

A Cost-Benefit Assessment of Gasification-Based Biorefining in the Kraft Pulp and Paper Industry

Volume 2 Detailed Biorefinery Design and Performance Simulation

FINAL REPORT

Under contract DE-FC26-04NT42260 with the U.S. Department of Energy
and with cost-sharing by the American Forest and Paper Association

21 December 2006

Eric D. Larson
Princeton Environmental Institute
Princeton University
Princeton, NJ
elarson@princeton.edu

Princeton University

Stefano Consonni and Silvia Napoletano
Department of Energy Engineering
Politecnico di Milano
Milan, Italy
stefano.consonni@polimi.it



Ryan E. Katofsky
Navigant Consulting, Inc.
Burlington, MA
rkatofsky@navigantconsulting.com

NAVIGANT
CONSULTING

Kristiina Iisa and Jim Frederick
Institute of Paper Science and Technology
School of Chemical and Biomolecular Engineering
Georgia Institute of Technology
Atlanta, GA
Kristiina.Iisa@ipst.gatech.edu
Jim.Frederick@ipst.gatech.edu



With contributions from:

Wang Xun
Department of Energy Engineering
Politecnico di Milano

Table of contents

1	SUMMARY	7
2	SYSTEMS OF INTEREST	8
2.1	Summary and nomenclature of plant configurations.....	9
3	CALCULATION OF MASS AND ENERGY BALANCES	10
3.1	GS	11
3.1	Aspen Plus.....	12
3.2	Calculation of fully integrated system.....	13
4	ASSUMPTIONS AND TECHNOLOGICAL ISSUES	16
4.1	Black liquor gasifier	16
4.2	Biomass boiler.....	17
4.3	Biomass dryer.....	18
4.4	Biomass gasifier	18
4.5	Syngas clean-up system.....	20
4.5.1	Syngas generated by the black liquor gasifier.....	20
4.5.2	Syngas generated by the biomass gasifier.....	20
4.5.2.1	<i>Tar control</i>	20
4.5.2.2	<i>Biomass syngas to the gas turbine</i>	21
4.5.2.3	<i>Biomass syngas to the Fuel Synthesis Island</i>	22
4.6	Gas turbine	22
4.7	HRSG and steam turbine	24
4.8	Heat integration	25
4.9	Oxygen production	26
4.10	Lime Kiln	27
4.11	Sulfur Recovery system.....	27
4.11.1	Rectisol system.....	28
4.11.2	Selexol system	29
4.11.3	Claus/SCOT unit.....	30
4.12	DME synthesis	31
4.12.1	DME synthesis kinetics model	31
4.12.2	DME reactor	32
4.12.3	Heat exchang design of DME synthesis section.....	33
4.13	Fischer-Tropsch (FT) synthesis.....	33
4.13.1	Kinetic model	33
4.13.2	FT reactor	34
4.13.3	FT liquid product.....	35
4.14	Mixed alcohols synthesis	35
4.14.1	Mixed alcohols synthesis kinetic model	35
4.14.1.1	<i>CO₂ removal in the recycle loop</i>	36
4.14.2	Mixed alcohols reactor.....	36

5	PROCESS CONFIGURATIONS AND OPERATING CONDITIONS	38
5.1	Summary of technologies adopted for the major subsystems.....	38
5.2	Input to Fuel Synthesis Island.....	38
5.2.1	Fuel synthesis fed with syngas from BLG	38
5.2.2	Fuel synthesis fed with syngas from BLG and from biomass gasification.....	39
5.3	Design and basic features of major subsystems.....	39
5.3.1	BL gasification	39
5.3.2	Biomass Gasification	40
5.3.2.1	<i>Biomass gasification with syngas cooler</i>	40
5.3.2.2	<i>Biomass gasification with quench</i>	41
5.3.3	Combined cycle	42
5.3.4	Rectisol system.....	42
5.3.4.1	<i>Total H₂S and CO₂ removal</i>	42
5.3.4.2	<i>H₂S removal</i>	44
5.3.5	DME synthesis island	45
5.3.6	FT synthesis island.....	47
5.3.7	Mixed alcohols synthesis island	48
5.4	DME cases	49
5.4.1	DMEa case: BLG with DME recycle island	49
5.4.1.1	<i>BL syngas cooling</i>	49
5.4.1.2	<i>Power boiler and steam cycle</i>	50
5.4.2	DMEb case: BLG and BGCC with DME recycle	50
5.4.3	DMEc case: BLG and BGCC with DME once-through production	51
5.5	FT cases	51
5.5.1	FTa case: BLG with FT production and BGCC with medium GT.....	51
5.5.2	FTb case: BLG with FT production and BGCC with large GT	51
5.5.3	FTc case: BLG and BG with FT production and CC with medium GT.....	51
5.6	MixOH case: BLG and BG with mixed alcohols production and CC with medium GT.....	52
6	PROCESS SIMULATION RESULTS	60
6.1	Overall performances.....	60
6.2	Energy efficiencies	62
6.3	Biorefinery designs vs. conventional Tomlinson systems.....	64
7	REFERENCES.....	67

APPENDIX A: DME AND FT SYNTHESIS	A.1
A.1 DME synthesis	A.1
A.1.1 Kinetics equations.....	A.1
A.1.2 Reactor model.....	A.3
A.1.3 Comparisons with experiment results.....	A.3
A.1.4 Sensitivity study of DME synthesis section	A.5
A.1.4.1 <i>Effect of reactor pressure variation</i>	A.6
A.1.4.2 <i>Effect of unconverted gas recycle</i>	A.7
A.2 FT synthesis	A.10

A.2.1	Kinetics equations.....	A.10
A.2.2	Reactor model.....	A.12

APPENDIX B: KINETIC MODEL FOR MIXED ALCOHOL SYNTHESIS B.1

B.1	Model development and preliminary results.....	B.1
<i>B.1.1</i>	Introduction	B.1
<i>B.1.2</i>	Scope of the work	B.1
<i>B.1.3</i>	Development of the kinetic model.....	B.2
<i>B.1.4</i>	Reactor simulation and validation of the kinetic model	B.6
<i>B.1.5</i>	Simulation study of the effects of the operating variables.....	B.13
<i>B.1.6</i>	Implementation of the kinetic model in a Fortran subroutine.....	B.17
<i>B.1.7</i>	Comparison between the results obtained using ASPEN and the Fortran program.....	B.18
<i>B.1.8</i>	Conclusions	B.19
B.2	Additional results and model validation	B.19
<i>B.2.1</i>	Introduction	B.19
<i>B.2.2</i>	Validation of the kinetic model	B.20
<i>B.2.3</i>	Conclusions	B.27
B.3	Literature cited	B.28

APPENDIX C: ANALYSIS AND SIMULATION OF A RECTISOL-BASED ACID GAS PURIFICATION PROCESS C.1

C.1	Background.....	C.1
<i>C.1.1</i>	The selected Rectisol process layout	C.1
C.2	“Rectisol-based” process design & features	C.2
<i>C.2.1</i>	Process principles	C.2
<i>C.2.2</i>	Process duties	C.2
<i>C.2.3</i>	Process bases	C.2
<i>C.2.4</i>	Process description	C.3
<i>C.2.4.1</i>	<i>The Acid Gas Absorber C1</i>	C.5
<i>C.2.4.2</i>	<i>The H₂S Concentrator C2</i>	C.5
<i>C.2.4.3</i>	<i>The CO₂ Stripper C3</i>	C.6
<i>C.2.4.4</i>	<i>The Solvent Regenerator C4</i>	C.6
<i>C.2.5</i>	Key process data & variables	C.6
<i>C.2.5.1</i>	<i>CO₂ heat of absorption in methanol</i>	C.6
<i>C.2.5.2</i>	<i>Different H₂S and CO₂ solubility in methanol</i>	C.7
<i>C.2.5.3</i>	<i>Methanol volatility</i>	C.7
<i>C.2.6</i>	Aspen Plus Model.....	C.7
<i>C.2.7</i>	Aspen Plus Model results and discussion.....	C.7
<i>C.2.7.1</i>	<i>Discussion</i>	C.10
<i>C.2.7.2</i>	<i>Addenda</i>	C.10
<i>C.2.8</i>	Aspen Plus Model for the abatement of H ₂ S only	C.11
C.3	Absorption column: model and thermodynamics	C.24
<i>C.3.1</i>	Nomenclature	C.25
<i>C.3.2</i>	Acid gas solubility	C.25
<i>C.3.3</i>	Heat of absorption of CO ₂ in methanol (-ΔH abs).....	C.25

C.3.4	Thermodynamic model	C.27
C.3.5	Heat and material balance equations in the absorption column	C.27
C.3.6	ABSORBER.xls user interface.....	C.29
C.3.7	Results and discussion	C.29
C.4	Aspen Plus thermodynamic model.....	C.35
C.5	References.....	C.36

Note: “Navigant is a service mark of Navigant International, Inc. Navigant Consulting, Inc. (NCI) is not affiliated, associated, or in any way connected with Navigant International, Inc., and NCI’s use of “Navigant” is made under license from Navigant International, Inc.

NOMENCLATURE

ASF	Anderson-Schulz-Flory (distribution)
BLGCC	Black Liquor Gasification Combined Cycle
BLGF	Black Liquor Gasification Fuel
CC	Combined Cycle
CSTR	Continuous Stirred Tank Reactor
DME	Dimethyl Ether
FSI	Fuel Synthesis Island
FT	Fischer Tropsch
GHSV	Gas Hourly Space Velocity
GI	Gasification Island
GT	Gas Turbine
GTL	Gas To Liquid
HRSG	Heat Recovery Steam Generator
HP	High Pressure
IGCC	Integrated Gasification Combined Cycle
IP	Intermediate Pressure
LP	Low Pressure
LPDME	Liquid Phase DME (reactor)
MixOH	Mixed Alcohols
MP	Medium Pressure
PFR	Plug-Flow Reactor
ppmv	parts per million by volume
SRU	Sulfur Recovery Unit
WGS	Water Gas Shift

1 SUMMARY

This volume illustrates the technologies, the assumptions and the modelization adopted to estimate the heat and mass balances of the biorefinery systems considered in this study.

Accurately calculating the mass/heat balances is crucial not only to verify the feasibility of a conceptual design and the applicability of a technological option, but also to estimate economic returns and environmental impacts. The modelization presented in this volume allows calculating all the parameters needed to appraise the overall plant performances:

- operating conditions of the most important components;
- extra-biomass input required to satisfy the mill steam demand;
- auxiliary power consumption;
- steam and cold duties;
- net power production;
- net fuel production.

These data are the basis to estimate capital and operating costs, and thus economic returns. The plant scheme and the operating conditions considered for each case are the outcome of significant screening work, which included the test of a considerable number of alternatives and sensitivity analyses. The basic feature that characterizes a plant scheme is the liquid fuel generated in the Fuel Synthesis Island (FSI), for which we've considered three cases:

- DME
- raw Fischer-Tropsch
- Mixed Alcohol

The type of fuel however does not fully characterize our plant configurations. The other basic options specified are:

- the arrangement of the Fuel Synthesis Island (with or without syngas recycle);
- the type of gas turbine (if any);
- the type of biomass gasifier (if any).

The combination of these options generates a relatively large number of alternative configurations. In this study we've focused on a total of seven cases which appear particularly meaningful and interesting: three for DME, three for Fischer-Tropsch and one for Mixed Alcohol. Although these seven cases do not exhaust the range of possible options, they give clear indications on the potential and the implications of pulp mill biorefinery systems.

Given the complexity of the systems to be modeled and the variety of the technologies involved, the modelization has been particularly challenging. A BLGF plant comprises sub-systems that fall in the realm of combustion and process technology (gasifier, heat exchangers, burners, etc.), others typical of the chemical industry (gas clean-up system, reactors, distillation columns, etc.) and others belonging to power plant technology (steam cycle, gas turbine, compressors and expanders, etc.). As a consequence, no single simulation tool is ideally suited for modeling the whole integrated biorefinery. In this study we've combined the use of two computer codes:

- GS, a code developed for research purposes at Politecnico di Milano and Princeton University;
- Aspen Plus, a code originally developed at MIT and now commercialized by AspenTech Inc.

Despite some complexity, the calculation algorithm based on these two codes provides an accuracy similar (or higher) to that of the most detailed engineering studies that can be found in the literature.

The technologies and the design parameters considered for each major sub-system are in between the state-of-the-art and the projections for the timeframe of the “Nth plant” biorefinery.

The results summarized in the last chapter of this volume allow appraising the merits of each plant option. The variety of the plant configurations analyzed in the study gives a wide range of power and fuel productions, as well as of efficiencies.

2 SYSTEMS OF INTEREST

The systems considered in this study are determined by alternative combinations of a few key processes:

- black liquor gasification
- biomass gasification (in one case biomass combustion)
- syngas cooling and clean-up
- catalytic synthesis of a liquid fuel from syngas
- co-generation of power and heat

The various technologies that can be used for these basic processes give rise to a large number of alternative configurations. The configurations considered in this study have been selected as among the most interesting and viable options to co-produce electricity, heat and liquid fuels under the constraint of handling all of the available black liquor and meeting the steam demand of the reference pulp and paper mill.

The plant scheme and the operating conditions considered for each case are the outcome of significant screening work, which included the test of a considerable number of alternatives and sensitivity analyses. This doesn't mean that the schemes and the set of operating parameters considered here are necessarily optimal, although we believe the performance improvements achievable by a more thorough optimization would be marginal. Significant improvements of efficiencies, power output or fuel output are likely to be achieved only by significant changes in the characteristics of the basic technologies, e.g. more effective catalysts, more efficient gas turbine, different gasification technology, etc.

Schematically, the systems modelled in this study consist of five basic “islands”:

- black liquor gasification island
- biomass gasification island (or, in one scheme, biomass boilers)
- syngas heat recovery and syngas clean-up island
- fuel synthesis island
- power island

The gasification island includes a cryogenic Air Separation Unit for the production of oxygen. The black liquor and biomass gasification islands are essentially the same for all the cases considered (except for the size of the biomass gasification island, which changes very significantly from one case to another). The heat recovery section has been tailored to the characteristics of each plant scheme to maximize the benefits of heat integration. The syngas clean-up island is centered around a Rectisol unit, except for the mixed alcohol case which adopts a Selexol system. The fuel synthesis island is the section that gives the basic characterization to the plant scheme. We have considered the following cases:

- production of DME from black liquor syngas, with no syngas recycle
- production of DME from black liquor syngas, with syngas recycle
- production of raw Fischer-Tropsch fuel from black liquor syngas, no syngas recycle
- production of raw Fischer-Tropsch fuel from a mix of black liquor and biomass syngas, no syngas recycle

- production of mixed alcohol from a mix of black liquor and biomass syngas, with syngas recycle.

The cases of DME with syngas recycle and Fischer-Tropsch fuel from black liquor syngas have been further differentiated based on the type of power island. For DME with syngas recycle we've considered a case with power boilers (no biomass gasifier) and just a steam cycle, and a case with a biomass gasifier and a combined cycle. For the case of Fischer-Tropsch fuel from black liquor syngas we've considered a case with a medium-size, 70 MW class gas turbine (GE 6FA) and another case with a large, 170 MW class gas turbine (GE 7FA).

2.1 Summary and nomenclature of plant configurations

As already mentioned, the basic feature that characterizes a plant scheme is the type of liquid fuel generated in the Fuel Synthesis Island (FSI):

- DME
- raw Fischer-Tropsch
- Mixed Alcohol

The type of fuel however is not enough to fully characterize the plant configuration. The other basic options specified are:

- the arrangement of the Fuel Synthesis Island (with or without syngas recycle);
- the type of gas turbine (if any);
- the type of biomass gasifier (if any)

Arrangement of Fuel Synthesis Island		with syngas recycle		once-through		syngas utilization
		none	medium scale (6FA)	medium scale (6FA)	large scale (7FA)	
Gas turbine:	NO (power boilers)	DMEa				syngas from BL goes to FSI
	YES, with syngas cooler		DMEb	DMEc FTa	FTb	syngas from BL goes to FSI, syngas from biomass gasifier goes to gas turbine
	YES, with quench		MixOH	FTc		syngas from BL and from biomass gasifier are mixed, and the whole flow goes to FSI

light blue background = back-pressure steam turbine
orange background = duct burner + back-pressure steam turbine
yellow background = steam turbine with low pressure section

Tab. 1. Overview of plant configurations

The overall picture is summarized in Tab. 1, where the nomenclature is as follows:

- DMEa** Production of DME, FSI with syngas recycle, no gas turbine (power island comprises just a steam cycle). The extra steam required to meet the mill demand is generated by power boilers and the FSI is fed (necessarily) with the syngas generated by black liquor. Given the need for the power boilers, no excess steam is available and the steam turbine is backpressure.
- DMEb** Like DMEa, but with a biomass gasifier that generates enough syngas to fully fire a medium-scale gas turbine. In this case the steam demand of the mill is met by burning some syngas in a duct burner ahead of the HRSG of the combined cycle.

Given the need for the duct burner, no excess steam is available and the steam turbine is backpressure.

- DMEc Like DMEb, but without syngas recycle in the FSI. Similarly to DMEb, also in this case some syngas must be burnt into a duct burner ahead of the HRSG of the combined cycle and the steam turbine is backpressure.
- FTa Production of Fischer-Tropsch fuel, once-through FSI, biomass gasifier that generates enough syngas to fully fire a medium-scale gas turbine. The steam demand of the mill is met by burning some syngas in a duct burner ahead of the HRSG of the combined cycle and the steam turbine is backpressure.
- FTb Like FTa, but with a large scale, 170 MW class gas turbine. The much larger size of the gas turbine eliminates the need for the duct burner. Steam production is much larger than needed by the mill, so the steam turbine includes a low pressure (condensing) section to increase power generation.
- FTc Like FTa, but with the FSI fed by the mix of all the syngas generated by black liquor and all the syngas generated by biomass. The much higher fuel production increases steam production in the exothermic FT reactor and eliminates the need for a duct burner to meet the mill steam demand. Similarly to FTb, steam production is larger than needed by the mill and the steam turbine includes a low pressure condensing section.
- MixOH Production of mixed alcohols with the same rationale of scheme FTc, i.e. the FSI is fed by the mix of all the syngas generated by black liquor and all the syngas generated by biomass. In this case however, the low conversion achievable in the mixed alcohol reactor makes syngas recycle in the FSI imperative. Despite the syngas recycle, fuel conversion and thus steam production in the FSI are relatively low and the steam demand of the mill can be met only by burning some syngas in a duct burner placed, as usual, ahead of the HRSG of the combined cycle. Since no excess steam is available, the steam turbine is backpressure.

When biomass syngas feeds the gas turbine (DMEb, DMEc, FTb, FTc) we've considered a biomass gasifier with syngas cooler. The syngas exiting the syngas cooler is filtered through ceramic candles and then fed to the gas turbine. Although not yet demonstrated at commercial scale, pilot-scale testing has been successful (e.g., at Varnamo, Sweden), and it is believed that this arrangement can be compatible with requirements of the gas turbine in commercial service.

When the syngas generated from biomass is mixed with the syngas generated from black liquor and the mixture feeds the FSI we've considered a biomass gasifier with quench. In this case the catalyst of the FSI requires deep removal of all contaminants from the syngas and gas clean-up must necessarily take place at low temperature. The penalties brought about by quenching the syngas are therefore limited, because the syngas has to be cooled to low temperature anyhow. On the other hand, a quench gasifier would be lower cost than the gasifier with syngas cooler design.

3 CALCULATION OF MASS AND ENERGY BALANCES

The calculation of mass and energy balances is the fundamental step required to estimate performances and costs of the technologies considered in this study. Mass and energy balances determine how much electricity and fuel can be generated by a given black liquor flow, as well as how much extra fuel (biomass or possibly fossil fuel) is needed to supply the mill steam

requirements. Mass and energy balances also give the basic information needed to size and to estimate the cost of the most relevant equipment. All this allows estimating the capital costs and the operating costs, as well as the unit cost of the final products (electricity and/or fuel).

The mass and energy balances and the overall performances of each pulpmill biorefinery configuration have been evaluated by combining the use of two computer codes:

- GS, a code developed for research purposes at Politecnico di Milano and Princeton University;
- Aspen Plus, a code originally developed at MIT and now managed and commercialized by AspenTech Inc.

The following gives a brief description of each code and of the algorithm adopted to calculate the mass and energy balances.

3.1 GS

GS is a computer code originally developed at Politecnico di Milano and Princeton University to predict the performance of complex Gas-Steam cycles. The code is a powerful and flexible tool that can accurately predict the performances of a wide variety of systems for electricity production or cogeneration, including systems where the feedstock is gasified to generate a syngas that undergoes a sequence of physical and chemical processes. As such, GS has also been used extensively for the analysis of gasification-based power systems, including black liquor gasification plants.

The system of interest is defined as an ensemble of components, each belonging to one of sixteen basic types: pump, compressor, turbine, heat exchanger, combustor, gas turbine expander, chemical reactor, mixer, flow splitter, heat recovery steam cycle, air splitter plant, shaft connecting different machines, saturator, solid oxide fuel cell, intercooled compressor, steam cycle. The variety of elementary components and the possibility to interconnect them modularly provide high flexibility.

Once the system to be calculated has been defined and the coherence of the component characteristics and their inter-connections have been verified, the code sequentially calculates the mass, energy and atomic species balances of all plant components until it reaches the convergence of thermodynamic conditions and component characteristics calculated at each iteration. After reaching convergence, the code can carry out a complete entropy (or "Second-Law") analysis to calculate the destruction of exergy and reversible work within each component and their input/output flows for the whole system.

The model accounts for all major phenomena and mechanisms affecting the performances of a wide variety of energy conversion systems: heat losses; variation of turbomachinery efficiency with scale and stage similarity parameters; constraints imposed by choking of flow at the gas turbine expander inlet, gas turbine cooling, incomplete chemical reactions, etc.; with proper input adjustments it can also predict basic off-design conditions.

The thermodynamic properties of all molecular species are calculated using a consistent methodology and the same data bases: JANAF tables for all gaseous species; SI steam tables for water and steam¹. Chemical equilibrium is predicted by the same algorithm adopted in STANJAN, a code originally developed at Stanford by prof. William Reynolds. Thus, GS can simulate accurately the performance of reactors where the whole output flow or a subset of it is at chemical equilibrium.

¹ For methanol, ethanol, butane and butane, enthalpy and entropy are taken from Perry, Nasa coefficients by Bonnie McBride of NASA Lewis Center [from EDL website: www.galcit.caltech.edu/EDL/index.html].

3.1 Aspen Plus

Aspen Plus is a widely used commercial chemical process simulation package originally developed for petrochemical refining applications. Due to its capability to simulate the operating conditions of chemical plants and to accommodate calculation of chemical kinetics, it well suited to calculate the chemical processing of syngas and the refining of the resulting products.

Aspen plus was originally developed at the MIT under a DOE project to simulate coal conversion processes. Now it has been widely accepted in the chemical industry as a design tool because of its ability to simulate a variety of steady-state processes ranging from single unit operations to complex processes involving many units.

Aspen plus was chosen as the simulation platform for our modeling of the syngas to fuel/chemical synthesis/separation process, as well as the gas purification section. The purpose of developing this simulation is to understand how co-production is affected by the constraints imposed by the chemical process, to evaluate different kinds of plant configurations, to find out ways to improve the performance of current designs. The features that make Aspen plus suitable to these purposes are:

Powerful database of chemical species properties. Compared to power production systems, the fuel synthesis island and the gas purification section include more types of chemicals (hydrocarbons, oxycompounds, sulfides, etc) which exhibit real gas behavior (i.e. departure from ideal gas law, including phase change). Having the correct thermophysical properties for such a large amount of compounds is crucial to predicting the performances of processes based on real gas effects like distillation columns, vapor-liquid separators, absorbers, strippers, etc. Aspen includes powerful packages with a variety of methods to predict the thermodynamic properties of the species and the mixtures being calculated.

A variety of models for the processes (flash, two-phase reaction, distillation, absorption, regeneration, etc.) carried out in syngas to liquid plants. Unlike power production, the synthesis of chemicals or fuels is often controlled by chemical kinetics and its simulation requires some form of kinetic model. In addition to simple models based on stoichiometry or chemical equilibrium, Aspen includes generalized models for kinetically-controlled reactors which can be used to estimate the mass and energy balance of the basic types reactors: fixed bed, stirred, slurry bed or bubbling slurry bed. The model library of Aspen also includes a number of gas-solid, gas-liquid and gas-gas separators that allow estimating the yield and the utilities load of the whole synthesis island. The Aspen model can be used to illustrate the trade-offs among the design parameters that determine the performance of a co-production system, as well as to test the sensitivity to the operating conditions and the specifications of the major components.

The ability to embed user-compiled models into the simulation process. While the framework of the physical and chemical models that can be run with Aspen has general applicability, it is obviously impossible to include beforehand all types of compounds, reactors or kinetic rate expressions that can be encountered in specific applications. The lack of data on a specific process can be easily overcome by interfaces that allow users to embed their own models into Aspen simulations. In fact, for this project the fuel synthesis island has been simulated by embedding kinetic models of DME, Fischer-Tropsch and Mixed Alcohol synthesis into the Aspen framework. The specific kinetic expressions and the kinetic models required to simulate the synthesis of each type of fuel have been implemented in a Fortran subroutine called by the Aspen module that calculates the synthesis reactor. By developing appropriate in-house models, each user can tailor the simulation procedure to address specific

requirements, not only for kinetic expressions, but also for aspects related to fluid dynamics, heat transfer, etc.

3.2 Calculation of fully integrated system

Aspen or GS alone cannot carry out satisfactory simulations of the fully integrated systems targeted in this project. This is why after a number of tests it was decided to use each code only for the systems for which it is most suited (Fig. 1 and Fig. 2): Aspen, for the Rectisol system and the fuel synthesis island; GS, for the gasification island and the power island.

In addition, GS was also used for the final pass giving the heat and mass balances of the whole integrated system, i.e. the actual final output for each plant configuration. This approach gives the maximum possible accuracy at the expense of the complexity of the calculation procedure, which requires a somewhat awkward but unavoidable sequence of GS and Aspen runs. The overall performances of each integrated system are calculated by going through the following steps, with the output generated at each step being the input required for one of the subsequent steps.

1. Run the GS model of the BL gasification island to predict the flow rate and the characteristics (composition, temperature, pressure) of the raw syngas at the inlet of the gas clean-up island, which are the inputs for the Aspen model of the Rectisol process.
2. Run the Aspen model of the Rectisol process to calculate flow rate and conditions of the clean syngas, as well as all other parameters needed to calculate the energy balance of the whole plant (cold and heat duty, flow rate and characteristics of streams other than the clean gas, etc.). In the MixOH case, syngas cleaning is carried out by the Selexol process and its utilities and material balances have been provided directly by UOP, licensor of the process.
3. Run the Aspen model of the fuel synthesis island using as input the outputs of the GS simulation of the gasification island and the Aspen simulation of the Rectisol system. This gives the amount of fuel available for export, as well as the flow rate and conditions (composition, temperature, pressure) of the unconverted syngas available for the power island, the refrigeration duty of the fuel synthesis island, the heat exchanged with power island, etc.
4. Run the GS model of the gasification island and power island altogether to predict the performances of the fully integrated system. This final calculation takes into account the Rectisol process and the fuel synthesis island as previously calculated by Aspen (heat exchanges, refrigeration duty, output flows, utilities, etc.), as well as the requirements of ancillary systems like the Claus and SCOT plant.

As long as no iteration is needed, this procedure requires a total of four runs in series (one GS + two Aspen + one final GS) and can be managed without excessive penalties, as shown in Fig. 3. This is the case for all plant configurations considered here except two: FTc and MixOH. In these cases the syngas generated by the biomass gasifier is mixed with the syngas generated from black liquor and the whole syngas flow is used for fuel production. The gas turbine is fed with the unconverted syngas from the fuel synthesis area (calculated by Aspen) and its flow rate must match the amount needed to fully fire the gas turbine. This requires repeating iteratively the calculation from step 2 to step 4, changing the amount of biomass fed to the biomass gasifier until the amount of unconverted syngas calculated by Aspen at step 3 equals the amount estimated by GS at step 4 for the gas turbine (Fig. 4). The complexity of this iteration procedure

makes it difficult (though not impossible) to carry out systematic investigations like sensitivity or parametric analyses.

A more straightforward procedure would obviously be desirable, but it would require the development of new software tools for the integration of Aspen and GS (or possibly other pieces of software). Aside from issues of software intellectual property (Aspen is a highly protected commercial package), such effort is much beyond the scope of this project. Despite its complexity, the calculation procedure adopted here appears therefore the best way to take advantage of the tools currently available. The approach provides an accuracy similar to (or greater than) that of the most detailed engineering studies that can be found in the literature.

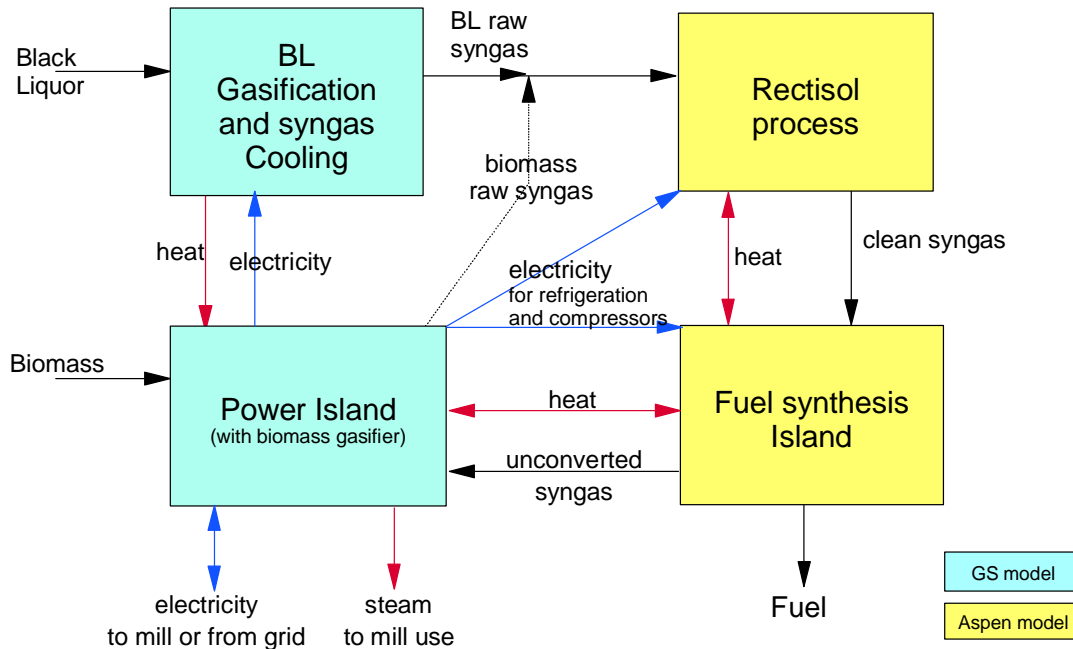


Fig. 1. Diagram of computer codes used for DME and FT cases. The BL gasification island is calculated first with GS. Then, Aspen is run twice to simulate the Rectisol system and the fuel synthesis island. Finally, GS is run again to simulate the whole integrated system, taking into account the results generated by Aspen for the Rectisol system and the fuel synthesis island.

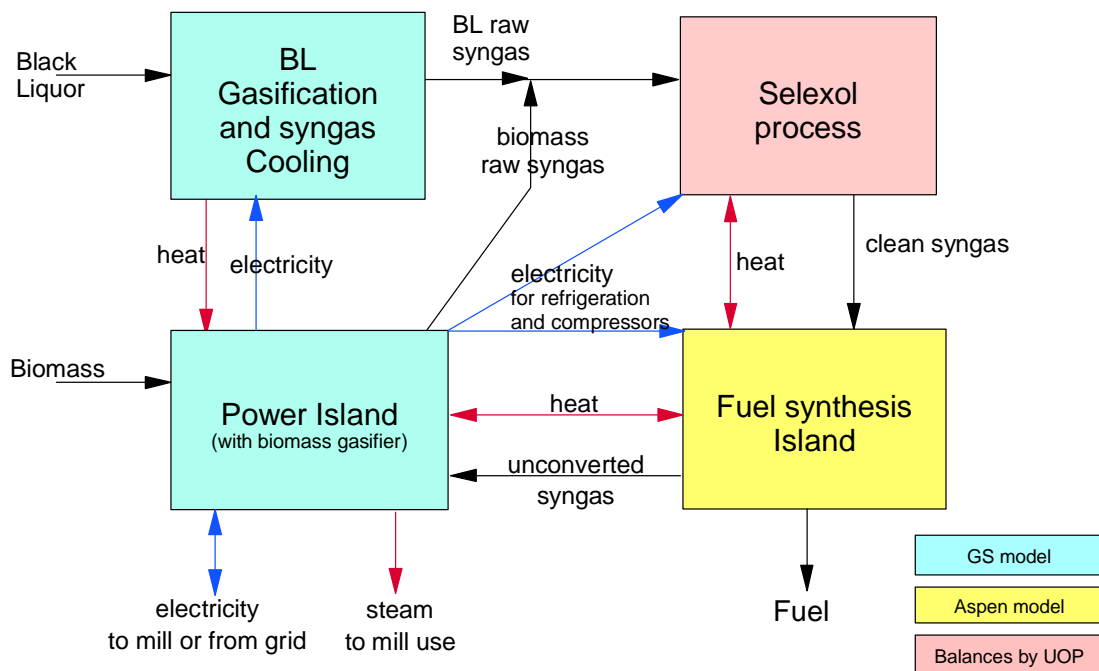


Fig. 2. Diagram of computer codes use for the MixOH configuration. The mass and energy balances of the Selexol system were provided directly by UOP, licensor of the process.

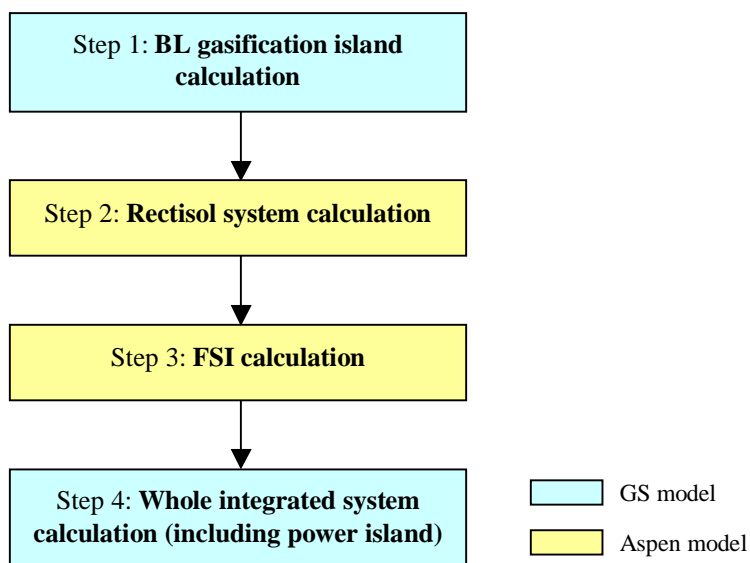


Fig. 3. Calculation algorithm for DMEa, DMEb, DMEc, FTa and FTb.

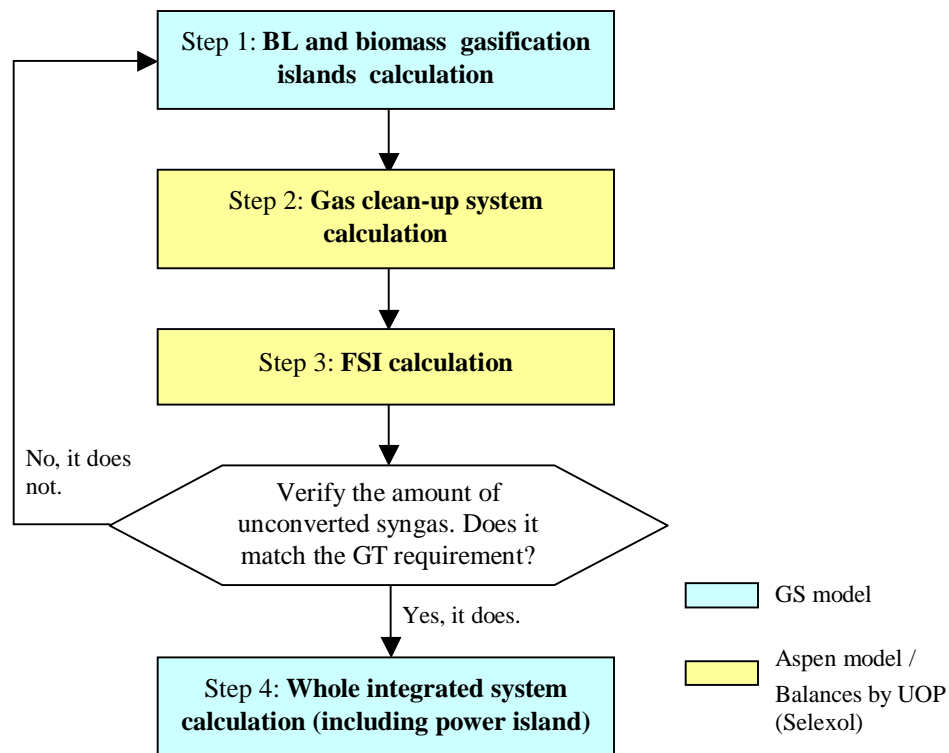


Fig. 4. Calculation algorithm for FTc and MixOH. The iteration between the final calculation by GS and the Aspen calculation of the Rectisol system (only for the FTc case) and of the FSI is required to adjust the amount of unconverted syngas to the value needed to fully fire the gas turbine. For MixOH, the mass and energy balances of the Selexol system have been provided directly by UOP, licensor of the process.

4 ASSUMPTIONS AND TECHNOLOGICAL ISSUES

4.1 *Black liquor gasifier*

The black liquor gasifier considered in this study refers to the technology under development by Chemrec, a Swedish company. The gasifier is a high-temperature, high-pressure, entrained flow, oxygen-blown reactor comprising two main sections: an upper section where black liquor is gasified at temperatures around 1000°C and a bottom section where the syngas is quenched and the smelt is collected in a bath to produce green liquor.

The gasifier basic operating conditions (Tab. 2) have been chosen in accordance with data published in the literature and information provided by the manufacturer. The composition of the syngas exiting the gasifier has been calculated assuming that:

- Carbon conversion and methane in raw gas are as specified in Tab. 2 (unconverted carbon leaves the gasifier together with the green liquor);
- Ash and chlorides behave as inert material;
- All the remaining material constitutes a gas/condensed-phase mixture at equilibrium comprising the following species: Ar, CO, CO₂, COS, H₂, H₂O, H₂S, NH₃, N₂,

Na_2CO_3 , Na_2SO_4 , Na_2S , NaOH , K_2CO_3 , K_2SO_4 , where the species containing sodium and potassium can be either liquid or solid or both, depending on temperature and pressure.

This calculation scheme, which determines the sulfur split between the syngas and the solid/liquid phase, gives satisfactory agreement with specific information provided by the manufacturer of the gasifier, as well as with qualitative indications found in the literature.

Black Liquor Gasifier	
Pressure of raw syngas	35 bar (483 psig)
Temperature of raw syngas before quench	1000°C (1832°F)
Heat loss to environment	0.5% of BL HHV
Heat to cooling flows	2.0% of BL HHV
Carbon conversion	99.9%
Methane in raw syngas	1.5% mass in raw gas

Tab. 2. Basic BL gasifier operating parameters

4.2 Biomass boiler

In the DMEa plant, the waste heat recoverable from the gasification island and the fuel synthesis island is insufficient to meet the mill steam demand, and additional steam is generated by a biomass boiler. The thermal power that must be supplied by this boiler is larger than the assumed capacity of the biomass boiler already existing at the mill; thus, additional biomass boiler capacity is needed (for our reference mill, existing biomass boilers are assumed to be able to accommodate 100 MW HHV of biomass input, while in DMEa, meeting the mill steam demand requires around 200 MW HHV of biomass input).

For added biomass boiler capacity, we have assumed the same design specifications as for the existing boilers, i.e. generation of steam at 87.2 bar, 480°C. This allows keeping the same back-pressure steam turbine at the existing plant. The new boiler would also provide saturated water at 38 bar to the DME reactor, where steam is generated to maintain a constant reaction temperature of 260°C. Saturated steam from the DME reactor is superheated up to 480°C in the boiler and then admitted to the steam turbine. The basic operating parameters assumed for the wood residual boiler are summarized in Tab. 3.

Wood Residual Boiler	
Air T, preheater outlet	145°C (293°F)
Gas T, preheater outlet	230°C (446°F)
Outlet flue oxygen (vol. wet)	4.0%
Evaporation pressure	87.2 bar (1250 psig)
Superheater outlet	480°C (896°F)
Superheater Δp	10.0%
Heat loss to environment	1.0%
Deaerator pressure	4.8 bar (55 psig)

Tab. 3. Basic operating parameters of additional power boiler fed with wood residuals

4.3 Biomass dryer

In the plants where the power island includes a gas turbine (i.e. all cases except DMEa), a mixture of hog fuel and purchased wood wastes are fed to a biomass gasifier; the syngas generated by such gasifier is either fed to the gas turbine (DMEb, DMEc, FTa and FTb) or mixed with the syngas generated by the black liquor gasifier prior to the fuel synthesis island (FTc and MixOH).

Operating experiences have shown that the moisture content of the biomass fed to the gasifier should be in the range 10-20% [Lau et al., 2003]. This is much below the typical moisture content of hog fuel and wood wastes, which is around 50%. To obtain proper gasification conditions, we have assumed therefore that the biomass feedstock is dried by direct contact with the flue gas exiting the HRSG to reduce its moisture content from 50% to 20%².

The temperature of the flue gas exiting the HRSG is adjusted to give a temperature of the moist gas exiting the drier of 90°C. A high drier inlet temperature must be avoided to minimize release of volatile organic compounds (VOCs) and risk of ignition; Brammer and Bridgwater [1999] mention a maximum value of 250°C. To achieve this temperature, the moist gas at the drier exit is recycled to the drier inlet and mixed with the gas exiting the HRSG at a temperature higher than 250°C; the fraction to be recycled is calculated to give a drier inlet temperature (downstream of mixing with the HRSG exhausts), of 250°C.

As for auxiliary power consumption, based on data reported by Consonni and Larson [1996] we've assumed an electricity consumption of 20 kJ per kg of wet biomass for biomass handling and drying (5.6 kWh per tonne of wet biomass).

4.4 Biomass gasifier

The biomass gasifier considered in this study is a pressurized oxygen- and steam-blown, fluidized-bed reactor similar to the one being developed by GTI [Lau et al., 2003]. In our case the use of oxygen as the oxidant does not imply major economic penalties because an Air Separation Unit (ASU) must be present anyhow to supply the oxygen needed by the black liquor gasifier. On the other hand, the oxygen-blown design gives a syngas with superior heating value, with benefits on equipment size (and cost) and the operation of crucial components downstream: higher combustion stability for the gas turbine combustor, higher fuel conversion for the fuel synthesis reactor. The amount of oxygen supplied to the gasifier determines the partial oxidation of biomass and thus the gasification temperature, which is assumed to be 950°C. This value appears a reasonable compromise between the need to avoid ash softening, which becomes more likely when temperature increases, and the need to minimize tar in the syngas, which increases when the syngas outlet temperature decreases. This temperature is selected to avoid any ash softening.

In the designs currently being pursued, the gasifier vessel is actually followed by a cracker for the breakup of the large molecules that constitute tar. In our simulations the gasifier and the cracker are calculated altogether in a single step, assuming that the syngas at the cracker exit is at 950°C, with all species at chemical equilibrium except for methane and tar, the latter modeled as phenol (C₆H₆O). The concentration of methane and tar at the cracker exit are specified in input at approximately the same values detected experimentally by Simell et al. [1996]. Given the presence of a catalyst in the cracker (nickel-based catalysts appear most suited) and the relatively

² We actually model the dryer as a mixer and an indirect-contact heat exchanger. First, the water to be evaporated to obtain the required outlet moisture content (in our case 20%) is mixed with the flue gas exiting the HRSG; then, the moisturized gas heats the dried biomass from the ambient temperature (20°C) to the temperature assumed at the drier exit, in our case 70°C.

high temperature, assuming that all species but methane and tar are at chemical equilibrium at the cracker outlet appears reasonable. Experimental data reported by Simell et al. [1996] show equilibrium is nearly reached even at the moderate conditions of 5 bar and 900°C.

In addition to oxygen, the gasifier is fed also with steam to fluidize the bed. The operating pressure is 36 bar, which is in the range of pressurized systems under development [Lau et al. 1993; Blackadder et al. 1994]. In the configurations where the biomass syngas is mixed with the BL syngas (i.e. FTc and MixOH), pressurized gasification allows mixing the two streams without the need for biomass syngas gas compression; this is beneficial, because the losses due to fuel gas compression are typically higher than those due to the compression of the fluidizing agent. On the other hand, in the configurations where the biomass syngas is supplied to the gas turbine, pressurized gasification allows the production of useful power by a gas expander. These benefits will have to be weighed against the complexity and the operating costs of biomass feeding to a pressurized reactor. In our case biomass is pressurized in lock hoppers with a stream of pure N₂ provided from the ASU plant; the lock-hoppers energy consumption is that for inert gas compression.

Tab. 4 summarizes the assumptions adopted for the biomass gasifier, while Tab. 5 gives the composition and the heating value of hog fuel and purchased wood wastes, which are assumed to be the same.

Biomass gasifier	
Pressure	36 bar (507 psig)
Steam mass flow	28% of DS
Steam pressure	38 bar (536 psig)
Outlet temperature	950°C (1742°F)
Heat loss	0.5% of biomass HHV
Mol fraction at cracker outlet	CH ₄ 1%
	Tar 0.2 g/Nm ³

Tab. 4. Basic biomass gasifier operating parameters

Bone dry wood: mass fraction	
C	49,98 %
H	6,12 %
O	42,49 %
N	0,55 %
S	0,06 %
Ash	0,80 %
LHV	18,66 MJ/kg
HHV	20 MJ/kg
Feed wood:	
Moisture	50 %
HHV	10,01 MJ/kg
LHV	8,12 MJ/kg
Dried wood:	
Moisture	20 %
HHV	16,01 MJ/kg
LHV	14,45 MJ/kg

Tab. 5. Composition and heating value of hog fuel and wood waste

4.5 *Syngas clean-up system*

The syngas generated by the gasification of black liquor or biomass must be cooled and properly treated to insure proper and reliable operation of the equipment fed with the syngas. The technologies to be used and the extent to which the gas must be purified depend on the syngas composition and the requirements of the systems downstream. Consequently, the arrangement and the processes assumed here have been tailored to the characteristics of the various system configurations.

4.5.1 Syngas generated by the black liquor gasifier

The syngas generated from black liquor exhibits relatively high concentrations of particulates, alkali, chlorine and sulfur. In the high-temperature gasification technology considered here most of the particulates and the alkali should be removed by the quench and in the heat exchanger placed immediately downstream of the gasifier, where the condensate generated by cooling the saturated syngas below its dew point flows counter-current with the gas, thus acting like a scrubber. This condensation cooling alone should remove most of the soluble species (alkali and acid gases) and particulates. On the other hand, given the very stringent requirements of the FSI downstream, we've considered two further treatments to achieve deep gas clean-up: low-temperature wet scrubbing and Rectisol. Despite its high cost, the latter is the most reliable process now available to achieve the purity required by the catalysts adopted to synthesize DME and FT fuels. In the MixOH case, the MoS₂ catalyst considered for the mixed alcohol synthesis requires some H₂S in the syngas and the very deep removal achievable with Rectisol is unnecessary. In this case we've therefore considered a wet scrubber followed by a Selexol system, which is less costly than Rectisol.

4.5.2 Syngas generated by the biomass gasifier

The clean-up requirements for the syngas generated by biomass are different depending on whether the syngas is fed to the gas turbine or the FSI. The following summarizes the technologies and the operating parameters assumed in each case. The need to control tar is the same in both cases.

4.5.2.1 Tar control

Tars are condensable organic compounds formed during gasification. They condense at temperatures around 350°C and their deposition on cool surfaces can cause severe operating problems: fouled heat transfer surfaces, constricted piping, clogged valves, etc. The tar concentration in the syngas is a function of gasification temperature and of the properties of the feedstock. Wood gasification (and biomass gasification in general) generates much more tar than coal gasification due to lower reactor temperatures utilized. A number of design features (e.g. splitting oxidant injection into a primary and secondary flow) can be effective in reducing tar formation; however, a process for tar destruction is likely to be necessary to achieve the low concentrations required for reliable plant operation. In our case we have assumed that the gas leaving the gasifier goes through a fixed bed catalytic reactor where tars are cracked into species with lower molecular weight. A nickel-based catalyst appears preferable, because at high pressure the catalytic action of dolomite or other carbonate rocks may be inadequate, even at 950°C. Pilot-scale tests have shown that nickel-based catalysts at elevated temperature (around 900°C) have high activity for tar destruction; they also catalyze ammonia decomposition, and about 80% ammonia conversion are achieved in the cracker. Then the amount of ammonia in the

product gas at the cracker exit is slightly higher than at equilibrium³ [Simell et al., 1996]. High temperature is needed also to avoid the formation of solid carbon, which could deposit and cause catalyst deactivation, as well as to compensate the deactivation caused at high pressure by H₂S.

At present, many nickel-based catalysts are commercially available because of their application in the steam reforming of hydrocarbons. They have demonstrated high activity also for tar destruction, although they undergo rapid deactivation due to poisoning by impurities and coke formation. Additional research is needed to develop formulations with longer lifetime.

In the model adopted here, the total oxygen flow supplied to the gasifier and the cracker is adjusted to achieve the specified temperature of 950°C at the cracker exit, assuming that the gas composition is at equilibrium except for methane and tar. In the configurations with the syngas cooler, where the biomass syngas is treated with just a ceramic candle filter, its temperature is maintained always above 375°C to prevent tar condensation. In the configurations with the quench, the biomass syngas is mixed with the black liquor syngas and treated in a Rectisol or Selexol system at low temperature.

4.5.2.2 Biomass syngas to the gas turbine

In cases DMEa, DMEb, FTa and FTb the gas turbine is fed with a mixture of syngas generated by the biomass gasifier and unconverted syngas from the fuel production island. In cases FTc and MixOH the gas turbine is fed solely with unconverted syngas.

The fuel gas fed to the gas turbine must not contain particulate or contaminants that can damage the turbine blades by erosion or corrosion. Additional contaminants of concern from an emission standpoint are nitrogen compounds, especially ammonia derived from nitrogen in biomass feedstock.

Unlike unconverted syngas, the syngas generated by the biomass gasifier contains contaminants that must be removed to prevent damage to the equipment downstream. In the configurations where the biomass syngas goes only to the GT (DMEa, DMEb, FTa and FTb) we have considered hot clean-up (ceramic filter operating around 450°C) that allows maintaining the syngas at high temperature. A commercially proven, low-temperature technology like quench and wet scrubbing would be simpler and safer, but less efficient. Consistent with our overall analysis, we assume that hot gas cleaning will be equally reliable in a commercial Nth plant.

4.5.2.2.1 *Particulate removal*

Particulates can cause severe turbine blade erosion even at very small concentrations. This is why gas turbine manufacturers specify stringent limits (around 5 ppm by weight) for their concentration in the fuel gas. Since conventional cyclones can't attain such low concentrations, high efficiency filtration devices like ceramic or metallic candle filters must be placed at an appropriate point of the syngas path.

In our modelization we have assumed that the bulk of the ash in the raw gas is removed by a cyclone at the gasifier exit, while all remaining particulates are separated by a ceramic (or metallic) filter operating at the temperature that allows maintaining the syngas above 375°C also downstream of the syngas expander and after mixing with unconverted syngas. Maintaining the syngas above 375°C is supposed to prevent the condensation of tars. At the same time, the operating temperature of the filter (around 450°C) is low enough to induce the condensation of most alkali on the solid particles removed by the filter.

³ At equilibrium the ammonia content is 60-50 ppm at 905-960°C.

At present, high temperature filters are not a commercial process yet. They are being tested in some pilot-plant gasifier and additional development and demonstrations are required to prove their effectiveness and commercial viability.

4.5.2.2.2 Alkali removal

Alkali compounds cause corrosion of the ceramic filter and of turbine blades. The alkali in the biomass are vaporized during gasification and end up in the product gas. At high temperatures these contaminants are volatile, but below 500°C the vapors condense and deposit on entrained solids. Thus, cooling below 500°C before particulate removal may be sufficient to remove alkali compounds down to levels specified by gas turbine manufacturers.

In the process design considered here, raw syngas is first cooled in a syngas cooler to about 450°C, and then filtered. As already mentioned, this would result in the removal of alkali in the filter while avoiding tar condensation.

Syngas cooler	
$\Delta p/p$	2%
Heat loss	2%
Min temperature at GT inlet	375°C (662°F)
Filter	
$\Delta p/p$	3%

Tab. 6. Basic operating parameters for the biomass syngas cooler and filter

4.5.2.3 Biomass syngas to the Fuel Synthesis Island

In cases FTc and MixOH all the syngas generated by the biomass gasifier and by the BL gasifier is used to produce liquid fuel. The two streams originated by the two gasifiers merge into a single flow which is treated in a physical absorption system: Rectisol for FTc, Selexol for MixOH. Rectisol can achieve the deep removal of sulfur required by FT catalysts (less than 1 ppm of H₂S). Selexol can attain a more moderate H₂S removal (H₂S around 10 ppm), which however is adequate for the sulfur-tolerant MoS catalyst of the MixOH reactor⁴.

Unlike the case where the syngas generated from biomass feeds the gas turbine, in this case quenching and scrubbing the syngas doesn't result in a reduction of system efficiency, because the physical clean-up system requires low temperature anyhow. This is why we have assumed that the syngas generated from biomass is quenched into a scrubber both to reduce its temperature and to remove alkali, tars and impurities, as well as most of the water vapor. Wet scrubbing has several advantages: it is a well-known and widely used technology and it removes particulates, tar and other contaminants very effectively; on the other hand, it generates contaminated water, which requires waste water treatment.

4.6 Gas turbine

The calculations carried out for this study refer to two General Electric engines: 6FA (medium scale) and 7FA (large scale). These machines belong to the most advanced generation of heavy-duty machines now in wide commercial service, also known as "F" technology.

⁴ In a system based on a MoS catalyst some H₂S in the syngas is actually necessary to make up for the small amounts of sulfur inevitably lost in the catalytic process.

Performance predictions have been calibrated based on data published by General Electric; a few relevant inputs to the gas turbine model have been fine tuned to achieve the best possible agreement with the overall performance published by GE. Tab. 7 compares the performances quoted by GE with those generated by the calculation model for operation on natural gas fuel at ISO conditions (15°C, 1 atm).

Compared to natural gas firing, feeding the gas turbine with a biomass-derived syngas increased mass flow through the turbine because, due to the relatively low heating value of the biomass syngas, a larger fuel flow rate is needed to reach a given Turbine Inlet Temperature (TIT). The larger mass flow through the turbine affects the match between the turbine and the compressor, which must obviously operate in such a way that the compressor outlet pressure equals (once combustor pressure drop is accounted for) the turbine inlet pressure.

The calculation carried out in GS assumes that the expander operates under aerodynamically choked conditions i.e. its “reduced” (non-dimensional) mass flow is constant. This corresponds to the operating conditions of essentially all commercial gas turbines. In this situation a larger mass flow can be accommodated only by increasing the pressure ahead of the turbine, i.e. by increasing the compressor pressure ratio. Higher pressure ratios move the compressor toward the stall limit, and thus there is a limit to the mass flow increase that can be tolerated by the gas turbine. In our calculations we have assumed that:

- The Turbine Inlet Temperature (TIT) is the same as with natural gas firing;
- The compressor can operate with a compression ratio up to 5% above its value with natural gas;
- Further increases in fuel flow must be accommodated by reducing the air flow entering the compressor, which in most engines can be easily accomplished by adjusting the inlet guide vanes.

Due to the different flow rate and thermo-physical properties of syngas compared to natural gas, maintaining the same TIT of the natural-gas version implies higher temperatures throughout the expansion and thus – everything else equal – higher blade metal temperatures and shorter life of the hot parts of the engine. This is why syngas-fired gas turbines are typically de-rated (TIT lower by 10-30°C) to maintain the same life and reliability of the natural gas-fired version. Our assumption of no change in TIT implies an increase in Turbine Outlet Temperature (TOT) of 10-20°C and can be justified by considering that by the time the Nth pulp mill biorefinery plant is realized, TIT and TOT of state-of-the-art gas turbines will be significantly higher than those adopted today.

As to the 5% increase in pressure ratio, it is within the range typically tolerable by the compressors of heavy-duty engines. Whether such an increase is compatible with lower air flow can only be verified by the gas turbine manufacturer (when air flow is decreased by closing the Inlet Guide Vanes, the compressor stall margin decreases).

Other issues raised by the use of syngas in a gas turbine are related to combustor stability, emissions and fuel injector pressure loss, which may be substantially different from those with natural gas. The first two are mainly related to syngas chemical composition and heating value; the third is related to flow rate. Based on pilot-scale experimental work and the experience accumulated in Integrated Gasification Combined Cycles (IGCC), refineries and steel plants, combustion stability should not be a major issue as long as the fuel calorific value is above 4-6 MJ/m_n³ (1 m_n³ = 1 m³ at the "normal" conditions of 1 atm, 0°C). In the systems considered here, the fuel fed to the gas turbine has a heating value higher than 6 MJ/m_n³, so no particular flame stability problems are envisaged. The increase in pressure loss to be applied across the fuel injectors can be accommodated either by increasing the fuel pressure (which however will

increase fuel compression work and thus reduce overall net efficiency) or by increasing the injector cross-sectional area (which requires some extra design work and thus would increase cost for the first units built). In our calculations we assumed a fuel pressure at least 50% higher than the combustor pressure.

Although special provisions may be needed to operate gas turbines on syngas, it is worth noting that a great deal of development work has been done and significant operating experience has been accumulated in coal-fired IGCC plants. For example, General Electric offers eight different gas turbines models, ranging from 10-300 MW, for use with syngas, including the two models evaluated here (www.gepower.com).

	6FA, 60 Hz						7FA, 60 Hz			
	conventional applications	Case DMEb	Case DMEc	Case FTa	Case FTc	Case MixOH	conventional applications	Case FTb		
fuel	natural gas	syngas	syngas	syngas	syngas	syngas	natural gas	syngas		
ambient conditions	ISO (15°C, 1 atm)	20°C, 1 atm					ISO (15°C, 1 atm)	20°C, 1atm		
air flow, kg/s	204.0	204.0	177.8	192.4	189.0	176.4	180.0	432.0	432.0	387.9
compressor outlet T, °C	n.a.	409	431	431	431	431	431	n.a.	402	420
fuel flow, kg/s	n.a.	4.43	32.2	25.5	29.0	39.9	14.9	n.a.	9.6	64.9
fuel LHV, MJ/kg	n.a.	48.91	6.95	8.60	7.61	5.95	8.80	n.a.	48.91	7.28
fuel mol weight, kg/Mol	n.a.	16.3	20.5	20.5	22.6	25.1	21.1	n.a.	16.3	21.5
exhaust flow, kg/s	n.a.	208.43	210.0	217.9	218.0	216.3	218.4	n.a.	441.6	452.8
pressure ratio	15.7	15.7	16.5	16.5	16.5	16.5	16.5	15.5	15.5	16.0
TIT, °C	n.a.	1,316	1,316	1,316	1,316	1,316	1,316	n.a.	1,316	1,316
TOT, °C	604	604	635	620	624	635	633	602	603	626
power output, MW	75.9	75.7	89.5	82.9	83.9	89.7	89.7	171.7	171.6	186.5
LHV efficiency, %	34.8	34.9	-	-	-	-	-	36.2	36.7	-
DP at compr. inlet, kPa	n.a.	0.0	1.0	1.0	1.0	1.0	1.0	n.a.	0.0	1.0
DP at turbine outlet, kPa	n.a.	0.0	4.0	4.0	4.0	4.0	4.0	n.a.	0.0	4.0
	GE data	our calculation					GE data	our calculation		

Tab. 7. Comparison between gas turbine performance published by General Electric and predictions with simulation software GS

4.7 HRSG and steam turbine

In the plant configurations with a gas turbine (all but DMEa), the gas turbine exhaust generates steam in a Heat Recovery Steam Generator (HRSG). The steam evaporation pressure and superheat temperature assumed here (130 bar and 540/565°C) correspond to the state-of-the-art of combined cycle systems and are more advanced than those adopted in the biomass boilers because the combustion products discharged by the gas turbine are much “cleaner” than those generated in the biomass boiler and do not raise severe erosion or corrosion issues. To take advantage of these more advanced steam conditions we’ve assumed that the existing steam turbine is replaced by a new machine designed for such admission conditions, as well as sized for the nominal flow of the new, integrated plant.

For DMEa, where steam is generated at more moderate conditions by recovering waste heat from the black liquor gasification island and the FSI, as well as by the existing hog fuel boilers; in this case we’ve assumed to maintain the existing steam turbine, which will have to be slightly modified (basically, introduce partial admission and modify the first few stages) to adapt it to the new operating conditions.

HRSG	
Evaporation pressure	130 bar (1870 psig)
Evaporation pressure in DME and FT reactors	38 bar (536 psig)
Evaporation pressure in MixOH reactor	130 bar (1870 psig)
Superheater $\Delta p/p$	10%
Superheater temperature (large scale GT)	565°C (1049°F)
Superheater temperature (medium scale GT)	540°C (1004°F)
Heat loss	0.7% of heat released by gas
Blow-down	1.14 kg/s
Deaerator pressure	4.8 bar (55 psig)
Condenser pressure (plants FTb and FTc)	0.074 bar (1.07 psia)

Tab. 8. Basic operating parameters for the HRSG and the steam cycle

At the scale of our power islands, a combined cycle would normally feature at least two evaporation pressures in the HRSG. In our case however we've considered only one evaporation pressure at 130 bar because for our back-pressure cycle with massive steam extraction at relatively high pressure (13 bar) additional evaporation pressures would give negligible benefits.

The heat released by the exothermic fuel synthesis reactions is carried away by generating saturated steam. Such steam generation is crucial to maintain the reactor at constant temperature and ensure its proper operation and expected life. In the MixOH case we've assumed a reactor temperature of 350°C and thus steam can be generated at the same pressure of the HRSG drum (saturation temperature at 130 bar is 330.8°C). Instead, the DME and FT reactors work at 260°C and generate steam at 38 bar (saturation temperature 247.3°C). In these cases the HRSG provides saturated water to the fuel reactors, and the saturated steam generated there goes back to the HRSG to be superheated. After being superheated, this medium-pressure steam is admitted to the steam turbine through a secondary port. The optimal superheat temperature of the medium-pressure steam admitted to the steam turbine is approximately equal to that of the mainstream flow at the secondary admission port, i.e. the value that minimizes the irreversibilities of mixing between the mainstream flow and the additional flow admitted at medium pressure. In our DME and FT cases we've assumed a superheat temperature of 370-400°C, very near to the optimum value that maximizes the electrical efficiency.

Steam reheat has not been considered because at the scale of our power islands and given the large amount of steam extracted for the mill it would be economically questionable.

Tab. 8 summarizes the design parameters assumed for the HRSG. In plants FTb and FTc the steam recovered using the gas turbine exhaust heat, the gasification island heat, and the FSI heat is more than the amount needed by the mill, and thus the steam turbine includes a low pressure section that expands the steam down to 0.074 bar (condensation temperature 40°C). In all other cases the steam turbine is back pressure and steam production is adjusted (by changing the biomass input to the biomass boilers or the biomass gasifier) to match the mill demand.

4.8 Heat integration

Given the large amounts of waste heat made available by syngas cooling, syngas clean-up and fuel synthesis, a proper integration ensuring the best use of such heat is crucial to the achievement of superior performances. A good match between the processes that generate heat and those that require heat can also reduce costs and refrigeration requirements; this is particularly true for the Rectisol system, which requires a refrigeration plant of considerable size

(several MW_{ref}) to cool the syngas much below ambient temperature. The design of heat transfer processes is also crucial to the achievement of proper operating conditions of key components: in the syngas coolers, the generation of steam gives the high heat transfer coefficients needed to maintain acceptable metal temperatures; in the fuel synthesis reactor, steam generation is essential to prevent catalyst overheating and achieve high conversion efficiencies.

The heat released by high temperature syngas streams from the black liquor gasifier and the biomass gasifier are cooled to generate HP steam for the power island and the mill. Whenever possible, the heat made available at medium or low temperature is used to preheat make-up water. This is particularly relevant for the plants with a large biomass gasifier, where the biomass dryer placed ahead of the gasifier and fed with the HRSG exhausts requires a large thermal input. Higher thermal inputs to the dryer are provided by increasing the temperature of the gas at the outlet of the HRSG, which therefore exhibits a deficit of the low-temperature heat needed to pre-heat the water.

Despite the efforts to optimize the heat exchanger network, some low temperature heat must be rejected to the environment and requires a cooling medium. We've assumed that enough cooling water is available at the plant to bring the temperature of the streams to be cooled down to 35°C. This is particularly relevant for the Rectisol system, where to limit the refrigeration power it is important that the syngas be cooled to the lowest possible temperature prior to its input into the refrigeration plant. Without adequate amounts of cooling water, net electricity production can be significantly lower than reported here, with somewhat higher capital costs.

To minimize irreversibilities and thus maximize efficiency, we've assumed that heat is transferred across relatively small temperature differences: minimum temperature difference 10°C for gas-liquid heat transfer; minimum temperature difference ~ 15°C for gas-gas heat transfer. In an actual situation these temperature differences are subject to economic optimization, to determine the best trade-off between efficiency and capital costs.

Heat exchangers operating at medium or low temperature are assumed to incur negligible heat losses, whereas for the HRSG we've assumed a heat loss of 0.7% of the heat transferred (Tab. 8). For the syngas cooler of the biomass gasifier, which handles gas between 950°C and 450-500°C, we've assumed a heat loss of 2% of heat transferred.

4.9 Oxygen production

95% pure oxygen (with 3.65% Ar and 1.35% N₂) is supplied to the oxygen-blown gasifiers by a stand-alone, conventional cryogenic Air Separation Unit (ASU) which generates oxygen at atmospheric pressure. Compression up to gasification pressure (36 bar) is carried out by an intercooled oxygen compressor. Some performance improvement may be gained by integrating the ASU with the power plant, which however should be carefully weighed against the implications and the unknowns of the added complexity of the plant and the start-up and shut-down procedures. We assume a non-integrated ASU in our designs.

The oxygen consumption of the gasifiers is determined by the composition, moisture content and heating value of the material to be gasified, as well as by the temperature to be reached (in our case, 1000°C for the black liquor gasifier, 950°C for the biomass gasifier). The BL gasifier oxygen requirement – as well as the whole heat/mass balances – is very sensitive to the Oxygen/Carbon ratio in the dry BL solids. Given the uncertainties about the actual composition of black liquor under polysulfide operating conditions, further work is needed to get reliable estimates of dry solids composition and properties at the conditions at which a mill would operate when integrated with a BL gasification system.

With gasification, the load of the lime kiln increases as a consequence of different smelt composition and a different breakdown between the sulfur that goes in the gas and in the smelt. Since the load increase is limited, we've assumed that it can be accommodated by firing the kiln with oxygen enriched air. A small increase in the size of the Air Separation Unit provides a low-cost source of oxygen for this purpose. The ASU size is further increased a little to also provide oxygen for the O₂ delignification unit existing at the mill. (See additional discussion on this topic in Volume 1.)

In the configurations with a biomass gasifier, the ASU also provides the nitrogen required by the biomass lock-hoppers.

4.10 Lime Kiln

Because of an increase of sodium carbonate leaving the gasifier in the condensed phase, black liquor gasification requires a higher causticization load compared to processing in a Tomlinson boiler. The higher causticization load requires a higher lime kiln capacity and higher lime kiln fuel consumption per unit of black liquor solids processed.

In the previous BLGCC study [Larson, Consonni and Katofsky, 2003] we've estimated a 16% increase in lime kiln load based on the assumption that the ratio of Active Alkali in the pulping liquor to the wood feed to the digester for the polysulfide process is the same of the conventional process utilizing Tomlinson recovery boilers. This assumption must be verified based on a more careful estimate of the heat/mass balances of polysulfide pulping. It is worth noting that, due to the higher yield of the polysulfide process assumed with gasification, the increase in kiln load (kW or kg/s of fuel oil) is significantly smaller than the increase in specific lime requirements (t of lime per t of BLS), which is 28%.

Given the relatively modest increase in the capacity required for the lime kiln, it is assumed that the extra capacity needed is met by oxygen-enrichment of combustion air.

4.11 Sulfur Recovery system

The H₂S in the gas phase at the exit of the BL gasifier must be removed both to recover the sulfur for the pulp mill and to prevent damages to the equipment downstream. Sulfur compounds and other contaminants can poison the catalysts used for fuel synthesis, as well as corrode the gas turbine and the heat transfer equipment.

The removal of H₂S and other contaminants can be carried out by a number of technologies based on chemical or physical absorption. The latter is favored by high pressures and low temperatures, which increase the solubility of the species to be captured into the liquid solvent used to carry them away. Unlike chemical absorption, physical absorption does not require large amounts of heat to regenerate the solvent; on the other hand, it requires high partial pressure of the gases to be removed. In our schemes gas clean-up is carried out at pressures between 32 and 105 bar; this situation is favorable for physical absorption, which therefore has been assumed in all cases.

Specifically, we've considered two of the most widespread commercial physical absorption processes that have accumulated significant operating experience with syngas treatment: Rectisol and Selexol. The former makes use of methanol as the solvent and operates at cryogenic temperatures (from -25°C to -60°C or even lower); the latter makes use of dimethyl ether of polyethylene glycol and typically operates at nearly ambient temperature (20-30°C). Rectisol can reduce the concentration of H₂S to much lower levels than Selexol; however, its much lower operating temperatures give higher power consumption and the complex plant arrangement results in higher capital costs.

The catalysts considered here for the production of DME and FT are very sensitive to sulfur poisoning and require very low concentrations of H₂S, of the order of 0.1 ppmv. Such a concentration is beyond reach for Selexol and necessarily requires Rectisol, which therefore has been assumed for all DME and FT cases. In addition to H₂S, Rectisol also captures most of the CO₂: without special provisions, up to 80% of the amount at inlet. This is a desirable feature because low CO₂ concentrations in the gas fed to the FSI improve its conversion to liquid fuel. The removal of all the CO₂ requires a more complex and thus more expensive design, which has been adopted only when the unconverted syngas is recycled (cases DMEa and DMEb), to avoid excessive CO₂ build-up in the recycle loop.

The catalysts considered for the production of mixed alcohols is a Mo-based sulfide that can tolerate H₂S concentration three orders of magnitude higher, around 100 ppmv; some H₂S is actually needed in the gas to make up for the sulfur inevitably lost by the catalyst. This circumstance suggests Selexol as a more suitable process for the MixOH case, and this is the option we have used.

4.11.1 Rectisol system

Given the significant consumption of utilities (especially refrigeration power, which translates to electric power requirements), the Rectisol system has been modeled in detail with Aspen Plus to quantify the requirements of refrigeration power, steam and electricity with an accuracy comparable to the estimates for the other major subsystems. The model, the configurations and the results generated with Aspen Plus are illustrated in detail in Appendix C. Although this model cannot provide detailed design information, it is helpful to define the plant configuration, choose the most suitable operating conditions and estimate the mass and heat balances.

The base configuration has been set up to achieve a concentration of H₂S + COS below 1 ppm and a concentration of CO₂ below 1% by volume. As reported in Tab. 9, the acid gases removed from the syngas are released in three streams:

- one containing essentially all the H₂S and COS removed from the syngas; the concentration of H₂S + COS in this stream is higher than 40% by vol., making it fully compatible with treatment in a Claus plant;
- one consisting mainly of CO₂ (more than 97% by volume) with no H₂S nor COS, which can be vented to the atmosphere or used in chemical industry.
- a tailgas with about 50% CO₂ and 50% N₂, also with no H₂S nor COS. This tailgas stream can be discharged to atmosphere. However, if some ppm of H₂S would still be present in this flow, a LO-CAT or other process can effectively remove trace H₂S.

The base configuration has been adopted for cases DMEa and DMEb, where the very high recycle rate in the FSI (97%) necessarily requires a thorough removal of the CO₂ to prevent its build-up in the recycle loop of the unconverted syngas. When the FSI is without unconverted syngas recycle, (as DMEc, FTa, FTb and FTc) the complete removal of CO₂ is unnecessary and the Rectisol plant can be significantly simplified to use only a single absorption column⁵. In this case the concentration of CO₂ in the clean syngas is about 5%, depending on the inlet raw syngas composition (Tab. 9).

⁵ Two columns are required for complete removal of CO₂.

		H ₂ S+CO ₂ total removal, BL syngas DMEa, DMEb	H ₂ S removal, BL syngas DMEc, FTa, FTb	H ₂ S removal, BL+biomass syngas FTc
Clean gas				
H ₂ S+CO ₂ content	ppm vol	< 0.1 (a)	< 0.1 (a)	< 0.1 (a)
CO ₂ content	% vol	< 1 (a)	6	5
CO₂-concentrated gas				
CO ₂ content	% vol	98	98	99
H ₂ S+CO ₂ content	% vol	none (a)	none (a)	none (a)
Tailgas				
CO ₂ content	% vol	50	32	38
N ₂ content	% vol	49	68	62
H ₂ S+CO ₂ content	% vol	none (a)	none (a)	none (a)
Acid gas stream (feed to Claus/SCOT plant)				
H ₂ S+CO ₂ content	% vol	44	41	13
CO ₂	% vol	53	56	84
Duties				
Heat	MWt	4	4	10
Refrigeration	MWref	6.8	5 - 6.6 (b)	16.0
Power consumption				
Refrigeration system	MWel	2.1	2 - 2.1 (b)	5.1
Other auxiliaries	MWel	1.0	0.96	2.6

(a) Values adopted as specifications for the Rectisol system.

(b) Values depending on inlet raw gas temperature.

Tab. 9. Main operating conditions of Rectisol system

4.11.2 Selexol system

Selexol is a proprietary technology licensed by UOP where the gas to be treated is contacted with dimethyl ether of polyethylene glycol at nearly ambient temperatures. The concentration of H₂S + COS can be brought down to around 10 ppmv, a value that is too high for the DME and FT catalysts but is acceptable for the MoS₂ catalyst assumed for MixOH synthesis.

In the arrangement with unconverted gas recycle assumed for the MixOH synthesis island it is convenient to operate the Selexol absorber and the mixed alcohol reactor at the same pressure to avoid the need to expand and recompress the recycle gas. Typical pressures in Selexol absorbers are 30-70 bar; higher pressures would favor the absorption of acid gases and most likely improve performances, but are beyond the experience gained by the licensor of the technology. Alcohol synthesis is favored by high pressures and a desirable value for the mixed alcohol reactor is 135-140 bar. In our case we have assumed that both the Selexol absorber and the mixed alcohol reactor operate at about 100 bar, which appears to be a reasonable compromise between the need to favor alcohol synthesis and the extensions of operating parameters that could be accepted by the supplier of a Selexol plant.

The Selexol system has not been modeled in detail. Estimates of performance and utilities consumption have been supplied directly by UOP (Tab. 10). These estimates have been used as inputs for the calculation of the overall performance of the whole biorefinery plant by GS.

Selexol Design Information	
Feed gas gas:	
Temperature	45°C
Pressure	104.5 bar
Mass flow	36 kg/s
H ₂ S content	1.2% vol
CO ₂ content	20% vol
Clean gas:	
Temperature	25°C
Pressure	104 bar
H ₂ S content	30 ppm vol
CO ₂ content	18%
Acid gas stream (feed to Claus/SCOT plant):	
Temperature	35°C
Pressure	1.9 bar
Mass flow	3.7 kg/s
H ₂ S content	24% vol
CO ₂ content	70% vol

Tab. 10. Main flows characteristics of the Selexol system

4.11.3 Claus/SCOT unit

The acid gas flow from the Rectisol process is treated in a Claus plant where H₂S is converted into elemental sulfur. This sulfur is dissolved into a low-sulfidity white liquor (containing the Na₂S formed in the gasifier smelt) to regenerate the polysulfide pulping liquor.

The Claus plant generates MP (13 bar) and LP (4.8 bar) steam, which is exported to the MP and LP headers that feed the mill. The amount of steam generated is assumed to be proportional to the amount of H₂S converted to elemental sulfur. The tail gas of the Claus plant is treated in a SCOT unit, which requires IP steam (6.5 bar) to regenerate the solvent used to absorb SO₂. The assumptions adopted for the Claus/SCOT unit are reported in Tab. 11.

The single components of the Claus/SCOT plant have not been modeled in detail. Power consumption, steam production and steam consumption (Tab. 11) are estimated base on data taken from [Larson, Consonni and Katofsky, 2003] and from Nexant [S. Kramer, personal communication, June 2006] for the whole Sulfur Recovery Unit (SRU).

In the FTc case the concentration of H₂S in the gas sent to the Claus plant is below 15% and the attainment of the temperatures needed by the Claus process may require a non conventional arrangement, for example with some pre-heating of the gas to be burned in the furnace.

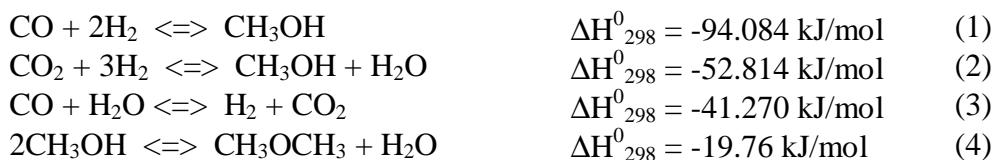
Claus/SCOT steam	
IP steam to SCOT plant	6.5 bar (80 psig) 2.4 kg/kg H ₂ S captured
MP steam from Claus plant to mill	13 bar (175 psig) 3.3 kg/kg H ₂ S captured
LP steam from Claus plant to mill	4.8 bar (55 psig) 1.8 kg/kg H ₂ S captured

Tab. 11. Assumptions adopted in this study for production and consumption of steam

4.12 DME synthesis

4.12.1 DME synthesis kinetics model

The direct synthesis of DME from syngas assumed in our FSI takes place in two steps: methanol synthesis and in situ methanol dehydration. The process comprises the following reactions:



Reactions (1)-(3) are catalyzed by a methanol synthesis catalyst (e.g. CuO/ZnO/Al₂O₃) and reaction (4) is catalyzed by an acidic catalyst (e.g. γ -aluminum). Reactions (1) to (4) show a high degree of synergy provided that the operation conditions are optimized enough to remove methanol effectively. Water formed in reactions (1) and (2) is removed via the water gas shift (WGS) reaction (3) to produce hydrogen which kinetically favors the production of methanol.

The low H₂/CO ratio (0.5-1) of the syngas derived from coal or biomass makes it well suited to a Continuous Stirred Tank Reactor (CSTR) configuration. This is the case of the Liquid Phase process (LPDME), where the synthesis reaction takes place in a slurry of inert oil and liquid reaction products with powdered catalyst-laden particles. This working condition provides good mixing and an effective means to carry away heat. Based on this advantage, LPDME has been selected as the DME synthesis technology.

It was decided to base the analysis and the simulation of the process taking place in the LPDME reactor on the model for methanol synthesis proposed by Graaf [Graaf et al. 1988, Graaf et al. 1896], based on an extensive set of accurate kinetic experiments, and the methanol dehydration model developed by Ng et al. [1999]. The model we use was originally developed by Larson and Ren [2003] and further modified by Celik, et al. [2004].

The main assumptions of the kinetic model are the following:

- the slurry is thermally stable and chemically inert;
- the particles carrying the catalyst are small enough to allow neglecting internal diffusion;
- mass transfer is fast enough to make liquid-phase diffusion of negligible relevance;
- the catalyst is uniformly distributed across the reactor;
- the heat generated by the synthesis reactions is carried away fast enough to make the reactor isothermal;
- the methanol synthesis reaction is catalyzed only by CuO/ZnO/Al₂O₃; the dehydration reaction is catalyzed only by γ - alumina;

- g) by-products are ignored; the only species involved are CO, CO₂, H₂, H₂O, CH₄O, DME, CH₄, N₂ and Ar.

Under stirred conditions the LPDME process can be treated as a CSTR and modeled by the Aspen block RCSTR. The kinetic mechanism with the characteristics listed above is supplied to Aspen in the form of a user-defined kinetic model. Tab. 12 reports the input of this user-defined model adopted for this study. See Appendix A for further details about the kinetic model assumed for the DME synthesis.

	Block Input parameters
<i>Reaction temperature</i>	260°C
<i>Reaction pressure</i>	62.5 bar
<i>Real variables</i>	
<i>No.1</i>	Catalyst A loading for methanol synthesis reaction
<i>No.2</i>	GHSV (gas hourly space velocity)
<i>No.3</i>	Catalyst B loading for methanol dehydration reaction
<i>No.4</i>	Ratio of catalyst B/ catalyst A

Tab. 12. Parameter inputs required for the Aspen RCSTR block used to model the DME reactor

4.12.2 DME reactor

DME can be synthesized by two types of reactors: fixed bed and slurry bed. As already mentioned, in this project we focus on the slurry bed reactor, where the syngas is bubbled through a slurry of high-boiling inert oil and suspended powdered catalyst particles. The reason of this choice is two-fold:

CO conversion and power co-production

The CO conversion ratios achievable in a single pass through the synthesis reactor can vary within a wide range. Low one-pass yields require the recycle of large amounts of unconverted gas to achieve acceptable CO conversion ratios and liquid fuel production. The nearly isothermal conditions and the effective gas-liquid-solid heat/mass transfer of the LPDME allows reaching DME molar fractions in the reactor output gas of the order of 5%⁶. Such one-pass performance is inadequate for a plant aimed at producing just DME; however, in our co-production schemes unconverted syngas is effectively used to produce power, so that moderate CO conversion ratios can still be attractive. In fact, the basic goal of a co-production system is achieving the most favorable breakdown of useful outputs (in our case fuel, power and heat), rather than maximizing a single product. In addition to higher energy utilization efficiency and higher economic benefits, co-production may also bring about lower overall emissions.

Temperature control

The temperature within the DME reactor must be controlled accurately both to prevent hot spots that could damage the catalyst and because temperature increases would shift the exothermic reactions that form DME away from the products. The relatively high heat of

⁶ The heat generated by the exothermic synthesis reaction tends to increase temperature and thus to slow down the reaction. The high heat fluxes achievable in the slurry bed reactor help in maintaining nearly isothermal conditions and thus high reaction speeds. High mass transfer rates are desirable to prevent the build-up of products around the catalyst particles, which would also slow down the reaction by shifting chemical equilibrium towards the reactants.

reaction of DME synthesis (significantly higher than that of methanol) makes this issue particularly relevant.

The operating conditions of the slurry bed reactor are particularly favorable for effective temperature control. The reactant gas forms small bubbles which react and exchange heat as they rise through the slurry. The heat taken up by the slurry is released to tubes immersed into the reactor which carry a two-phase mixture of water and steam. The high overall heat transfer coefficients of the two-phase mixture inside the tubes and the liquid outside allows handling high fluxes, giving a compact and relatively inexpensive reactor design. An added, important benefit of good temperature control is the longer life of the catalyst.

4.12.3 Heat exchange design of DME synthesis section

The production of high purity DME requires both heat duties and cold duties. Heat is needed to heat the reactants of the DME reactor and the dehydration reactor, as well as for the reboilers of the distillation columns. Cooling is needed for the condensers of the distillation towers that separates light gases, DME, methanol and water. Besides, different streams (reactants, reactors effluents, etc.) must be heated or cooled to pre-determined temperatures.

To ensure the most efficient use of the energy available, the heat exchangers within the FSI have been arranged to match the heat duties and the cold duties as much as possible. Some cooling is provided by the expansion of an in-process stream at high pressure; the remainder by cooling water and a refrigeration plant.

4.13 *Fischer-Tropsch (FT) synthesis*

4.13.1 Kinetic model

The simplest kinetic models for Fischer-Tropsch synthesis are single- α models such as that proposed by Lox and Froment [1993], who assume fixed growth probability for all olefins (C_nH_{2n}) and paraffins (C_nH_{2n+2}). Fox and Tam [1995] present a triple- α model for FT synthesis, which can more accurately predict product distributions than single- α models. We have adopted a model, based on Fox and Tam's approach, that was developed by Larson et al. [2005]. With Fox and Tam's approach, the rate of olefin formation varies depending on the carbon number, and the paraffin formation rate is related to the olefin formation rate.

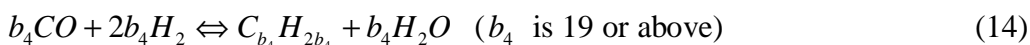
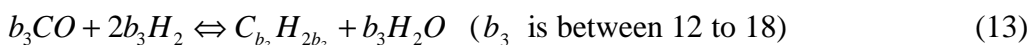
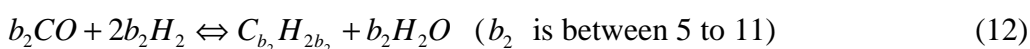
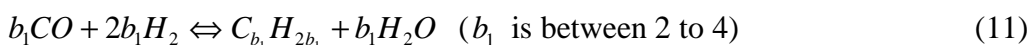
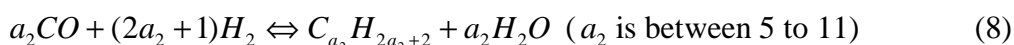
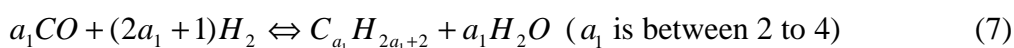
Our simulations assume a slurry bed reactor where an iron catalyst is dispersed in the FT wax product. The advantages of the slurry bed are the same already mentioned for DME, with the added benefit that for FT synthesis the CO conversion achievable with a single pass is extremely high: at the operating conditions considered here, the kinetic model of the FT reactor gives a CO conversion of nearly 65%. The main disadvantage is the complexity of catalyst separation from the FT waxes. Due to its WGS activity, the iron catalyst is particularly suited to the low H_2/CO syngas generated by the black liquor and biomass gasifiers.

The main assumptions adopted for the FT synthesis model are:

- the slurry is thermally stable and chemically inert,
- the particles carrying the catalyst are small enough to allow neglecting internal diffusion;
- mass transfer is fast enough to make liquid-phase diffusion of negligible relevance;
- the catalyst is uniformly distributed across the reactor;
- the heat generated by the synthesis reactions is carried away fast enough to make the reactor isothermal;

- Oxygenated by-products are ignored.
- FT components with two to four carbons (C2-C4) we lump together as light gases and represent as equivalent C4; C5-C11 are grouped as FT gasoline fraction and represented as equivalent C9. C12-C18 are grouped as FT diesel fraction and represented as equivalent C15 component. C19+ are grouped as FT wax fraction and represented as equivalent C21 pseudocomponent.

In addition to hydrocarbon reaction rates, there are also reaction rates to be considered for CO, H₂, CO₂ and H₂O. In this regard, our model considers the following reactions (see Appendix A for further details about the kinetic model assumed for FT synthesis):



4.13.2 FT reactor

Due to the high yields achievable with a single pass, in all cases we've considered a once-through arrangement. Like DME synthesis, under stirred conditions FT synthesis can also be treated as a CSTR and modeled by the Aspen block RCSTR. The kinetic mechanism is provided to Aspen in the form of a user-defined model. The input and output parameters for this user-defined kinetic model are reported in Tab. 13.

	Block Input parameters
<i>Reaction temperature</i>	260°C
<i>Reaction pressure</i>	30.7 bar
<i>Real variables</i>	
<i>No.1</i>	Catalyst loading for FT synthesis reaction
<i>No.2</i>	GHSV = 5800 liters/kgcata.h ⁷

Tab. 13. Assumptions adopted for the Aspen RCSTR block used to model the FT reactor

⁷ Liters are at normal temperature and pressure, i.e. at 20°C and 1,013 bar.

4.13.3 FT liquid product

The raw liquid product of the FT synthesis reactor is a mixture of distillate, naphtha and wax which needs further processing to upgrade it to gasoline and diesel fuel. Because of the complexity of this process and the small scale of our biorefinery (compared to refineries fed with fossil fuels), we've assumed that the raw liquid is exported to an existing petroleum refinery without further processing. The raw FT product must be kept warm in order to maintain the waxes as liquid, thus requiring trucks with heated tanks.

4.14 Mixed alcohols synthesis

4.14.1 Mixed alcohols synthesis kinetic model

Alcohols and other oxygenated liquids are viewed as desirable gasoline additives both to improve the octane number and to reduce engine emissions. Catalysts used for the production of higher alcohols from synthesis gas can be divided into four categories [Liu et al., 1997]:

- the first one is based on a soluble Ru complex used as an homogeneous catalyst;
- the second can be described as modified methanol catalysts, e.g. alkali-doped ZnO/chromia or Cu-based catalysts;
- the third comprises mixed-metal Fischer-Tropsch catalysts, e.g. Co and Fe on a support;
- the last comprises alkali-promoted MoS₂ catalysts.

Mo-based systems are promising due to their high tolerance to sulfur compounds in the feed gas, high WGS reaction activity, high activity and selectivity for linear alcohols. The last characteristic is very important, because the formation of hydrocarbons (α -olefins and n -paraffins) from CO and H₂ is thermodynamically favored with respect to the formation of higher alcohols, i.e. K_{eq} (the equilibrium constant) of hydrocarbons are higher than K_{eq} of alcohols; consequently, the synthesis of higher alcohols requires selective catalysts capable of finding a way around the tendency favoured by thermodynamics to drive the process toward alcohols.

Given the lack of any published models in the literature, for this study a new kinetic model has been developed to estimate CO conversion and alcohols formation over a Mo-based catalyst. The model has been developed at the Dept. of Chemistry of Politecnico di Milano by the group led by prof. P. Forzatti, who for many years has been at the forefront of research on heterogeneous catalytic processes (see Appendix B for a full description of the model developed by prof. Lietti and Tronconi). The kinetic model is based on the experimental data published by Gunturu et al. [1998] on the synthesis of methanol and higher alcohols from syngas by means of a C-supported, K-promoted Co-Mo sulfide catalyst (Mo-Co-K/C). The work of Gunturu et al. provides data on the whole set of reactions for higher alcohols synthesis, as well as rate expressions and estimates of kinetic parameters.

The kinetic model based on Gunturu's data has been implemented into a Fortran code, which has been subsequently embedded into the Aspen model of the plant section devoted to mixed alcohol synthesis. Similarly to the model for DME synthesis and FT synthesis, the model of mixed alcohol synthesis is executed by Aspen when calculating the mass and energy balance of the Fuel Synthesis Island.

The simplified reaction scheme adopted for the synthesis of higher alcohols is the following:





In this lumped reaction scheme, the production of methanol from CO and H₂ (reaction 15) is considered reversible and limited by chemical equilibrium. Further, it is assumed that all hydrocarbon products are produced from methanol and comprise only methane (reaction 16). The formation of ethanol (reaction 17) and the formation of propanol (reaction 18) proceed by reaction of CO and H₂ with methanol and with ethanol, respectively, according to a consecutive scheme. CO₂ formation is accounted for by the WGS reaction (reaction 19) which is assumed to be always at equilibrium.

Alcohols with carbon number higher than three (C₄₊ alcohols) are formed in quantities so small that they are irrelevant to the mass/energy balances and thus are neglected; in fact, C₄₊ carbon selectivity is less than 4% [Aden et al. 2005]. As for ethers (dimethyl ether, diethyl ether) and other oxygenates not explicitly identified as alcohols, they have been lumped into the hydrocarbon fraction, i.e. methane.

Since the experimental data reported by Gunturu refer to an inlet flow with no CO₂, in the kinetic model developed here CO₂ is assumed to behave as an inert and its influence on the reaction rates is due solely to the decrease of the partial pressure of the reactants. As long as the CO₂ concentration in the syngas is only a few percentage points, this assumption is most likely realistic. On the other hand, large concentrations of CO₂ could influence the kinetic characteristics of the catalyst and reduce its activity and/or its selectivity to higher alcohols. In the MixOH case considered here the concentration of CO₂ in the reactor inlet gas is about 30%, a value for which an impact on the catalyst behavior cannot be excluded. Consequently, the alcohols production calculated by our model may be optimistic and requires verification with further experimental data on conditions with high CO₂ concentration.

4.14.1.1 CO₂ removal in the recycle loop

The high CO₂ content in the syngas fed to the mixed alcohol reactor is due to the recycle loop, which returns to the reactor the by-product CO₂ generated by the alcohol synthesis. The CO₂ concentration at the reactor inlet could be drastically reduced by removing nearly all the CO₂ in the recycle flow by the same Selexol system that removes H₂S. This arrangement would be more expensive due not only to the larger mass flow through the Selexol (which would handle the recycled syngas together with the fresh syngas) but also to the more complex and costly arrangement of the Selexol plant required to remove both H₂S and CO₂. Moreover, the recycled stream includes a large amount of methane (a byproduct of the synthesis reactions) which would be captured in significant amounts in the column designed to capture the CO₂. Most of this methane would be subsequently released together with CO₂ in the flash chambers for Selexol regeneration and its effective recovery would be problematic. Since the penalties due to methane capture appear much more severe than those possibly due to lower catalyst activity, we've considered a scheme without thorough CO₂ removal from the syngas.

4.14.2 Mixed alcohols reactor

Similarly to the synthesis of DME and FT fuel, alcohol synthesis is also exothermic and the heat of reaction must be effectively removed to prevent temperature increases that may sinter and thus deactivate the catalyst.

Differently from what we assumed for DME and FT, for mixed alcohols we've assumed a fixed bed reactor because slurry technology for mixed alcohol synthesis is not commercially proven. In particular, the availability of a suitable inert liquid and the feasibility of an appropriate catalyst/liquid separation system are yet to be demonstrated. On the other hand, in a fixed bed reactor the arrangement of the evaporator tubes that carry away heat is particularly critical. Due to these factors, the best arrangement and the actual design of the mixed alcohol reactor need further investigation. Tab. 14 summarizes the main assumptions adopted for the mixed alcohol island.

<i>Clean syngas gas parameters</i>	H ₂ S molar fraction = 50 ppm
<i>Unconverted syngas recycle ratio</i>	90%
<i>Methanol recycle ratio</i>	100%
<i>Reactor</i>	Type: Fixed bed Reaction temperature = 350°C Pressure = 100 bar GHSV = 3000 liters/H.kgcata
<i>Molecular Sieve</i>	20% of ethanol and 97% of water are removed to purge gas

Tab. 14. Assumptions adopted for the Aspen block used to model the Mixed Alcohols reactor

5 PROCESS CONFIGURATIONS AND OPERATING CONDITIONS

5.1 Summary of technologies adopted for the major subsystems

Tab. 15 summarizes the technologies adopted for the major subsystems, as described in the previous chapters. The following paragraphs give a detailed description of the plant arrangement and the operating conditions calculated for each case.

		DMEa	DMEb	DMEc	FTa	FTb	FTc	MixOH
Technology for energy recovery from BL	Entrained-Flow Gasifier	X	X	X	X	X	X	X
	Quench	X	X	X	X	X	X	X
	Oxygen feed	X	X	X	X	X	X	X
Technology for energy recovery from biomass	Fluidized Bed Gasifier		X	X	X	X	X	X
	Syngas Cooler		X	X	X	X		
	Quench						X	X
	Oxygen feed		X	X	X	X	X	X
	Power Boilers	X						
Technology for Gas Clean-Up ahead of FSI	Rectisol	X	X	X	X	X	X	
	Selexol							X
Syngas treatment ahead of Gas Turbine	Ceramic Filter		X	X	X	X		
	Syngas Expander		X	X	X	X		
	Saturator						X	X
Technology for Fuel Synthesis	Feed from BL gasifier	X	X	X	X	X	X	X
	Feed from biomass gasifier						X	X
	Slurry Bed	X	X	X	X	X	X	
	Fixed Bed							X
	Unconverted Gas Recycle	X	X					X
Technology used to meet mill steam demand	Power Boilers	X						
	Duct Burner ahead of HRSG		X	X	X			X
	Backpressure Steam Turbine	X	X	X	X			X
Technology for Power Production	Condensing Steam Turbine					X	X	
	Medium-scale Gas Turbine		X	X	X		X	X
	Large-scale Gas Turbine					X		

Tab. 15. Technologies adopted for the major subsystems

5.2 Input to Fuel Synthesis Island

As shown in Tab. 15, in all cases the syngas generated in the black liquor gasifier is cooled, cleaned and then fed to the FSI. In schemes DMEa, DMEb, DMEc, FTa and FTb this syngas is the only input to the FSI. Instead, in schemes FTc and MixOH the FSI is fed by a mixture of the syngas generated by the BL gasifier and the syngas generated by the biomass gasifier.

5.2.1 Fuel synthesis fed with syngas from BLG

The process designs of cases DMEa, DMEb, DMEc, FTa and FTb are similar: the syngas generated by BL gasification is cooled and cleaned in the Rectisol system and then sent to fuel synthesis. Some of the mill steam demand is met by recovering waste heat from the biorefinery; the remainder is provided by the power island. We have considered two basic configurations:

In case DMEa, the mill steam demand is matched by burning hog fuel and purchased wood wastes in a boiler.

In the other cases (DMEb, DMEc, FTa, FTb), hog fuel and wood residuals feed a biomass gasifier that generates syngas that is burned in a gas turbine. The gas turbine exhaust gases raise steam in a heat recovery steam generator (HRSG) which feeds the steam turbine. The mill steam

demand is matched by adjusting the fuel input to a duct burner placed between the gas turbine and the HRSG; the only exception is case FTb, where the steam generated in the HRSG is more than enough to feed the mill and so no duct burner is needed. Both the gas turbine combustor and the duct burner are fed with a mixture of biomass syngas and unconverted syngas from the FSI. The amount of purchased wood wastes fed to the biomass gasifier (in addition to hog fuel) must be such that the biomass syngas plus unconverted syngas from the FSI are enough to fully fire the gas turbine and provide the required input to the duct burner.

In all cases the high pressure steam generated in the biomass boilers (case DMEa) or the HRSG expands through a steam turbine prior to being sent to the mill. In case FTb, the steam in excess of the mill demand expands through the LP section of the steam turbine.

5.2.2 Fuel synthesis fed with syngas from BLG and from biomass gasification

In cases FTc and MixOH the syngas generated by BL gasification and by biomass gasification are mixed together. The mixture is cleaned and sent to the FSI. Ahead of mixing, the biomass syngas is quenched to remove tar, particulates and alkali to very low levels. The unconverted syngas exiting the fuel synthesis island is used to fuel the GT. If needed, some unconverted syngas is also burned in a duct burner to match the mill steam demand.

The amount of purchased wood wastes sent to the biomass gasifier (in addition to hog fuel) is set to a value that gives enough unconverted syngas to fully fire the gas turbine and to feed the duct burner.

5.3 Design and basic features of major subsystems

5.3.1 BL gasification

Concentrated black liquor with a solid content of 80% is gasified in an entrained-flow oxygen-blow reactor at 32 bar pressure and at a temperature of about 1000°C. The black liquor is partially oxidized to produce a molten smelt of sodium and sulfur compounds, as well as a combustible gas consisting mainly of CO, CO₂ and H₂; the gas also includes part of the sulfur from the black liquor in the form of H₂S. The raw gas and the smelt droplets flow into the lower section of the gasifier vessel, where they are cooled by injection of the condensate coming from the downstream syngas cooler. The smelt dissolves in the quench liquid to form green liquor, which is sent to chemical recovery after being cooled by heating the condensate used for the quench. The smelt-free raw gas leaves the quench at 217°C and 35 bar and is subsequently cooled to about 120°C through a heat exchanger. The heat released by the syngas in the first sections of the heat exchanger generates MP and LP steam, while the heat released in the last section is used to heat feed water. Most of the water in the syngas condenses, thereby releasing most of the energy picked-up in the quench. Chemrec, the developer of the BL gasifier design modeled here, claims that the counter-current arrangement envisaged for the heat exchanger design to cool the syngas can remove alkali down to very low concentrations.

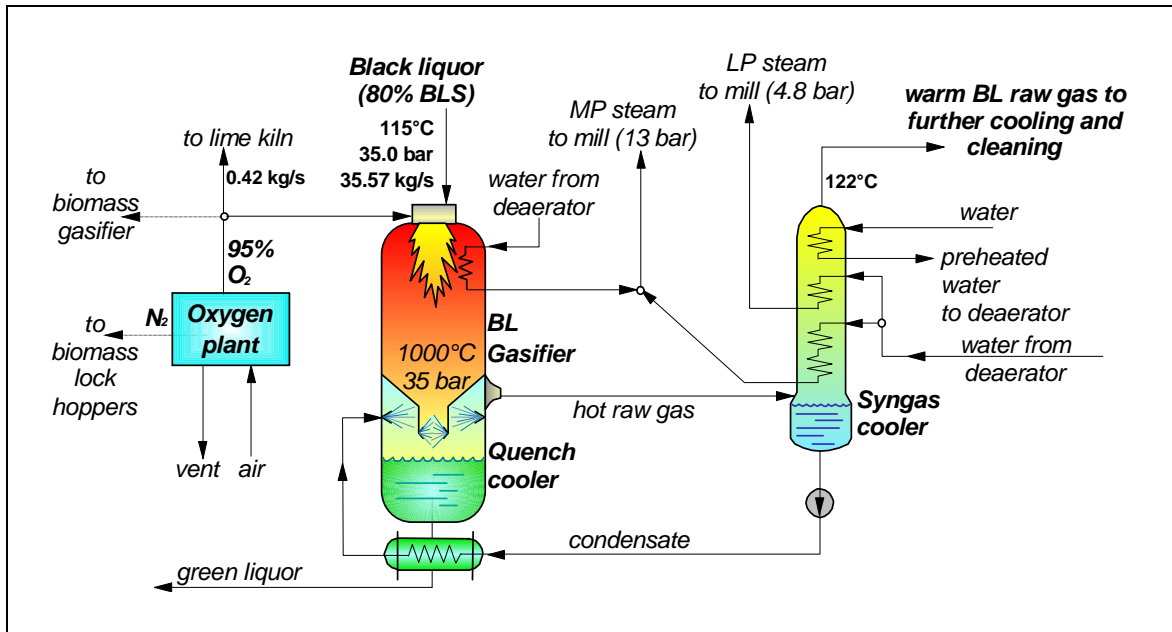


Fig. 5. Plant configuration for BL gasification

5.3.2 Biomass Gasification

Hog fuel and purchased wood wastes are chipped and dried from 50% to 20% moisture content using heat from the gas leaving the HRSG. The dried biomass is then pressurized in a lock-hopper system with inert gas and then fed to the fluidized-bed gasifier operating at 36 bar. N₂ from the ASU is used as inert gas for the lock-hoppers. An intercooled compressor pressurizes the nitrogen made available by the ASU at atmospheric pressure up to 37.7 bar.

Steam at 38 bar generated in the fuel synthesis reactor (except for MixOH, where steam is extracted from the steam turbine) is used to fluidize the bed. The gasifying agent is oxygen provided by the same ASU that supplies the BL gasifier. The syngas produced in the gasifier passes first through a cyclone to remove most of the solids, which are returned to the gasification vessel, and then in another reactor designed to crack the tar by means of a catalyst like nickel. The heat and mass balance of the gasifier have been calculated by assuming that the syngas composition at the cracker exit is at equilibrium except for methane and tar, for which we've imposed the concentration suggested by data found in the literature (as discussed earlier).

5.3.2.1 Biomass gasification with syngas cooler

In the configurations where the syngas generated in the biomass gasifier feeds the gas turbine, the gas exiting the cracker is cooled in a steam generator that feeds the same drum of the HRSG. The syngas at 495-420°C⁸ exiting the syngas cooler goes through a high-temperature candle filter and subsequently expands through a radial turbine to generate some electricity using the difference in pressure between the filter (approximately 34 bar) and the pressure assumed to be necessary for fuel injection into the gas turbine combustor (24 bar). Ahead of the gas turbine combustor, the syngas from biomass gasification is mixed with the unconverted syngas (from the

⁸ The syngas temperature at the outlet of the syngas cooler is such that the temperature of the flow fed to the gas turbine is 375°C, thereby avoiding tar condensation. The relatively large variation of the temperature at the outlet of the syngas cooler is due to the large variation, from one case to another, of the amount of relatively cold unconverted syngas added ahead of the gas turbine feed.

FSI) not needed by the duct burner. To avoid tar deposition, the syngas temperature at the exit of the syngas cooler is set to a value that ensures a syngas temperature above 375°C along the whole syngas line, i.e. a temperature of at least 375°C after mixing with the unconverted syngas from the FSI.

The amount of wood residues fed to the gasifier is adjusted to generate the amount of syngas needed to fully fire the gas turbine (together with the available fraction of unconverted syngas). Fig. 6 illustrates the design of biomass gasification system with syngas cooler.

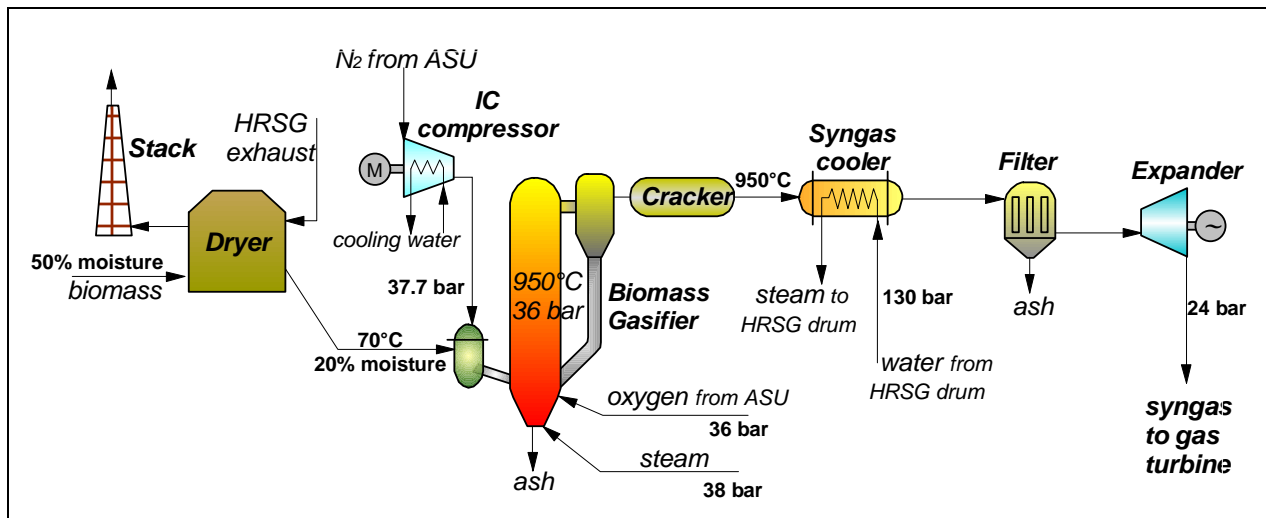


Fig. 6. Biomass gasification system with syngas cooler

5.3.2.2 Biomass gasification with quench

When the biomass syngas is sent to the FSI to produce liquid fuel the syngas exiting the cracker is quenched with water. The saturated syngas leaving the quench (at the saturated temperature of water at its outlet partial pressure, i.e. about 200°C) goes through a boiler and a water heater that recover the large amounts of heat released by water vapour condensation. The flow of condensate at about 120°C exiting these heat exchangers is recycled and used as quench water. The cool biomass syngas is mixed with the BL syngas at about the same temperature (to minimize mixing losses), and the whole flow is sent to the gas clean-up system (Rectisol or Selexol).

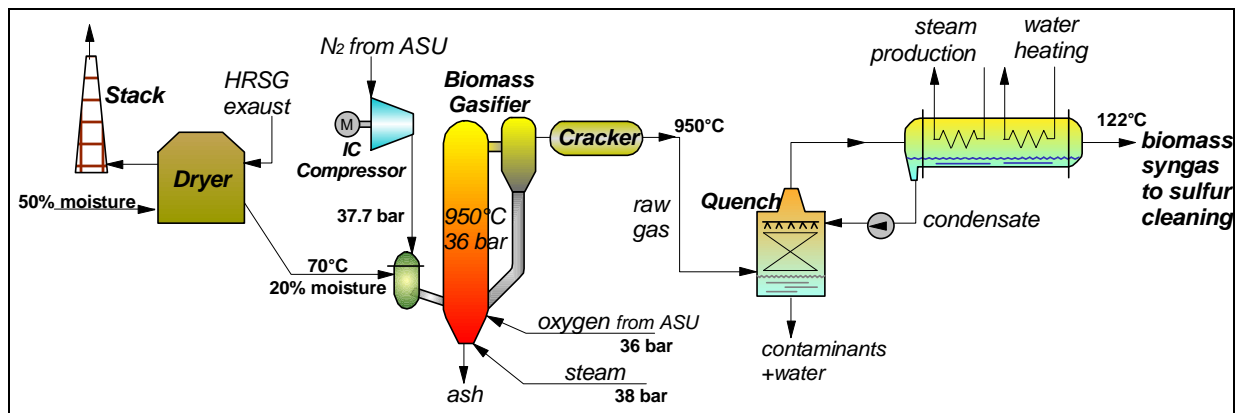


Fig. 7. Biomass gasification system with quench

reduce the solvent losses in the product gas. As the CO₂ absorption in polar solvents is a relatively highly exothermic process, the methanol solvent needs to be fed to the *absorber* column at a very low temperature (-60°C) in order to maintain a low operating temperature in the column.

With this configuration, the methanol fed at the top of the upper column is nearly pure, while the methanol used to scrub H₂S in the lower column is rich in CO₂. The liquid stream exiting at the bottom of the upper section is rich in CO₂ with nearly no H₂S, while the liquid collected at the bottom of the bottom section is rich in both acid gases H₂S and CO₂.

In addition to H₂S and CO₂, methanol may absorb significant fractions of possibly valuable gases. To avoid losing such gases, our scheme includes two flash drums (D2 and D3) at an intermediate pressure (7.5 bar) between the *Absorber* and the *Solvent Regenerator* pressure: the less soluble gas (such as CO, H₂, Ar,..) are re-transferred in the gas phase and recycled by compressing and mixing them with the raw syngas.

The process is composed of three other main blocks:

- *H₂S Concentrator (C2)*, where methanol rich in H₂S is concentrated at the bottom while CO₂, the more volatile compound, is obtained almost pure at the top.
- *CO₂ Stripper (C3)*, where the methanol stream rich in H₂S is contacted with nitrogen to strip another fraction of the CO₂ absorbed in the *Acid Gas Absorber*, which is transferred back to the gas phase; a mixture of N₂ and CO₂ is extracted at the top of the stripper.
- *Solvent Regenerator (C4)*, where the liquid from the bottom of the *CO₂ Stripper*, containing the H₂S absorbed in the *Acid Gas Absorber* and the remaining CO₂ is regenerated in the regeneration column via indirect heating with steam. Following cooling at low temperature to condense any methanol in the gas phase, the mixture of H₂S and CO₂ exiting the top of the column is routed to a Claus/SCOT unit.

The acid gas stream of H₂S and CO₂ goes first through a regenerative heat exchanger and then to a Claus/SCOT plant where H₂S is converted to elemental sulfur. According to the literature, with Rectisol the sulfur content in the CO₂ and tail gas flow is so low that they can be discharged into the atmosphere (or used in the process industry).

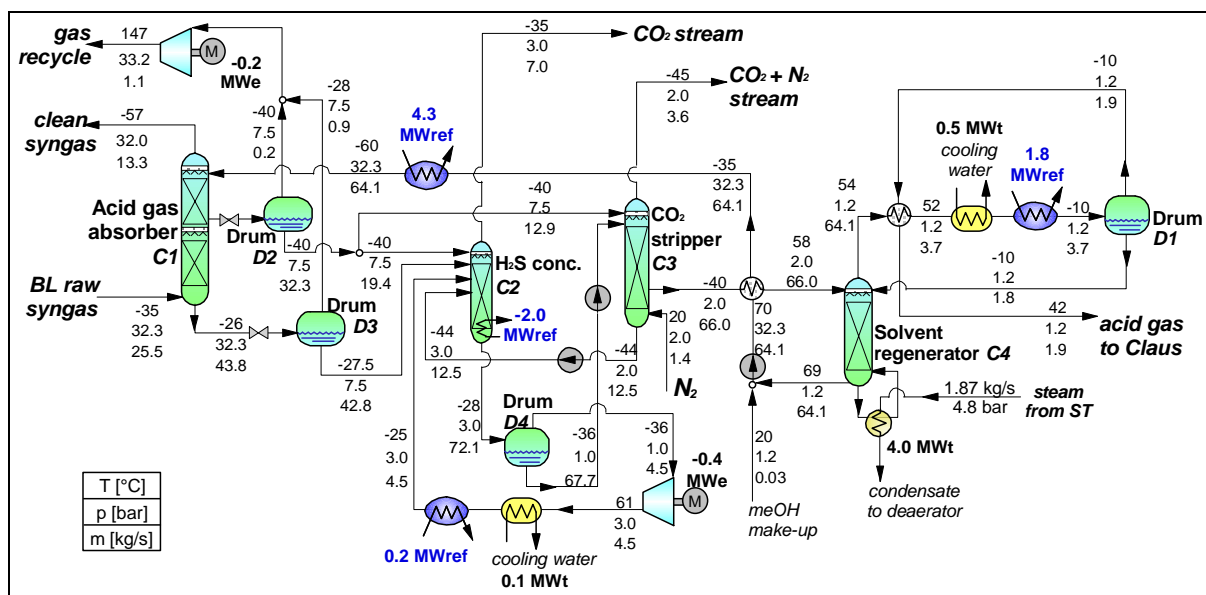


Fig. 9. Energy and mass balances for DMEa and DMEb cases of Rectisol model with H₂S and CO₂ abatement.

5.3.4.2 H₂S removal

The scheme developed for the removal of both H₂S and CO₂ was modified and adapted to the case where no specific target is set on CO₂ removal. In this case *Absorber (C1)* comprises only 1 column and the process scheme becomes the one shown in Fig. 10 and Fig. 11.

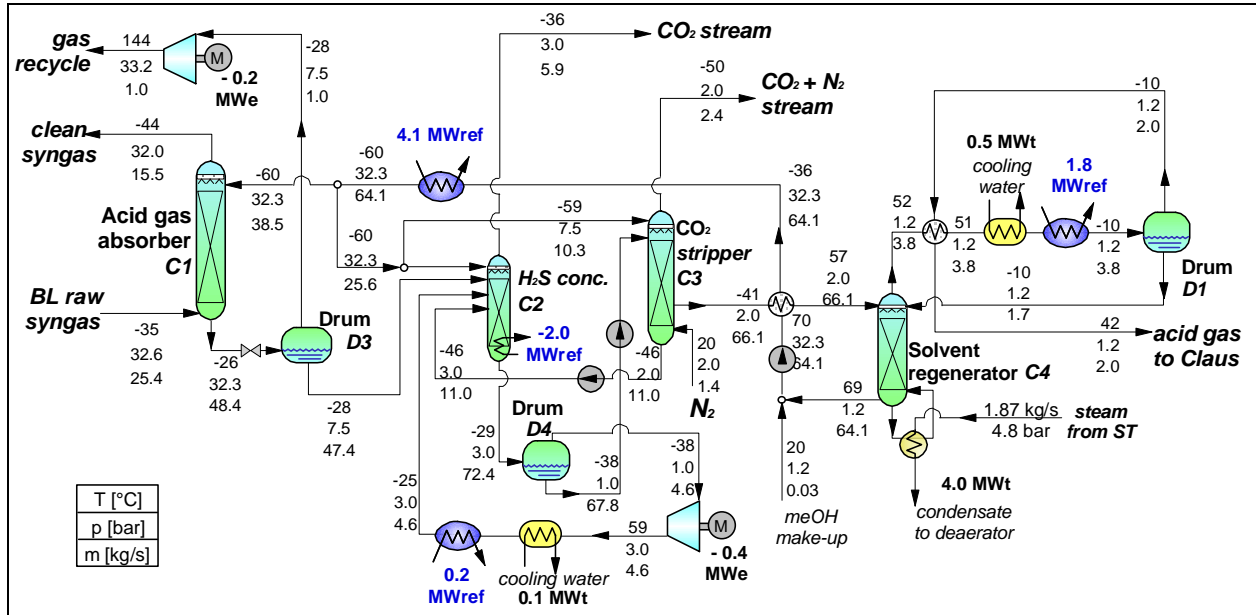


Fig. 10. Energy and mass balances of the Rectisol system adopted for cases DMEc, FTa and FTb, where H₂S is removed with no specific target on the removal of CO₂.

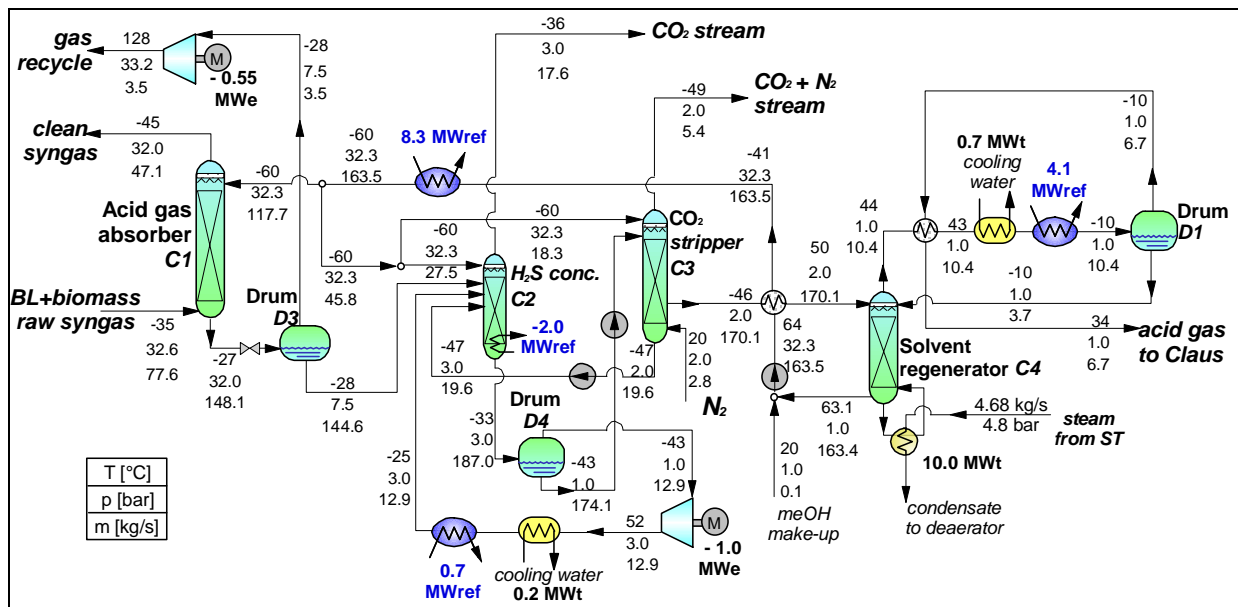


Fig. 11. Energy and mass balances of the Rectisol system adopted for case FTc, where H₂S is removed with no specific target on the removal of CO₂. The syngas entering absorber C1 is a mixture of the syngas coming from the BL and the biomass gasifier.

5.3.5 DME synthesis island

The clean BL syngas at 66 bar is heated to 240°C using the product stream from the synthesis reactor and then fed to the DME reactor. To maintain isothermal synthesis conditions at 260°C, steam is generated in boiler tubes immersed in the liquid reactor bed. In a single pass of gas through the DME reactor only a portion of CO and H₂ is converted to DME.

The mixture of gases leaving the reactor passes to the product separation area, where DME with high purity 99.8% is separated from methanol, unconverted syngas, and water. A series of flash tanks separate most of unconverted synthesis gas, then the separation is achieved by cryogenic distillation, cooling the gasses and separating based on boiling points. DME, methanol, and water all have boiling points higher than those of syngas components, so they are cooled and condensed, and then separated from each other. In this project, three columns are applied. The first is used to separate DME/methanol/water from CO₂ and other light gases (CO, H₂, etc.). The second is used to separate DME from methanol/water. The last one separates water from methanol.

The methanol flow is heated to 250°C, in a regenerative heat exchanger using steam, and then sent to an adiabatic reactor where DME is produced by methanol dehydration. A downstream flash tank separates the most volatile part of the product, including all DME produced, and this is sent to the second distillation column. The liquid fraction is recycled to the third distillation column.

Separating CO₂ and DME is difficult due to similar boiling points. Getting the last DME out of CO₂-laden gas is very difficult, and some small losses are tolerated.

The heat exchangers in the DME separation area are arranged in order to optimize heat integration by minimizing heat and refrigeration requirements. The net heat duty of the area is provided by steam from the power island.

The methanol separated out using the 2nd column can be recycled to the synthesis reactor inlet. However, we chose instead to separately dehydrate the methanol to DME for several reasons, including increasing the partial pressures of reactants, eliminating the recycle pump and additional heat exchangers, and other factors.

About the use of the unconverted gas, we have considered two plant configurations:

1. most of the unconverted gas (97%) from the separation area is returned, via compressor, to the synthesis reactor to generate additional DME (*recycle* configuration), the small remaining unconverted is sent to the power island (Fig. 12);
2. all the unconverted gas from the separation area goes to the power island (*once-through* configuration). In this case, the syngas passes only once through the synthesis reactor (Fig. 13).

5.3.6 FT synthesis island

The design configuration and main results of the FT synthesis island are illustrated in Fig. 14 and Fig. 15. The clean syngas is preheated and sent to the FT slurry-bed reactor using an iron-based catalyst. Two streams exit from the reactor at 260°C: a liquid reactor effluent stream, and an overhead vapor stream. The gas flow is used to preheat reactor inlet syngas to 245°C and heat purge gas or generate steam (depending on the case). These heat exchangers cool the stream to 38°C, then a gas-liquid separator is used to recover more FT products from the mixture and to separate a waste water stream. The gas flow exiting this separator is unconverted syngas that is sent to the power island. In FT synthesis island, the unconverted gas recycle design is not considered, because the single pass conversion is already relatively high.

A mixture of distillate, naphtha, and wax from the reactor, together with the liquid hydrocarbons recovered in the gas-liquid separator, constitute the liquid final product of FT synthesis.

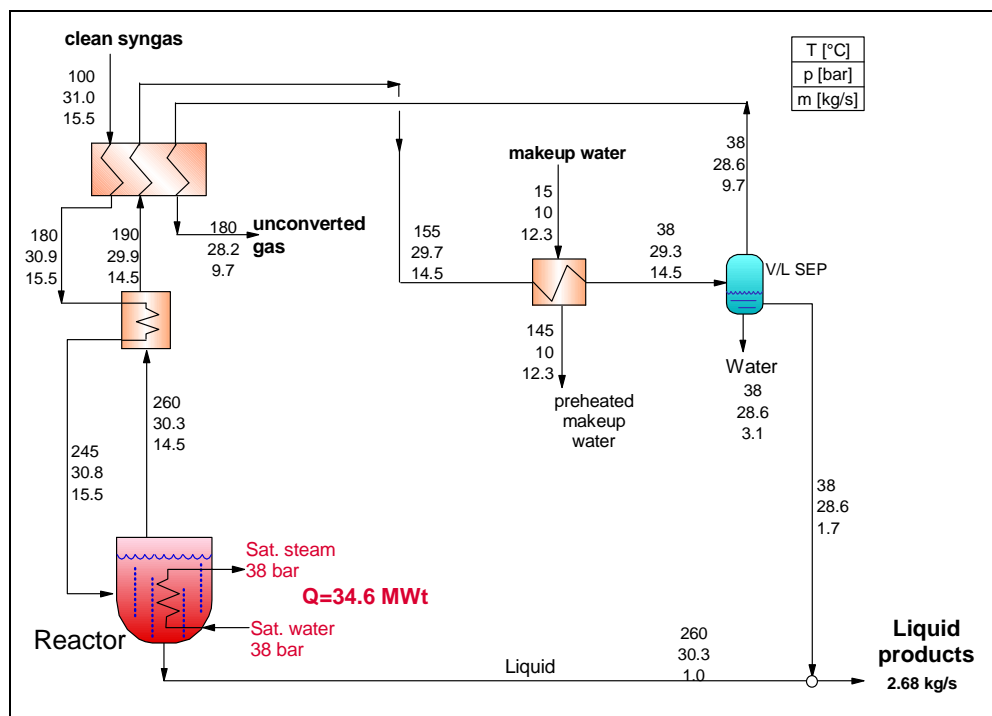


Fig. 14. Energy and mass balances of FT synthesis island for FTa and FTb cases (syngas from BL gasification)

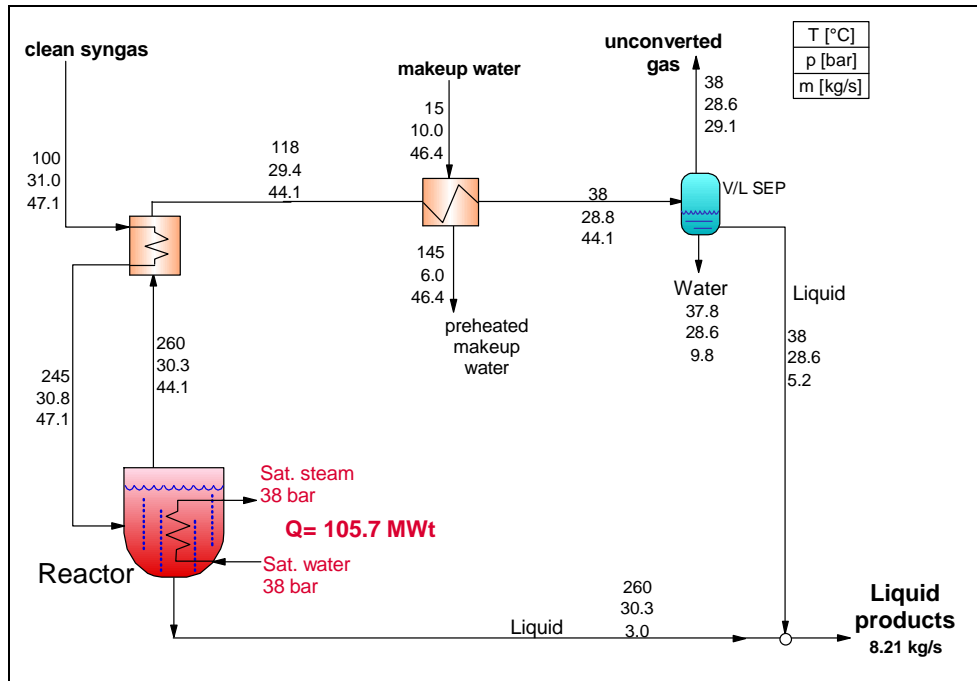


Fig. 15. Energy and mass balances of FT synthesis island for FTc cases (syngas from both BL and biomass gasification)

5.3.7 Mixed alcohols synthesis island

Fig. 16 show the design and the energy and mass balances of the Selexol system and mixed alcohols synthesis island.

The fresh clean syngas from the Selexol system is mixed with two recycle flows, then it is preheated to 330°C by cooling the outlet flow and is fed to the synthesis reactor. The heat released during reaction is used for HP steam raising, so as the reactor temperature is maintained at 350°C. After reaction, the hot effluent is cooled first by the reactor inlet flow and then by cooling water to 36°C. At this temperature the majority of alcohols condense, so the unconverted gas is separated from the liquid alcohols in a vapor/liquid separator. The gas stream is divided into two flows: part (76% of the unconverted syngas) is compressed and recycled back to the synthesis reactor. The remaining gas is preheated, expanded to about 25 bar for power production, humidified and finally used to fuel the GT.

The liquid flow, after a pressure drop to 3.5 bar via a valve, goes to a distillation column where methanol and other gases are separated, recompressed to the reactor operating pressure and recycled to the synthesis reactor. The flow from the bottom of the distillation column containing higher alcohols (C2+ alcohols) goes to a molecular sieve, where water is separated from the liquid alcohols. The purge gas from the molecular sieve, composed of water with a small percentage of alcohols, is compressed and sent to the gas turbine to recover the energy content and also to increase the mass flow of the fuel so as to increase power production.

The mixture with C2+ alcohol is treated as the final product of this section.

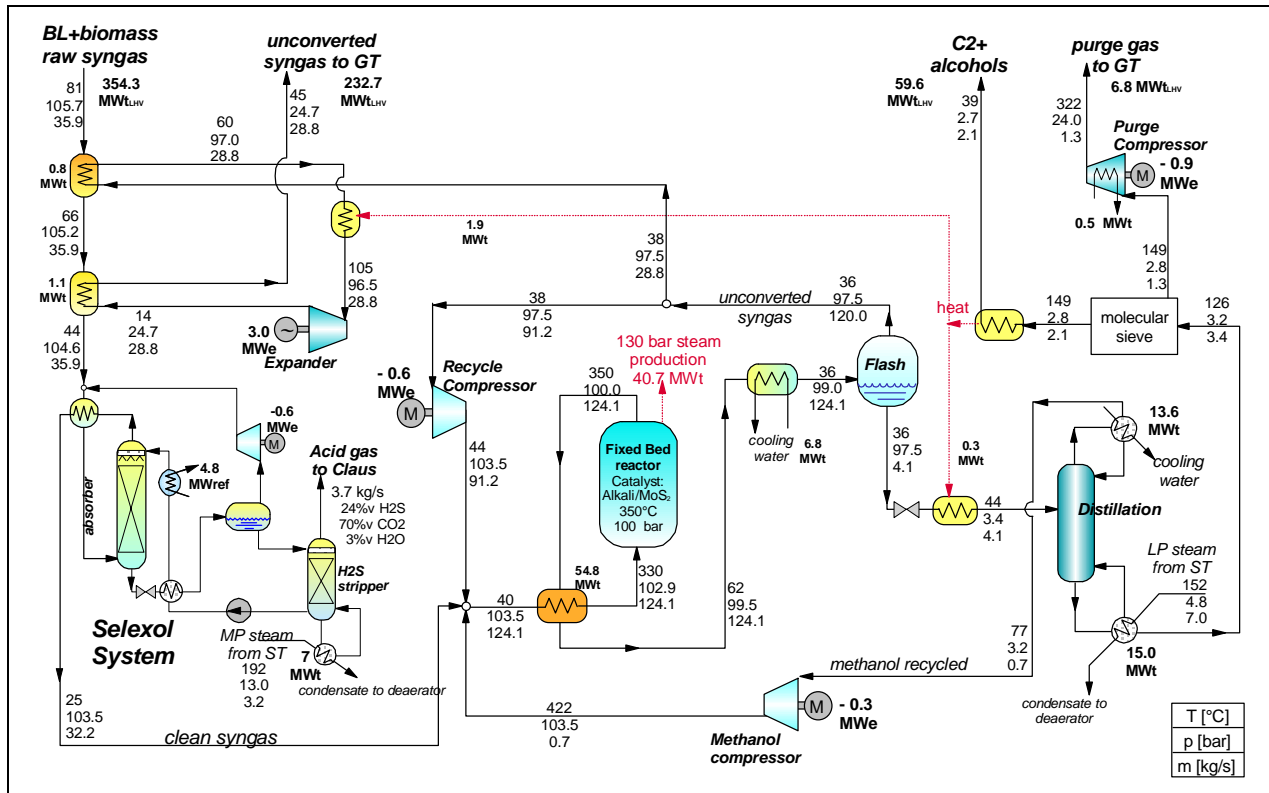


Fig. 16. Energy and mass balances of Selexol system and mixed alcohols synthesis island

5.4 DME cases

5.4.1 DMEa case: BLG with DME recycle island

In DMEa case (Fig. 18) the fuel synthesis island is designed to maximize the DME production: since in a single pass through the synthesis reactor only a portion of syngas is converted to the fuel, most of the unconverted syngas is recycled to the reactor to increase DME output. Because of the recycle of unconverted syngas, the Rectisol plant removes almost completely the CO₂ in the BL syngas, in addition to sulfur compounds.

The mill process steam is provided by burning in a boiler the hog fuel, the purge unconverted syngas and additional wood residues. The only electricity produced is from a back-pressure steam turbine through which steam is expanded before it goes to meet mill process demands.

5.4.1.1 BL syngas cooling

The BL is gasified and the syngas is quenched and cooled to 120°C, as described in par. 5.3.1 *BL gasification*. Then the syngas has to be cooled down to about -35°C, before entering the absorption column of the Rectisol plant. Since the cold clean syngas must be fed to the fuel synthesis reactor at high temperature (around 200°C), a regenerative heat exchanger is used to cool the raw syngas to about 120°C by heating to 100°C the clean syngas leaving the Rectisol process. The raw syngas is further cooled to 35°C through a water heater, in which make-up water is preheated, and then chilled to -35°C by a refrigeration system.

The clean syngas at the Rectisol plant outlet is compressed to the pressure required by the DME reactor (about 65 bar) before entering the regenerative heat exchanger and then sent to the DME synthesis island (described in par. 5.3.5 *DME synthesis island*). This compression is

carried out at low temperature, the Rectisol absorber exit temperature, so as to reduce compression power.

5.4.1.2 Power boiler and steam cycle

In DMEa, biomass is used in a boiler rather than being gasified. Hog fuel available as a by-product of the pulpwood feed to the mill (9% of the pulpwood logs), together with the purge gas from the DME synthesis island, is burned in a boiler. Additional wood wastes are purchased in order to generate enough steam to meet the mill demand.

The power boiler generates steam at 87.2 bar and 480°C. It also produces saturated water at 38 bar for the DME synthesis reactor cooling and superheats to 480°C the saturated steam coming back. These two steam flows expand through a back-pressure steam turbine with two main extractions. The first extraction at 13 bar provides the MP process steam for the mill and the second extraction at 6.5 bar supplies the IP steam to the SCOT unit. The balance of steam exhausts at 4.8 bar to provide the LP steam required by the mill. The

Fig. 17 shows the plant configuration for the biomass boiler and the steam cycle.

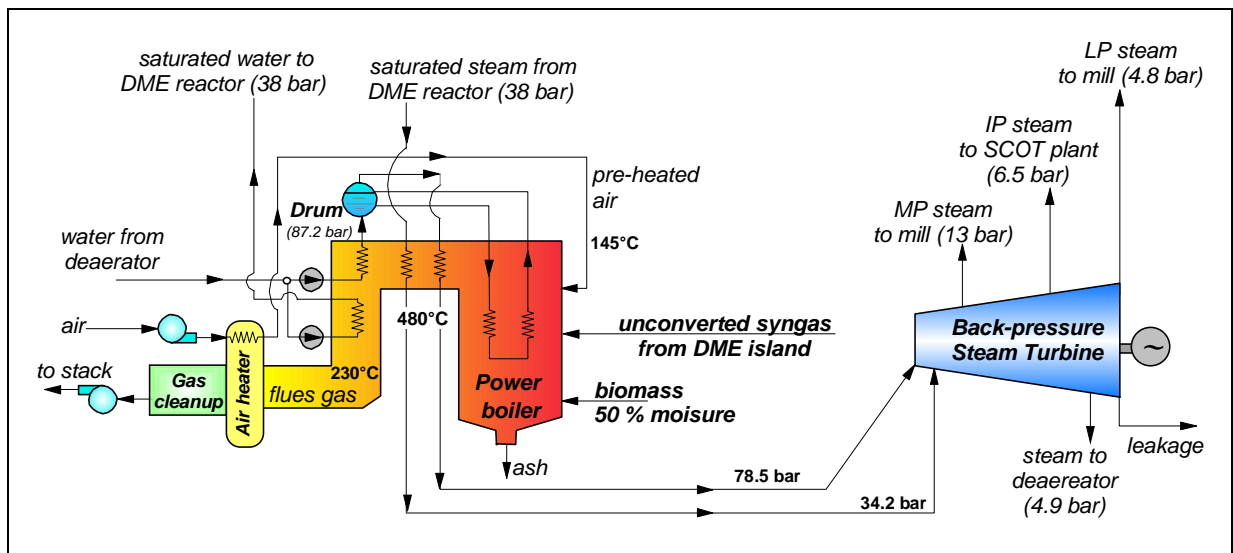


Fig. 17. Power island configuration for DMEa case

5.4.2 DMEb case: BLG and BGCC with DME recycle

In DMEb, as in DMEa, the syngas from black liquor gasification is cooled and cleaned in the Rectisol plant and sent to the DME synthesis island with unconverted gas recycle. This portion of the plant is identical to the one adopted for DMEa., The power island is different: the wood residuals are gasified, as described in par. 5.3.2.1 *Biomass gasification with syngas cooler*, and the produced syngas feeds a medium scale gas turbine (6FA). Part of the biomass syngas together with the unconverted syngas from the DME island, is sent to the duct burner. The steam generated in the HRSG by recovering heat from the gas turbine exhaust drives a back-pressure steam turbine and then is sent to the mill (Fig. 19).

The gas turbine enables more electricity production than in DMEa, and the combined cycle provides a significant amount of the power required by the mill, but the amount of purchased biomass increases compared to DMEa.

5.4.3 DMEc case: BLG and BGCC with DME once-through production

In DMEc, the syngas from black liquor gasification is used for making DME, as in the two other DME cases, but the syngas is passed only once through the synthesis reactor instead of recycling the unconverted syngas. DME production is reduced as a result. The configuration of BL syngas cooling and cleaning is similar to the other DME cases, except for the lower CO₂ removal requirement at the Rectisol plant: without the recycle loop in the synthesis island, total CO₂ abatement is not necessary.

The power island configuration is essentially the same as DMEb: it includes a biomass gasifier and a downstream combined cycle with a medium scale gas turbine (Fig. 20).

Without recycle, the unconverted syngas mass flow to the power island is higher. Part of this syngas is used to feed the duct burner, so that the HRSG produces enough steam to meet the mill process demands, and the remainder is sent to the gas turbine combustor. Because a significant amount of unconverted syngas goes to the gas turbine, the amount of biomass syngas required to fully fire the gas turbine is reduced compared to DMEb.

5.5 *FT cases*

5.5.1 FTa case: BLG with FT production and BGCC with medium GT

As in the DME cases, the black liquor is gasified and cooled, then all sulfur and a large amount of CO₂ are absorbed from the product syngas by a Rectisol system. Since all of our FT designs adopt a once-through synthesis configuration, total CO₂ capture at the Rectisol island is not required.

The FT synthesis reactor operates at about 31 bar. Unlike for the DME cases, a syngas compressor is not necessary before the FT island. The chilled clean syngas at the Rectisol absorption column exit is used to cool down the raw syngas, so as to reduce the duty of the refrigeration system upstream of the Rectisol absorption column. Then the clean syngas is heated to 100°C by cooling the raw BL syngas, as in the DME cases, and sent to the FT synthesis island. The unconverted syngas after synthesis is sent to the power island: part to the duct burner and the remainder to the gas turbine (Fig. 21).

The power section configuration, including a biomass gasifier with syngas cooler and a combined cycle with back-pressure steam turbine, is very similar to the DMEb and DMEc cases.

5.5.2 FTb case: BLG with FT production and BGCC with large GT

The FTb plant configuration (Fig. 22) is similar to the FTa design with one major difference: the gas turbine adopted is a large scale one (7FA). As a consequence a larger amount of exhaust gas is available from the gas turbine for steam production in the HSRG, and no duct burner is needed because the steam raised is more than the mill requires. The excess steam is expanded in a condensing section of the steam turbine to generate additional electricity.

5.5.3 FTc case: BLG and BG with FT production and CC with medium GT

In the FTc case (Fig. 23) BL syngas and biomass syngas are both used for fuel production: the raw BL syngas at 122°C is mixed with the syngas from biomass gasification, with the design

described in par. 5.3.2.2 *Biomass gasification with quench*, at the same temperature. The subsequent configuration of raw syngas cooling, cleaning in Rectisol plant and reheating is the same as in the other FT cases. Unlike the other FT cases, the gas turbine is fed only with unconverted syngas from the fuel synthesis island. It passes through a saturator, wherein it is humidified and pre-heated by mixing with water at 185°C. The saturator recovers low temperature heat and also leads to increased power production from the gas turbine because of the increase of syngas mass flow. Moreover, the humidified gas also results in a lower flame temperature in the gas turbine combustor, thereby reducing thermal NO_x emissions. In previous cases the syngas sent to the gas turbine doesn't pass through a saturator because the gas comes from a biomass gasification with syngas cooler; it already has a high temperature and a high water vapor content.

Using the biomass syngas to produce fuel, in addition to BL syngas, enables production of a larger amount of FT liquid. Also, more heat for steam raising is available in the synthesis reactor, so a duct burner is not necessary to raise sufficient steam to meet mill process demands. In fact, there is an excess of steam produced, so a condensing section in the steam turbine is used to recover a larger amount of electricity.

5.6 *MixOH case: BLG and BG with mixed alcohols production and CC with medium GT*

The configuration of the MixOH plant (Fig. 24) is similar to the FTc case design. The mixture of BL syngas and syngas from biomass gasification with quench design is cooled by preheating makeup water and compressed in an intercooled compressor to about 106 bar, the assumed operating pressure of the synthesis reactor. Then the raw syngas goes through heat exchangers that cool the gas to about 45°C before entering the Selexol system where most of H₂S and part of CO₂ are removed.

Following the Selexol acid gas removal system, the clean syngas is used as the feed for mixed alcohols synthesis. The unconverted syngas leaving the mixed alcohols synthesis island (described in 5.3.7 *Mixed alcohols synthesis island*) is humidified in a saturator, mixed with the purge gas from the alcohols separation area and burned in the gas turbine. Steam required by the mill and by the biorefinery plant (Selexol process, biomass gasifier, SCOT plant, alcohol distillation, etc.) is provided by the HRSG, integrated with the synthesis reactor steam generation. Since heat recovered from the gas turbine exhaust is not sufficient to raise all required process steam, additional syngas from biomass gasification is burned in a duct burner to increase steam generation.

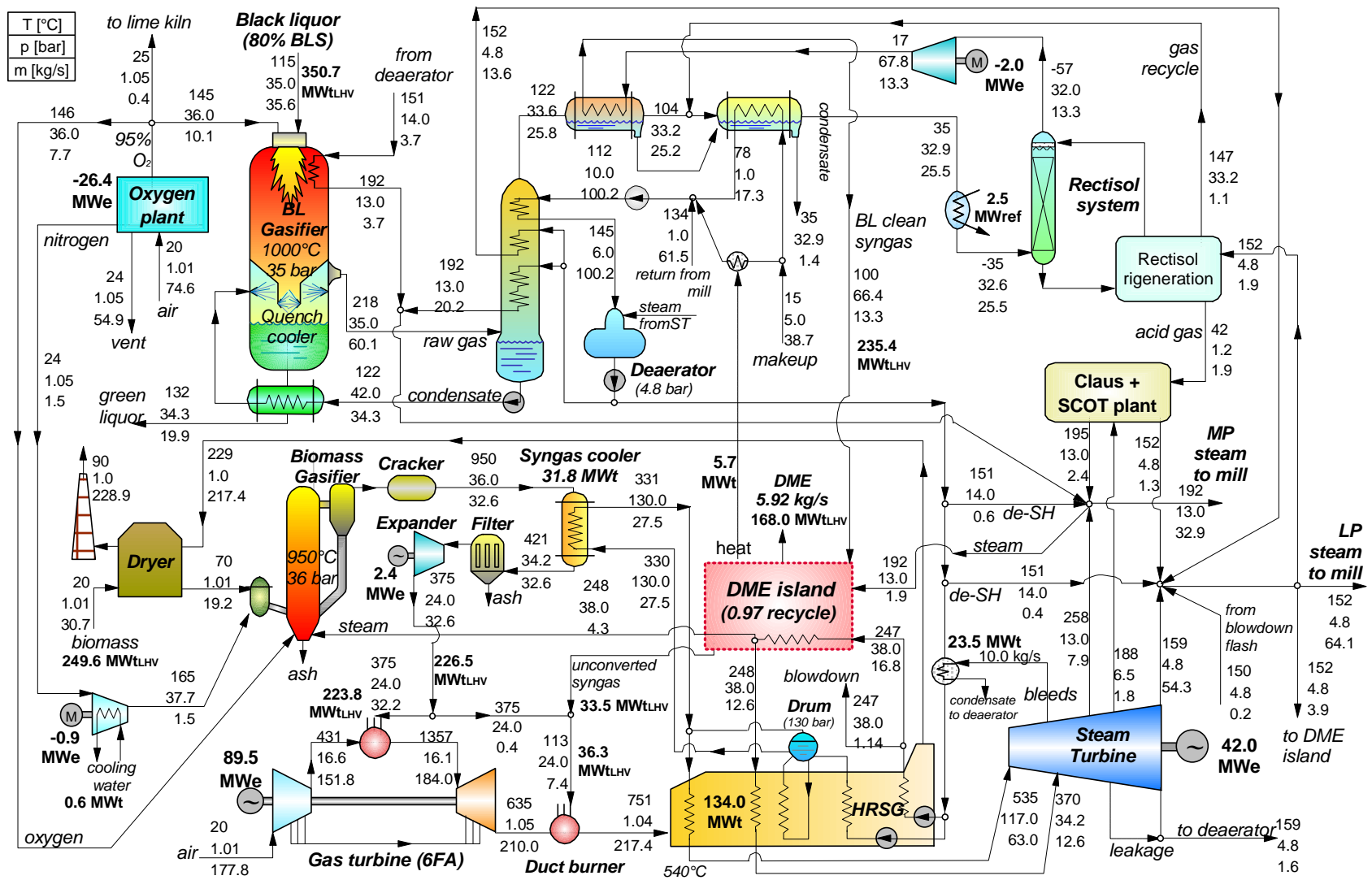


Fig. 19. Plant configuration and mass/energy balances for DMEb case

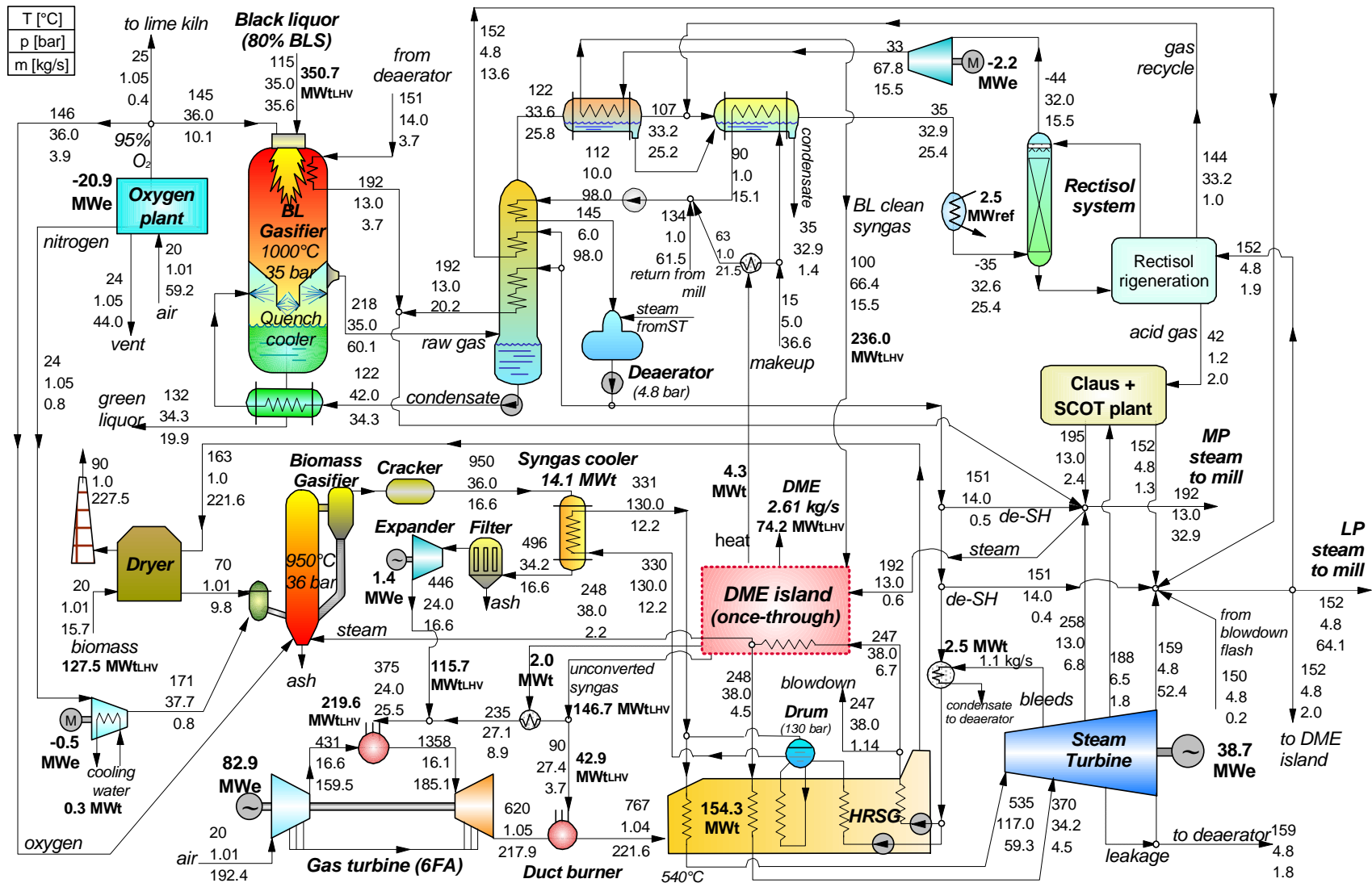


Fig. 20. Plant configuration and mass/energy balances for DMEc case

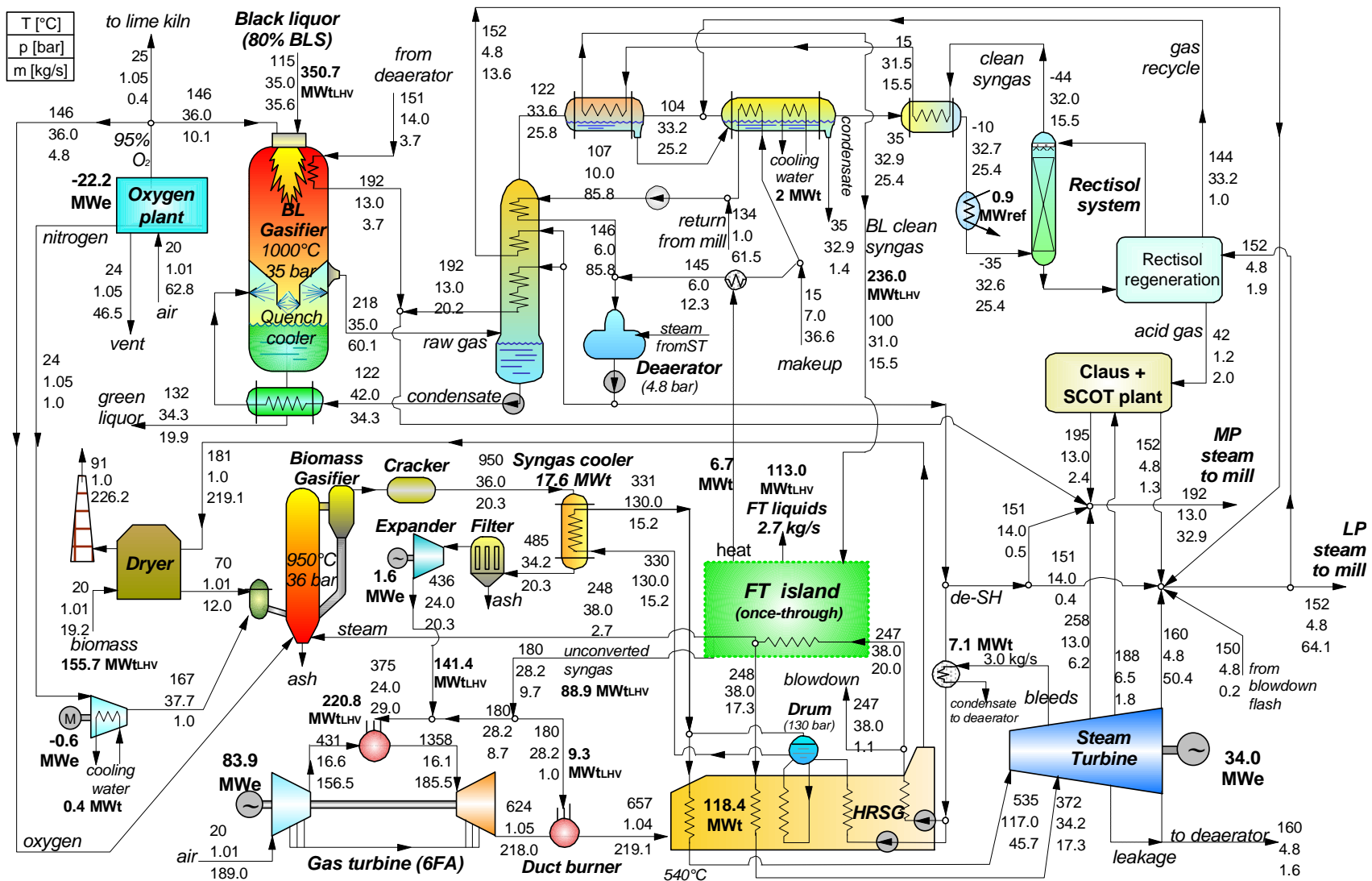


Fig. 21. Plant configuration and mass/energy balances for FTa case

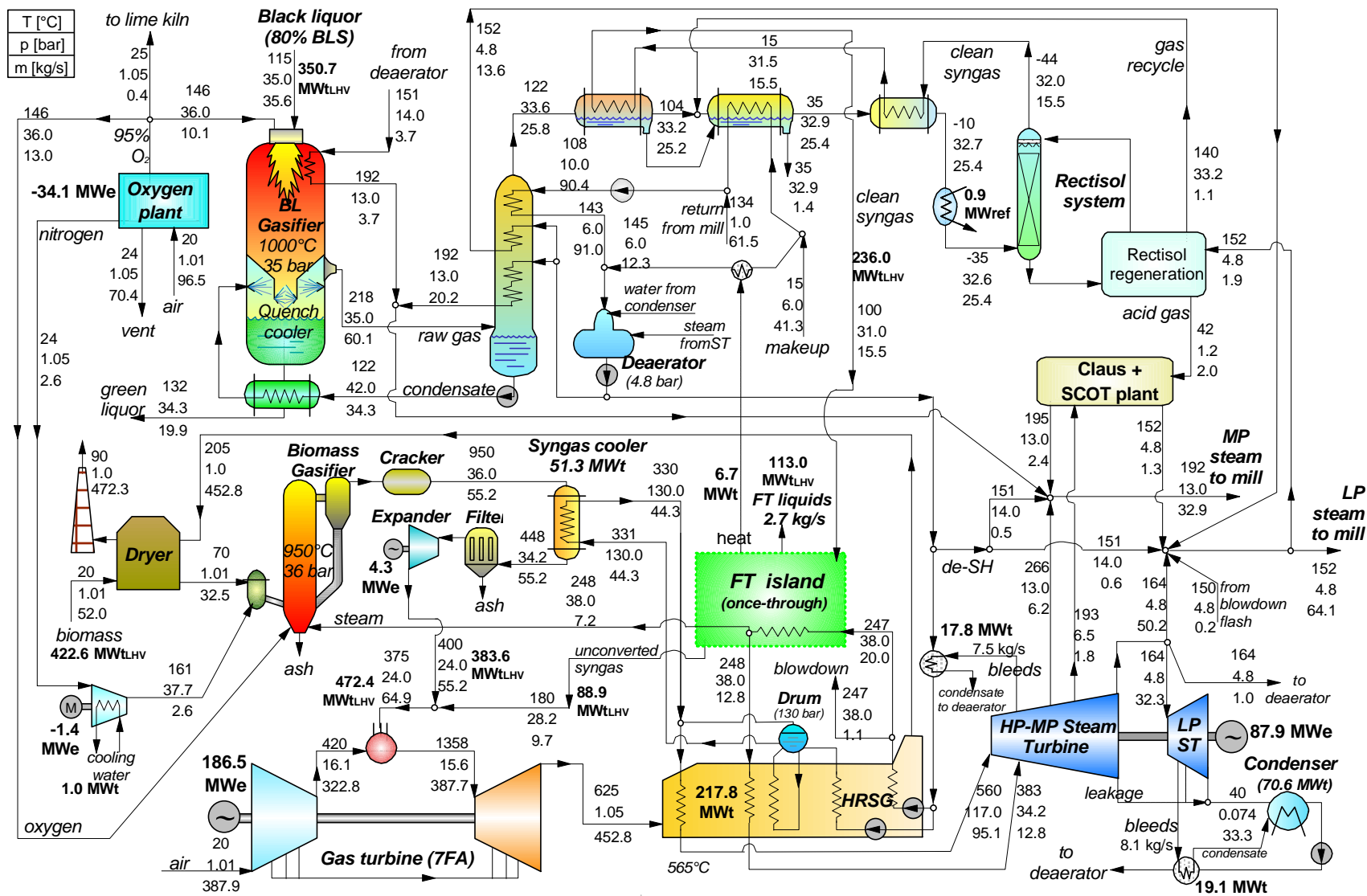


Fig. 22. Plant configuration and mass/energy balances for FTb case

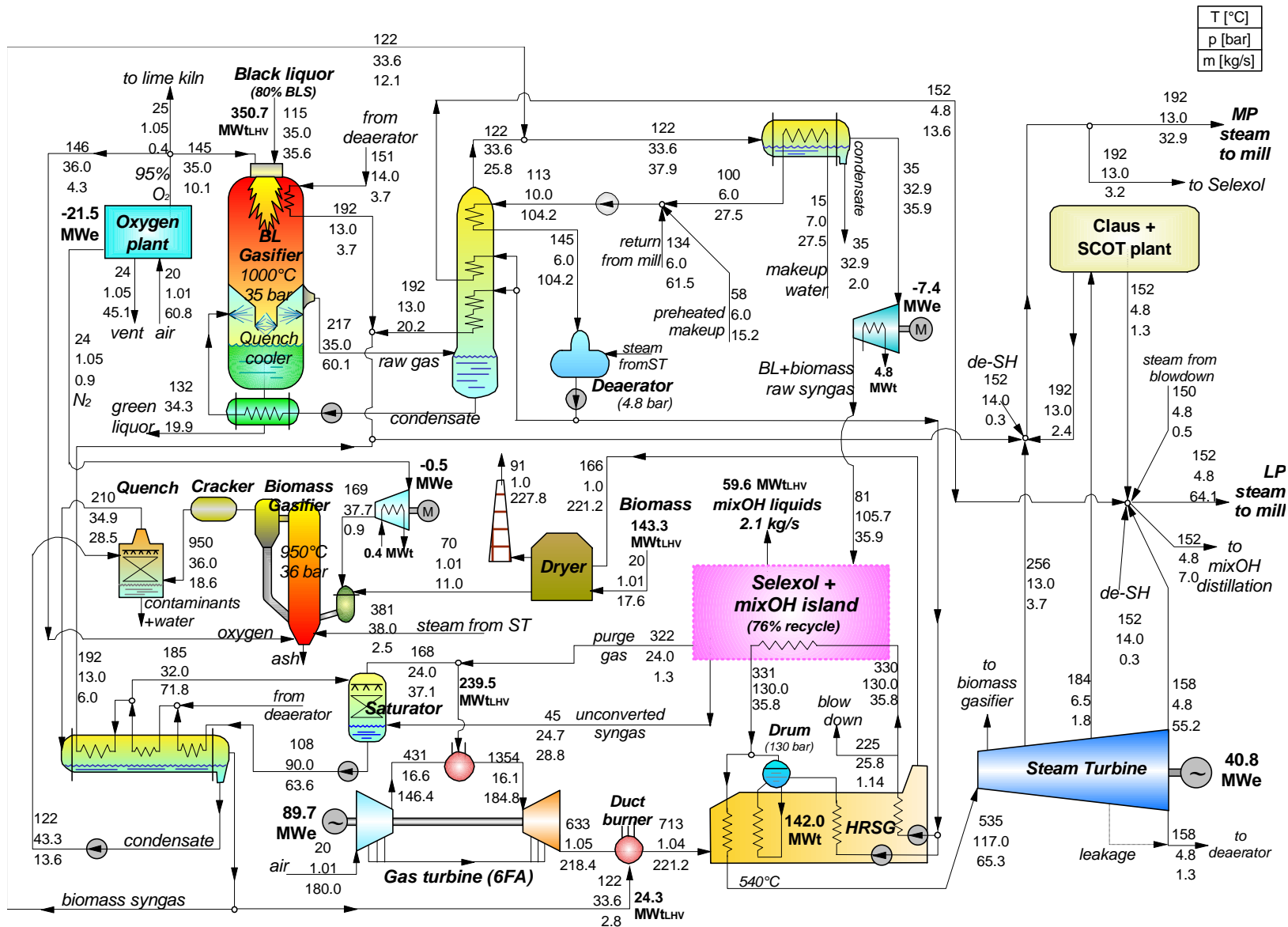


Fig. 24. Plant configuration and mass/energy balances for MixOH case

6 PROCESS SIMULATION RESULTS

6.1 Overall performances

Tab. 16 to Tab. 18 and Fig. 25 show the energy balance and the overall performances predicted in our simulations. The tables and the figure report also the conventional Tomlinson boiler system described and calculated by Larson, Consonni and Katofsky [2003].

		Tomlinson boiler	BL Gasifier						
			Case DMEa	Case DMEb	Case DMEc	Case FTa	Case FTb	Case FTc	Case MixOH
FUEL INPUT									
DS flow	kg/s	31.5	28.5	28.5	28.5	28.5	28.5	28.5	28.5
DS in black liquor	%	80.0	80.0	80.0	80.0	80.0	80.0	80.0	80.0
Total black liquor	kg/s	39.4	35.6	35.6	35.6	35.6	35.6	35.6	35.6
	MWt LHV	392.6	350.7						
Total wood residuals	kg/s	7.1	16.2	30.7	15.7	19.2	52.0	62.2	17.6
	MWt LHV	57.8	131.5	249.6	127.5	155.7	422.6	505.4	143.3
	from mill MWt LHV	57.8	54.1	54.1	54.1	54.1	54.1	54.1	54.1
	purchased MWt LHV	0.0	77.4	195.5	73.4	101.6	368.5	451.3	89.2
Lime kiln fuel oil	MWt LHV	31.1	35.9	35.9	35.9	35.9	35.9	35.9	35.9
FUEL PRODUCTION									
Fresh clean syngas to fuel synthesis area	kg/s	-	13.3	13.3	15.5	15.5	15.5	47.1	32.2
	MWt LHV	-	235.4	235.4	236.0	236.0	236.0	692.8	342.3
	H ₂ /CO ratio mol/mol	-	1.04	1.04	1.04	1.04	1.04	1.11	1.08
Syngas from biomass gasification	kg/s	-	-	32.6	16.6	20.3	55.2	52.5	14.9
	LHV	-	-	7.0	7.0	7.0	7.0	8.7	8.8
	MWt LHV	-	-	226.5	115.7	141.3	383.6	457.9	130.9
Syngas recycle in fuel synthesis island	%	-	0.97	0.97	0	0	0	0	0.76
Unconverted syngas to power island	kg/s	-	7.0	7.0	12.6	9.7	9.7	29.1	28.8
	MWt LHV	-	33.5	33.5	146.7	88.9	88.9	237.5	232.7
DME	kg/s	-	5.92	5.92	2.61	-	-	-	-
	MWt LHV	-	168.0	168.0	74.2	-	-	-	-
FT liquids	kg/s	-	-	-	-	2.57	2.57	7.90	-
	MWt LHV	-	-	-	-	111.6	111.6	342.7	-
Mixed Alcohols	kg/s	-	-	-	-	-	-	-	2.10
	MWt LHV	-	-	-	-	-	-	-	59.6

Tab. 16. Summary of performance estimates: mass and energy balances of fuel inputs and fuel productions

		Tomlinson boiler	BL Gasifier						
			Case DMEa	Case DMEb	Case DMEc	Case FTa	Case FTb	Case FTc	Case MixOH
REFRIGERATION DUTY									
Rectisol/Selexol plant	MWref	-	6.8	6.8	6.6	5.0	5.0	16.0	4.8
DME island	MWref	-	3.9	3.9	1.7	-	-	-	-
STEAM									
HP steam from power boiler (87.2 bar)	kg/s	125.56	47.7	-	-	-	-	-	-
HP steam from HRSG (130 bar)	kg/s	-	-	35.5	47.1	30.5	50.8	22.3	29.5
HP steam from biomass syngas cooler (130 bar)	kg/s	-	-	27.5	12.2	15.2	44.3	-	-
	MWt	-	-	31.8	14.1	17.6	51.3	-	-
Steam from DME/FT reactor to power island (38 bar)	kg/s	-	16.8	16.8	6.7	20.0	20.0	61.1	-
	MWt	-	29.1	29.1	11.5	34.6	34.6	105.7	-
Steam from MixOH reactor to power island (130 bar)	kg/s	-	-	-	-	-	-	-	35.8
	MWt	-	-	-	-	-	-	-	40.7
MP steam from Claus plant (13 bar)	kg/s	-	2.4	2.4	2.4	2.4	2.4	2.4	2.4
	MWt	-	4.7	4.7	4.7	4.7	4.7	4.7	4.7
LP steam from Claus plant (4.8 bar)	kg/s	-	1.3	1.3	1.3	1.3	1.3	1.3	1.3
	MWt	-	2.7	2.7	2.7	2.7	2.7	2.7	2.7
MP steam to Selexol and to fuel synthesis island (13 bar)	kg/s	-	1.9	1.9	0.6	-	-	-	3.2
	MWt	-	4.0	4.0	1.3	-	-	-	7.0
IP steam to SCOT plant (6.5 bar)	kg/s	-	1.8	1.8	1.8	1.8	1.8	1.8	1.8
	MWt	-	3.6	3.6	3.6	3.6	3.6	3.6	3.6
LP steam to Rectisol and to fuel synthesis island (4.8 bar)	kg/s	-	5.8	5.8	3.9	1.9	1.9	4.7	7.0
	MWt	-	12.3	12.3	8.3	4.0	4.0	10.0	15.0
MP steam to mill (13 bar)	kg/s	35.15	32.9	32.9	32.9	32.9	32.9	32.9	32.9
	MWt	69.28	64.8	64.8	64.8	64.8	64.8	64.8	64.8
LP steam to mill (4.8 bar)	kg/s	67.60	64.1	64.1	64.1	64.1	64.1	64.1	64.1
	MWt	142.78	135.3	135.3	135.3	135.3	135.3	135.3	135.3

Tab. 17. Summary of performance estimates: refrigeration duties and steam balance

		Tomlinson boiler	BL Gasifier						
			Case DMEa	Case DMEb	Case DMEc	Case FTa	Case FTb	Case FTc	Case MixOH
POWER									
Steam turbine gross output	MWel	72.00	32.88	41.96	38.71	33.97	87.90	48.57	40.80
Gas turbine output	MWel	-	-	89.54	82.91	83.90	186.51	89.68	89.73
Expander output	MWel	-	2.58	5.01	1.96	1.65	4.26	-	2.99
<i>Total gross production</i>	MWel	<i>72.00</i>	<i>35.46</i>	<i>136.51</i>	<i>123.58</i>	<i>119.52</i>	<i>278.67</i>	<i>138.25</i>	<i>133.52</i>
Aux for steam cycle/HRSG	MWel	6.70	1.38	2.30	1.52	1.31	3.76	5.40	2.75
Aux for biomass boiler	MWel	1.00	1.75	-	-	-	-	-	-
Aux for BL gasification island	MWel	-	2.67	2.67	2.67	2.67	2.67	2.67	2.67
Aux for biomass gasification island	MWel	-	-	1.90	0.97	1.18	3.21	3.84	1.09
Biomass handling and drying	MWel	-	-	0.61	0.31	0.38	1.04	1.24	0.35
Lock hoppers	MWel	-	-	0.86	0.46	0.55	1.41	1.67	0.51
Clean syngas compressor	MWel	-	1.95	1.95	2.17	-	-	-	7.37
Gas compressors	MWel	-	7.26	7.26	-	-	-	-	1.77
ASU	MWel	-	15.19	26.40	20.93	22.20	34.14	37.84	21.53
Aux for Rectisol/Selexol	MWel	-	0.97	0.97	0.96	0.96	0.96	2.59	1.81
Rectisol/Selexol process refrigeration	MWel	-	2.15	2.15	2.07	2.01	2.01	5.11	1.21
DME island consumption	MWel	-	1.00	1.00	0.40	-	-	-	-
<i>Total use</i>	MWel	<i>7.70</i>	<i>34.32</i>	<i>48.07</i>	<i>32.44</i>	<i>31.26</i>	<i>49.19</i>	<i>60.36</i>	<i>41.05</i>
Net power production	MWel	64.30	1.14	88.44	91.13	88.27	229.48	77.89	92.47
Mill electricity consumption	MWel	100.10	100.10	100.10	100.10	100.10	100.10	100.10	100.10
ASU (delignification use)	MWel	-	0.58	0.58	0.58	0.58	0.58	0.58	0.58
Power purchased from grid	MWel	35.80	98.38	11.08	8.38	11.25	-129.97	21.63	7.05

Tab. 18. Summary of performance estimates: electricity balance

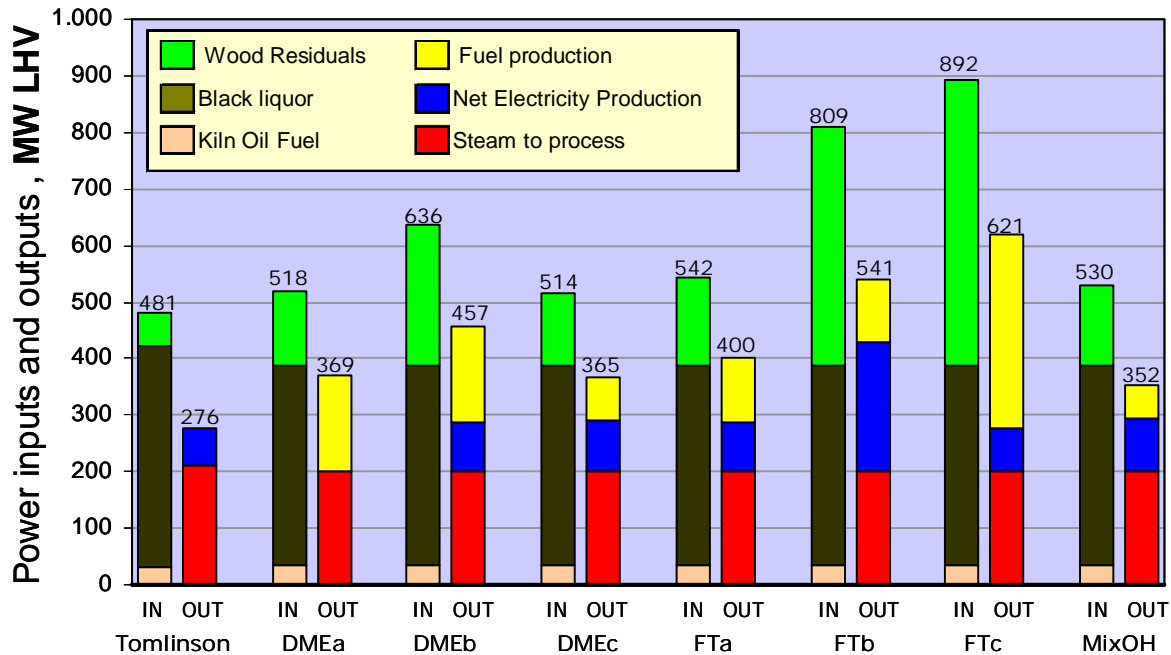


Fig. 25. Energy balance of biorefinery simulations and Tomlinson system

6.2 Energy efficiencies

Tab. 19 shows the value of various energy efficiency parameters for the biorefinery designs and of the Tomlinson system. *ETA electricity* is the ratio of net electricity production to total fuel inputs. *ETA fuel* is the ratio of exportable fuel to total fuel inputs. *ETA heat* is the ratio of process steam heat to total fuel inputs. *ETA 1st* is the efficiency with which primary energy is converted to useful outputs (1st law thermodynamic efficiency), i.e. *ETA electricity* + *ETA fuel* + *ETA heat*.

ETA 1st is helpful to appreciate the energy balance of the biorefinery system; however, it is not an appropriate performance indicator because electricity, fuel and heat have quite different thermodynamic (and economic) relevance and their mere sum (the numerator of *ETA 1st*) does not account for their actual “value”.

In an attempt to quantify the actual thermodynamic quality or “value” of the outputs generated by each plant, in the last row of Tab. 19 we’ve introduced *ETA equivalent electricity total*, defined as the ratio between the electricity that could be produced by converting all outputs to electricity and the primary energy input. This enables an “apples-to-apples” thermodynamic comparison among systems that produce no liquid fuel (e.g. Tomlinson system) and those that produce some fuel. Clean liquid fuels like DME and MixOH could generate electricity by a combined cycle (the most efficient technology now available) with an efficiency of 0.55 $MW_{el}/MW_{LHV_{fuel}}$. This is not the case for the raw FT fuel, which would require further upgrading; assuming that the raw FT liquid could be converted to light fuels with 91% efficiency, the overall electric efficiency achievable with FT raw products is 0.50 $MW_{el}/MW_{LHV_{fuel}}$. The steam exported from the biorefinery could be fed to a steam turbine and expanded to the condenser pressure assumed here of 0.074 bar; this would generate 610 kJ_{el} per kg of MP steam at 13 bar, 510 kJ_{el} per kg of LP steam 4.8 bar (these conversion factors account for an expansion efficiency equal to the one of the LP turbines considered in this study).

Fig. 26 shows the contribution of each output (heat, fuel and electricity) to *ETA 1st* and to *ETA equivalent electricity total*.

From the point of view of just the energy balance ($ETA\ 1^{st}$) the three DME cases are about equivalent, FTa is the best case while FTb and MixOH stay behind (but still much better than Tomlinson). This ranking is misleading, because it doesn't account for the different "quality" of the three forms of energy generated by each plant. Energy quality is accounted for in the $ETA\ equivalent\ electricity\ total$ parameter. The best option with this measure is FTb, which reaches $ETA\ equivalent\ electricity\ total$ close to 42% thanks to the high electric efficiency of the large scale combined cycle. Instead, the worst biorefinery option is DMEa which, being without a combined cycle, suffers from no net electricity production. This situation indicates that generating electricity from black liquor and biomass is thermodynamically more efficient than generating fuels. Or, from a different point of view, that significant margins do exist to improve the thermodynamic efficiencies of the processes for the production of fuels via the thermochemical route.

The comparison between Tomlinson and DMEa shows that generating DME is thermodynamically more efficient than the conventional Tomlinson technology. On the other hand, the higher values of $ETA\ equivalent\ electricity\ total$ of all other BLGF cases with respect to DMEa show that co-producing fuel and electricity is a more rational way of taking advantage of the black liquor resource and of the opportunity of heat integration with the mill.

		Tomlinson boiler	BL Gasifier						
			Case DMEa	Case DMEb	Case DMEc	Case FTa	Case FTb	Case FTc	Case MixOH
EFFICIENCIES (LHV basis)									
ETA electricity	%	13.4	0.2	13.9	17.7	16.3	28.4	8.7	17.4
ETA fuel	%	0	32.4	26.4	14.4	20.6	13.8	38.4	11.2
ETA heat	%	44.0	38.6	31.4	38.9	36.9	24.7	22.4	37.8
ETA 1st	%	57.4	71.3	71.8	71.1	73.7	66.9	69.6	66.4
ETA equivalent electricity total	%	25.0	28.2	36.7	35.9	36.3	41.8	33.9	33.6

Tab. 19. Energy efficiencies:

$ETA\ electricity = \text{net electricity production} / \text{sum of all fuel energy inputs};$

$ETA\ fuel = \text{liquid fuel energy} / \text{sum of all fuel energy inputs};$

$ETA\ heat = \text{process steam heat} / \text{sum of all fuel energy inputs};$

$ETA\ 1st = ETA\ electricity + ETA\ fuel + ETA\ heat;$

$ETA\ electricity\ equivalent\ tot. = (\text{net electricity production} + K1* \text{liquid fuel energy} + K2* \text{MPsteam flow} + K3* \text{LPsteam flow}) / \text{sum of all fuel energy inputs};$

where $\text{sum of all fuel energy inputs} = \text{total residual wood} + \text{BL} + \text{lime kiln oil}$. For details on $K1$, $K2$ and $K3$ see Tab. 20 and text.

		DME	FT	MixOH	MPsteam	LPsteam
K1	MW _{el} /MW _{fuelLHV}	0.55	0.50	0.55	--	--
K2	kJ _{el} /kg _{steam}	--	--	--	610	--
K3	kJ _{el} /kg _{steam}	--	--	--	--	510

Tab. 20. Coefficients of liquid fuels and steam conversions to electricity.

K1 = Electricity that could be produced by a combined cycle fed with the liquid fuel. The electrical efficiency of the CC is assumed 55% for DME and MixOH and 50% for FT raw liquid (thus assuming 91% of efficiency for the conversion from raw FT to light fuels).

K2 = Electricity that could be produced by MP (13 bar) steam expansion to 0.074 bar in steam turbine. Isentropic eff. = 0.81; mechanical-electrical eff. = 0.98. The resulting ratio between electricity and heat is 0.31.

K3 = Electricity that could be produced by LP (4.8 bar) steam expansion to 0.074 bar in steam turbine. Isentropic eff. = 0.84; mechanical-electrical eff. = 0.98. The resulting ratio between electricity and heat is 0.24.

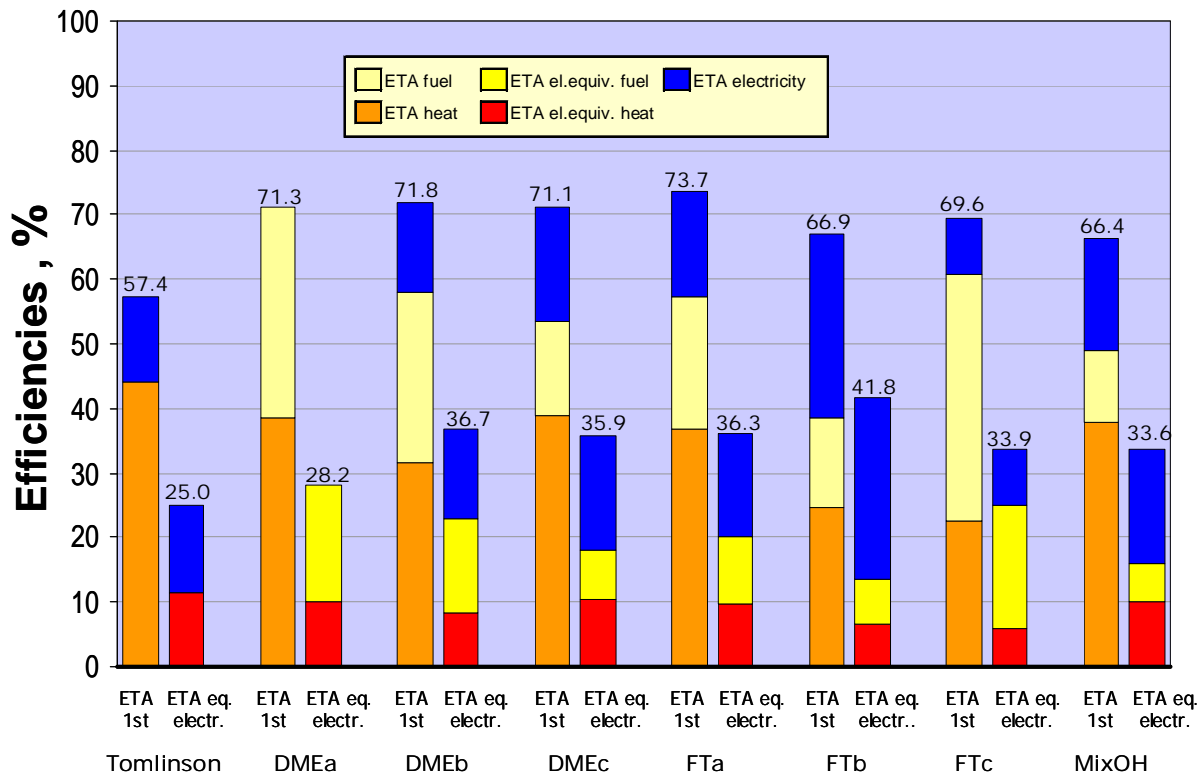


Fig. 26. Energy efficiencies and contribution of each output (steam heat, liquid fuel and electricity) to ETA1st and to ETA equivalent electricity total

6.3 Biorefinery designs vs. conventional Tomlinson systems

Fig. 27 shows the increment of energy inputs required by biorefineries and their additional electricity generation, both relative to the Tomlinson case. The production of liquid fuels is always an extra output with respect to the Tomlinson system.

The marginal biorefinery efficiencies reported in Tab. 21 show the effectiveness with which biorefinery designs utilize the extra fuel (compared to the Tomlinson case) to generate extra electricity (*Marginal electrical efficiency*) and to produce liquid fuels (*Marginal fuel efficiency*).

The third column of Tab. 21 shows the *Marginal equivalent electricity efficiency*, i.e the ratio between the extra equivalent electricity generated by BLGF (numerator of *ETA equivalent electricity total* minus electricity generated in the Tomlinson case) divided by the extra-fuel consumption. From a thermodynamic perspective, this is the “fairest” measure of comparison. The very high values reached by this marginal efficiency indicate that BLGF is a way to compensate the inefficiencies of the reference Tomlinson system. The larger the “marginal” system added to the reference mill, the lower the marginal gains, because the relevance of compensating the inefficiencies of the reference Tomlinson decreases. This explains why the marginal efficiency of the largest plants (FTb and FTc) is relatively low.

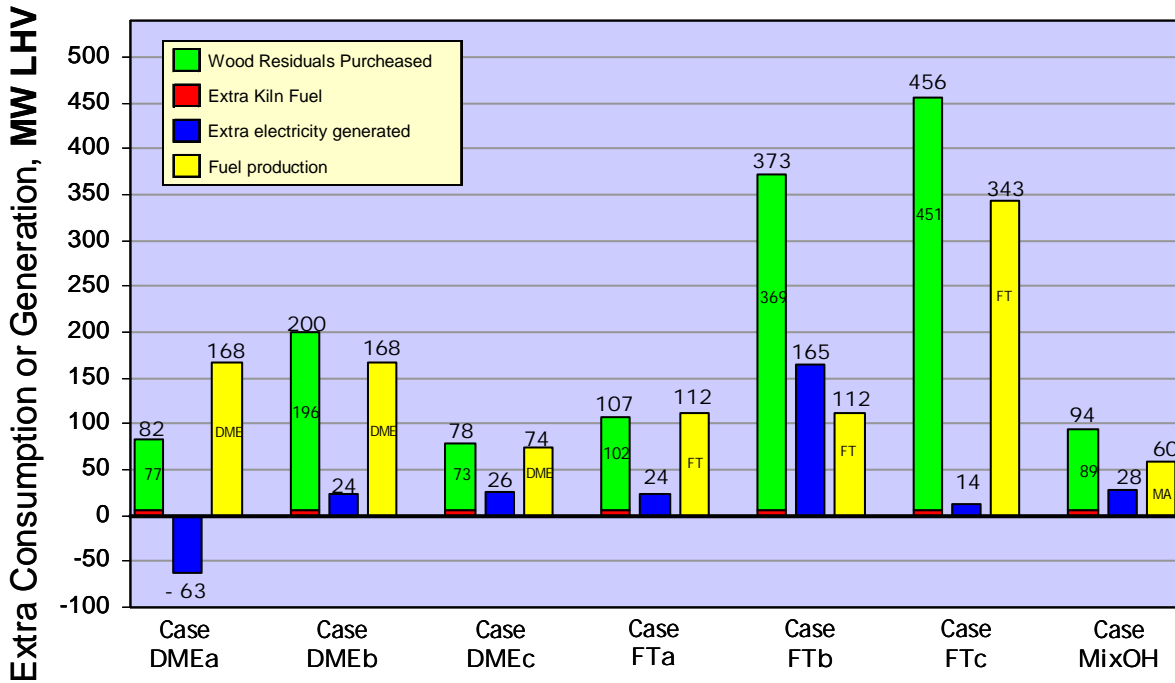


Fig. 27. Biorefinery energy inputs and outputs variations with respect to Tomlinson system

	“Marginal” electric efficiency %	“Marginal” fuel production efficiency %	“Marginal” equivalent electricity production efficiency %
Case DMEa	-76.1	204.4	36.3
Case DMEb	12.3	83.9	58.5
Case DMEc	35.0	94.8	87.2
Case FTa	23.1	104.8	75.4
Case FTb	44.4	29.9	59.3
Case FTc	3.1	75.1	40.7
Case MixOH	30.6	63.4	65.4

Tab. 21. Marginal efficiencies with respect to Tomlinson system.

Marginal electric efficiency = extra net electricity production / extra total fuel consumption

Marginal fuel production efficiency = liquid fuel production / extra total fuel consumption

Marginal equivalent electricity efficiency = (extra net electricity production + liquid fuel production* *K1*) / extra total fuel consumption

K1 is the efficiency of liquid fuel conversion to electricity in a combined cycle, as described in Tab. 20.

7 REFERENCES

- Aden A., Spath P., Atherton B., 2005. "The Potential of Thermochemical Ethanol Via Mixed Alcohols Production", Milestone Completion Report, National Renewable Energy Laboratory (NREL), October 31
- Bechtel, 1998. "Aspen Process Flowsheet Simulation Model of a Battelle Biomass-Based Gasification, Fischer-Tropsch Liquefaction and Combined-Cycle Power Plant", DE-AC22-93PC91029-16, May, US Dept. of Energy, Pittsburgh, Pennsylvania.
- Blackadder W.H., Lundberg H., Rensfelt E., and Waldheim L., 1994. "Heat and Power Production via Gasification in the Range 5 50 MWe," in *Advanced In Biomass Thermochemical Conversion*, A.V. Bridgwater (ed.), Balckie Academic & Professional Press, London.
- Brammer J.G. and Bridgwater A.V., 1999. "Drying technologies for an integrated gasification bio-energy plant", *Renewable and Sustainable Energy Reviews*, 3: 243-289
- Bridgwater A.V., 1995. "The technical and economic feasibility of biomass gasification for power generation", *Fuel* 74(5):631-53.
- Celik, F.E., Larson, E.D. and Williams, R.H. "Transportation fuels from coal with low CO₂ emissions," paper presented at the 7th International Conference on Greenhouse Gas Control Technologies, Vancouver, BC, 5-9 September, 2004.
- Consonni S. and Larson E.D., 1998. "Biomass-Gasifier/Aeroderivative Gas Turbine Combined Cycle: Part A – Technologies and Performance Modeling, and Part B – Performance Calculations and Economic Assessment", *J. of Engineering for Gas Turbines and Power*, 118: 507-525.
- Cummer K. and Brown R., 2002. "Ancillary equipment for biomass gasification", *Biomass and Bioenergy*, 23: 113-128
- Dayton D., 2002. "A Review of the Literature on Catalytic Biomass Tar Destruction", NREL/TP-510-32815, National Renewable Energy Laboratory (NREL), December
- Devi L., Ptasinski K. and Janssen F., 2003. "A review of the primary measures for tar elimination in biomass gasification processes", *Biomass and Bioenergy* 24:125 – 140
- Dry M.E., 2002. "The Fischer-Tropsch process: 1950-2000", *Catalysis Today* 71:227-241
- Ekbom T., Lindblom M., Berglin N. and Ahlvik P., 2003. "Technical and Commercial Feasibility Study of Black Liquor Gasification with Methanol/DME Production as Motor Fuels for Automotive Uses – BLGMF"
- Fox J.M. and Tam S.S., 1995. "Correlation of slurry reactor Fischer-Tropsch yield data", *Topics in Catalysis*, 2:285-300

- Graaf G.H., Winkelman J.G.M., and Stamhuis E.J., 1988. "Kinetics of three-phase methanol synthesis", *Chemical Engineering Science*, 43 (8), pp. 2161-2168.
- Graaf G.H., and Beenackers A.A.C.M., 1996. "Comparison of two-phase and three-phase methanol synthesis processes", *Chemical Engineering and Processing*, 35, pp. 413-427.
- Gunturu A.K., Kugler E.L., Cropley J.B. and Dadyburjor D.B., 1998. "A Kinetic Model for the Synthesis of High-Molecular-Weight Alcohols over a Sulfided Co-K-Mo/C Catalyst", *Ind. Eng. Chem. Res.* 37: 2107-2115
- Hamelinck C. Faaij A., den Uil H. and Boerrigter H., 2004. "Production of FT transportation fuels from biomass; technical options, process analysis and optimisation, and development potential", *Energy* 29:1743-1771
- Larson E.D. and Tingjin R., 2003. "Synthetic fuel production by indirect coal liquefaction", *Energy for Sustainable Development*, Volume VII No. 4
- Larson, E.D., Consonni, S., and Katofsky, R.E., 2003. "A Cost-Benefit Assessment of Biomass Gasification Power Generation in the Pulp and Paper Industry, Final Report" final report, Princeton Environmental Institute, Princeton, NJ, October.
- Larson, E.D., Kreutz, T.G. and Consonni, S., 1999. "Combined Biomass and Black Liquor Gasifier/Gas Turbine Cogeneration at Pulp and Paper Mills," *J. of Engineering for Gas Turbines and Power*, 121: 394-400.
- Lau F.S., Bowen D.A., DiHu R., Doong S., Hughes E.E., Remick, R., Slimane R., Turn S.Q., and Zabransky R., 2003. "Techno-Economic Analysis of Hydrogen Production by Gasification of Biomass", Gas Technology Institute (GTI), contract DE-FC36-01GO11089 for DOE, June
- Lau F.S., Carty R.H., Onischak M., and Bain R.L., 1993. "Development of the IGT Renugas Process," Conference on Strategic Benefits of Biomass and Waste Fuels, Electric Power Research Institute, Washington, DC, 30 March – 1 April, 1993.
- Liu Z., Li X., Close M.R., Kugler E.L., Peterson J.L., Dadyburjor D.B., 1997. *Ind. Eng. Chem. Res.*, 36, 3085-3093
- Milne T.A., Evans R.J. and Abatzoglou N., 1998. "Biomass gasifier "Tars": Their Nature, Formation and Conversion", NREL/TP-570-25357, National Renewable Energy Laboratory, November
- Ng K.L., Chadwick D., and Toseland B.A., 1999. "Kinetics and modeling of dimethyl ether synthesis from synthesis gas", *Chemical Engineering Science*, 54, pp. 3587-3592. Contract DE-AC26-99FT40675 for US DOE by Research Triangle Institute, Research Triangle
- Pan Y.G., Roca X., Velo E., Puigjaner L., 1999. "Removal of tar by secondary air injection in fluidized bed gasification of residual biomass and coal", *Fuel*; 78:1703-9.
- Ranke, G. and Weiss, H., "Separation of Gaseous Components from a Gaseous Mixture by Physical Scrubbing", United States patent 4,324,567, 1982

- Riesenfeld F.C., Kohl, A., "Gas Purification", II Edition, Gulf Publishing Company, 1974
- Simell P., Kurkela, E., Stahlberg P. and Hepola, J., 1996. "Catalytic hot gas cleaning of gasification gas." *Catalysis Today* 27(1-2), 55-62.
- Spath P.L., Dyton D.C., 2003. "Preliminary Screening — Technical and Economic Assessment of Synthesis Gas to Fuels and Chemicals with Emphasis on the Potential for Biomass-Derived Syngas", NREL/TP-510-34929, National Renewable Energy Laboratory (NREL), December
- SRI Consulting, 2002. "Dimethyl ether as alternate fuel", Report No. 245, June
- The Rectisol® Process for Gas Purification, Lurgi Engineering Oel-Gas-Chemie, brochure available @ <http://www.lurgi.com>
- Tijmensen M., Faaij A., Hamelinck C. and van Hardeveld M., 2002. "Exploration of the possibilities for production of Fischer Tropsch liquids and power via biomass gasification", *Biomass and Bioenergy* 23:129 – 152
- U.S. Department of Energy, 1998. "Baseline Design/Economics for Advanced Fischer-Tropsch Technology, Final report", April

APPENDIX A: DME AND FT SYNTHESIS

A.1 DME synthesis

A.1.1 Kinetics equations

Direct synthesis of DME from syngas involves two parallel steps, methanol synthesis and methanol dehydration. This process can be represented by following reactions:



The rates for reactions (A1), (A2) and (A3) use in our kinetic model, expressed in terms of partial fugacity, results:

$$r_{A1} = \frac{k_{A1} K_{CO} \left(f_{CO} f_{H_2}^{3/2} - \frac{f_{MeOH}}{f_{H_2}^{1/2} K_{A1}^0} \right)}{\left(1 + K_{CO} f_{CO} + K_{CO_2} f_{CO_2} \right) \left(f_{H_2}^{1/2} + \frac{K_{H_2O}}{K_{H_2}^{1/2}} f_{H_2O} \right)} \quad (\text{A5})$$

$$r_{A2} = \frac{k_{A2} K_{CO_2} \left(f_{CO_2} f_{H_2}^{3/2} - \frac{f_{H_2O} f_{MeOH}}{f_{H_2}^{3/2} K_{A2}^0} \right)}{\left(1 + K_{CO} f_{CO} + K_{CO_2} f_{CO_2} \right) \left(f_{H_2}^{1/2} + \frac{K_{H_2O}}{K_{H_2}^{1/2}} f_{H_2O} \right)} \quad (\text{A6})$$

$$r_{A3} = \frac{k_{A3} K_{CO_2} \left(f_{CO_2} f_{H_2} - \frac{f_{H_2O} f_{CO}}{K_{A3}^0} \right)}{\left(1 + K_{CO} f_{CO} + K_{CO_2} f_{CO_2} \right) \left(f_{H_2}^{1/2} + \frac{K_{H_2O}}{K_{H_2}^{1/2}} f_{H_2O} \right)} \quad (\text{A7})$$

where f_i is component fugacity (bar), r is reaction rate based on weight of catalyst (mol/s·kg_{cat}).

The temperature dependencies of rate parameters and adsorption coefficients can be expressed as

$$K = A \exp\left(\frac{B}{RT}\right)$$

where R is ideal gas constant, 8.314 J/K-mol; T is reaction temperature, K; A , B are constants listed in Tab. A1 for liquid-phase methanol synthesis reactions.

Parameter	Liquid Phase	
	Constant A	Constant B
k_{A1}	2.12×106	-98800
k_{A2}	2.58×1018	-220000
k_{A3}	1.09×101	-48300
K_{CO}	5.15×10 ⁻¹¹	91500
K_{CO_2}	7.83×10 ⁻⁵	41000
$K_{H_2O} / \sqrt{K_{H_2}}$	2.30×10 ⁻¹²	114100
K_{A1}^0	2.391×10 ⁻¹³	98388
K_{A2}^0	1.068×10 ²	-39683
K_{A3}^0	2.544×10 ⁻¹¹	58705

Tab. A1. Parameters of Graaf methanol synthesis kinetic models⁹

For reaction (A4), in terms of liquid concentration, the left to right reaction rate is given by r_{A4} , proposed by Ng¹⁰:

$$r_{A4} = k_{A4} K_{MeOH}^2 \left[\frac{C_{MeOH}^2 - \frac{C_{H_2O} C_{DME}}{K_{A4,A3}}}{\left(1 + 2\sqrt{K_{MeOH} C_{MeOH}} + K_{H_2O} C_{H_2O}\right)^4} \right] \quad (A8)$$

where C_i is the concentration of component i , and the constants are as follows:

$$k_{A4} = 3.7 \times 10^{10} \exp\left(-\frac{105000}{RT}\right)$$

$$K_{MeOH} = 7.9 \times 10^{-4}$$

⁹ Graaf G.H., Winkelman J.G.M., and Stamhuis E.J., 1988. "Kinetics of three-phase methanol synthesis", *Chemical Engineering Science*, 43 (8), pp. 2161-2168; Graaf G.H., and Beenackers A.A.C.M., 1996. "Comparison of two-phase and three-phase methanol synthesis processes", *Chemical Engineering and Processing*, 35, pp. 413-427.

¹⁰ Ng, K.L., Chadwick, D., and Toseland, B.A., 1999, "Kinetics and modeling of dimethyl ether synthesis from synthesis gas," *Chemical Engineering Science*, **54**: 3587-3592.

$K_{A4,A3}$ is the equilibrium constant expressed in terms of concentration. We have assumed the fix value¹¹ of 8.571.

A.1.2 Reactor model

Performance of the reactor is defined by the following material and energy balances:

$$F_i^{in} - F_i^{out} = k_L \alpha(i) V_{comp} (P_{G,i} / H_i - c_{L,i})$$

$$k_L \alpha(i) V_{comp} (P_{G,i} / H_i - c_{L,i}) = k_s \alpha_s (C_{G,i} / H_i - C_{L,i})$$

$$k_s \alpha_s (C_{G,i} / H_i - C_{L,i}) = \sum W_{cata} r_{i,j}$$

If include the factors of mass transfer into reaction rates, the above model can be simplified as:

$$F_i^{in} - F_i^{out} = \sum W_{cata} r_{i,j}$$

where $r_{i,j}$ stands for the reaction rates of component i in reaction j. The total consumption/formation rates of components considered in the DME reaction are as follows:

$$r_{MeOH} = r_{A1} + r_{A2} - 2r_{A4}$$

$$r_{CO} = -r_{A1} + r_{A3}$$

$$r_{H_2} = -2r_{A1} - 3r_{A2} - r_{A3}$$

$$r_{CO_2} = -r_{A2} - r_{A3}$$

$$r_{H_2O} = r_{A2} + r_{A3} + r_{A4}$$

$$r_{DME} = r_{A4}$$

in which r_{A1} , r_{A2} , r_{A3} and r_{A4} are defined by equations (A5), (A6), (A7), and (A8).

A.1.3 Comparisons with experiment results

In order to test this kinetic model, comparisons with experimental results were made. Experimental data are from Gogate and Lee¹². The properties of the catalysts used in it that work are listed in Tab. A2. Tab. A3 shows the operating conditions considered. Tab. A4 shows a comparison of experimental results with predictions using our model for three different ratios of

¹¹ Seidel, A., 1990, "Calculating chemical reaction equilibrium for a homogeneous phase from the material balance of a batch reactor," *Chemical Engineering Science*, 45(9): 2970-2973.

¹² Gogate, M.R., and Vijayaraghavan, P., 1992. "A single-stage, liquid-phase dimethyl ether synthesis process from syngas: thermodynamic analysis of the LPDME process system", *Fuel Science and Technology International*, 10 (3), pp. 281-311.

the mass of methanol synthesis catalyst and dehydration catalyst: 1, 0.5, and 0. The comparison is satisfactory.

Methanol Synthesis Catalyst		
Identification	EPJ-19	
Manufacturer	United Catalysts, Inc.	
Composition	CuO	55%
	ZnO	36%
	Al ₂ O ₃	8%
	SiO ₂	1%
Geometry	2.38 mm cylindrical extrudates	
Length	Varying between 3 to 15 mm	
Specific Area	92 m ² /g	
Pore Volume	0.43 cm ³ /g	
Methanol Dehydration Catalyst		
Identification	Gamma-Alumina (AL-3916P)	
Manufacturer	Harshaw-Filterol Partnership	
Specific Area	198 m ² /g	
Pore Volume	0.43 cm ³ /g	
<u>Inert Liquid Medium</u>	Witco-40 white mineral oil	
<u>Reactor</u>	One-liter stirred autoclave by Autoclave Engineers, inc.	

Tab. A2. Assumptions adopted for catalysts in DME synthesis model

Temperature	250°C
Pressure	70 bar
Oil	550 mL of Witco 40 oil
Impeller speed	1500 rpm
Feed flow rate	1 SLPM ¹³

Tab. A3. Co-production of methanol and DME operating conditions considered for comparison

¹³ Standard Liters per Minute.

Co-production of Methanol and DME								
Content			Literature	Model	Literature	Model	Literature	Model
Catalyst	EPJ-19 (g)		15		15		15	
	Gamma-Alumina to EPJ-19 ratio		0		0.5		1	
Reactor Feed Flow Rate and Mol Fractions	Flow	mol/h	2.6787	2.6787	2.6787	2.6787	2.6786	2.6786
	H2	mol%	0.3815	0.3815	0.3696	0.3696	0.3616	0.3616
	CO		0.4564	0.4564	0.4727	0.4727	0.4836	0.4836
	CH4		0.0860	0.0860	0.0826	0.0826	0.0790	0.0790
	CO2		0.0762	0.0762	0.0752	0.0752	0.0757	0.0757
Reactor Exit Flow Rate and Mol Fractions	Flow	mol/h	2.1093	2.1413	1.9953	2.1290	1.9557	2.1172
	H2	mol%	0.2150	0.2252	0.1918	0.2219	0.1956	0.2214
	CO		0.4556	0.4465	0.4494	0.4506	0.4469	0.4502
	CH4		0.1097	0.1076	0.1109	0.1038	0.1082	0.1001
	CO2		0.0946	0.0941	0.1247	0.1097	0.1425	0.1248
	MEOH		0.1242	0.1255	0.1038	0.0959	0.0755	0.0695
	H2O		0.0009	0.0011	0.0011	0.0016	0.0012	0.0025
	DME		0.0000	0.0000	0.0184	0.0166	0.0300	0.0315
GHSV				4545		4545		4545
Syngas Conv.	Conv.	%	31.0365	30.0922	34.6148	29.4633	34.6907	28.9465
	Error			-3.0%		-14.9%		-16.6%
Carbon Conv.	Conv.	%	18.3626	18.8336	19.1147	18.7288	17.6884	18.7360
	Error			2.6%		-2.0%		5.9%
MeOH Yield	Yield	mol/h	0.2620	0.2687	0.2071	0.2041	0.1477	0.1472
	Error			2.6%		-1.4%		-0.3%
DME Yield	Yield	mol/h	0.0000	0.0000	0.0367	0.0354	0.0587	0.0667
	Error					-3.6%		13.7%

Tab. A4. Comparisons between results calculated with the model adopted and experimental data

A.1.4 Sensitivity study of DME synthesis section

The kinetic model enables us to simulate performance under different operating conditions. Reactor pressure and syngas recycle fraction were varied to see the performance impact (Tab. A5).

Reaction pressure	35 bar – 150 bar
Unconverted gas recycle ratio	0 – 0.97
Reactor operation temperature	260°C
GSHV	6000 liters/h.gcat
CATAdme/CATAmeth	0.3
Turbine outlet pressure	28.5 bar
1st distillator pressure	25 bar

Tab. A5. Assumptions and parameters investigated in sensitivity analysis of DME production

A.1.4.1 Effect of reactor pressure variation

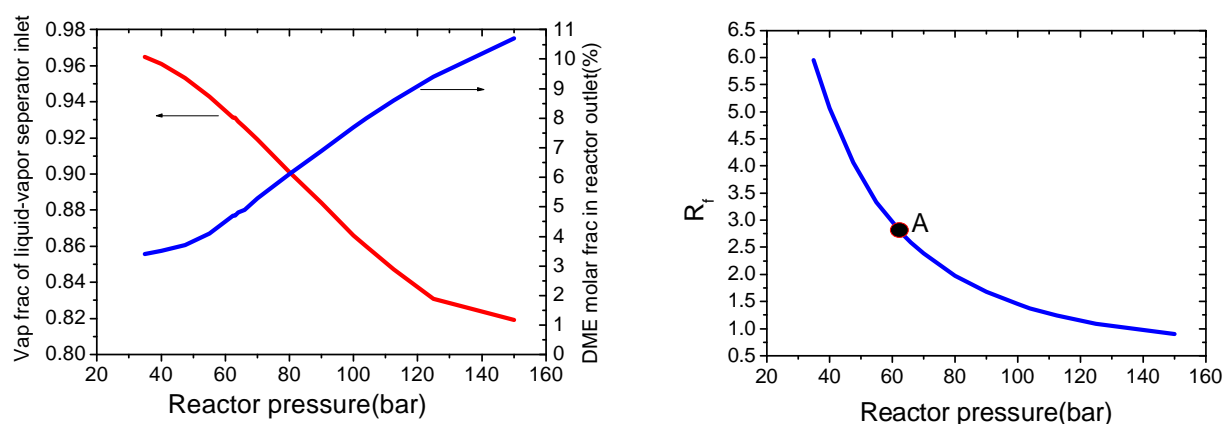


Fig. A1. Effect of reactor pressure variation on vapor fraction of products at 40°C, on DME molar fraction in products and on unconverted recycled gas-to-fresh gas ratio (R_f). The unconverted recycle ratio is fixed at 0.97. Point A shows the pressure adopted in this study (62.5 bar).

With increasing reactor pressure, the vapor fraction at the reactor outlet decreases (Fig. A1, red curve), so less unconverted syngas is separated from the product mixture. Assuming that the fraction of unconverted gas recycled back to the reactor inlet is constant (in our case, 97%), lower unconverted syngas mass flow means lower ratio R_f between the mass flow of unconverted syngas recycled to the reactor inlet and the mass flow of fresh syngas; in turn, this implies that the composition of the syngas at the reactor inlet becomes closer to the composition of the fresh syngas.

The DME molar fraction in exiting reactor stream increases with increasing reactor pressures (Fig. A1). This is augmented by less inert gas dilution due to the decreased amount of unconverted syngas recycled. Both these effects give a DME yield increment. At the same time the mass flow at the reactor outlet decreases when the pressure increases because of a inlet reactor flow decrement.

The combined effects of these factors give a DME production increment with reaction pressure at pressures lower than 100 bar, while the DME production begins to decrease with reaction pressure at higher pressures.

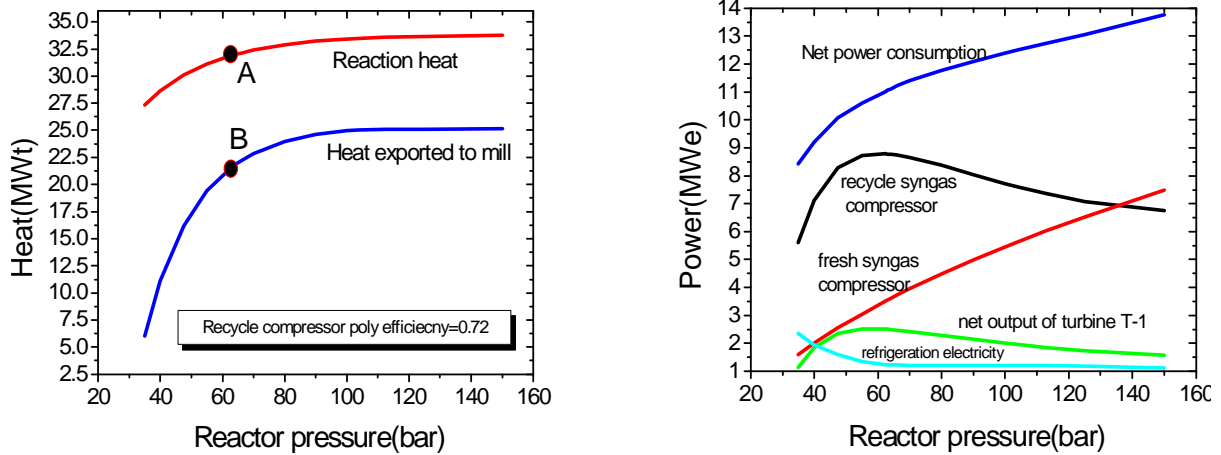


Fig. A2. Effect of reactor pressure variation on heat released in reaction, on heat exported to mill and on electricity consumed and generated by the DME synthesis island. The unconverted recycle ratio is fixed at 0.97. Point A and point B show the pressure adopted in this study (62.5 bar).

With increasing pressure, the CO + H₂ molar fraction in the unconverted gas decreases, which reduces the heating value of the purge gas. At pressures higher than 100 bar, this decrement is minor.

Synthesis reactions are favored by higher reaction pressure, thus more reaction heat is produced as pressure increases (Fig. A2). Moreover, the steam usage in the DME synthesis section decreases with pressure, so that increasing amounts of export steam are available for other uses (e.g., export to the mill) as pressure increases (Fig. A2). But at pressures higher than 100 bar this increment becomes negligible.

The fresh syngas compressor power consumption increases with reaction pressure (Fig. A2, right). With syngas recycle, the recycle compressor pressure ratio increases with the reaction pressure but, at the same time, the flow of gas recycled back to the reactor decreases for a fixed unconverted gas recycle ratio. These two factors lead to an increase in power consumption of the recycle compressor when reactor pressure increases up to about 60 bar, and to a decrease at pressures higher than 60 bar. The total compressor power consumption (considering both the fresh feed and recycle compressors) increases continuously with increasing reaction pressure.

In summary, when reaction pressures are varied from 35bar—150bar:

- the maximum DME mass flow production can be achieved at around 100 bar,
- the DME yield variation is about 0.01 kg/s/bar,
- at reaction pressures higher than 100 bar, the heat available for export from the synthesis reactor and the purge gas energy content changes very little,
- total compressor work increases steadily with increasing pressure.

From the results above, a suitable pressure range for the DME synthesis reactor is 60-80 bar.

A.1.4.2 Effect of unconverted gas recycle

The recycle of a fraction of the unconverted gas to the reactor can be changed to increase the ratio of DME output to purge gas energy

The recycle ratio (R) is defined as the portion of the unconverted gas recycled back to the reactor.

By increasing R , an increase of DME production is achieved. But at R higher than 0.97, this effect becomes very trivial. Moreover, a purge gas flow taken from the recycle loop is necessary to prevent an excessive built-up of inert gases. For these reasons, the recycle ratio selected in DMEa and DMEb cases is 0.97.

The Fig. A3 shows the relation between R and R_f , and the values adopted in this study (point A). The figures A4, A5 and A6 show the effects of R_f change.

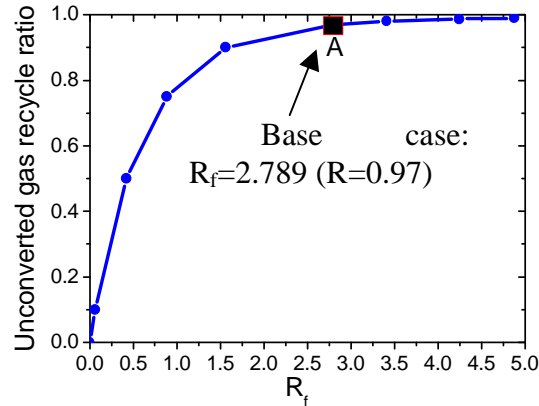


Fig. A3. The unconverted gas recycle ratio is the fraction of unconverted syngas recycled back to reactor. This value determines the unconverted recycled gas-to-fresh gas ratio (R_f). Point A shows the value of R_f adopted in this study (2.79, given by a recycle ratio of 0.97).

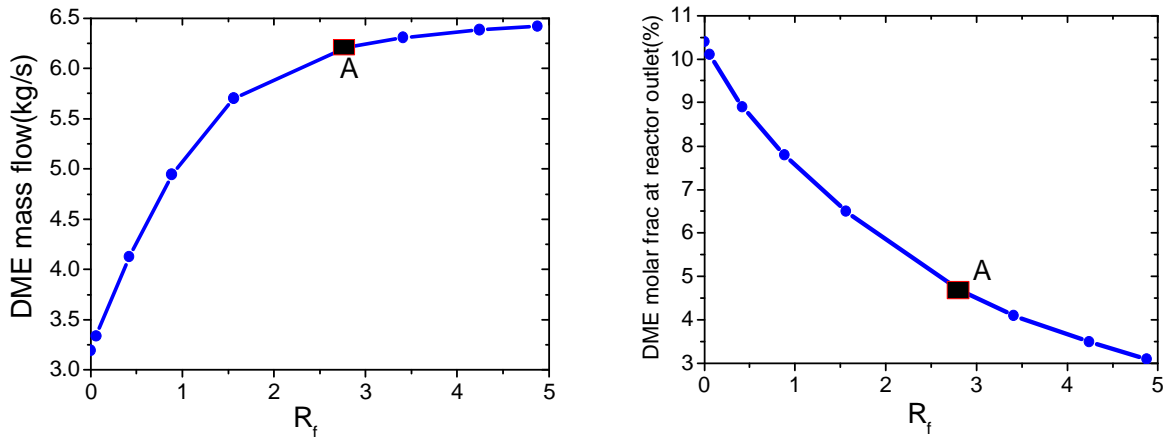


Fig. A4. Effect of unconverted recycled gas-to-fresh gas ratio (R_f) on DME production and on DME molar fraction at reactor outlet. The reactor pressure is fixed at 62.5 bar. Point A shows the value of R_f adopted in this study (2.79, given by a recycle ratio of 0.97).

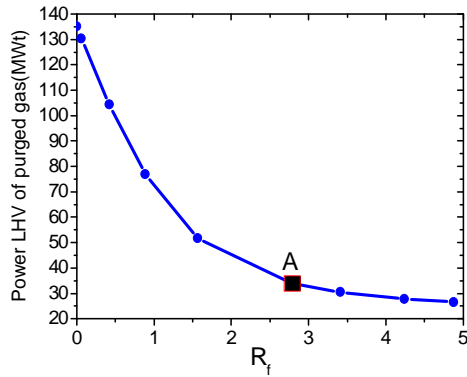


Fig. A5. Effect of unconverted recycled gas-to-fresh gas ratio (R_f) on purged gas energy content. The reactor pressure is fixed at 62.5 bar. Point A shows the values of R_f adopted in this study (2.79, given by a recycle ratio of 0.97).

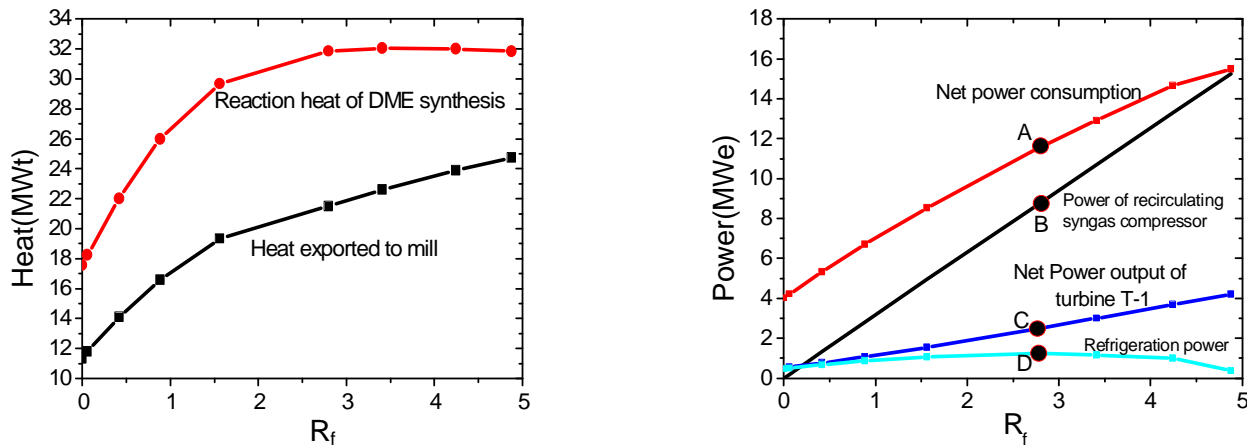


Fig. A6. Effect of unconverted recycled gas-to-fresh gas ratio (R_f) on heat released in reaction, on heat exported from the synthesis island for other uses (e.g., for the mill) and on electricity consumed and generated by the DME synthesis island. The reactor pressure is fixed at 62.5 bar. Points A, B, C, D show the value of R_f adopted in this study (2.79, given by a recycle ratio of 0.97).

The power consumption of the recycle gas compressor increases almost linearly with increasing recycle ratio. Also the reaction heat increases when the recycle ratio increases, but at high recycle ratio the variation becomes small.

In summary, at recycle ratio higher than 0.97:

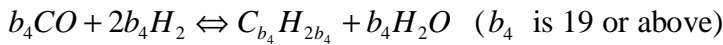
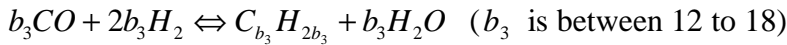
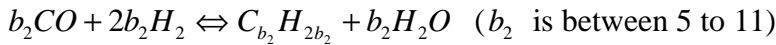
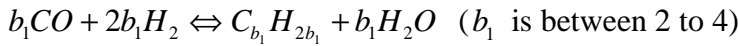
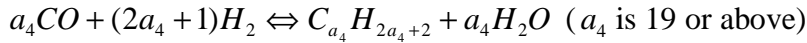
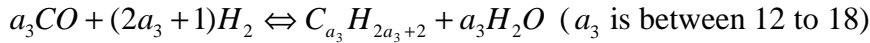
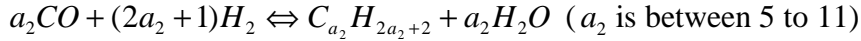
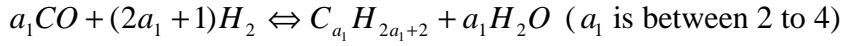
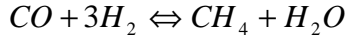
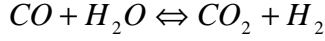
- the DME yield increases only slowly,
- the purge gas energy content decreases, and
- heat export from, and power consumption in, the synthesis section increase.

From these results, the most suitable unconverted gas recycle ratio is about 0.97.

A.2 FT synthesis

A.2.1 Kinetics equations

The reactions considered in the FT reactor are:



The following are expressions used to determine reaction rates:

- methane

$$R_{CH_4} = k_{HC5}P_{H_2} \frac{\left(\frac{k_{HC1}P_{CO}}{k_{HC1}P_{CO} + k_{HC5}P_{H_2}} \right)}{1 + \left(\frac{k_{HC1}P_{CO}}{k_{HC1}P_{CO} + k_{HC5}P_{H_2}} \right) \frac{1}{1-\alpha}} \quad (A9)$$

- C₂-C₄ (light gases)

$$R_{C_nH_{2n}} = \sum_{i=2}^4 \left(\left(k_{HC6} \frac{\left(\frac{k_{HC1}P_{CO}}{k_{HC1}P_{CO} + k_{HC5}P_{H_2}} \right) \alpha^{n-1}}{1 + \left(\frac{k_{HC1}P_{CO}}{k_{HC1}P_{CO} + k_{HC5}P_{H_2}} \right) \frac{1}{1-\alpha}} \right) \times \frac{i}{n} \right) \quad (A10)$$

n is a number between 2 to 4.

If we define the fraction of olefins for C₂–C₄ as fO_{2-4} , the general reaction rate for paraffins is:

$$R_{C_nH_{2n+2}} = R_{C_nH_{2n}} (1 - fO_{2-4}) / fO_{2-4}. \quad (A11)$$

- C₅-C₁₁ (FT gasoline)

Similarly, for C₅-C₁₁ FT gasoline, the general reaction rate for olefins is:

$$R_{C_n H_{2n}} = \sum_{i=5}^{11} \left(\left(k_{HC6} \frac{\left(\frac{k_{HC1} P_{co}}{k_{HC1} P_{co} + k_{HC5} P_{H_2}} \right) \alpha^{n-1}}{1 + \left(\frac{k_{HC1} P_{co}}{k_{HC1} P_{co} + k_{HC5} P_{H_2}} \right) \frac{1}{1-\alpha}} \right) \times \frac{i}{n} \right) \quad (A12)$$

n is a number between 5 to 11.

If we define the fraction of olefins for C₅ – C₁₁ as fO_{5-11} , the general reaction rate for paraffins is:

$$R_{C_n H_{2n+2}} = R_{C_n H_{2n}} (1 - fO_{5-11}) / fO_{5-11}. \quad (A13)$$

- C₁₂-C₁₈ (FT diesel)

$$R_{C_n H_{2n}} = \sum_{i=12}^{18} \left(\left(k_{HC6} \frac{\left(\frac{k_{HC1} P_{co}}{k_{HC1} P_{co} + k_{HC5} P_{H_2}} \right) \alpha^{n-1}}{1 + \left(\frac{k_{HC1} P_{co}}{k_{HC1} P_{co} + k_{HC5} P_{H_2}} \right) \frac{1}{1-\alpha}} \right) \times \frac{i}{n} \right) \quad (A14)$$

n is a number between 12 to 18.

Is we define the fraction of olefins for C₁₂ – C₁₈ as fO_{12-18} , the general reaction rate for paraffins is:

$$R_{C_n H_{2n+2}} = R_{C_n H_{2n}} (1 - fO_{12-18}) / fO_{12-18}. \quad (A15)$$

- C₁₉₊ (wax)

$$R_{C_n H_{2n}} = \sum_{i=19}^{100} \left(\left(k_{HC6} \frac{\left(\frac{k_{HC1} P_{co}}{k_{HC1} P_{co} + k_{HC5} P_{H_2}} \right) \alpha^{n-1}}{1 + \left(\frac{k_{HC1} P_{co}}{k_{HC1} P_{co} + k_{HC5} P_{H_2}} \right) \frac{1}{1-\alpha}} \right) \times \frac{i}{n} \right) \quad (A16)$$

n is a number between 19 to 30.

If we define the fraction of olefins for C₁₉ + as fO_{19+} , the general reaction rate for paraffin is:

$$R_{C_n H_{2n+2}} = R_{C_n H_{2n}} (1 - fO_{19+}) / fO_{19+} \quad (A16)$$

A.2.2 Reactor model

The performance of the reactor is defined by the following material and energy balances:
Gas phase:

$$F_i^{in} - F_i^{out} = k_L \alpha (i) V_{comp} (P_{G,i} / H_i - c_{L,i})$$

$$k_L \alpha (i) V_{comp} (P_{G,i} / H_i - c_{L,i}) = k_s \alpha_s (C_{G,i} / H_i - C_{L,i})$$

$$k_s \alpha_s (C_{G,i} / H_i - C_{L,i}) = \sum W_{cata} r_{i,j}$$

Accounting for the influence of mass transfer on reaction rates, the above model can be simplified as:

$$F_i^{in} - F_i^{out} = \sum W_{cata} r_{i,j}$$

$r_{i,j}$ stands for the reaction rates of component i in reaction j .

The total consumption/formation rates of components considered in FT reaction (CO, CO₂, H₂O, H₂ and FT products) are defined as follows:

$$r_{CO} = -r_{WGS} - r_{CH_4} - \sum_{i=1}^4 a_i R_{C_i H_{2i+2}} - \sum_{j=1}^4 b_j R_{C_j H_{2j}}$$

$$r_{H_2} = r_{WGS} - 3r_{CH_4} - \sum_{i=1}^4 (2a_i + 1) R_{C_i H_{2i+2}} - \sum_{j=1}^4 2b_j R_{C_j H_{2j}}$$

$$r_{CO_2} = r_{WGS}$$

$$r_{H_2O} = -r_{WGS} + r_{CH_4} + \sum_{i=1}^4 a_i R_{C_i H_{2i+2}} + \sum_{j=1}^4 b_j R_{C_j H_{2j}}$$

APPENDIX B: KINETIC MODEL FOR MIXED ALCOHOL SYNTHESIS¹⁴

B.1 *Model development and preliminary results*

B.1.1 Introduction

It has been known for many decades that mixtures of methanol and higher alcohols (i.e. long chain alcohols) could be used directly as fuel, as fuel additives for octane or cetane enhancement, or as oxygenate fuel additives for environmental reasons [1 - 4 and references therein]. In the '90s, the abrupt development of MTBE demand and the prognoses for a mid-term shortage of oil-derived isobutene has led to a renewed interest in the synthesis, particularly over methanol-modified synthesis catalysts which lead to the production of mainly methanol and isobutanol. The consecutive dehydration of isobutanol to isobutene, the precursor of MTBE along with methanol, is state of the art: in this way, a syngas route to MTBE would be accessible [3]. However to date the synthesis of higher alcohols, particularly of isobutanol, still suffers from poor selectivity, so that the synthesis of methanol and Fischer-Tropsch liquid fuels are preferably considered nowadays as a way of exploitation the huge reserves of natural gas located in remote areas, via syngas production (Gas-to-liquid, GTL).

Catalysts used for the production of higher alcohols from synthesis gas (mixtures of CO and H₂) can be divided into four categories [2, 5 and references therein]. The first one is based on a soluble Ru complex used as an homogeneous catalyst. The second one can be described as modified methanol catalysts (e.g. alkali-doped ZnO/chromia or Cu-based catalysts). The third category of catalysts comprises mixed-metal Fischer-Tropsch catalysts (e.g. Co and Fe on a support). Finally, the last category includes alkali-promoted MoS₂ catalysts.

Among the various catalysts, Mo-based systems are the catalysts of choice in the case of S-containing feed due to their high tolerance for sulfur compounds. They also show high activity in the water-gas shift reaction and high activity and selectivity for linear alcohols. The last characteristic is important in view of the fact that there are several possible reactions between CO and H₂, that are thermodynamically competitive to the synthesis of higher alcohols. In particular, the formation of hydrocarbons (α -olefins and n-paraffins) from CO and H₂ is thermodynamically favored with respect to the formation of higher alcohols (i.e. Keq of hydrocarbons are higher than Keq of alcohols) [1]. For this reason, for the higher alcohols synthesis, the usage of an highly selective catalysts is necessary to guide the process selectivity toward alcohols.

B.1.2 Scope of the work

The scope of this work is to build a Fortran code able to estimate, given a set of process conditions (temperature, pressure, feed composition), the rates of formation of the main products (i.e. methanol, ethanol, propanol, methane, carbon dioxide and water) involved in the higher alcohols synthesis over a Mo-based catalyst.

For this reason we first selected, based on literature indications, a set of rate expressions describing the kinetic behavior of the species involved in the mechanism of formation of the higher alcohols; based on such rate equations, we then constructed a Fortran code able to estimate directly the CO conversion and alcohols productivity given a set of process conditions.

¹⁴ **Authors:** Prof. Enrico Tronconi, Prof. Luca Lietti, Eng. Zuzana Vallusova, Eng. Carlo Giorgio Visconti. Milano, July 2006

B.1.3 Development of the kinetic model

In a paper recently published by Gunturu et al. [6] a C-supported, K-promoted Co-Mo sulfide catalyst (Mo-Co-K/C) was used to study the kinetics of the synthesis of methanol and higher alcohols from syngas. The content of Mo in the catalyst was 18 wt. %, the molar ratio of K/Mo was equal to 1.3 and the ratio of Co/Mo was 0.34. The catalyst was tested in a gradientless Berty reactor, which was used as an internal recycle reactor. The kinetic runs were performed in the temperature range of 300-350°C, at the total pressure of 40.8-68.1 atm (400-1000 psig) with a CO/H₂ feed ratio ranging from 0.5 to 2. All the experiments were performed at a fixed gas hourly space velocity (GHSV) of 9000 L/h/kgcatalyst.

The article provides detailed experimental data for the whole set of higher alcohols synthesis kinetic runs. The results of the related kinetic study, including rate expressions and kinetic parameter estimates, are also published.

Accordingly, the kinetic model reported in [6] has been herein adopted as a starting point for the purposes of the present work. In the following we describe its structure, its implementation in a computer code, and its validation against data from other literature sources.

The adopted simplified reaction scheme for the synthesis of higher alcohols is shown below.



In this lumped reaction scheme, the production of methanol from CO and H₂, reaction (B1), is regarded as reversible, and limited by chemical equilibrium. Further, it is assumed that all the hydrocarbon products are produced from methanol and are composed exclusively by methane, reaction (B2). The formation of ethanol, reaction (B3), and the formation of propanol, reaction (B4), proceed by reaction of CO/H₂ with methanol and with ethanol, respectively, according to a consecutive scheme. The water-gas shift reaction, reaction (B5), which accounts for CO₂ formation, is assumed to be always in thermodynamic equilibrium.

Alcohols of carbon number higher than three (C4+ alcohols) are formed in quantities small enough to be neglected for present purposes (C4+ carbon selectivity < 4% [7]). In addition, all the formed ethers (dimethyl ether, diethyl ether) and other oxygenates not explicitly identified as alcohols were lumped into the methane (hydrocarbon) fraction.

The equation for the calculation of the gross rate of formation of methanol published in [6] contained some mistakes, possibly due to misprints. So we corrected this equation into the following form:

$$r_{CH_3OH}^{gross} = \frac{A_m e^{-(E_m/R)(1/T-1/T_{cp})} \left(\left[\frac{P_{CO}}{P_{CO}^{cp}} \right] \left[\frac{P_{H_2}}{P_{H_2}^{cp}} \right]^2 - \frac{1}{K_{eq}} \left[\frac{P_{CH_3OH}}{P_{CH_3OH}^{cp}} \right] \right)}{\left(1 + K_1 \left[\frac{P_{CO}}{P_{CO}^{cp}} \right] + K_2 \left[\frac{P_{H_2}}{P_{H_2}^{cp}} \right] + K_3 \left[\frac{P_{CH_3OH}}{P_{CH_3OH}^{cp}} \right] \right)^{nm}} \quad (B6)$$

with

$$K_{eq} = K_a / (K_z K^{CP}) \quad (B7)$$

$$K^{CP} = \frac{P_{CH3OH}^{CP}}{P_{CO}^{CP} (P_{H2}^{CP})^2} \quad (B8)$$

where r_i^{gross} is the rate of formation of species i in kmol/h/kgcat and p are the partial pressures of the reactants measured in atm. T_{cp} is the temperature and p_{cp} is the partial pressure of the center-point experiment ($T_{cp}=598$ K, $p_{cp}=47.6$ atm), E_m is activation energy for methanol formation, R is the ideal gas constant, the parameters K_1 , K_2 and K_3 are adsorption coefficients, K_{eq} is nondimensional equilibrium constant and K_a is equilibrium constant in kPa⁻². This experiment performed under CP conditions was replicated after every four runs made at different conditions. K_{CP} is the nondimensionalizing term represented by the ratio of the partial pressures at the central point (equation B8).

The expressions used for the calculation of ethanol, propanol and methane gross rates of formation were used exactly as reported in [6]:

$$r_{C2H5OH}^{gross} = \frac{A_e e^{-(E_e/R)(1/T-1/T_{cp})} \left[\frac{P_{CH3OH}}{P_{CH3OH}^{cp}} \right]}{\left(1 + K_e \left[\frac{P_{CH3OH}}{P_{CH3OH}^{cp}} \right] \right)^{n_e}} \quad (B9)$$

$$r_{C3H7OH}^{gross} = \frac{A_p e^{-(E_p/R)(1/T-1/T_{cp})} \left[\frac{P_{C2H5OH}}{P_{C2H5OH}^{cp}} \right]}{\left(1 + K_p \left[\frac{P_{C2H5OH}}{P_{C2H5OH}^{cp}} \right] \right)^{n_p}} \quad (B10)$$

$$r_{HC}^{gross} = \frac{A_h e^{-(E_h/R)(1/T-1/T_{cp})} \left[\frac{P_{CH3OH}}{P_{CH3OH}^{cp}} \right]}{\left(1 + K_h \left[\frac{P_{CH3OH}}{P_{CH3OH}^{cp}} \right] \right)^{n_h}} \quad (B11)$$

The net rates (defined as the difference between the gross rates of species i) were obtained as follows:

$$r_{CH3OH}^{net} = r_{CH3OH}^{gross} - r_{C2H5OH}^{gross} - r_{HC}^{gross} \quad (B12)$$

$$r_{C2H5OH}^{net} = r_{C2H5OH}^{gross} - r_{C3H7OH}^{gross} \quad (B13)$$

$$r_{C3H7OH}^{net} = r_{C3H7OH}^{gross} \quad (B14)$$

$$r_{HC}^{net} = r_{HC}^{gross} \quad (B15)$$

Gunturu et al. used a fugacity correction factor $K_z = 0.3359$ estimated by nonlinear regression.

On the other hand a value of K_z for the reaction (B1) estimated from the literature [8] at a

pressure of 54 atm and temperature of 598 K is 0.84. So, in order to use a fugacity correction factor closer to chemical reality we decided to replace K_z of Gunturu with the new value 0.84.

Using this value of K_z and the parameter estimates from Gunturu's article, summarized in Table B1, we calculated gross and net rates of formation of methanol, ethanol, propanol and hydrocarbons for all the experimental runs reported in Gunturu's paper.

Table B1. Parameters published in [6] for Methanol, Ethanol, Propanol and Hydrocarbon Synthesis Model ^a.

$A_m=4.9047$	$E_m=117.733$	$K_1=0.0696$	$K_2=0.6400$	$K_3=0.6940$	$n_m=2$
$K_z=0.8359$					
$A_e=1.5259$	$E_e=24.986$	$K_e=0.7367$	$n_e=1$		
$A_p=0.1101$	$E_p=89.943$	$K_p=0.2502$	$n_p=1$		
$A_h=4.6928$	$E_h=95.416$	$K_h=1.2472$	$n_h=1$		

^a A_m, A_e, A_p, A_h [mol/h/kg_{cat}], E_m, E_e, E_p, E_h [kJ/mol], all other parameters are dimensionless.

A comparison of the calculated and experimental values of the net rates of formation of all the species cited in the Gunturu's article is reported in the parity plots of Figures B1 – B4.

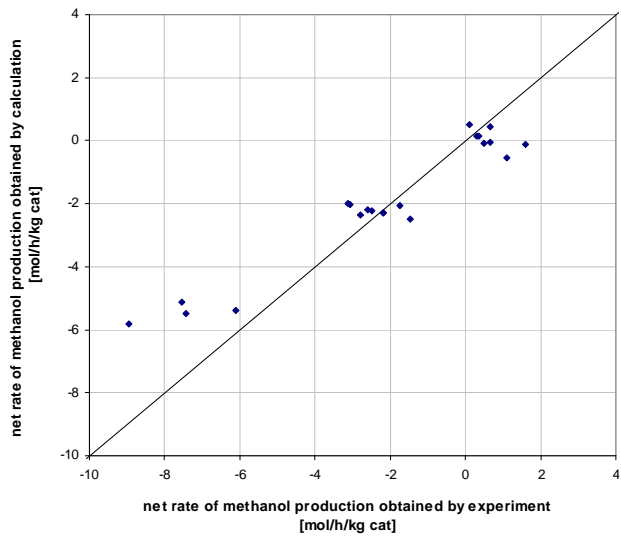


Figure B1. Parity plot for net rates of methanol production.

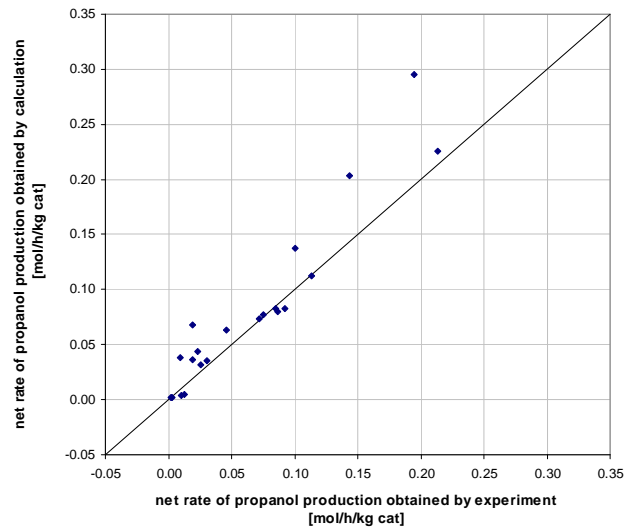


Figure B2. Parity plot for net rates of propanol production.

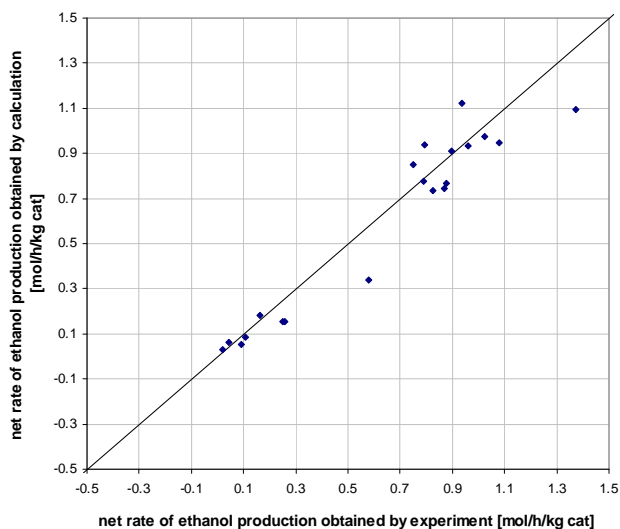


Figure B3. Parity plot for net rates of ethanol production.

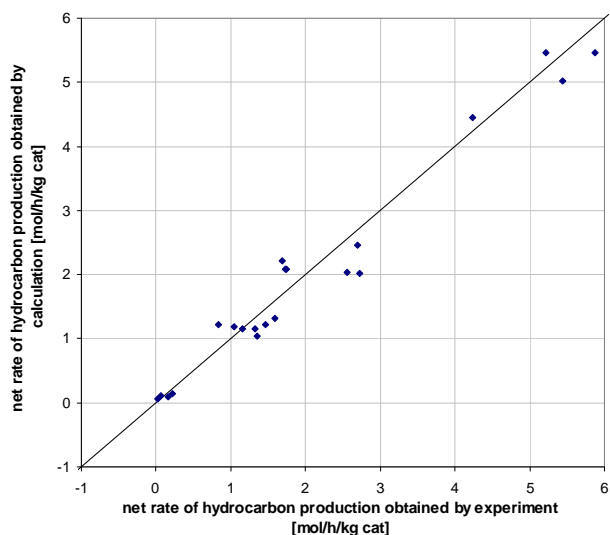


Figure B4. Parity plot for net rates of hydrocarbon production.

Figures B3 and B4 (parity plots for net rates of ethanol and hydrocarbon) are similar to the figures published in [6]. But in the case of figures B1 and B2 (plots for net rates of methanol and propanol) there results were somewhat at variance with those published in [6].

Hence a regression was performed using the experimental data of article [6] in order to obtain improved estimates of the parameters for methanol and propanol gross rates of formation.

We also implemented some additional changes concerning the parameter K_a used in these equations. In fact, in the article the values of the equilibrium constant K_a were given for the temperatures of 573, 598 and 623 K. We have replaced these values with the value of equilibrium constant K_a calculated as a function of temperature from equation B16 [8]. The new parameter estimates are shown in Table B2.

$$K_a = 0.99998 * \exp\left[21.225 + 9143.6/T - 7.492 * \ln T + 4.076E - 3 * T - 7.161E - 8 * T^2\right] \quad (\text{B16})$$

Table B2. Revised parameter estimates for the Methanol and Propanol Synthesis Model ^a.

$A_m=7.3117$	$E_m=143.472$	$K_1=7.6393E-9$	$K_2=0.6785$	$K_3=0.9987$	$n_m=3$
$K_z=0.8359$					
$A_p=0.1074$	$E_p=89.3328$	$K_p=0.6086$	$n_p=1$		

^a A_m, A_p [mol/h/kg_{cat}], E_m, E_p [kJ/mol], all other parameters are dimensionless.

Figures B5 and B6 show the parity plots for methanol and propanol obtained using the revised parameter estimates.

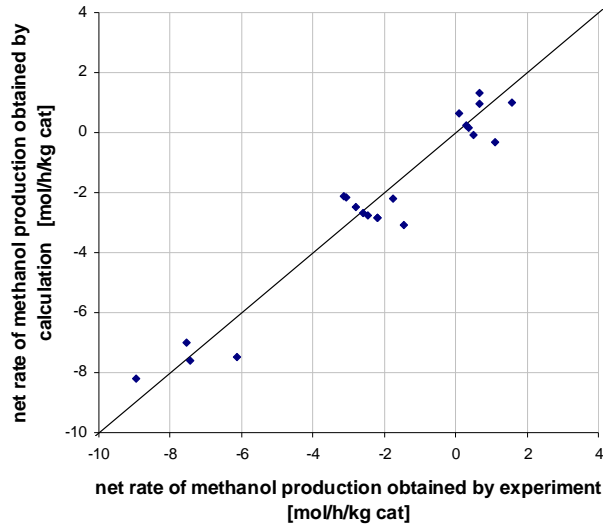


Figure B5. Comparison plot for net rates of methanol production: revised parameters in Table B2.

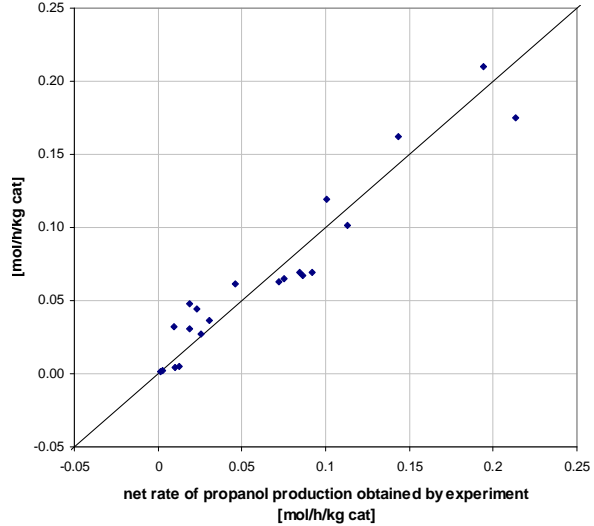


Figure B6. Comparison plot for net rates of propanol production: revised parameters in Table B2.

From these figures we can conclude that the new parameters allow a good fit of the experimental rate data from [6].

B.1.4 Reactor simulation and validation of the kinetic model

Once obtained “good” estimates of the kinetic parameters for methanol and higher alcohol synthesis, these were used to set up a Fortran program for simulation of the higher alcohols synthesis in ideal reactors. Both the options of perfectly-mixed reactor (CSTR) and plug-flow reactor (PFR) were considered.

The simulation program works with the following input data:

- Inlet flow rates of CO, H₂, N₂, methanol, ethanol, propanol and methane [kg/h]
- Temperature [K]
- Pressure [atm]
- Mass of catalyst [kg]
- Type of reactor (CSTR or PFR).

The simulation program used the subroutine LSODI [9] to integrate numerically a system of ordinary differential equations (reactor model for PFR case, system (a)) and the subroutine BUNLSI [10] to solve a system of nonlinear algebraic equations (reactor model for CSTR case, system (b)).

System (a):

$$\left\{ \begin{array}{l}
\frac{dF_{CO}}{dW_{cat}} = -2 \cdot r_{CH_3OH}^{gross} - r_{CH_4}^{gross} - 2 \cdot r_{C_2H_5OH}^{gross} - 2 \cdot r_{C_3H_7OH}^{gross} + r_{wgs} \\
\frac{dF_{H_2}}{dW_{cat}} = -r_{CH_3OH}^{gross} - r_{C_2H_5OH}^{gross} - r_{C_3H_7OH}^{gross} - r_{wgs} \\
\frac{dF_{CO_2}}{dW_{cat}} = r_{wgs} \\
\frac{dF_{H_2O}}{dW_{cat}} = r_{CH_4}^{gross} + r_{C_2H_5OH}^{gross} + r_{C_3H_7OH}^{gross} - r_{wgs} \\
\frac{dF_{CH_4}}{dW_{cat}} = r_{CH_4}^{gross} \\
\frac{dF_{CH_3OH}}{dW_{cat}} = r_{CH_3OH}^{gross} - r_{C_2H_5OH}^{gross} - r_{CH_4}^{gross} \\
\frac{dF_{C_2H_5OH}}{dW_{cat}} = r_{C_2H_5OH}^{gross} - r_{C_3H_7OH}^{gross} \\
\frac{dF_{C_3H_7OH}}{dW_{cat}} = r_{C_3H_7OH}^{gross} \\
\frac{dF_{N_2}}{dW_{cat}} = 0
\end{array} \right.$$

with initial conditions:

$$\left\{ \begin{array}{l}
F_{CO}(W_{cat} = 0) = F_{CO}^{IN} \\
F_{H_2}(W_{cat} = 0) = F_{H_2}^{IN} \\
F_{CO_2}(W_{cat} = 0) = F_{CO_2}^{IN} \\
F_{H_2O}(W_{cat} = 0) = F_{H_2O}^{IN} \\
F_{CH_4}(W_{cat} = 0) = F_{CH_4}^{IN} \\
F_{CH_3OH}(W_{cat} = 0) = F_{C_3OH}^{IN} \\
F_{C_2H_5OH}(W_{cat} = 0) = F_{C_2H_5OH}^{IN} \\
F_{C_3H_7OH}(W_{cat} = 0) = F_{C_3H_7OH}^{IN} \\
F_{N_2}(W_{cat} = 0) = F_{N_2}^{IN}
\end{array} \right.$$

where F_i^{IN} is the feed flow of the generic i-species [kmol/h] and W_{cat} the mass of catalyst [kg].

System (b):

$$\left\{ \begin{array}{l} \frac{F_{CO}^{OUT} - F_{CO}^{IN}}{W_{cat}} = -2 \cdot r_{CH_3OH}^{gross} - r_{CH_4}^{gross} - 2 \cdot r_{C_2H_5OH}^{gross} - 2 \cdot r_{C_3H_7OH}^{gross} + r_{wgs} \\ \frac{F_{H_2}^{OUT} - F_{H_2}^{IN}}{W_{cat}} = -r_{CH_3OH}^{gross} - r_{C_2H_5OH}^{gross} - r_{C_3H_7OH}^{gross} - r_{wgs} \\ \frac{F_{CO_2}^{OUT} - F_{CO_2}^{IN}}{W_{cat}} = r_{wgs} \\ \frac{F_{H_2O}^{OUT} - F_{H_2O}^{IN}}{W_{cat}} = r_{CH_4}^{gross} + r_{C_2H_5OH}^{gross} + r_{C_3H_7OH}^{gross} - r_{wgs} \\ \frac{F_{CH_4}^{OUT} - F_{CH_4}^{IN}}{W_{cat}} = r_{CH_4}^{gross} \\ \frac{F_{CH_3OH}^{OUT} - F_{CH_3OH}^{IN}}{W_{cat}} = r_{CH_3OH}^{gross} - r_{C_2H_5OH}^{gross} - r_{CH_4}^{gross} \\ \frac{F_{C_2H_5OH}^{OUT} - F_{C_2H_5OH}^{IN}}{W_{cat}} = r_{C_2H_5OH}^{gross} - r_{C_3H_7OH}^{gross} \\ \frac{F_{C_3H_7OH}^{OUT} - F_{C_3H_7OH}^{IN}}{W_{cat}} = r_{C_3H_7OH}^{gross} \\ \frac{F_{N_2}^{OUT} - F_{N_2}^{IN}}{W_{cat}} = 0 \end{array} \right.$$

The Fortran code included the system of kinetic equations described above (eq.s B6, B9-B11). In addition we inserted the water-gas shift reaction, with rate equation (17), into the model:

$$r_{wgs} = k_{wgs} (p_{CO} p_{H_2O} - 1/K_{weq} p_{CO_2} p_{H_2}) \quad (B17)$$

The equilibrium constant for the water gas shift reaction was calculated as a function of temperature according to equation (B18) [11].

$$K_{weq} = 1 / \exp \left[13.148 - 5639.5/T - 1.077 \cdot \ln T - 5.446E-4 \cdot T - 1.1251E-7 \cdot T^2 + 49170/T^2 \right] \quad (B18)$$

The rate constant of water gas shift reaction k_{wgs} was arbitrarily assumed to have the value 10000 kmol/h/kgcat/atm². It was verified, that in both cases (PFR reactor and CSTR reactor) the water-gas shift reaction was essentially at equilibrium under these conditions.

Figure B7 compares the CO conversions calculated using the CSTR (open symbols) and PFR (solid symbols) models with the data of Gunturu [6]. The two experimental data reported in the figure were obtained under the same experimental conditions ($T = 623$ K, $p = 54$ atm, GHSV = 9000 L/h/kgcatalyst, H_2/CO ratio = 1/1, mass of the catalyst 0.5 g), with and without the

addition of methanol in the feed flow (at a flow rate of 0.02 ml/min). In both cases, from the parity plot in figure B7 it is clear that the experimental CO conversion is underestimated by the model. Notably, due to the very limited CO conversions no significant differences are apparent using either the CSTR or the PFR models.

We have attempt to improve the model fit of CO conversion by multiplying the gross rates by a constant factor equal to 1.5 (triangles) and 2 (circles), respectively.

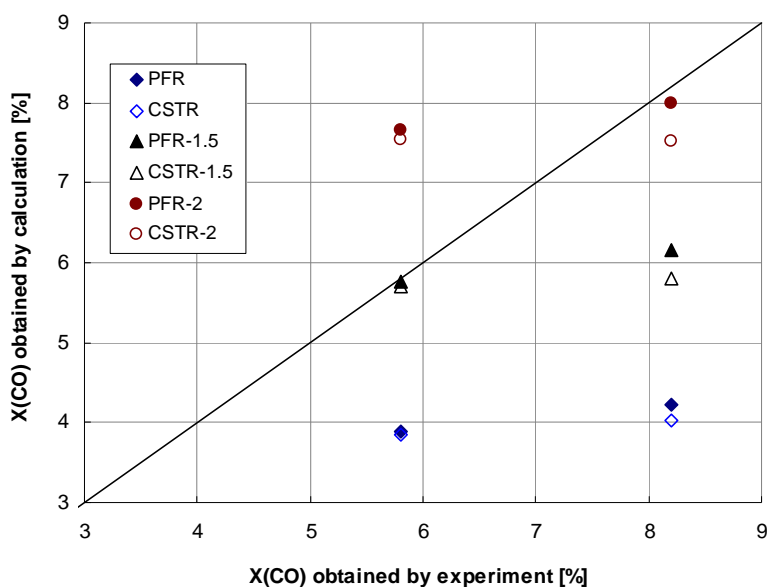


Figure B7. Parity plot for CO conversion - X(CO) of data form Gunturu using the gross rates without modification, the gross rates multiplied by the constant factor equal to 1.5 and 2, respectively.

Multiplying all the gross rates by 1.5 the fit improved. However it is difficult to evaluate the goodness of our result using the data from Gunturu because only two CO conversion values (out of 21 runs) are available in the paper.

Due to this reason, in order to better verify the validity of our simulation results, we used data from two additional papers, i.e. Li et al. [12] and Yun Park et al. [13].

Li et al. [12] used in his work a series of carbon-supported molybdenum-based catalysts for higher alcohols synthesis from synthesis gas. One of these used catalysts was also a catalyst with the same content of Mo (18 wt. %), the same ratios of K/Mo (1.3) and Co/Mo (0.34) and prepared in the same way as the catalyst used in [6] (except the way of sulfidation of the catalyst before the catalytic reaction, but also it was similar to Gunturu). Since Li et al. [12] work in the same Department of Gunturu (West Virginia University) it is likely that the same catalyst was used. However Li et al. tested the catalyst in a stainless-steel tubular reactor, the reaction temperature was varied from 200 to 400 °C, the total pressure was 51 atm (750 psig), CO/H₂ ratio was 1/1, GHSV varied from 6 to 21.6 m³/h/kg of catalyst (from 267.7 to 963.7 mol/h/kgcat) and the mass of the catalyst was 0.5 g.

In Figure B8 the results of calculation of CO conversion for data from Li et al. [12] for a PF and a CST reactor model (solid and open symbols, respectively) are compared with the published experimental data. The model clearly underestimated the experimental data. For this reason, as previously done with the data of Gunturu, we multiplied the gross rates by a constant factor equal to 1.5 (figure B9) and 2 (figure B10), respectively.

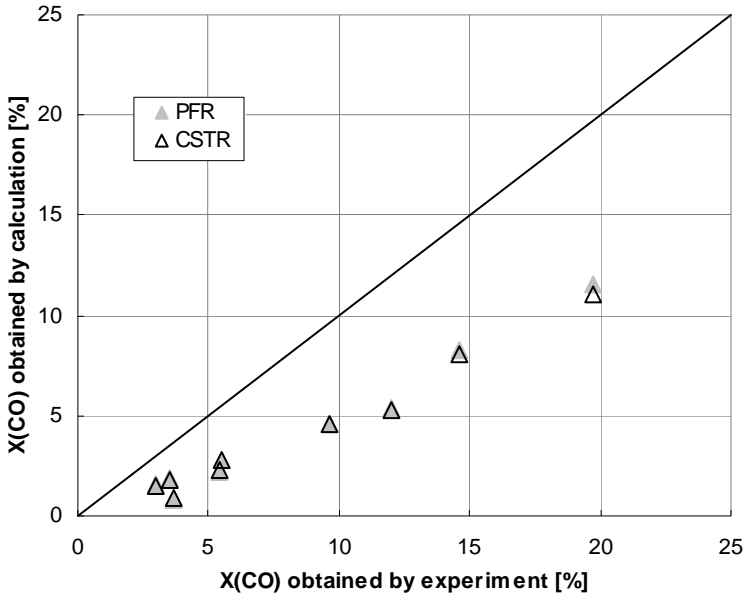


Figure B8. Parity plot for CO conversion - X(CO) calculated for PFR (solid points) and CSTR (open points) reactor on the basis of data from Li (Gunturu catalyst).

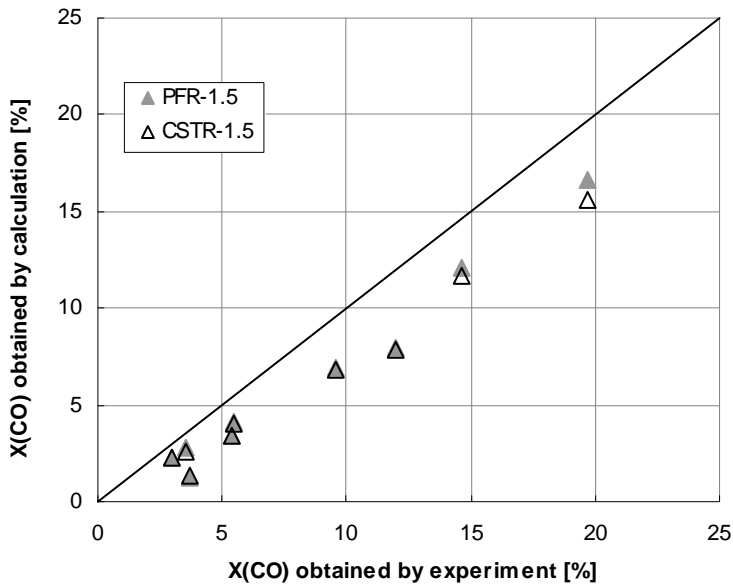


Figure B9. Parity plot for CO conversion - X(CO) of data from Li for Gunturu catalyst using the gross rates multiplied by the constant factor 1.5.

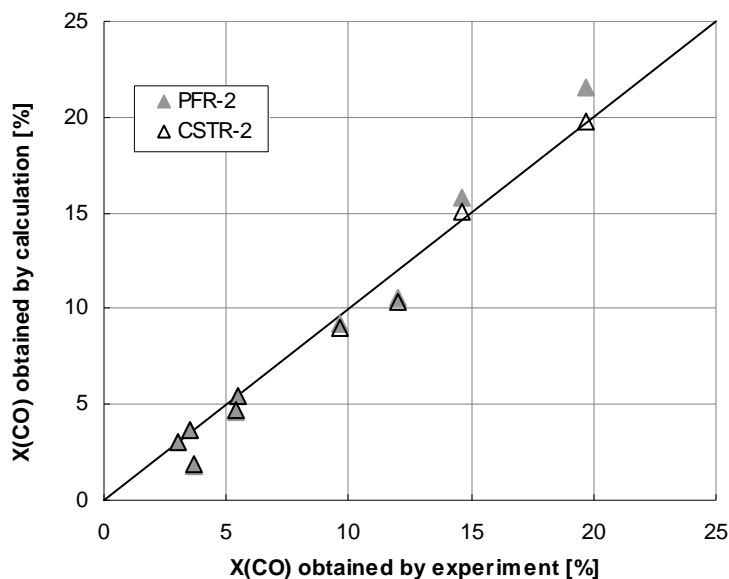


Figure B10. Parity plot for CO conversion - $X(\text{CO})$ of data from Li for Gunturu catalyst using the gross rates multiplied by the constant factor 2.

The best agreement between experimental and calculated data for both reactor models was obtained multiplying the gross rates by a constant factor equal to 2 (figure B10).

Yun Park et al. [13], on the contrary, used in their study a K/MoS_2 catalyst with a K_2CO_3 content of 17 wt. %. The alcohol synthesis reaction was carried out in a tubular fixed-bed integral reactor.

The reaction temperature was varied in the range 250-350 °C, the total pressure was varied from 15-90 atm, the space time $W/(\text{FCO})_0$ or τ was varied between 4-22 $\text{gcat}\cdot\text{h}/\text{mol}$ ($\text{GHSV} = 250\text{-}45 \text{ mol/h/kgcat}$), with the H_2/CO molar feed ratio ranging from 0.5 to 4 and with a catalyst mass of 1.0 g.

In Figure B11 the calculated CO conversion for data from Yun Park [13] for PF and CST reactor models (solid and open symbols, respectively) are compared with the published experimental data. The experimental data, as for the Gunturu [6] and the Li [12] data, are clearly underestimated.

The results obtained by multiplying the gross rates by a factor of 1.5 or 2 are shown in figures B12 and B13, respectively. In this case the best fit was observed using a factor equals to 1.5; however, considering that Yun Park [13] used in his work a different catalyst with respect to Gunturu's and Li's catalyst, the results obtained by using the factor 2 appear also very reasonable.

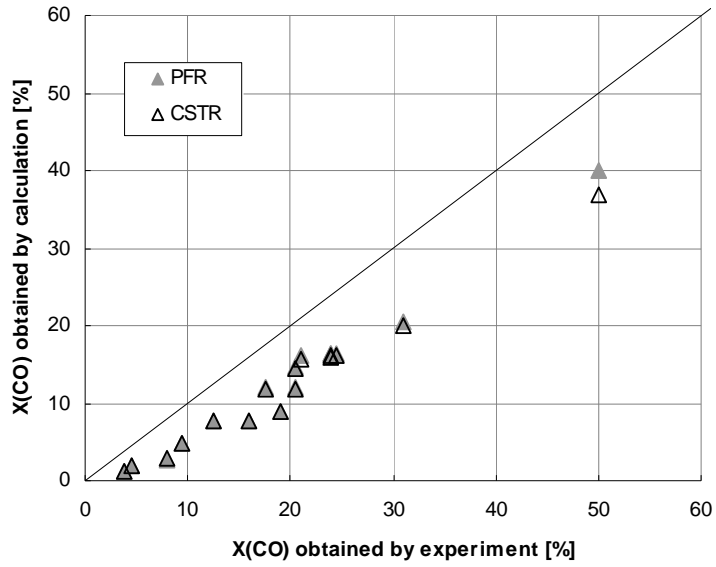


Figure B11. Parity plot for CO conversion - X(CO) of data from Yun Park catalyst.

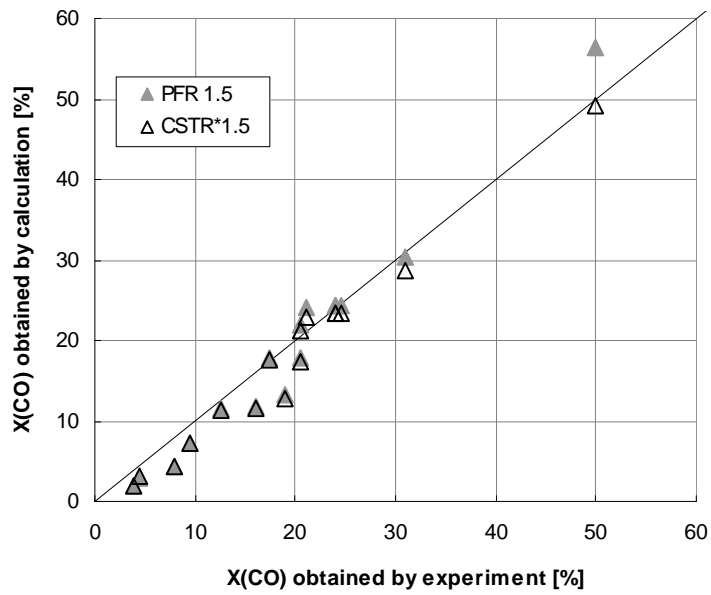


Figure B12. Parity plot for CO conversion - X(CO) of data from Yun Park catalyst - the rates of every components multiplied by 1.5.

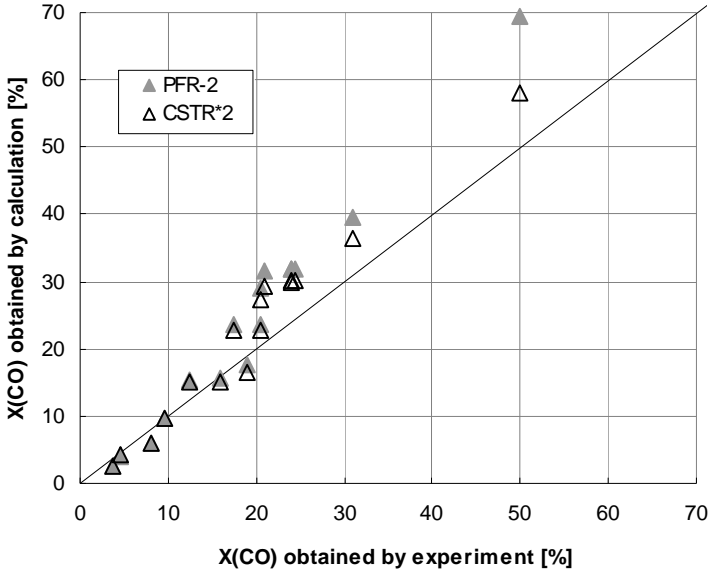


Figure B13. Parity plot for CO conversion - X(CO) of data from Yun Park catalyst– the rates of every components multiplied by 2.

As a conclusion, in the kinetic scheme the gross rates originally estimated from Gunturu’s paper [6] have been multiplied by a factor equal to 2. In particular, the pre-exponential factors in the rate constants (the parameters A_i) of the gross rate equations have been multiplied by 2.

These results are probably close to the best ones which is possible to obtain from the available data sets. In order to develop a more accurate kinetic model, a dedicated experimental work is required.

In any case, the final parameter estimates obtained from the available data for the methanol, ethanol, propanol and hydrocarbon formation rates are collected in table B3.

Table B3. Final parameter estimates for the Methanol, Ethanol, Propanol and Hydrocarbons Synthesis Model ^a.

$A_m=14.6233$	$E_m=143.472$	$K_1=7.6393E-9$	$K_2=0.6785$	$K_3=0.9987$	$n_m=3$
$K_z=0.8359$					
$A_e=3.0518$	$E_e=24.986$	$K_e=0.7367$	$n_e=1$		
$A_p=0.2148$	$E_p=89.3328$	$K_p=0.6086$	$n_p=1$		
$A_h=9.3856$	$E_h=95.416$	$K_h=1.2472$	$n_h=1$		

^a A_i [mol/h/kg_{cat}], E_i [kJ/mol], all other parameters are dimensionless.

B.1.5 Simulation study of the effects of the operating variables

In order to point out the effects of reaction conditions on both CO conversion and final product distribution we performed reactor simulations under the following conditions:

Temperature = 553-623 K

Pressure = 30-160 bar

H₂/CO ratio = 1.2

GHSV = 155 - 51.7 mol/h/kg_{cat}

The results of these calculations are shown in figures B14 and B15.

CO conversion increases with increasing temperature and pressure and with decreasing GHSV, as expected.

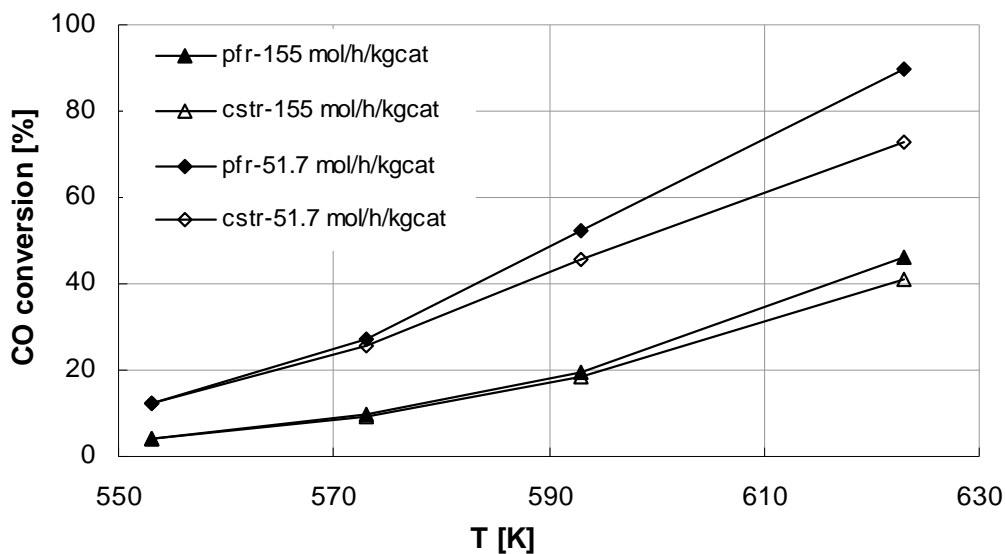


Figure B14. CO conversion, X_{CO} , calculated for PFR (solid symbols) and CSTR (open symbols) reactor models at 134.7 atm, H_2/CO ratio = 1.2 and GHSV equal to 155 and 51.7 mol/h/kg_{cat}.

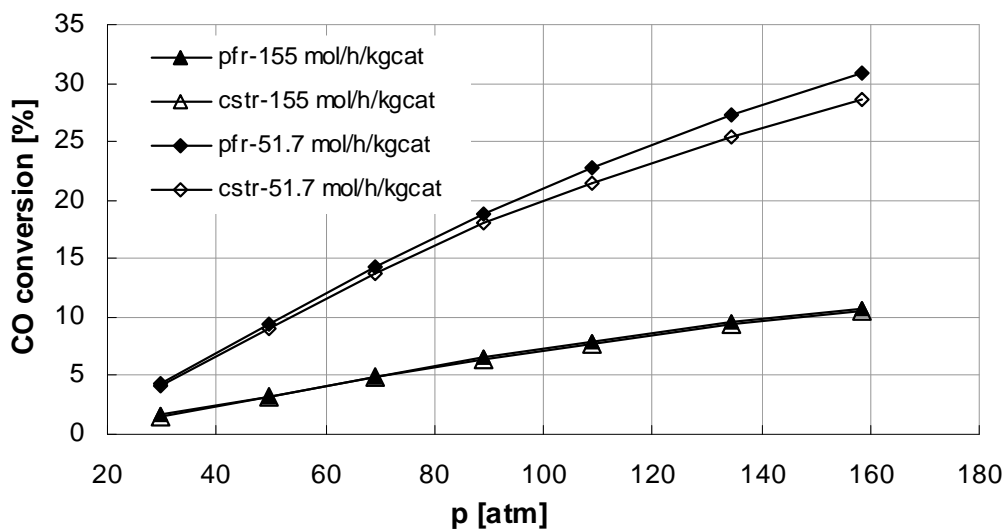


Figure B15. CO conversion, X_{CO} , calculated for PFR (solid symbols) and CSTR (open symbols) reactor models at 573 K, H_2/CO ratio = 1.2 and GHSV equal to 155 (triangles) and 51.7 (diamonds) mol/h/kg_{cat}.

It is of interest to analyze the results in term of productivity of the various species upon changing temperature (see Figure B16) and pressure (see Figure B17) as well as space velocity.

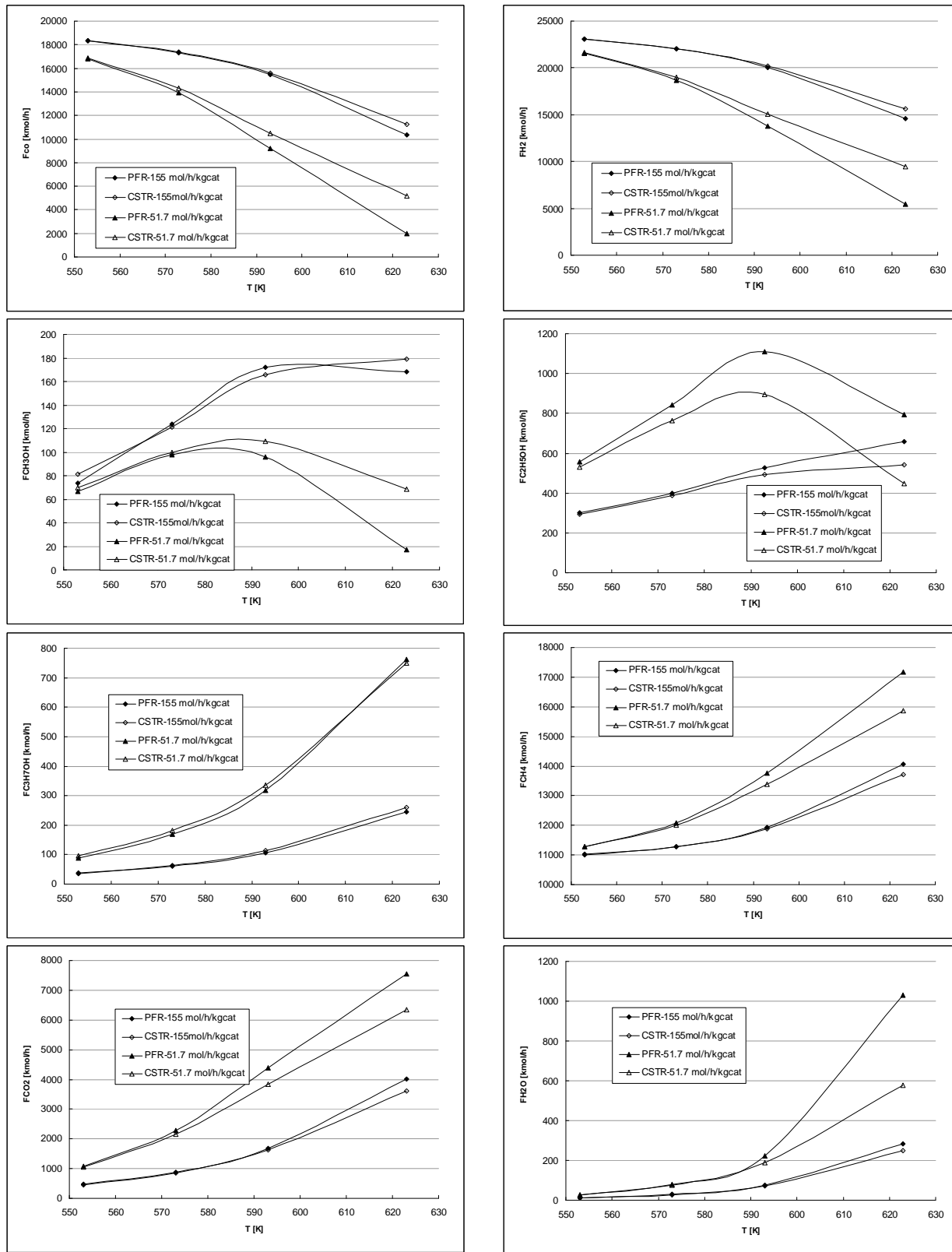


Figure B16. Outlet flow of CO, H₂, CH₃OH, C₂H₅OH, C₃H₇OH, CH₄, CO₂ and H₂O calculated for PF (solid symbols) and CST (open symbols) reactors with varying temperature at the following conditions: Pressure= 134.7 atm, H₂/CO ratio= 1.2 and GHSV= 155 (triangles) and 51.7 (diamonds) mol/h/kg_{cat}.

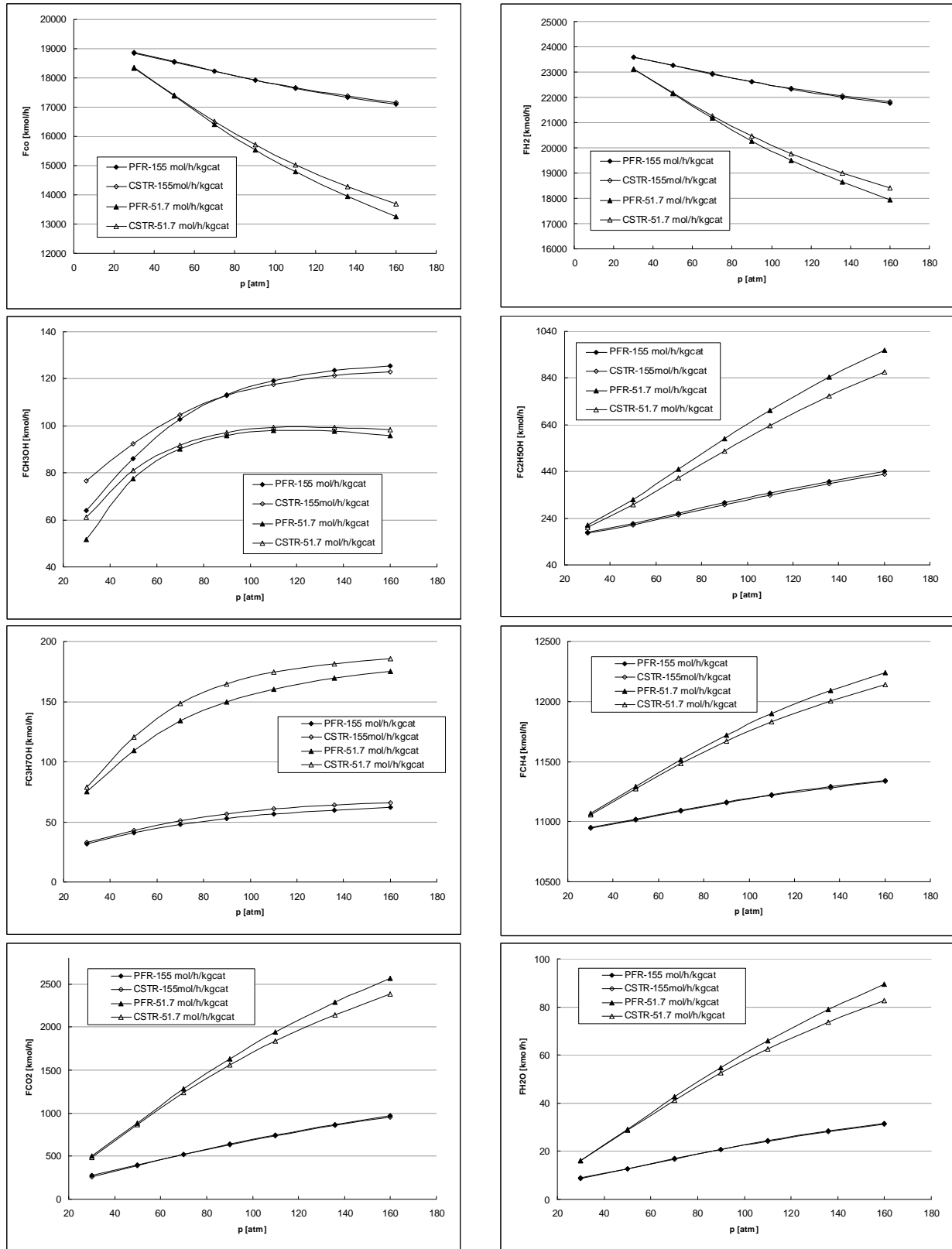


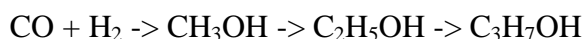
Figure B17. Outlet flow of CO, H₂, CH₃OH, C₂H₅OH, C₃H₇OH, CH₄, CO₂ and H₂O calculated for PF (solid symbols) and CST (open symbols) reactors with varying pressure at the following conditions: Temperature= 573K, H₂/CO ratio= 1.2 and GHSV= 155 (triangles) and 51.7 (diamonds) mol/h/kg_{cat}.

From Figure B16 it is clear that it is possible to increase the CO and the H₂ conversion simply by increasing the temperature and decreasing the GHSV. In addition, from Figure B16 it is evident that, working at fixed temperature and decreasing the GHSV, it is possible to maximize the selectivity to C₂+ alcohols. In the same manner, it is clear that increasing the temperature, at fixed GHSV, it is possible to maximize the C₃H₇OH selectivity.

These trends are typical of chemical systems in which there are consecutive reactions, i.e. reactions following the generic scheme:



In the case of the mixed alcohols synthesis, in particular, this generic scheme can be written as the sum of the two following reactions paths:



This means that methanol and ethanol are intermediates compounds in the higher alcohols synthesis reaction, so their outlet flows depend, as it is also clear from the balance equations (12-13), from the rates of formation of methanol, ethanol and methane in the case of methanol and from both the rates of formation of ethanol and propanol in the case of ethanol.

So, the effect of the temperature on the net reaction rate of these components (i.e. the outlet flows of these compounds) is complex, deriving from the linear combination of more than one “Arrhenius-type” equations. This justifies the graphs reported in Figure B16, which show a maximum in the outlet flow of methanol and ethanol with respect to the temperature.

Concerning the effects of pressure, from Figure B17 it is clear that increasing pressure results in higher conversions of the reactants and, in the investigated range, also in higher alcohols selectivities.

This monotonic and limited effect of the pressure on the CO conversion and alcohols selectivity can be ascribed to the limited effect of the pressure on the kinetic laws of the reactions involved in the mixed alcohols synthesis and it evidences that the temperature and the GHSV are the two major parameters to vary in order to optimize both the CO conversion and the higher alcohols selectivity.

B.1.6 Implementation of the kinetic model in a Fortran subroutine

On the basis of the received template USRKIN.f, we have developed two different Fortran codes to be interfaced with the process simulator ASPEN. Such routines are able to evaluate the gross rates of formation of CO, H₂, CH₃OH, C₂H₅OH, C₃H₇OH, CH₄, H₂O and CO₂ in a multitubular plug flow reactor and in a continuous stirred tank reactor on the basis of the following parameters supplied by Aspen:

- Molar fraction of the inlet components
- Temperature [K]
- Pressure [Pa]
- Mass of catalyst [kg]

In the program we used the system of kinetic equation represented by eq.s 6, 9-11, with parameter estimates as in Table B3. In addition we inserted into the model the water-gas shift reaction, with rate equation (17). The equilibrium constant for the water gas shift reaction was calculated as a function of temperature according to equation (18) [11].

B.1.7 Comparison between the results obtained using ASPEN and the Fortran program

In order to check the subroutine developed and its correct interface with Aspen, we simulated the two PF and CST reactors for a set of conditions supplied by Xun Wang, i.e.:

Temperature = 573 K

Pressure = 136 bar

Feed flow rates [kmol/s]:

H ₂	6.5691
CO	5.3216
Ar	0.369
N ₂	1.1275
CO ₂	0.0336
H ₂ O	0.0012
CH ₄	3.0101
METHANOL	0.03312359
ETHANOL	0.04081143
PROPANOL	0.00349779

The obtained CO conversion data, as well as the calculated product distributions are reported in table B4. The same table also shows the results calculated by Xun Wang using Aspen.

Table B4. The product distribution calculated for PF reactor with Aspen and with the Fortran code, for the reaction condition reported above

	Aspen (kmol/s)	Fortran (kmol/s)
CO	4.8099	4.8136
CO ₂	0.2435	0.2428
H ₂	6.0559	6.1102
Ar	0.369	1.6547*
N ₂	1.1275	
H ₂ O	0.0079	0.0079
CH ₃ OH	0.0344	0.0343
C ₂ H ₅ OH	0.1113	0.1113
C ₃ H ₇ OH	0.0167	0.0166
CH ₄	3.1298	3.1369
X _{CO} (%)	9.62	9.58

* In the FORTRAN code we used only one species representing all the inert gases together i.e., the lump of nitrogen and argon.

From the data reported in Table B4 it can be concluded that the two programs leads to essentially the same results.

We note that all calculations were performed for single-pass process (i.e., with no recycle). In the case of the presence of a recycle, large quantity of CO₂ would be present in the feed. Although the literature sources we have worked with did not investigate the effect of CO₂

content in the feed on the behaviour of the catalyst, it is likely that this compound affect the activity of the catalyst.

As matter of facts, the inhibiting effect of the presence of CO₂ in the feed on the higher alcohol synthesis has been demonstrated for a ZnCrO+15%Cs₂O catalyst [2]. In this case, the presence of 6% CO₂ in the feed depresses the yield of higher alcohols by a factor of three. Methanol formation is only marginally affected, however, so that the relative content of higher alcohol with respect to methanol is greatly reduced. It is also worth noticing that the presence of carbon dioxide in the feed causes greater amounts of water to be produced via the water gas shift reaction. The inhibiting effects of the CO₂ were explained by assuming that water rather than CO₂ inhibits the HAS reaction by competing for adsorption with the intermediate C1-species on the catalyst surface.

B.1.8 Conclusions

On the basis of a kinetic analysis reported in the literature for the synthesis of higher alcohols from CO/H₂ mixtures over a Mo-based catalyst [6], a Fortran subroutine to be integrated in Aspen able to estimate the rate of formation of the main products of the synthesis (i.e. methanol, ethanol, propanol, methane, carbon dioxide and water) was developed.

The ability of the lumped kinetic model to predict the CO conversion and the product distribution of the higher alcohol synthesis over Mo-based catalysts was validated against experimental data measured at different reaction conditions (type of reactor, catalyst, T, P, inlet flows, GHSV) obtained from various literature sources [6, 12, 13].

Finally, an analysis of the effect of temperature and pressure on the CO conversion and on the products distribution was performed. It was so verified that higher temperature and pressure and lower space velocities have a positive effect on the conversion of CO. The optimization of the process conditions, however, should be performed also on the basis of the products selectivities, that exhibit a complex trend with increasing temperature and pressure.

The lumped kinetic model has been implemented in a FORTRAN subroutine which has been successfully interfaced with the ASPEN process simulation program.

B.2 Additional results and model validation

B.2.1 Introduction

In our previous paragraphs of Appendix B we have discussed the results of a Fortran subroutine developed on the basis of a lumped kinetic analysis described in the literature [12] for the synthesis of higher alcohols from CO/H₂ mixtures over a Mo-based catalyst. The derived kinetics were able to estimate the rates of formation of the main products of the synthesis (i.e. methanol, ethanol, propanol, methane, carbon dioxide and water).

The ability of the lumped kinetic model to predict the CO conversion in the higher alcohol synthesis over Mo-based catalysts was validated against experimental data measured at different reaction conditions (type of reactor, catalyst, T, P, inlet flows, GHSV) obtained from various literature sources [6, 12, 13]. In our previous report we have shown that in order to obtain good fits of CO conversion the gross rates must be multiplied by a factor equal to 2. In this way we were able to achieve a good fit of the experimental CO conversion data from three different sources [6, 12, 13].

However, in our previous report we did not fully analyze the products distribution. It is the goal of the present addendum to investigate whether the introduction of the above mentioned factor is suitable to simulate the product distribution as well.

B.2.2 Validation of the kinetic model

Figures B18 and B19 show the comparison of experimental data (points) published in [12] with the simulations obtained by multiplying the gross rates by a factor 1 (1*PFR, i.e. without modifications) and a factor 2 (2*PFR) (experimental conditions are reported in the figure captions). Upon comparison of figures B18 and B19 we can conclude that multiplication of the gross rates by a constant factor of 2 has a positive effect not only on the prediction of CO conversion (see paragraphs B.1) but also on the prediction of the product distribution of alcohols. Indeed the yields of mixed alcohols is better estimated, even though a worse fit of the selectivity to mixed alcohols and yields of HC is obtained if compared to the case of 1*PFR.

In order to improve the prediction of the product distribution we have tried to change again the multiplication factor for gross rates of individual products. We have observed that the best fit of experimental data can be obtained using a multiplication factor of 2 for the gross rates of methanol, ethanol and propanol, and a multiplication factor of 1 for the gross rates of hydrocarbons (2*Alcohols, 1*HC). The results obtained with these multiplication factors are shown in figure B20. In this case also for the mole fraction of individual alcohols we have observed a good fit of experimental data [12].

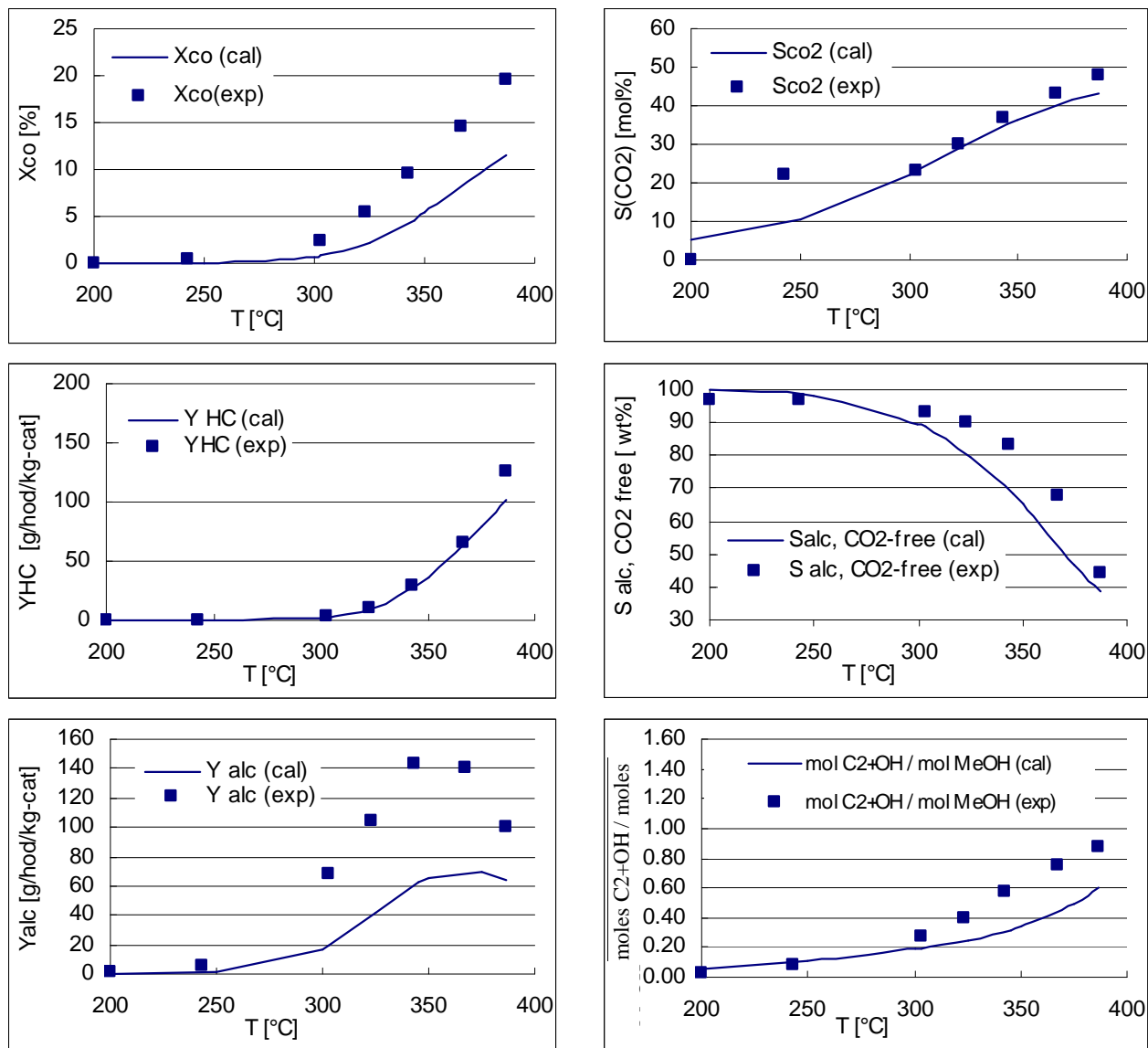


Figure B18. Comparison of experimental [12] and calculated data. Calculated data have been obtained for PF reactor using the gross rates of products without modifications (1*PFR). Experimental conditions: 51 atm, 0.5g cat., H₂=CO=25ml/min (268mol/h/kg-cat.). The following parameters are reported: X_{CO} , conversion of CO; Y_{HC} and Y_{alc} , space-time yields of hydrocarbons and total alcohols (CO₂-free basis), respectively; and $C_{2+OH} / MeOH$, molar ratio of higher alcohols to methanol.

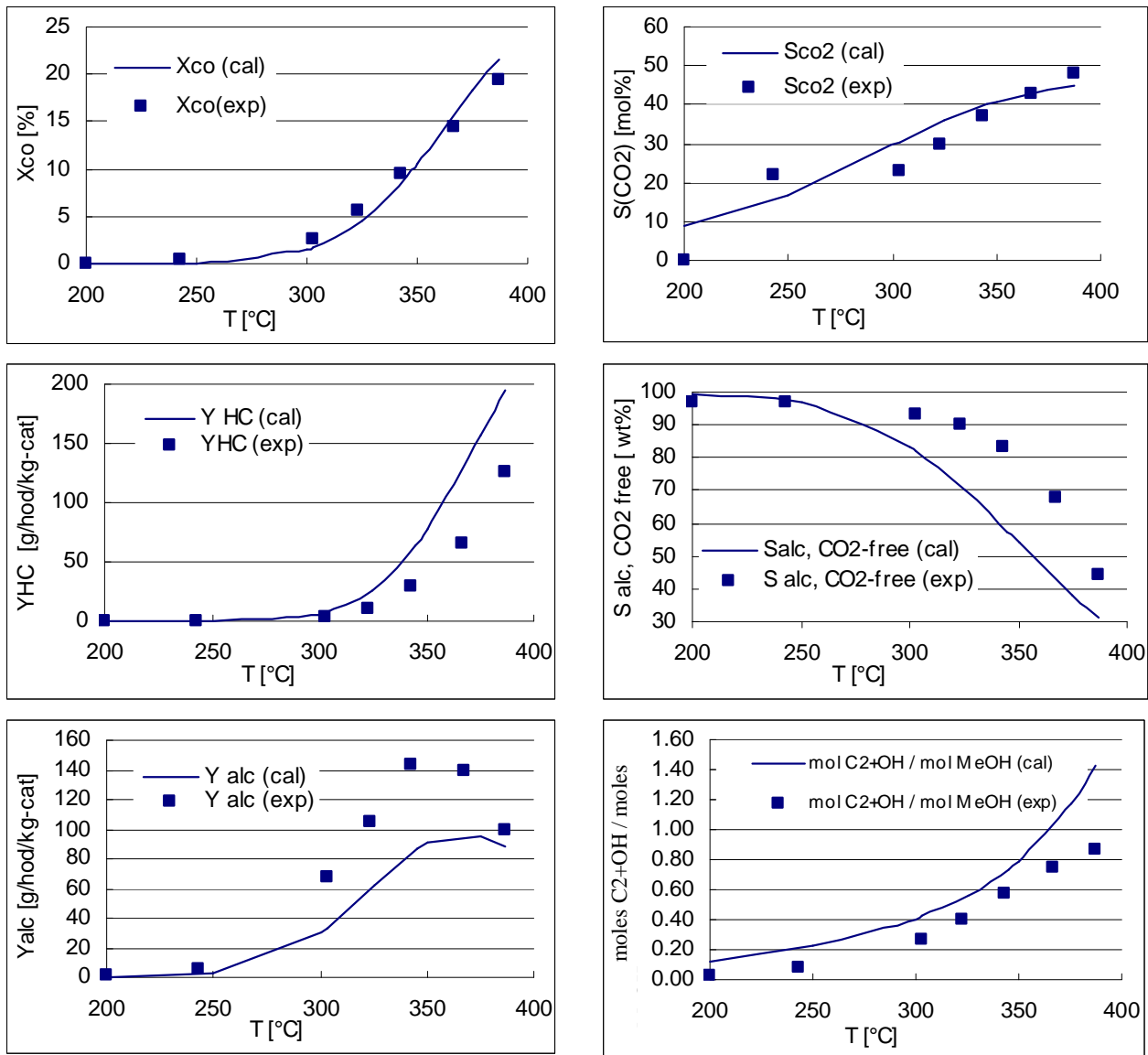


Figure B19. Comparison of experimental [12] and calculated data. Calculated data have been obtained for PF reactor using the constant factor of 2 for multiplication of the gross rates of all the species involved in the mechanism ($2 \cdot PFR$). Experimental conditions: 51 atm, 0.5g cat., $H_2=CO=25\text{ml/min}$ (268mol/h/kg-cat). Catalyst parameters are as defined in figure B18.

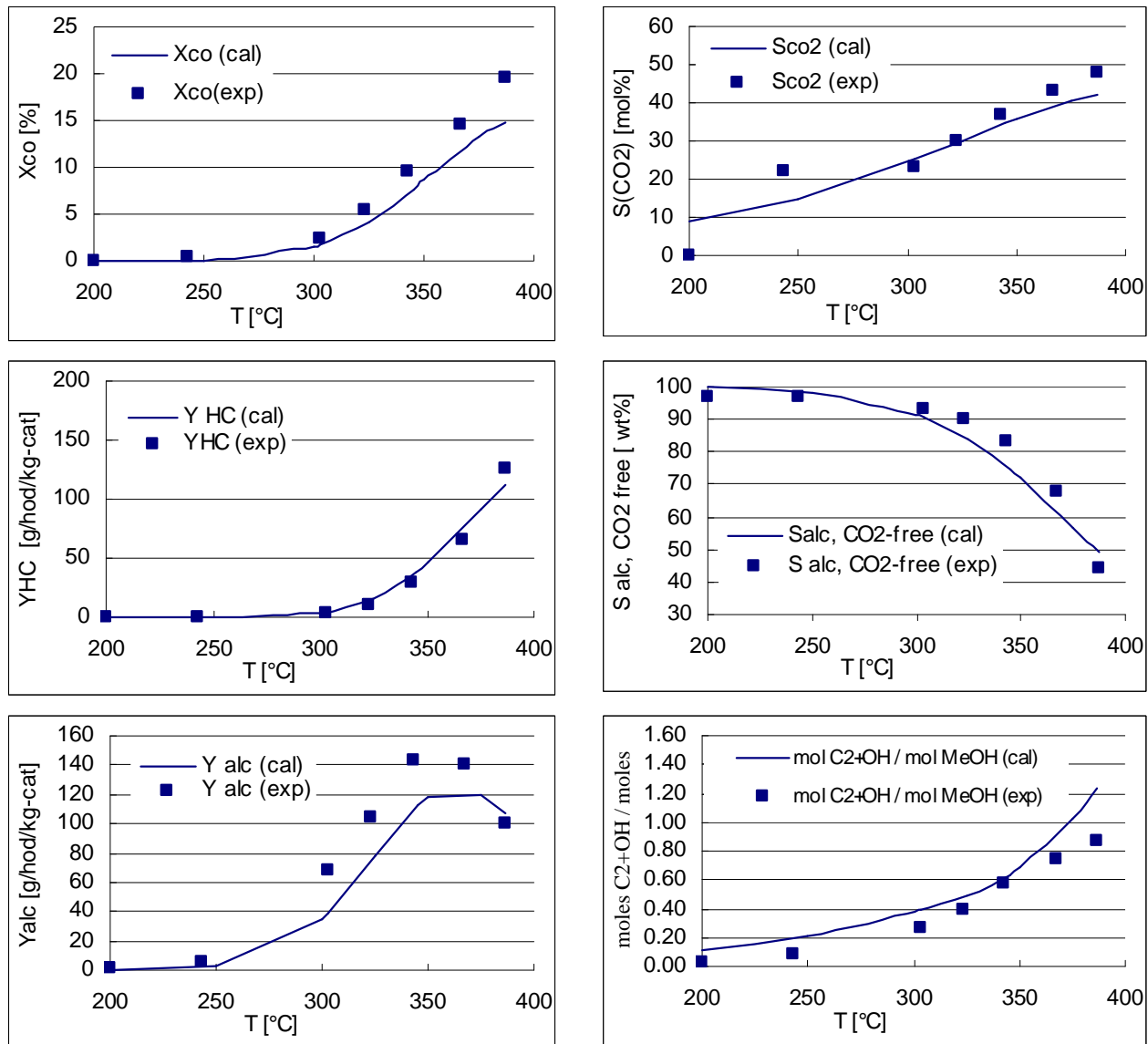


Figure B20. Comparison of experimental [12] and calculated data. Calculated data have been obtained for PF reactor using the constant factor of 2 for multiplication of the gross rates of all the alcohols and factor of 1 for gross rate of hydrocarbons ($2 \cdot \text{Alcohols}$, $1 \cdot \text{HC}$). Experimental conditions: 51 atm, 0.5g cat., $\text{H}_2 = \text{CO} = 25 \text{ ml/min}$ (268 mol/h/kg-cat). Catalyst parameters are as defined in figure B18.

Figures B21, B22 and B23 show the comparison between the experimental data (points) published in [13] and the calculated data (experimental conditions are reported in the figure captions). Calculated data have been obtained using the multiplication factors reported in the figure captions. In figures B21-B23 XCO is the CO % conversion, XCO₂ the CO₂ % yield, ΣX_{pi} the paraffins yield, ΣX_{ai} the mixed alcohols yield, defined as [13]:

$$X_{ij} = (\text{moles of CO consumed to produce } i \text{ component group with carbon number } j) / (\text{moles of CO fed to the reactor})$$

From the comparison the results obtained using 1*PFR and 2*PFR (figures B21 and B22, respectively) it is concluded that the model predictions obtained using 1*PFR underestimates the CO conversion and the selectivity to CO₂, while the prediction of selectivity to paraffins and alcohols for these experimental condition was quite good. On the other hand, when using the

multiplication factor of 2 the CO conversion is overestimated along with the selectivity to alcohols, whereas the selectivity to CO₂ (and hydrocarbons) are satisfactory.

Finally, we have also attempted in this case to improve the prediction of product distribution by multiplying the gross rate of methanol, ethanol and propanol by constant factor of 2 and that of hydrocarbons by a factor of 1 (2*Alcohols, 1*HC). The results obtained in this case are shown in figure B23. The new set of multiplication factors was able to predict nicely the experimental data, but for the selectivity to total alcohols. Also the selectivity of the individual alcohols are not adequately fitted (results not shown).

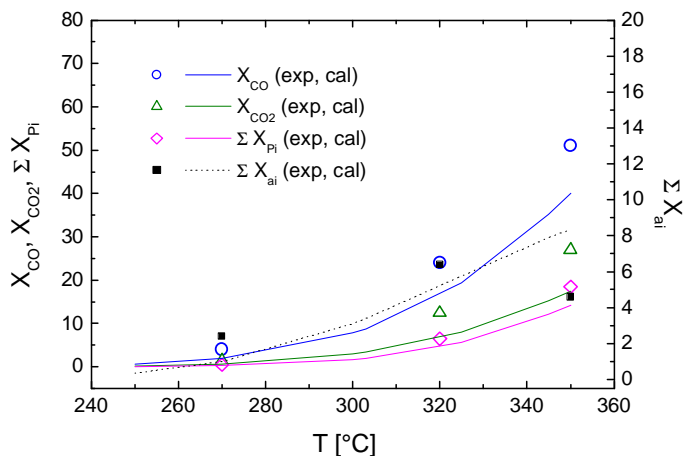


Figure B21. Comparison of experimental [13] and calculated data. Calculated data have been obtained for PF reactor using the gross rates of products without modifications (1*PFR). Experimental conditions: 90 atm, 1 g cat., H₂/CO=1.01 (17.1 g-cat .h/mol, 58.48 mol/h/kg-cat).

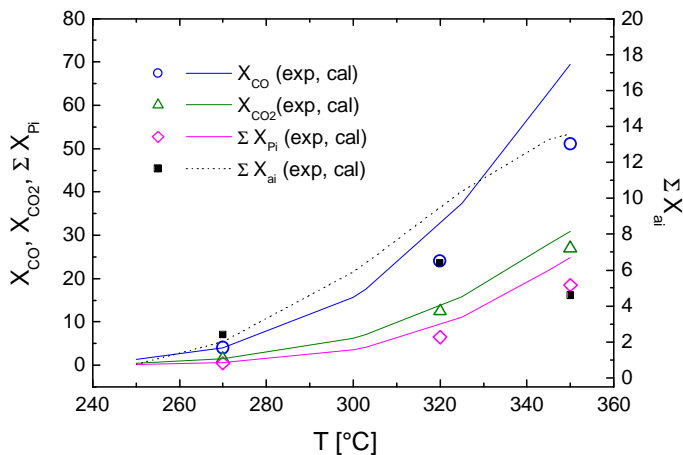


Figure B22. Comparison of experimental [13] and calculated data. Calculated data have been obtained for PF reactor using the constant factor of 2 for multiplication of the gross rates of all species involved in the mechanism (2*PFR). Experimental conditions: same as figure B21.

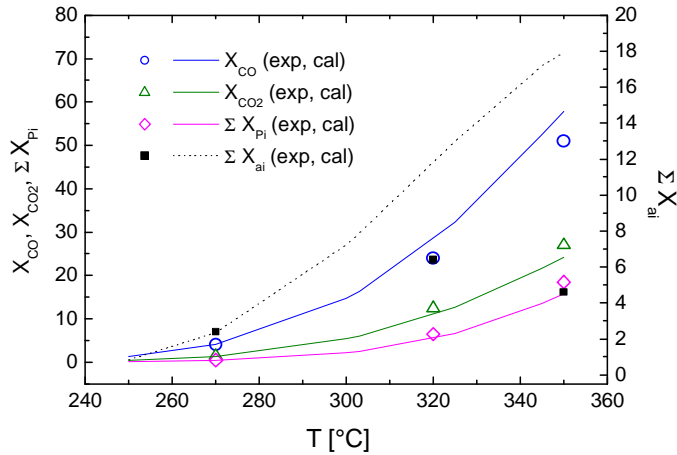


Figure B23. Comparison of experimental [13] and calculated data. Calculated data have been obtained for PF reactor using the constant factor of 2 for multiplication of the gross rates of all alcohols and factor of 1 for gross rate of hydrocarbons (2*Alcohols, 1*HC). Experimental conditions: same as figure B21.

Figures B24 and B25 compare the results obtained upon calculating the CO conversion from the data of Li et al. [12] for PF and a CST reactor model (solid and open symbols, respectively) with the published experimental data. When multiplying the gross rates by a constant factor of 2 (figure B25) the model well simulates the experimental data. On the other hand, when multiplying by factor of 2 only the gross rates of alcohols (figure B24) the model clearly underestimated the experimental data. However, considering that different multiplying factors for alcohols and hydrocarbons allowed to improve the product distribution, these results appear reasonable.

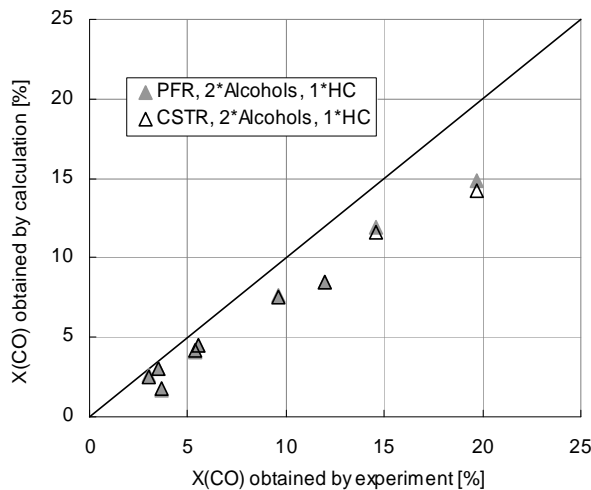


Figure B24. Parity plot for CO conversion - X(CO) calculated for PFR (solid points) and CSTR (open points) reactor using the gross rates multiplied by the constant factor 2 for alcohols and 1 for HC on the basis of data from [12].

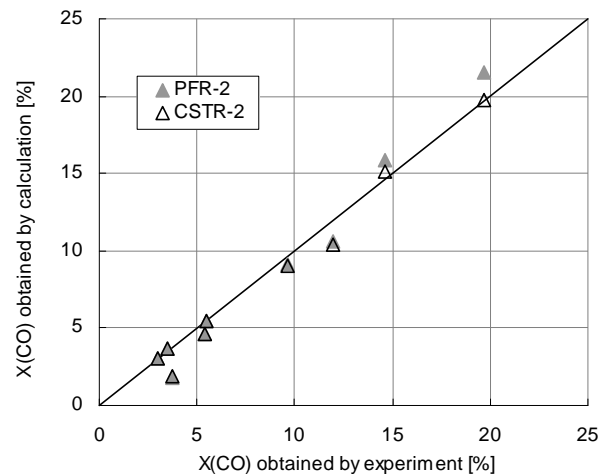


Figure B25. Parity plot for CO conversion - X(CO) calculated for PFR (solid points) and CSTR (open points) reactor using the gross rates multiplied by the constant factor 2 on the basis of data from [12] (Figure B10).

Figures B26 and B27 compare the results obtained upon calculating the CO conversion from the data of Yun Park et al. [13] for PF and a CST reactor model (solid and open symbols, respectively) with the published experimental data. When multiplying the gross rates by a

constant factor of 2 (figure B27) the model underestimates a few experimental data. Better fit was observed using multiplying factors equals to 2 for alcohols and to 1 for hydrocarbons (figure B26).

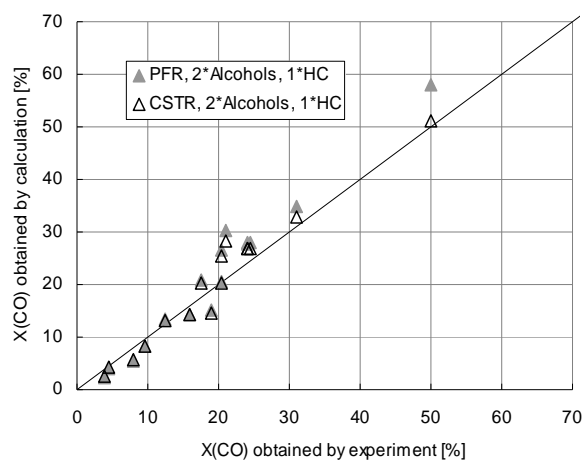


Figure B26. Parity plot for CO conversion - X(CO) calculated for PFR (solid points) and CSTR (open points) reactor using the gross rates multiplied by the *constant factor 2 for alcohols and 1 for HC* on the basis of data from [13].

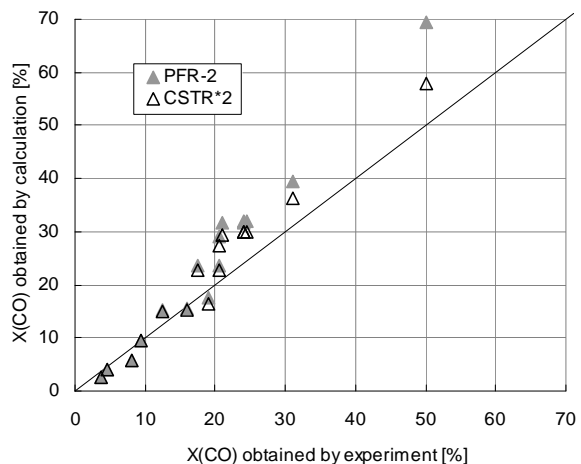


Figure B27. Parity plot for CO conversion - X(CO) calculated for PFR (solid points) and CSTR (open points) reactor using the gross rates multiplied by the *constant factor 2* on the basis of data from [13] (Figure B13).

Finally, we have tried to simulate also the experimental conditions of Quarderer [14]: temperature 262°C, total pressure 122 atm, GHSV 33,7 mol/h/kg-cat, H₂/CO ratio 1:1. Our predictions together with the experimental data are published in table B5. Unfortunately, at these experimental conditions (very low temperature and GHSV) our sets of kinetic parameters is not able to fit correctly the experimental data (neither CO conversion, nor distribution of alcohols).

Table B5. Comparison of experimental data published in Quarderer [14] with data calculated using the 2*PFR and PFR,2*Alcohols,1*HC, respectively.

wt. %	Experimental data	2*PFR	2*Alcohols, 1*HC
water	-	0.80	0.67
methanol	36	8.14	8.47
ethanol	38	79.40	80.40
propanol	13	11.66	10.46
butanol	3	-	-
X_{co}, %	29	6.54	6.66

Nevertheless in case of total carbon selectivities to mixed alcohols, on a carbon dioxide free basis, (Figures B28 and B29) when multiplying the gross rates of alcohols by constant factor of 2 and hydrocarbons by constant factor of 1, we have achieved good results. However for creating these plots we have fixed the H₂/CO ratio (1.2) [14] and we have supposed that the

authors used in these experiments a total pressure of 122 atm and a GHSV of 33,7 mol/h/kg-cat as in previous experiments.

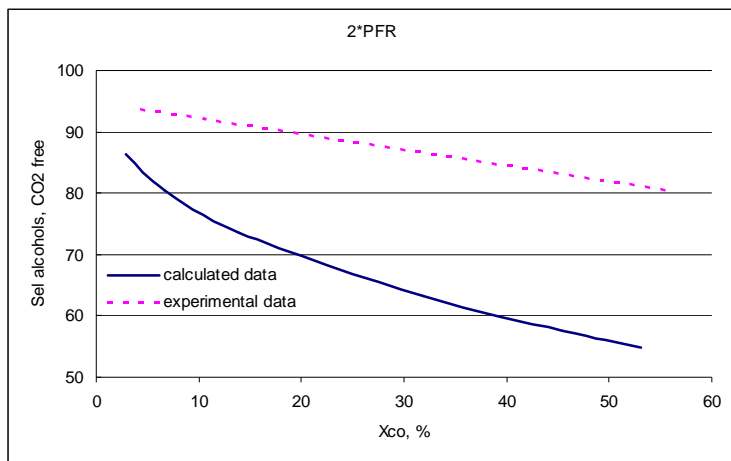


Figure B28. Carbon selectivity to mixed alcohols [%], experimental data [14] and data calculated using a constant factor of 2.

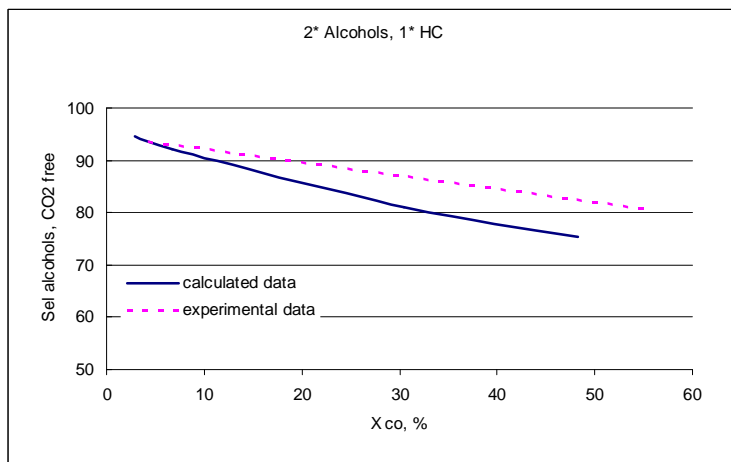


Figure B29. Carbon selectivity to mixed alcohols [%], experimental data [14] and data calculated using constant factor of 2 for alcohols rate of formation and 1 for HC.

B.2.3 Conclusions

The ability of the lumped kinetic model to predict both the CO conversion and the product distribution of the higher alcohol synthesis over Mo-based catalysts was tested against experimental data measured at different reaction conditions (type of reactor, catalyst, T, P, inlet flows, GHSV) obtained from various literature sources [12, 13, 14].

Considering that all the three sources make use of different catalysts and experimental conditions, the best agreement between experimental and calculated data for PFR reactor models, for both the CO conversion and distribution of products, was obtained by multiplying the gross rates of individual alcohols by a constant factor equal to 2 and the gross rate of hydrocarbons by a constant factor of 1.

B.3 Literature cited

- [1] G. Natta, U. Colombo, I. Pasquon, in *Catalysis* (P.H. Ammet, Ed.), Vol V., Charter 3, Reinhold, New York, 1957, p.131.
- [2] P. Forzatti, E. Tronconi, I. Pasquon, *Catal. Rev.-Sci.Eng.*, 33 (1&2), 109-168 (1991).
- [3] K.A.N. Verkerk, B. Jaeger, C.-H. Finkeldei, W. Keim, *Appl. Catal. A: General*, 186, 407-431 (1999).
- [4] R.G. Herman, *Catal. Today*, 55, 233-245 (2000).
- [5] Z. Liu, X. Li, M.R. Close, E.L. Kugler, J.L. Peterson, D.B. Dadyburjor, *Ind. Eng. Chem. Res.*, 36, 3085-3093 (1997).
- [6] A.N. Gunturu, E.L. Kugler, J.B. Cropley, D.B. Dadyburjor, *Ind. Eng. Chem. Res.*, 37, 2107-2115 (1998).
- [7] A. Aden, P. Spath, B. Atherton, NREL Milestone Completion Report "The Potential of thermochemical Ethanol Via Mixed Alcohols Production", (2005).
- [8] *Ullmann's Encyclopedia of Industrial Chemistry*, Fifth, Completely Revised Edition, Volume A16, B. Elvers, S. Hawkins, G. Schulz (Eds.), ISBN 3-527-20116-5 (VCH, Wienheim).
- [9] J.F. Painter and A.C. Hindmarsh, *Computing and mathematics research division*, 1-316, Lawrence Livermore national laboratory, Livermore, 1987.
- [10] G. Buzzi-Ferraris, E. Tronconi, "BUNLSI - A FORTRAN program for solution of systems of nonlinear algebraic equations", *Comput. Chem. Eng.* 10, 129-141 (1986).
- [11] L. Bisset, *Chem. Eng. (N.Y.)* 84 (1997) no.21, 155.
- [12] X. Li, L. Feng, Z. Liu, B. Zhong, D.B. Dadyburjor and E.L. Kugler, *Ind. Eng. Chem. Res.*, 37, 3853-3863 (1998).
- [13] T. Yun Park, I.S. Nam and Y. Gul Kim, *Ind. Eng. Chem. Res.*, 36, 5246-5257 (1997).
- [14] G.J. Quarderer, 78th Spring National AIChE Meeting, April 6-10, 1986, New Orleans, Louisiana.

APPENDIX C: ANALYSIS AND SIMULATION OF A RECTISOL-BASED ACID GAS PURIFICATION PROCESS¹⁵

C.1 Background

The study reported in this appendix analyses the performances of a commercially well-known process for acid gas washing with the major scope of quantifying the utilities consumptions in relation with the raw gas produced within a specific plant for the gasification of the black liquor produced by the US Pulp & Paper industry.

The process commercial name is *Rectisol* and its license is property of Lurgi Oel-Gas-Chemie GmbH and Linde AG.

The analysis was performed via a detailed study on the thermodynamics bases for the Rectisol and the *major Study outcome is an Aspen Plus simulation (Aspentech) (<http://www.aspentech.com>)*, a flexible tool able to provide basic information on a “*Rectisol-like*” process performances when the operating variables and feed characteristics are varied.

The Rectisol process is particularly suitable to turn the gas produced by the gasification of coal or other carbon-based materials into a valuable gas composed essentially of H₂ and CO in various ratios (so called *syngas*) by removing impurities such as H₂S, CO₂, HCN, NH₃, mercaptans, etc. which are the most frequent gasification by-products, depending of course on the gasifier feed.

Lurgi (Gas Generation and Purification Division) affirms [Ref. 5] that *Rectisol* is a technology that always requires a tailor-made design to the actual application: the design needs therefore to consider the upstream gasification technology, the downstream use of purified gas as well as the specifications for the offgases and the sulfur-rich gas streams.

Lurgi in fact claims that the design is certainly influenced by small “bugs” (e.g. trace contaminants in the raw gas) which might be present down to the ppb range. On the other hand, Lurgi confirms that even though, based on the previous statements, a non-proprietary simulation model such as an *Aspen* one, cannot provide detailed design information, it is useful to obtain general information on the main process components and the major process performances.

The present Study was conducted following this philosophy.

C.1.1 The selected Rectisol process layout

Several Rectisol process design configurations exist, in certain cases substantially different with each other, as the purified gas applications can be quite diverse.

In the present Study, the base-design was reproduced, following the original 1982 US Patent [Ref. 1] as this design definitely fits the needs for the black liquor gasification case and in addition the detailed description given in the Patent was a strong support to the comprehension of the process design.

Furthermore, the consistency of the results provided by the Aspen simulation could be verified against the information available in Literature [Refs. 2,3], most of all regarding the process utilities consumptions, as these information will be integrated in the Study on the Black Liquor Gasification Plant.

¹⁵ **Author:** Eng. Vittorio Felli

C.2 “Rectisol-based” process design & features

C.2.1 Process principles

The process presented here was designed to treat a raw acid gas containing sulphur compounds (H₂S & COS) and carbon dioxide which need to be entirely removed from the gas phase using a physical scrubbing liquid (methanol), in order to produce a “clean” gas to further process units. The acid gases on the other hand are separated in at least two gas streams.

The process presented in this Study was designed *trying inspiration* from the layout described in [Ref. 1] US Patent 4,324,567 (April 13, 1982), assigned to Linde: “Separation of Gaseous Components from a Gaseous Mixture by Physical Scrubbing”; this patented process received the market name of *Rectisol*®.

As already discussed in paragraph C.1, the results presented and the Aspen simulation itself is claimed to be representative of a “Rectisol-based” acid gas washing, and not of course of the *Rectisol* itself.

C.2.2 Process duties

Input stream:

The raw acid gas feed has the following characteristics (reference values):

- Flowrate: 90,000 Nm³/h
- H₂S content: 2% vol
- CO₂ content: 20% vol
- COS: 0.02% vol
- Present gas species: CH₄, CO, CO₂, H₂S, COS, H₂, NH₃, Ar

Products & duty specifications:

- Clean gas from the raw acid gas *Absorber*:
 - H₂S+COS content: < 0.1 ppm vol
 - CO₂ content: < 1 % vol
- CO₂-concentrated gas:
 - CO₂ content > 97% vol
 - H₂S+COS content: none
- Tailgas:
 - CO₂ content 50% vol
 - H₂S+COS content: none
- Acid gas stream (feed to a sulphur recovery unit, e.g. Claus®):
 - H₂S+COS content: > 40% vol
 - CO₂ remaining

Note that in the following description, “H₂S” will refer to both species H₂S and COS: this shortcut was adopted as only traces of COS are present in the feed gas. A further support to this simplification is given in paragraph C.4.

C.2.3 Process bases

The basic concepts for process design are underlined here below (refer to fig. C1). A more detailed description of the thermodynamics can be found in paragraph C.3.

- The acid gas CO_2 and H_2S are absorbed by a physical scrubbing liquid at high pressure without any chemical reaction, in order for the solvent to be easily regenerated via indirect heating at the *Regenerator* column (*C4* in fig. C1). At the same time, the solvent must be not volatile at the Absorber operating conditions in order to reduce the solvent losses in the product gas: methanol at low temperatures ($< -20^\circ\text{C}$) presents these characteristics.
- As the CO_2 absorption in polar solvents is a relatively highly exothermic process, the methanol solvent needs to be fed to the *Absorber* column (*C1* in fig. C1) at a low temperature (its value depends in turn on the operating pressure) in order also to maintain a low operating temperature in the column and consequently to reduce the volatility of the acid gas absorbed as much as possible. If the solvent feed temperature is not sufficiently low, the heat released by the absorbed CO_2 would raise the liquid temperature up to the point at which any further gas absorption would be prevented.
- The H_2S is roughly five times more soluble in methanol than CO_2 : this fact is used to separate the two absorbed acid gas. One single column might be used to separate a portion of the CO_2 absorbed in the loaded solvent (methanol + CO_2 + H_2S , stream *C1D3*) obtaining a pure CO_2 stream; in effect the physical characteristics of the system require the use of stripping nitrogen in a further column in order to increase the CO_2 volatility and to drastically reduce its content in the methanol liquid stream.

The process is composed of four main blocks (refer to fig. C1):

- *The Acid Gas Absorber C1*: the raw gas enters the column at the bottom section and it is contacted with the scrubbing methanol introduced at the top of the column.
- *The H_2S Concentrator C2*: the methanol rich in the absorbed acid gas is concentrated in hydrogen sulphide as the carbon dioxide, the more volatile compound, is obtained almost pure at the top of the column.
- *The CO_2 Stripper C3*: the methanol stream concentrated in H_2S is contacted with stripping nitrogen; another portion of the CO_2 absorbed in the *Acid Gas Absorber* is transferred back to the gas phase, so that a gas mixture of N_2 and CO_2 is obtained at the top of the stripper.
- *The Solvent Regenerator C4*: the liquid bottom from the *CO_2 Stripper*, containing the H_2S absorbed in the *Acid Gas Absorber* and the remaining CO_2 is regenerated in the regeneration column via indirect heating with steam. Following a further cooling at low temperature to condensate the methanol present in the gas phase, the gas exiting the top of the column is composed of H_2S and CO_2 and it can be routed to a Sulphur Recovery Unit (outside the scope of the present Study).

C.2.4 Process description

Refer to fig. C1.

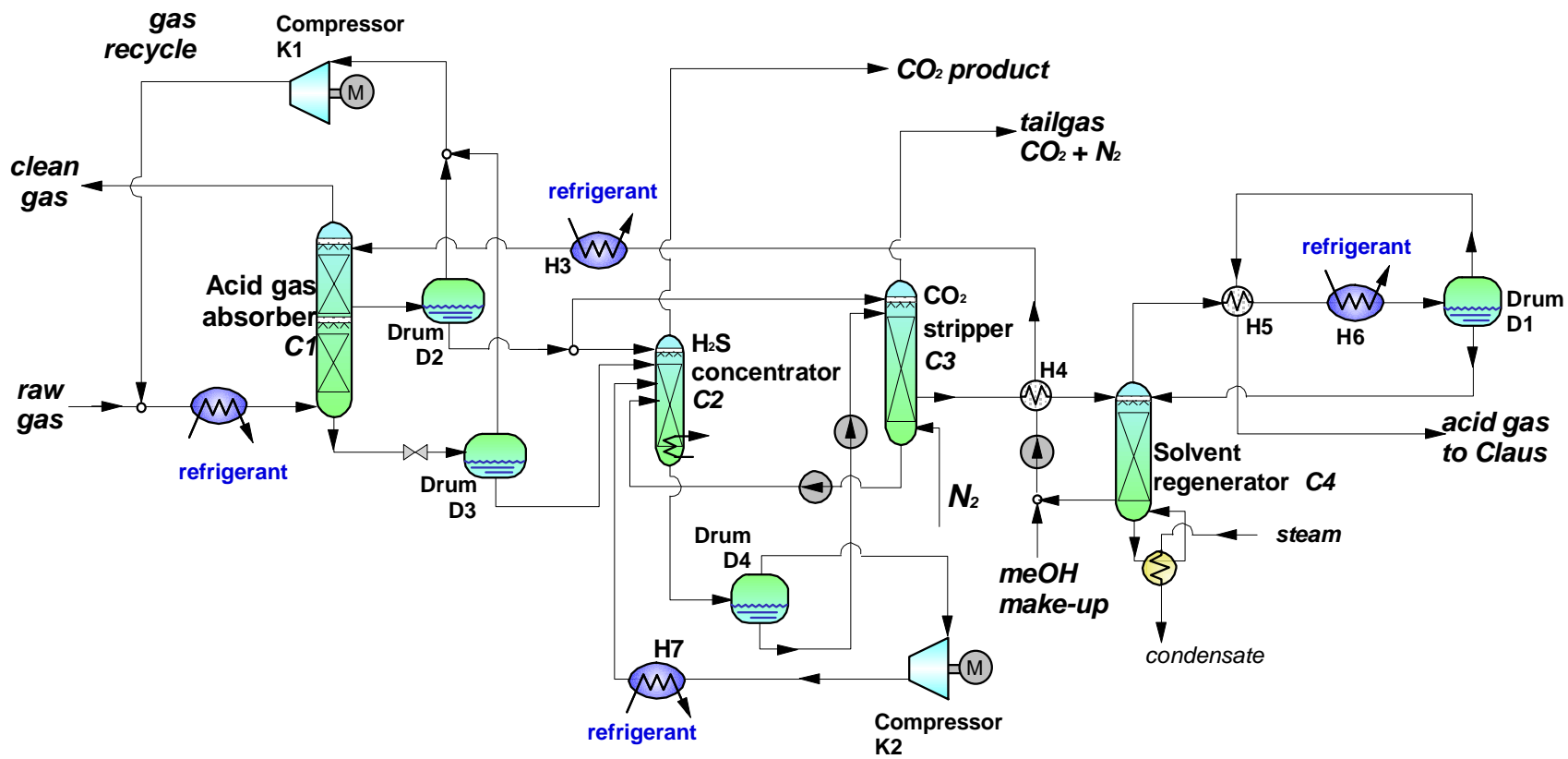


Figure C1: H₂S + CO₂ absorption

C.2.4.1 The Acid Gas Absorber C1

The pressure of the column was fixed at 32 bar based on the pressure of the raw feed gas (*EXH1*), which is an external input. This high pressure raw gas stream *EXH1* is pre-cooled in the exchanger *H1* by the lean gas stream *CIH1*; it is then mixed with the recycle gas *KIM2* to be finally cooled in the exchanger *H2* before being introduced at the bottom stage of the absorber column *C1*.

The absorber is composed of two columns, one on top of the other: part of the upper column bottom liquid is introduced at the top of the bottom column while the gas exiting the bottom column feeds the upper column.

- The bottom column is the *H₂S Absorption Section* where the H₂S originally present in the raw gas is totally absorbed by the scrubbing methanol, while only part of the CO₂ is absorbed, as this is less soluble than H₂S in methanol. Furthermore, as the CO₂ absorption in polar solvents is an exothermic phenomenon, the portion of absorbed CO₂ in the bottom section raises the liquid temperature in the column so that the driving force for the CO₂ absorption itself sharply decreases and the CO₂ remaining in the gas phase requires a further treatment in the upper section to be completely absorbed.
- In the upper section, the CO₂ which left in the gas phase is completely absorbed by means of the top low-temperature pure methanol liquid stream *H3C1*.

It is clear thereby that while pure methanol is fed at the top of the absorber *C1*, methanol rich in CO₂ is fed at the top of the H₂S absorber.

On the other hand, two liquid streams exit the absorber *C1*:

- *C1D2*: rich in CO₂ while no H₂S is present
- *C1D3*: rich in both acid gases H₂S and CO₂

Note that clearly other gases which are much less soluble in methanol with respect to H₂S and CO₂ at the operating conditions might still be partially absorbed in the liquid phase and this could be a problem as they might be valuable products for purposes of the *Process Designer*. To solve this issue, two flash drums *D2* and *D3* at an intermediate pressure (7.5 bar) between the *Absorber* and the *Solvent Regenerator* pressure were introduced: the less soluble gas (such as CO, H₂, Ar,...) are re-transferred in the gas phase and they can be recycled to the column via the compressor *K1*.

C.2.4.2 The H₂S Concentrator C2

This column is designed to enrich the down coming liquid in H₂S by a selective desorption of CO₂, the less soluble component. Column *C2* is composed of two sections:

- The bottom section is the stripping column: both H₂S-loaded streams *D3C2* from the absorber *C1* and *P4C2* from the *CO₂ Stripper* are fed to the column to let the gas being desorbed. The stripping gas is provided by the low pressure (1 bara) flash vaporization of the bottom *C2* residue *C2D4* in drum *D4*: the gas phase is re-compressed through compressor *K1*, cooled in exchanger *H7* and introduced at *C2* bottom.
- The top section is the H₂S absorber that in fact is absorbed by the stream *SIC2*, coming from the absorber *C1*, which is rich in CO₂ but does not contain any H₂S.

Therefore, two streams exit the *H₂S Concentrator C2*:

- *C2EX*: gas stream exiting the top stage of the *H₂S Concentrator*, which is composed of CO₂ (> 97% vol) and other gases, excluding H₂S.
- *P2C3*: liquid stream containing both CO₂ and H₂S; a portion of these gaseous components was already released in the low pressure vessel *D4*.

C.2.4.3 The CO₂ Stripper C3

This column leads to a further extent the CO₂ desorption from the acid gases rich solvent from column *C2* as it works at a lower pressure (2 bar) with respect to *C2* and stripping nitrogen is used in order to obtain a tailgas with no H₂S on top of the stripper. The *Stripper C3* is again composed of two sections:

- the bottom one is the stripping section: the stream *P2C3* is fed at the top (theoretic) plate while the stripping nitrogen is introduced at the bottom one. Both CO₂ and H₂S are stripped from the liquid solvent.
- The gas leaving the bottom section is then scrubbed in the top one via the liquid stream *S1C3* which comes from the absorber *C1* and it is rich in CO₂ but it does not contain any H₂S. In the top H₂S scrubbing section, H₂S is completely absorbed in the liquid phase.

Three product streams exit the *CO₂ Stripper C3*:

- *C3EX*: tailgas composed of CO₂ and nitrogen, roughly in the same ratio.
- *C3H4*: liquid stream containing the CO₂ left in the solvent after the stripping columns and practically the whole H₂S which is absorbed in the *Absorber C1*. This stream is routed to the *Solvent Regenerator C4*.
- *C3P4*: liquid stream to the bottom section of column *C2*.

C.2.4.4 The Solvent Regenerator C4

The methanol solvent is fed to an intermediate plate of the atmospheric *Regenerator C4* and the stripping heat is provided by the low pressure steam reboiler.

As methanol boiling temperature at atmospheric pressure is around 65°C and methanol is quite volatile at these operating conditions, the column top section is provided with a heat exchanger *H6*, fed by a refrigerant, which cools down the vapors to a temperature low enough (-10°C) that practically all the methanol is condensed and re-routed to the column *C4* as reflux.

H6 is represented in fig. C1 as external to column *C4*, but indeed it is quite common having it inside the very top section of the *Regenerator*, above the first plate.

This is a fundamental design item as it prevents high solvent losses.

C.2.5 Key process data & variables

C.2.5.1 CO₂ heat of absorption in methanol.

As already pointed out, the CO₂ absorption in polar solvents is an exothermic phenomenon: if the heat released increases the scrubbing liquid temperature above a certain point, depending on the *Absorber* pressure, the absorption cannot take place and only a very small part of the column is effective.

Two process variables are strictly dependent on this phenomenon:

- the scrubbing methanol circulation rate to the *Absorber C1* (and consequently, for a fixed gas rate fed to the column, the molar ratio liquid/gas);
- the scrubbing methanol feed temperature to *Absorber C1*.

Both variables contribute to maintain a sufficiently low operating temperature inside the *Absorber* and consequently a good acid gas absorption level: the first variable, which must be above a minimum, provides a sufficiently high liquid heat capacity, while the second variable, which must be below a maximum, prevents any *hot spot* throughout the column.

This basic equations and models governing the effect of the previous variables are extensively presented in paragraph C.3, while figures C2-C3 show the effect of the methanol circulation rate on the clean product gas quality.

C.2.5.2 Different H₂S and CO₂ solubility in methanol

This property guarantees the possibility of separating the two gases downstream of the *Absorber*, obtaining therefore two CO₂ rich gas streams containing no H₂S. The relative solubility of the two acid gases has a number of implications on the process design, mainly on the solvent flowrates selected for the various column of the layout of fig. C1: as an example, the flow ratio between streams *CID2* and *CID3* is quite important for the *Absorber* design.

Refer again to paragraph C.3 for details.

C.2.5.3 Methanol volatility

Among other polar solvents, methanol is used in *Rectisol* process as it is relatively cheap and at the selected *Absorber* operating conditions it is not volatile: it is generally assumed that the solvent losses to the product gas are negligible.

C.2.6 Aspen Plus Model

The model here presented was simulated with the *Aspen Plus Process Simulator*; the *Aspen Plus* file, the heat and material balance together with the most useful concentration and temperature profiles for the various column are reported in paragraph C.4.

The simulation performed provides all the information on the “*Rectisol*-based” plant included in the scope of the present Study.

It is quite important though reminding here that the process simulation performed in the present Study and the *Rectisol* process available on the market share the same design principles but of course a large amount of information related to *Rectisol* are not available in the Literature as they are property of the Licensor. This implies that the model designed here must be taken as a first approximation of the industrial plant. This is particularly true for the secondary product streams such as the “Tailgas” or the “CO₂ gas”: in certain cases the *Aspen Model* cannot provide for these streams *exactly* the same characteristics that the *Rectisol* would provide and this is only because of the lack of proprietary information.

C.2.7 Aspen Plus Model results and discussion

The results of the *Aspen Plus* process simulation are reported in detail in paragraph C.4.

Here below, the overall results and performance parameters are presented in comparison with the published data, in order to confirm the reliability of the Model.

- Table C1: the *Model* and the original *Patent* [Ref. 1] are compared in terms of main streams characteristics
- Table C2: the *Model* and the original *Patent* [Ref. 1] are compared in terms of overall performance parameters
- Table C3: the Model utilities consumptions are compared to the data available in Literature.

	raw gas to Absorber	lean scrubbing MeOH to Absorber	solvent to Absorber bottom section	clean gas product	CO2 gas product	stripping N2	Tailgas	Claus gas (to sulphur recovery unit)
Aspen Plus Model for present Study								
Absorber pressure (bara)	32							
Methanol top Absorber stage T(°C)	-60							
FLOW								
Nm3/h	91188			70338	12969	4035	8037	3954
t/h		230	113					
kmol/s	1.13	2.00	0.90	0.87	0.161	0.05	0.10	0.05
COMPOSITION								
CO2 (mol%)	20.95%			0.45%	97.95%		49.52%	53.21%
H2S+COS (mol% / ppm vol)	1.93%			0.0007	0.18%		0.14%	43.60%
CO2/S-compounds (mol/mol)	11							
H2 (mol%)	37.57%			48.65%				
CO (mol %)	36.09%			46.63%				
Ar (ml %)	1.01%			1.23%				
CH4 (mol %)	2.06%			2.54%				
N2 (mol %)	0.37%			0.41%			49.34%	
NH3 (mol %)	0.01%			0.00%				
Methanol (mol %)	0.00%	99.995%		0.00%	0.0955%		0.0563%	1.6546%
Rectisol Patent (Ref. 1)								
Absorber pressure (bara)	75							
Methanol top Absorber stage T(°C)	-50							
FLOW								
Nm3/h	100000			72500	23300	3000	5650	1480
t/h		100	45					
kmol/s	1.24	0.87	0.39	0.90	0.289	0.04	0.07	0.02
COMPOSITION								
CO2 (mol%)	26.00%			none	99.00%		47.75%	57.43%
H2S+COS (mol% / ppm vol)	0.63%			none	0.00%		0.00%	42.57%
CO2/S-compounds (mol/mol)	41							
H2 (mol%)	69.90%			96.24%				
CO (mol %)	1.70%							
Ar (ml %)				2.30%				
CH4 (mol %)								
N2 (mol %)	1.18%			1.61%			53.10%	
NH3 (mol %)	0.00%							
Methanol (mol %)		100.000%		0.00%				

Table C1

	Aspen Plus Model for present Study	Rectisol Patent (Ref. 1)
scrubbing MeOH to Absorber (top stage)/MeOH to Absorber bottom section (kg/kg)	2.0	2.2
lean MeOH/CO2 flow in raw gas (mol/mol)	8.4	2.7
lean MeOH/H2S flow in raw gas (mol/mol)	91.7	111.2
lean MeOH/raw gas (mol/mol)	1.8	0.7
CO2 in "pure" CO2 product / raw gas CO2 (mol/mol)	0.7	0.9
CO2 in Tailgas / raw gas CO2 (mol/mol)	0.2	0.1
CO2 in "Claus Gas" / raw gas CO2 (mol/mol)	0.1	0.0
H2S in "Claus Gas" / raw gas H2S (mol/mol)	1.0	1.0
CO2/S-compounds (mol/mol) in "Claus Gas"	1.2	1.3
overall CO2/S-compounds concentration ratio	8.9	30.6
overall methanol losses (t/h)	0.1	not available

Table C2

MODEL	Aspen Plus Simulation for present Study	Data published in Ref. 2	Data published in Ref. 3
Absorber pressure (bar)	32	56	78
Raw acid gas to the Absorber			
CO2 (kmol/s)	0.24	0.54	0.57
H2S (kmol/s)	0.02	0.02	0.004
MeOH circulation rate (kmol/s)	2.00	NA	NA
CO2 product			
Flow (kmol/s)	0.16	0.52	0.36
CO2 (vol%)	98%	99%	99%
Claus gas from Regenerator			
Flow (kmol/s)	0.05	0.05	0.02
CO2 (vol%)	53%	42%	68%
H2S (vol%)	44%	47%	27%
Methanol make-up (kg/h)	120	40	30
Refrigeration			
Duty (MW)	7.41	4.20	2.00
H3 - major solvent refrigeration (MW)	4.34		
Refrigerant temperature (°C)	< -60	-31	-38
H2 feed gas cooler (MW)	0.43		
H6 regenerator top condenser (MW)	2.31		
H7 Recycle gas cooler (MW)	0.33		
Cooling water @ regenerator top condenser (m3/h)	none	133	300
Heating duty @ regenerator reboiler (MW)	4.00	3.20	3.75
Shaft power @ methanol pumps (kW)	421	1640	1100

Table C3

C.2.7.1 Discussion

Tables C1 and C2 show a high reproducibility of the *Patent* data by the *Model*:

- the raw gas flow and the CO₂&H₂S compositions are very similar in the two cases in the different streams
- the distribution of the CO₂ in the feed raw gas into the product streams and the Claus Gas (to Sulphur Recovery Unit) is reproduced quite consistently in the two cases
- the Claus Gas composition is very close in the two cases
- the overall CO₂ concentration factor [(CO₂/S-compounds mol/mol) ratio between Claus Gas and the raw feed gas] has the same order of magnitude in the two cases

The two process layouts, although very similar, do present minor differences: the key ones are the *Absorber* pressure that in the *Patent* case is roughly 2.5 times as much the *Model Absorber* pressure. In addition, in the *Patent* case the *Absorber* column is provided of an inter-stage cooler which helps the absorption and which was not introduced in the *Model* layout.

The previous explain how the molar ratio methanol solvent/raw gas for the *Model* case is roughly 2 times as much the *Patent* value.

Table C3 compares the utilities consumption for the Aspen Model and the Rectisol typical plants data available in Literature.

The results have the same order of magnitude, which confirms again the *Model* consistency.

The heat duty to the Regenerator reboiler is higher in the Model case because the methanol circulation rate in the plant is higher, which in turn depends on the lower *Absorber* pressure in the Model case.

The previous considerations confirm that the main scope of the Present Study was achieved: the Model is a tool which allows a first evaluation of the *Rectisol* process performances in terms of lean gas characteristics, process key parameters and process utilities consumptions.

C.2.7.2 Addenda

1. It is clear from what previously explained that methanol circulation rate within the “*Rectisol*-based” plant has a very important effect on its utilities consumptions as they are mostly related to this key parameter.

It is important stressing the fact that the choice of the methanol circulation rate as per the Model results reported in paragraph C.4 is not unique: a smaller value could have been selected respecting nevertheless the specifications on the product clean gas from the *Absorber*.

The choice of 2 kmol/s (methanol stream to the Absorber) guarantees though the best compromise between the utilities consumption values reported in Literature and the Aspen simulation results (although not perfect!) for all the process product streams, including the tailgas and the CO₂ gas stream.

In this way, the utilities consumptions were slightly overestimated but the Aspen Model resulted being consistent.

The effects of methanol circulation rate on various process parameters are reported in figures C3 to C6.

2. Figures C7-C16 show the Aspen Model results in detail.

For each column or column section, the following variables are plot against the theoretic stages:

- temperature
- gas & liquid molar flow
- H₂S and CO₂ volume/molar concentration

Actually, it was thought that the previous figures, when compared to the explanations and the background given in paragraph C.3 could help to better understand the process basics.

Note that the numeration of the theoretic column stages always assigns the top column stage the number “1” (for each column section).

C.2.8 Aspen Plus Model for the abatement of H₂S only

The Model prepared for the abatement of both acid gases H₂S and CO₂ from the raw feed gas was modified and adapted to the case in which the specification on the H₂S in the clean product gas remains the same as in the previous model, while there is no target on the CO₂.

In practice, the *Absorber C1* (fig. C2) is composed of 1 column only (the upper one in the previous model is not required here) and the process scheme is adapted coherently.

As the process description is very similar to the one provided above, it is not reported here. The Aspen Plus process simulation was performed on two different acid gas feeds: one equal to the previous case fed, the other roughly 3 times as much in flow.

It is important to underline that:

- The simulated *Rectisol*-based process is able to achieve the desired separation even with this modified and unusual process layout.
- The utilities consumption are very close between the “H₂S&CO₂” and the “H₂S-only” abatement cases at constant acid gas feed rate.

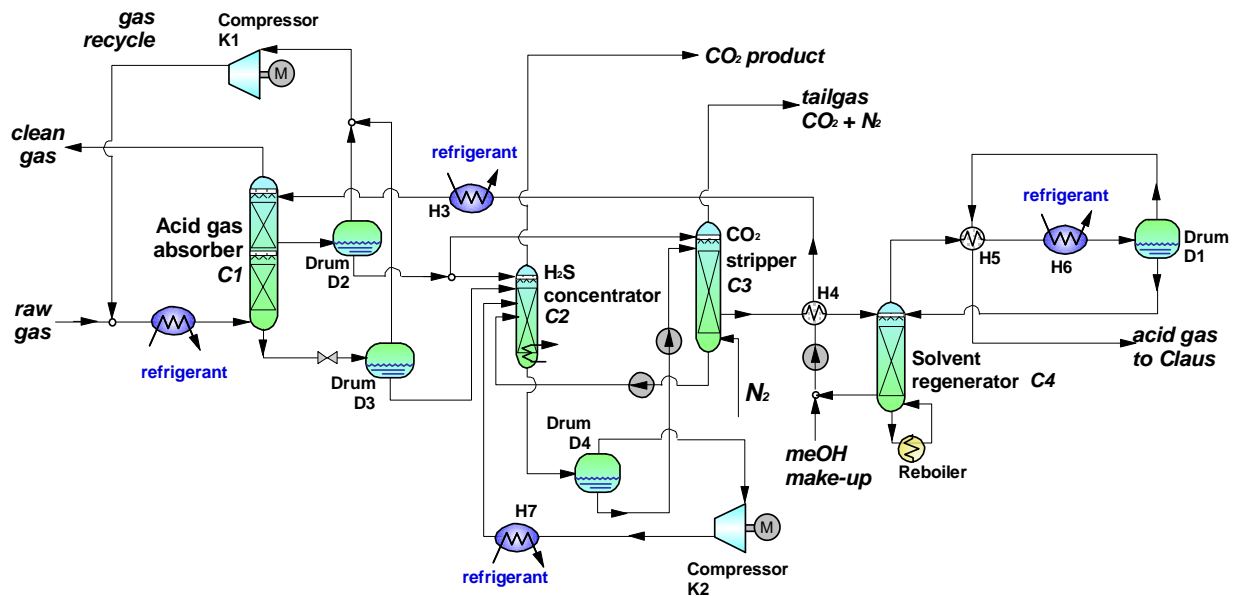


Figure C2: “H₂S only” absorption

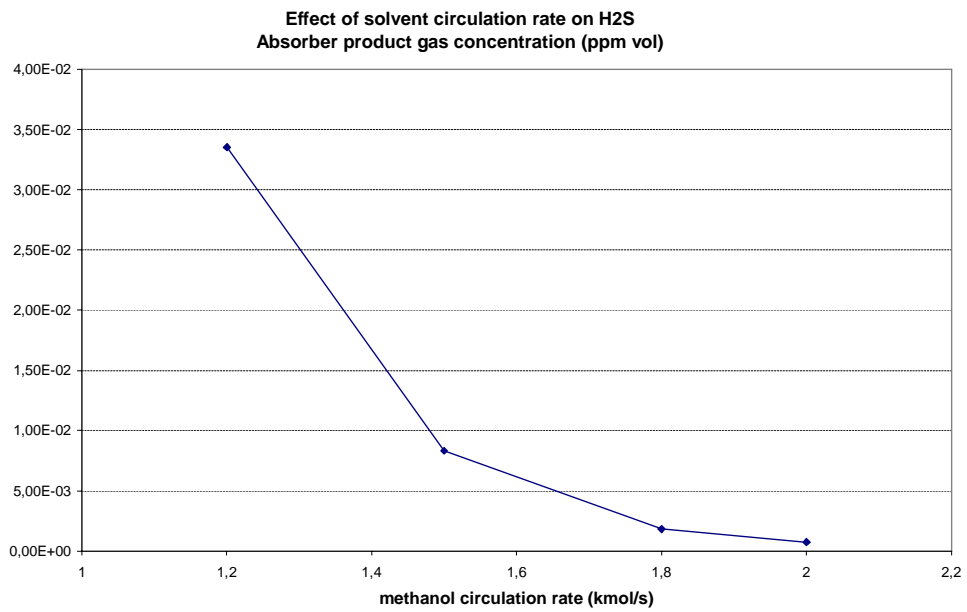
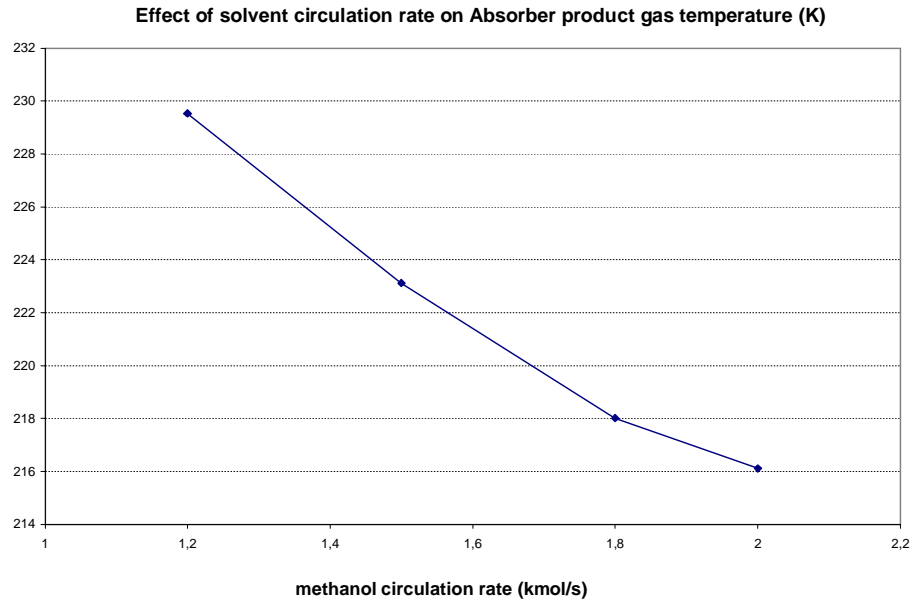


Figure C3: Effect of solvent circulation rate

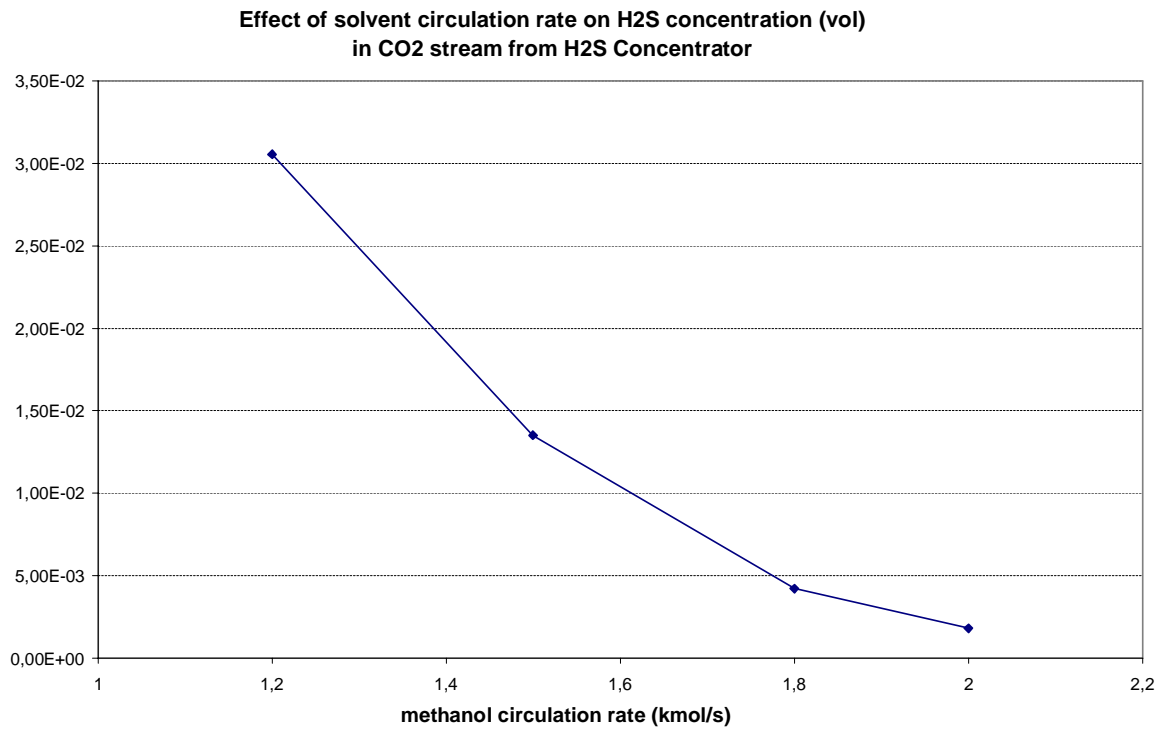
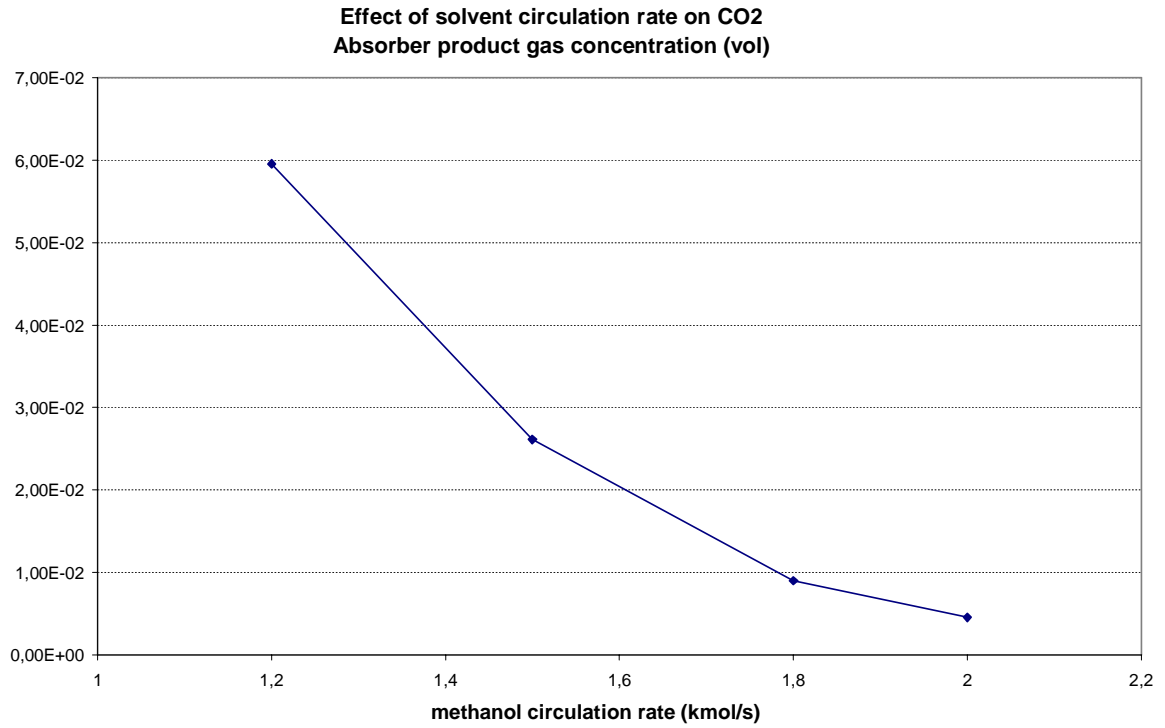
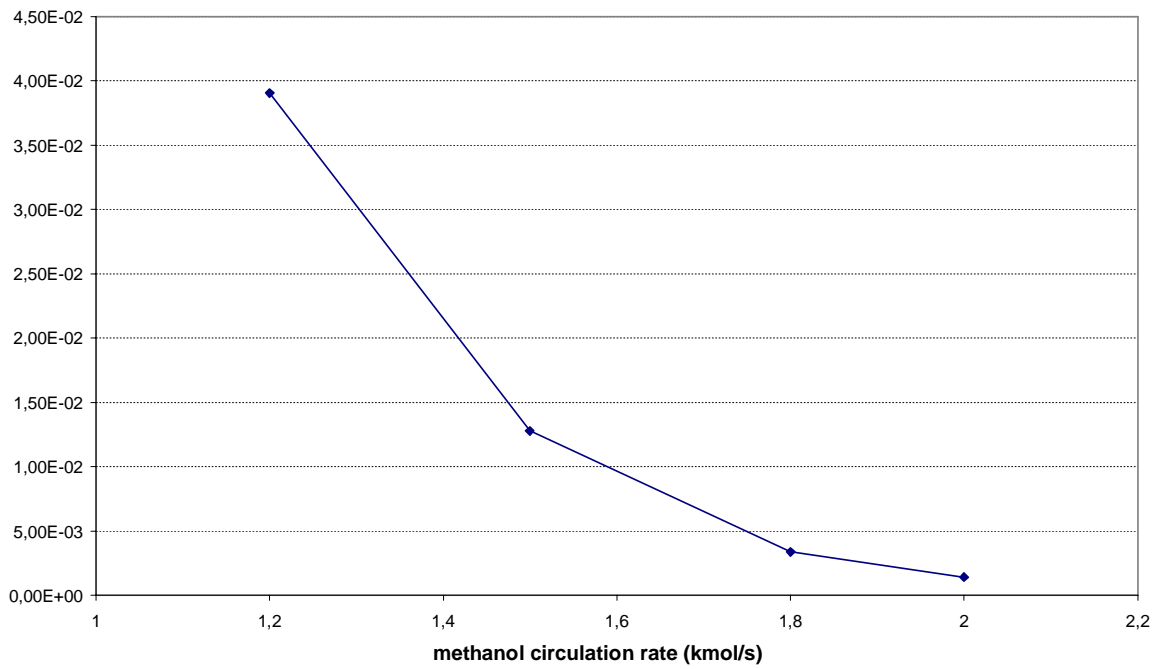


Figure C4: Effect of solvent circulation rate

Effect of solvent circulation rate on H2S concentration (vol) in Tailgas



Effect of solvent circulation rate on N2/CO2 concentration (vol) in Tailgas

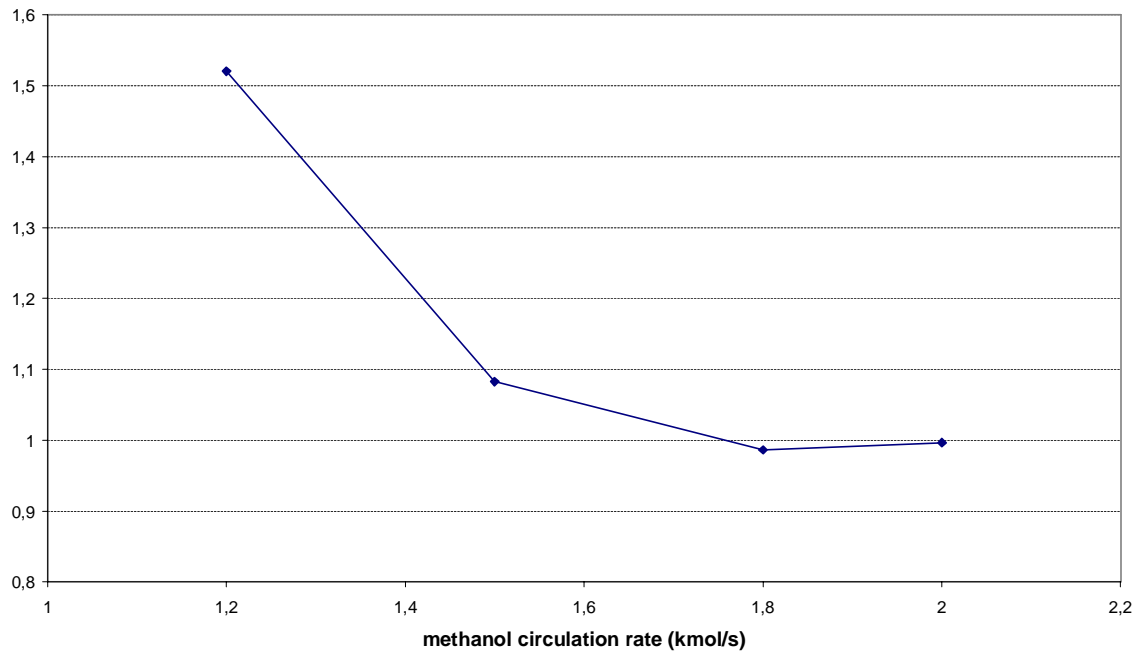


Figure C5: Effect of solvent circulation rate

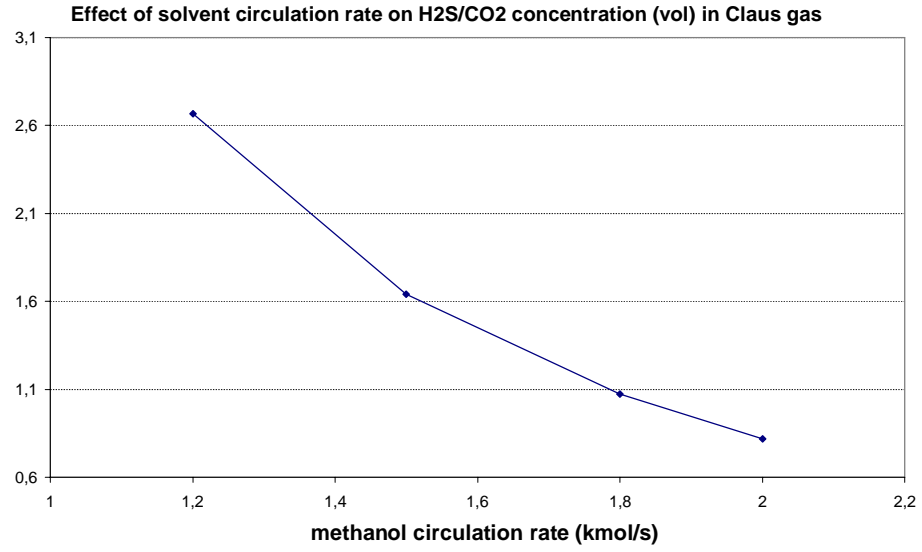


Figure C6: Effect of solvent circulation rate

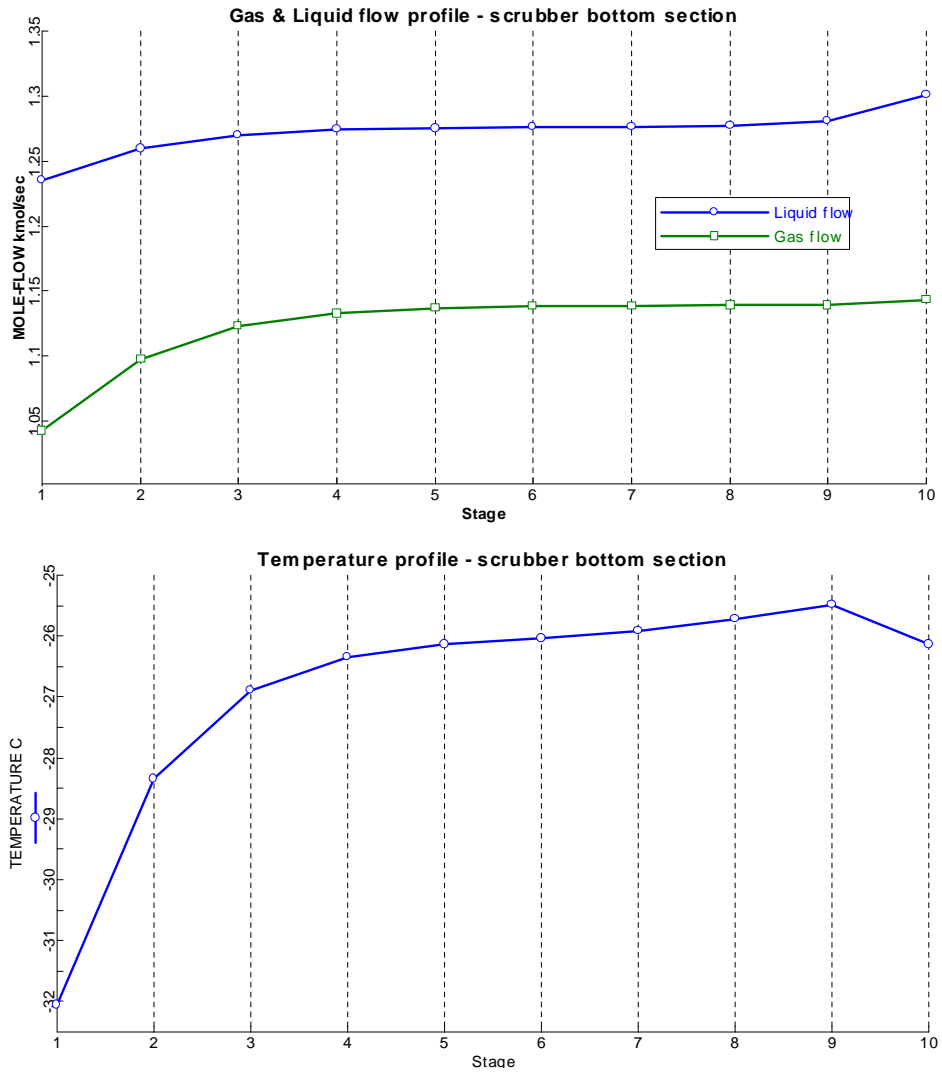


Figure C7: Aspen Model results

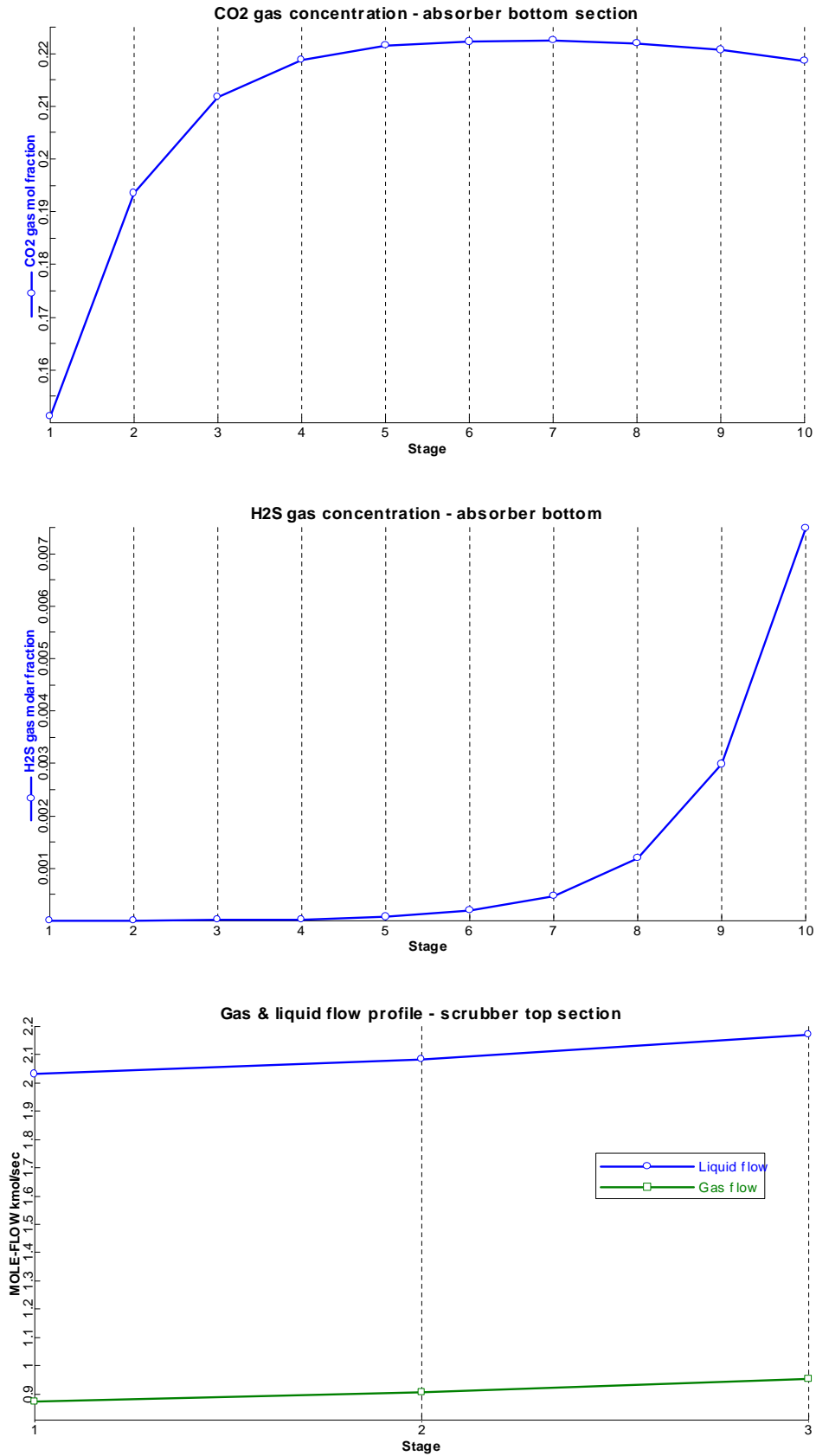


Figure C8: Aspen Model results

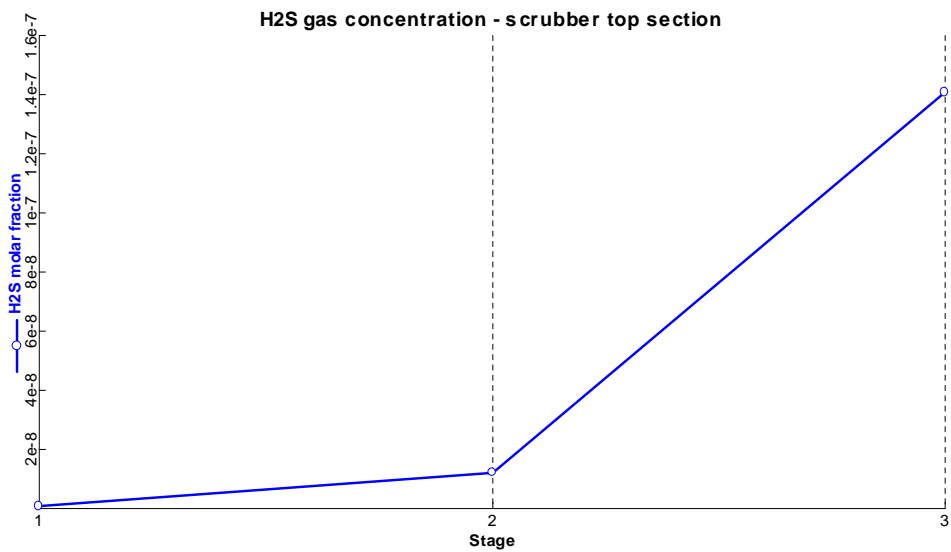
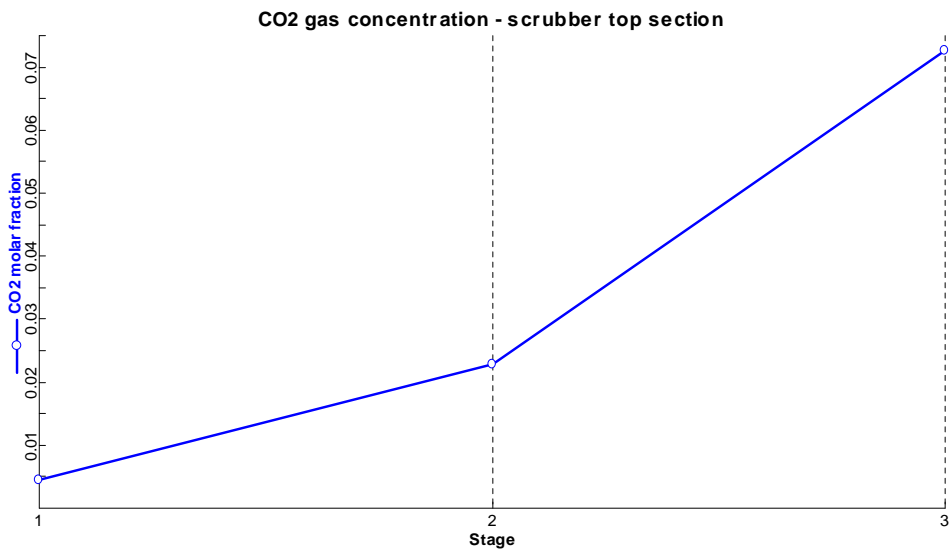
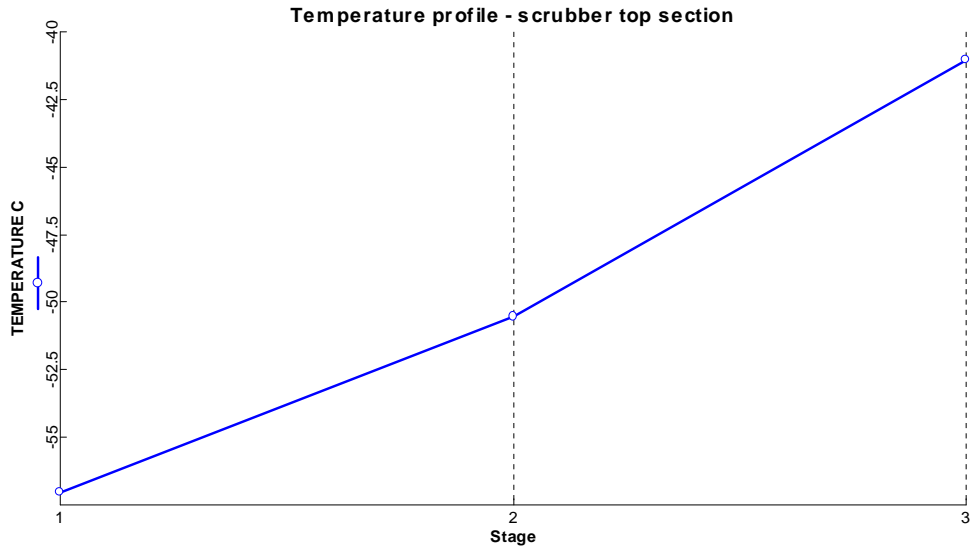


Figure C9: Aspen Model results

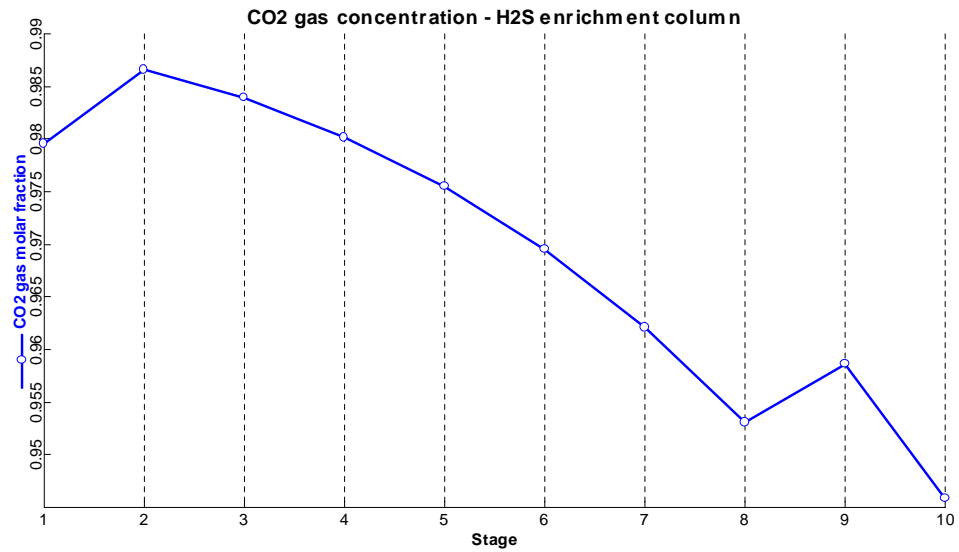
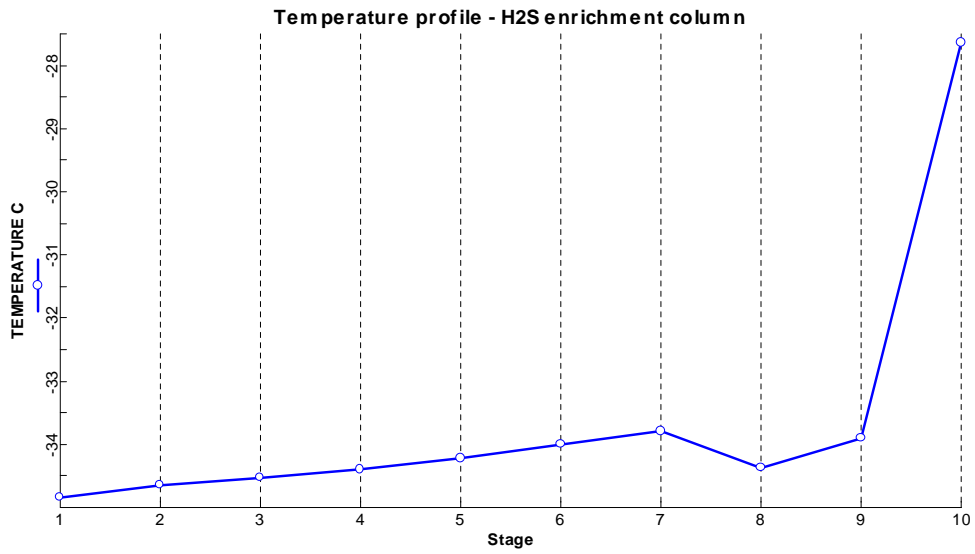
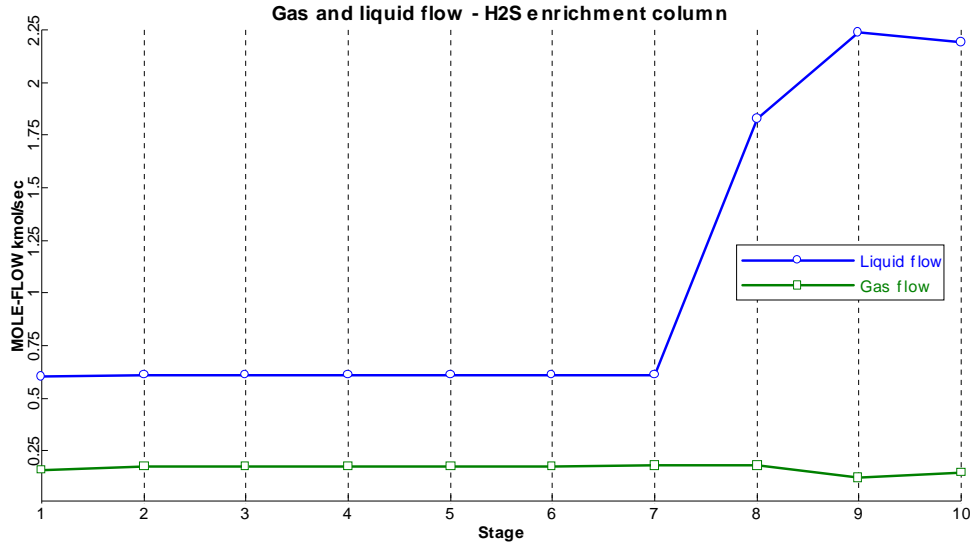


Figure C10: Aspen Model results

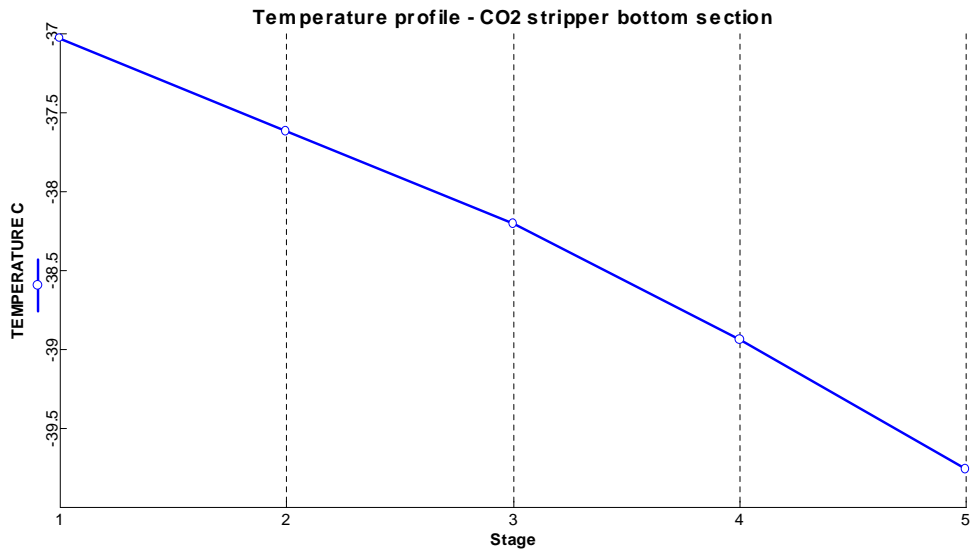
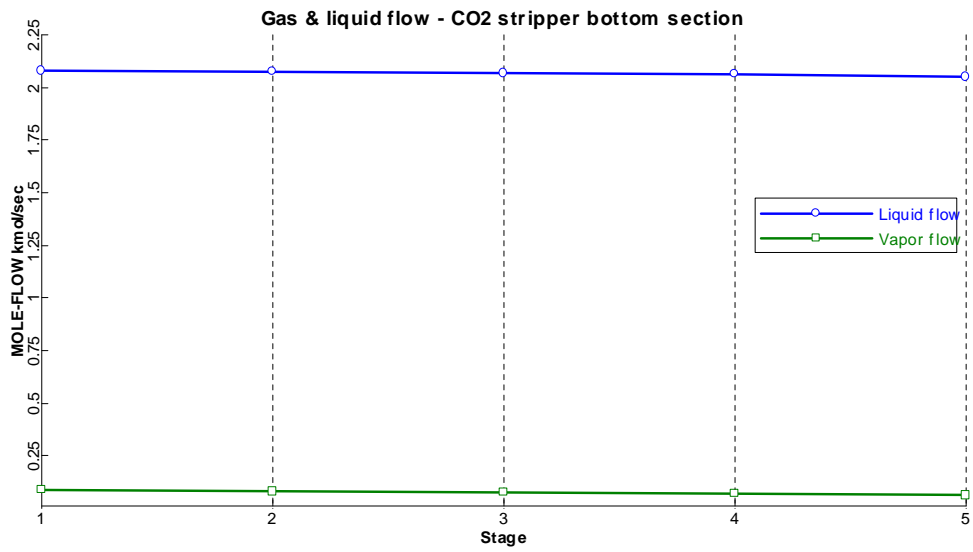
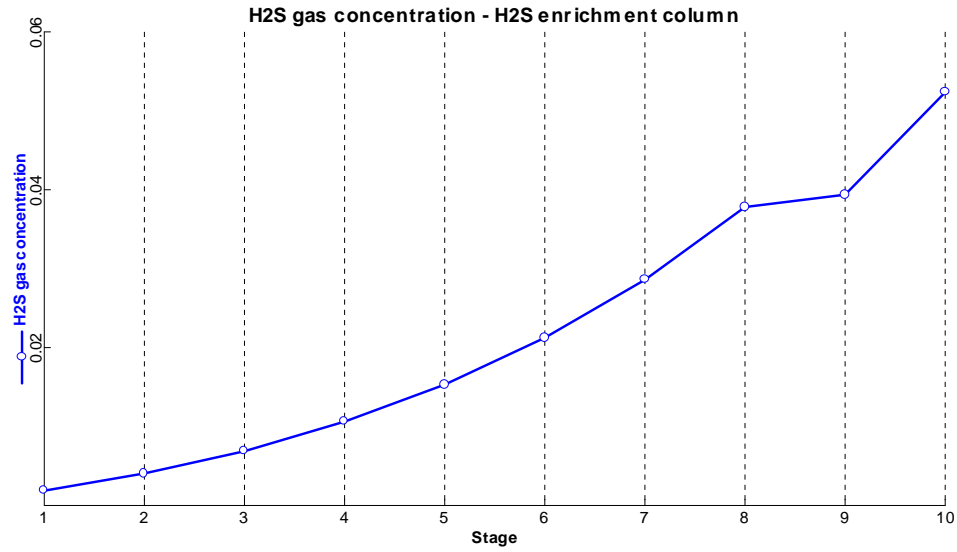


Figure C11: Aspen Model results

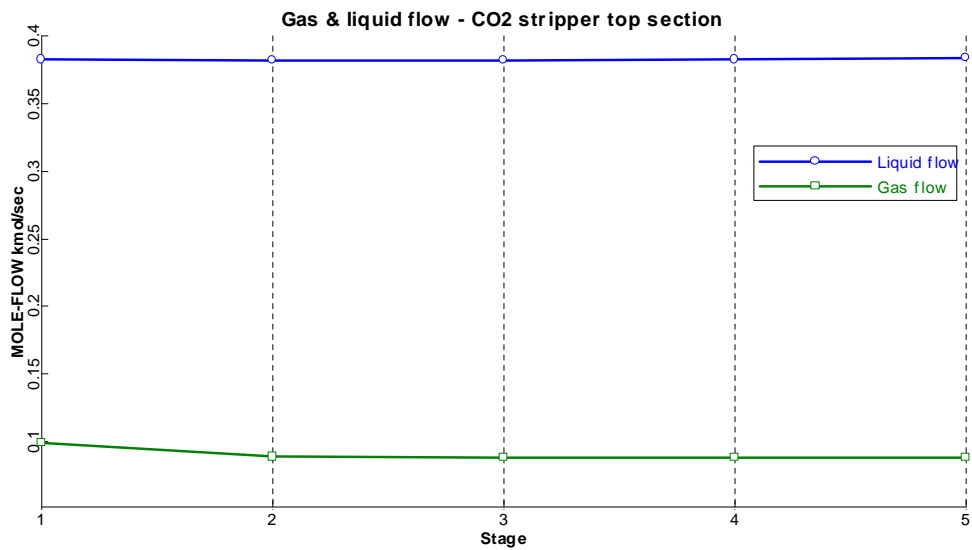
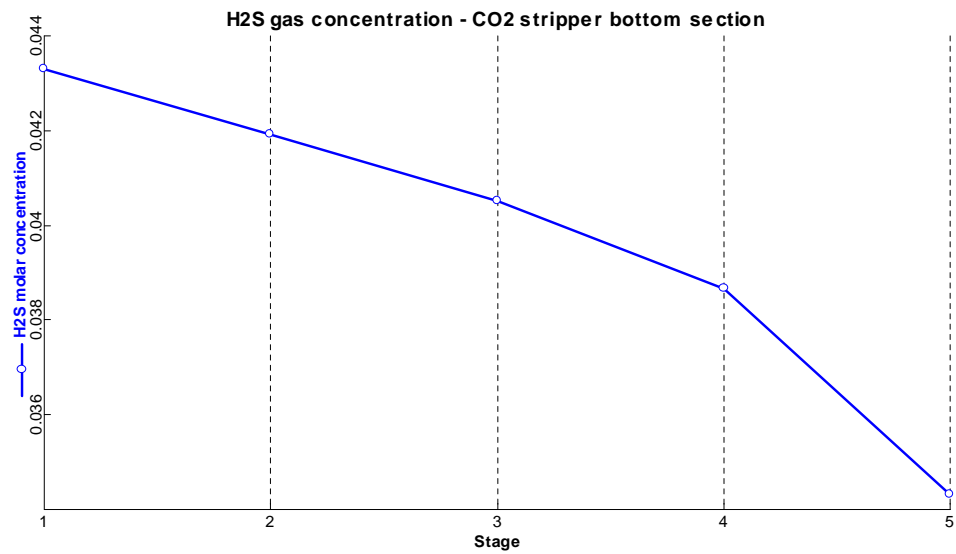
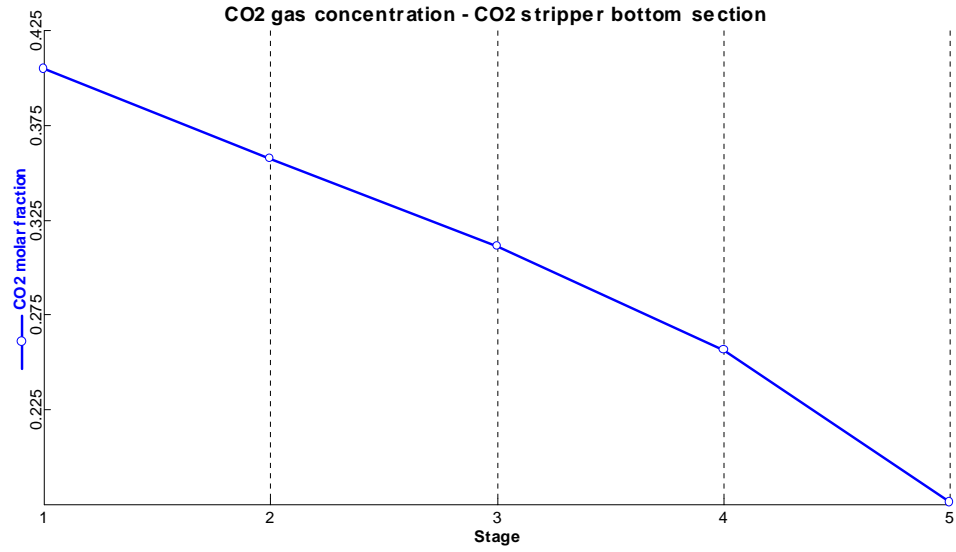


Figure C12: Aspen Model results

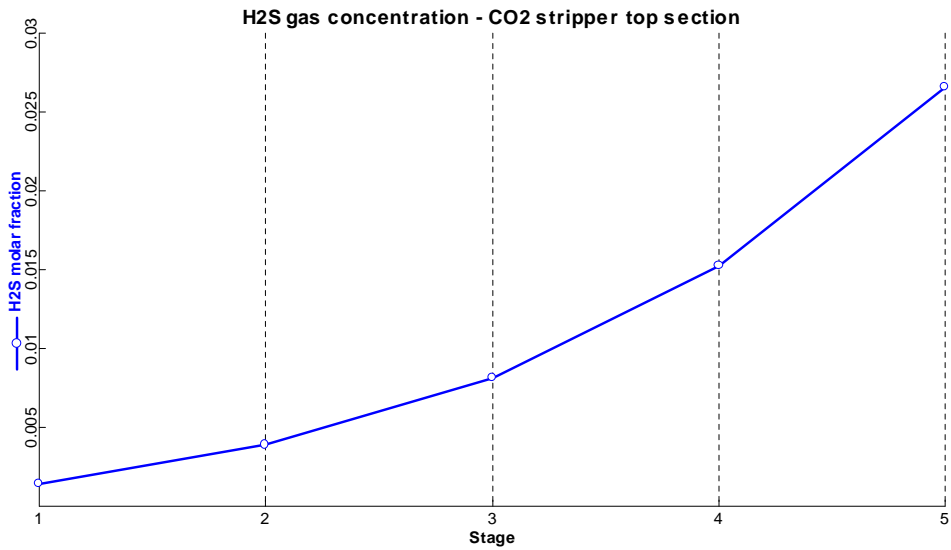
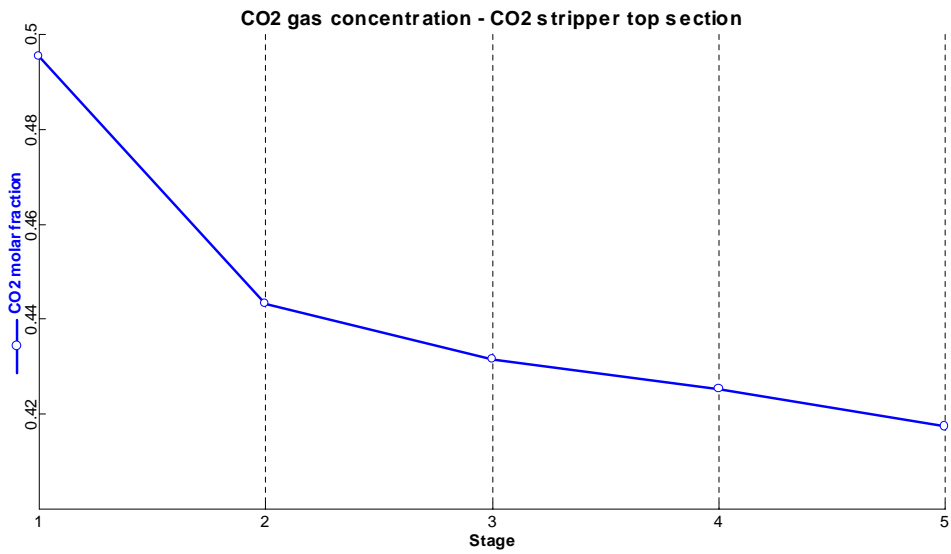
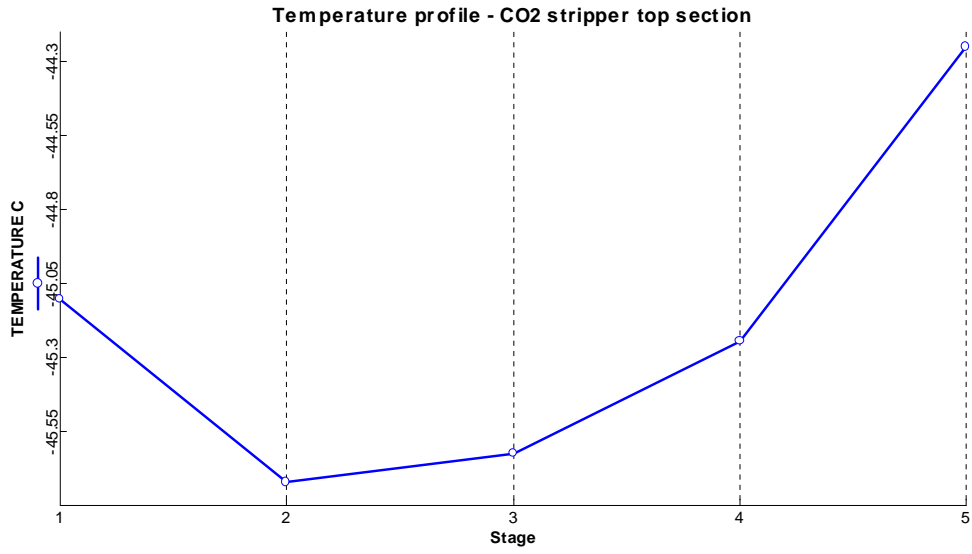


Figure C13: Aspen Model results

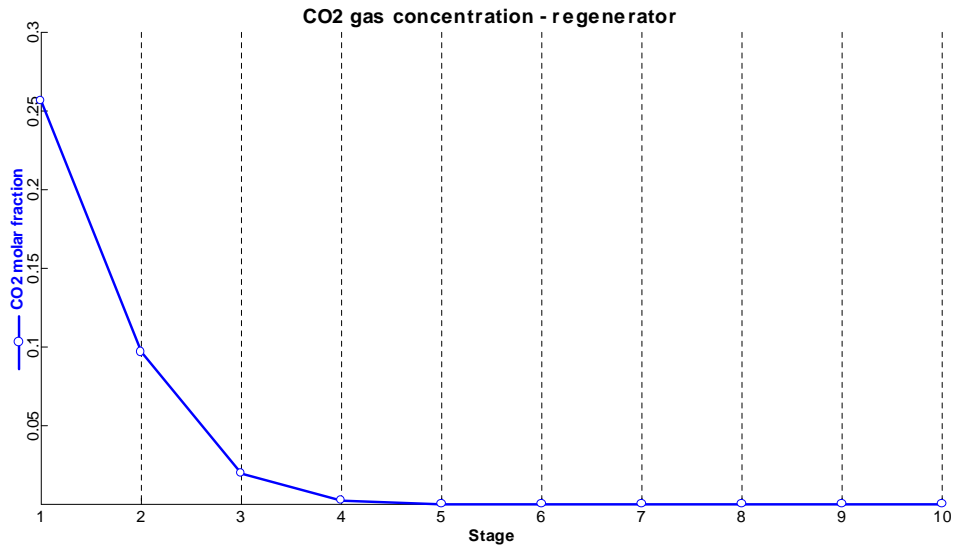
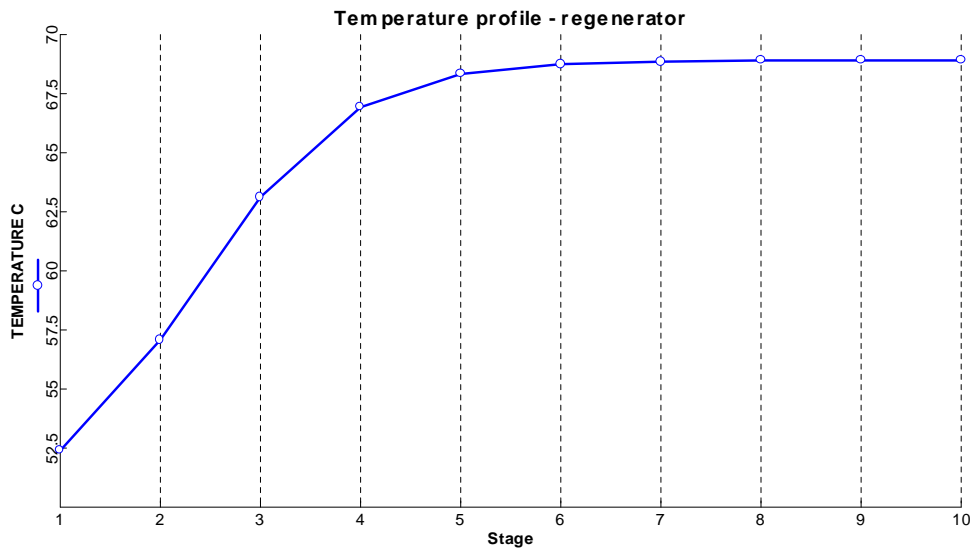
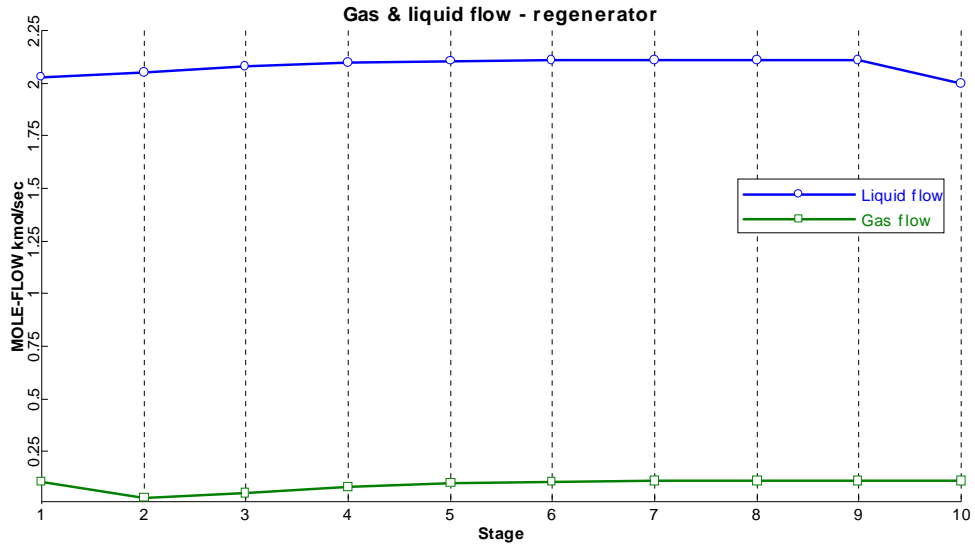


Figure C14: Aspen Model results

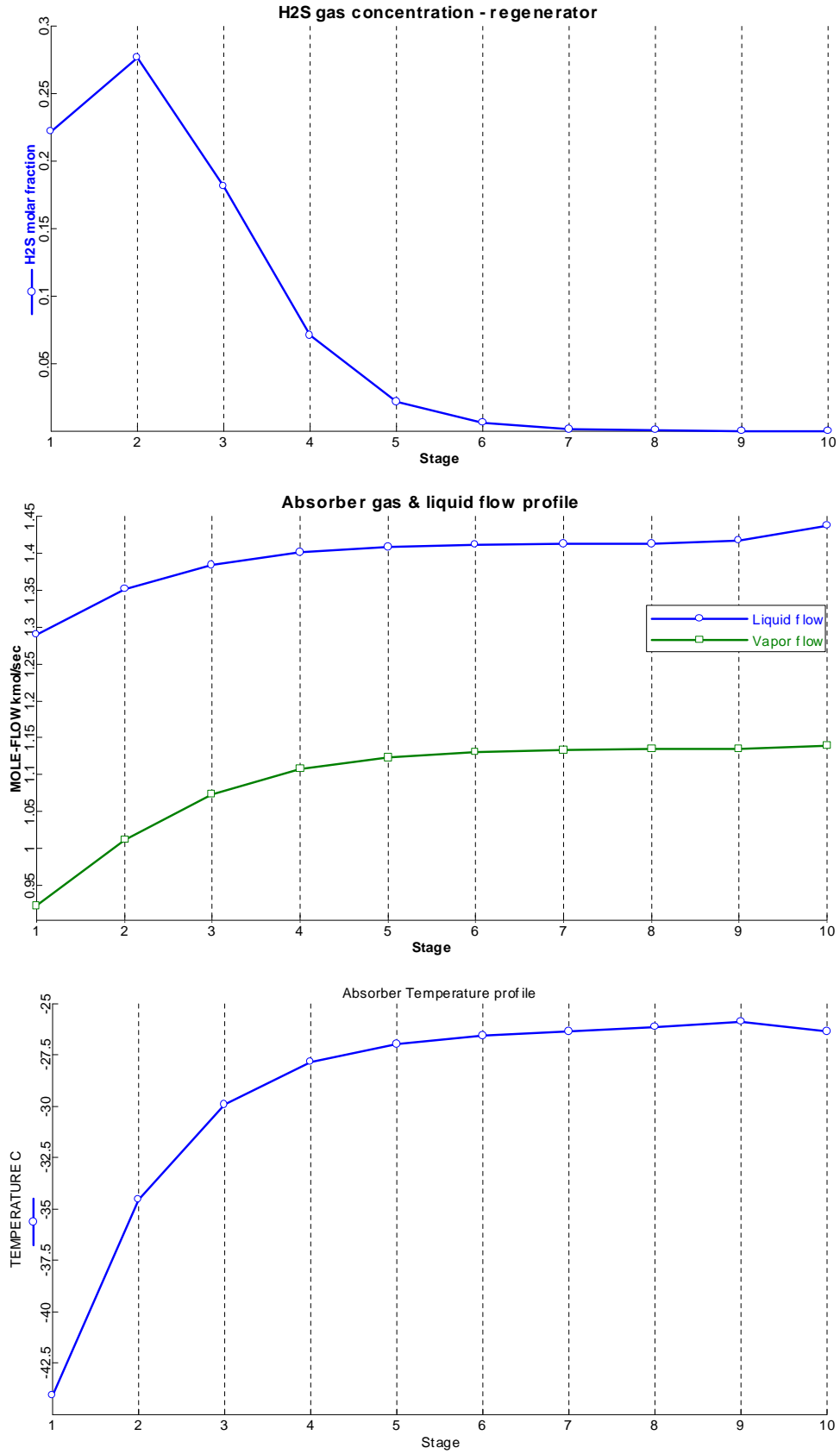


Figure C15: Aspen Model results

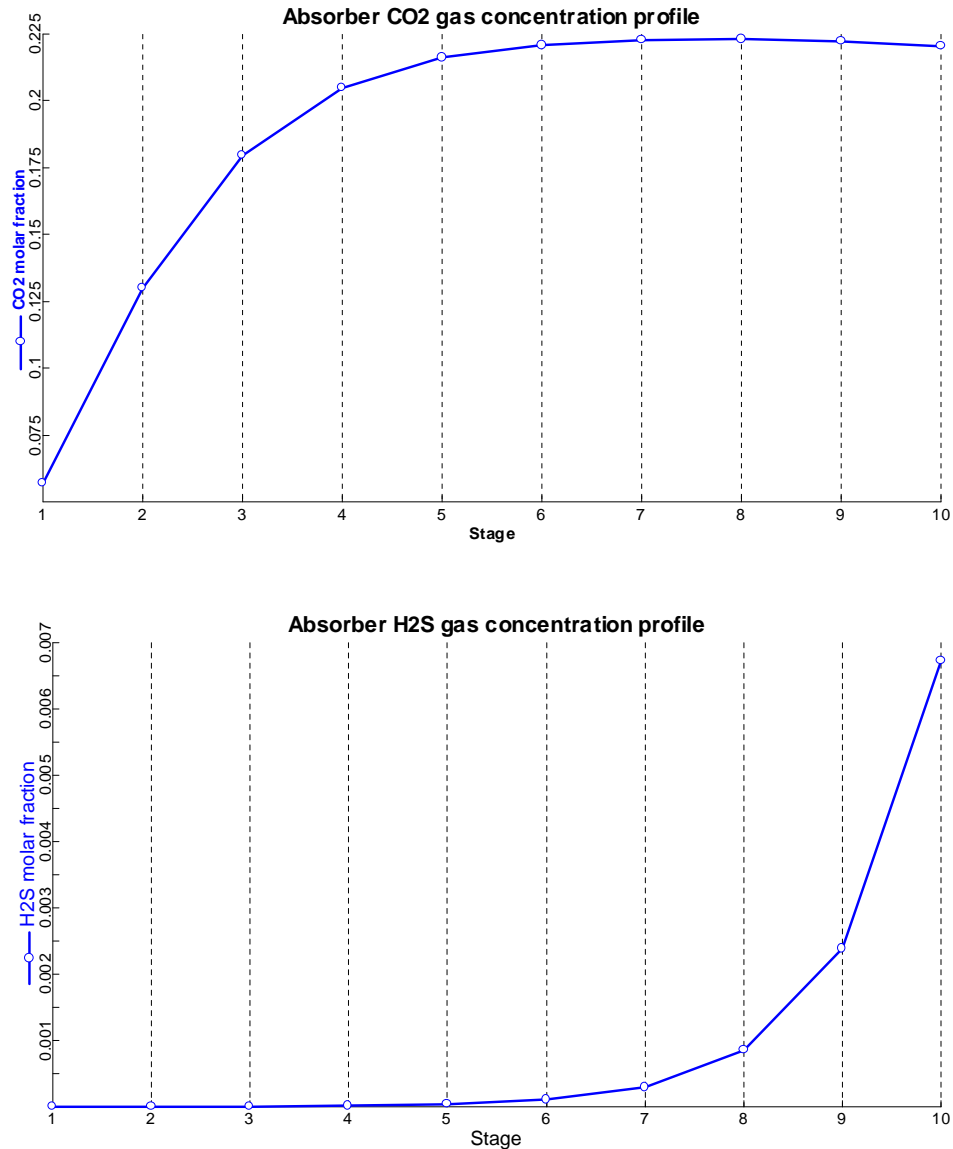


Figure C16: Aspen Model results

C.3 Absorption column: model and thermodynamics

Model and thermodynamics of an absorption column designed for an acid gas containing CO₂ and H₂S, using methanol at low temperatures as a solvent, with no chemical reaction involved.

The preliminary model presented in this chapter was prepared in order to provide a basic comprehension of the thermodynamic system for the highly exothermic absorption of a gas in a liquid, such as CO₂ in methanol.

This was achieved through simple material and energy balance equations written at various sections (theoretic stages) throughout the absorption column.

Above all, the two following issues were analyzed:

- the influence of the high heat of absorption of CO₂ in methanol on the scrubbing liquid temperature and consequently on the absorption kinetics

- the effect of the scrubbing methanol flowrate on the methanol temperature, as a result of the variation of the total liquid flow heat capacity, and on the acid gas concentration in the gas product.

The results of the model are expected to highlight potential problems for a *Process Simulation Software (Aspen Plus* in the present Study) on the “*Rectisol*-based” process, at the same time suggesting starting realistic operating conditions for the simulation itself.

A simple thermodynamic model was coupled with basic heat and material balance equations and it was applied to each theoretic stage of an absorption column: the mathematic model was implemented on the Excel file ABSORBER.xls (reported in paragraph C.4). The excel file output provides the details for the product gas from the scrubbing column (temperature, composition, flowrate), the number of ideal stages required and the profiles for the temperature, the H₂S and CO₂ gas and liquid concentration throughout the column.

C.3.1 Nomenclature

- x liquid molar fraction
- y gas molar fraction
- H Henry constant (pressure)
- P pressure
- T temperature
- L liquid molar flow
- G gas molar flow
- $d\dot{Q}_{abs}$ theoretic stage enthalpy balance
- $(-\Delta H_{abs})$ heat of absorption
- c_{pl} liquid specific heat @ const pressure
- c_{pg} gas specific heat @ const pressure

C.3.2 Acid gas solubility

CO₂ and H₂S are both soluble in methanol, even though the solubility of H₂S is higher than the CO₂ one: roughly 5 times as much. The following table C4 [Ref. 3] reports the equilibrium solubility of H₂S and CO₂ in methanol at two different temperatures when the acid gas partial pressure is equal to 1 atm:

temperature (°C)	solubility (vol/vol)		selectivity H2S/CO2
	H2S	CO2	
-10	41	8	5.1
-20	92	15	6.1

Table C4

C.3.3 Heat of absorption of CO₂ in methanol (-ΔH abs)

It is hard finding this experimental data in Literature, as the system CO₂/methanol (*physical absorption, no reaction*) is quite specific to the Rectisol process, and consequently very few experimental data have been published.

It is well known though that the CO₂ absorption in polar solvents is a quite exothermic process:

- CO_2 is commonly absorbed in water following the reaction: $\text{CO}_2 + \text{H}_2\text{O} = \text{H}_2\text{CO}_3$ and developing roughly 5830 kcal/kmol of absorbed CO_2
- CO_2 is commonly absorbed in alkaline basics following the reaction (e.g.): $\text{CO}_2 + \text{H}_2\text{O} + \text{NaCO}_2 = 2\text{NaHCO}_3$ and developing roughly 4930 kcal/kmol of absorbed CO_2
- CO_2 is commonly absorbed in aqueous solutions containing ethanol-amines, following again a highly exothermic reaction.

Therefore, in order to obtain a first approximation value, an *Aspen Plus* simulation based on the thermodynamic model presented in paragraph C.4 was used.

The process model is the following fig. C17:

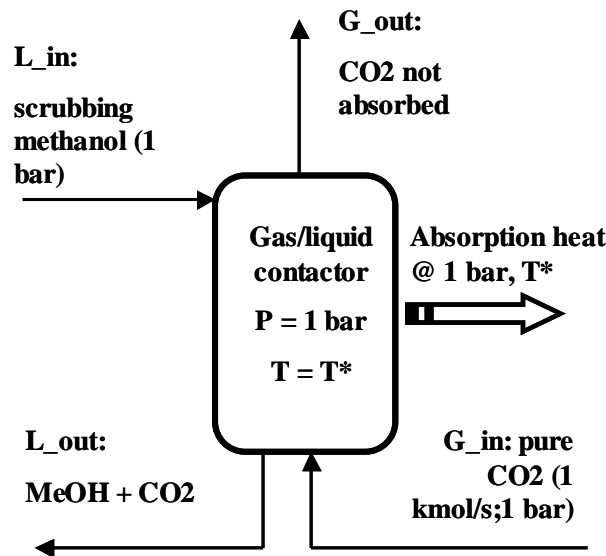


Figure C17: Model used to obtain the CO_2 absorption heat through an Aspen Plus simulation

- 1 kmol/s G_{in} gas stream composed of 100% CO_2 at conditions of 1 bar and a temperature T^* enters a gas/liquid contactor maintained at constant pressure (1 bar) and temperature T^*
- the gas is contacted with a continuous liquid stream L_{in} of pure methanol at 1 bar and a temperature T^* ; the flowrate is not an input
- the system calculates the methanol flowrate L_{in} required to entirely absorb G_{in} into the liquid phase, so that the output stream G_{out} (the gas exiting the contactor) is zero, while the inlet CO_2 is completely absorbed in the output liquid stream L_{out}
- the system at the same time calculates the heat power which must be withdrawn from the system in order to maintain a constant temperature T^* in the contactor: this value is the actual heat of absorption of CO_2 in methanol at atmospheric CO_2 partial pressure and a temperature equal to T^* .

The results of the *Aspen Plus* simulation are reported in table C5.

INPUT T (°C)	INPUT G_in (kmol/s)	OUTPUT L_in (kmol/s)	OUTPUT -ΔH (kcal/kmol)	CALCULATED solubility (vol CO ₂ /vol MeOH)
-35	1	35	4024	14
-60	1	25	4914	19

Table C5

The results for (-ΔH abs) are clearly of the same order of magnitude with respect to the ones published in Literature for similar systems and the calculated solubility values for CO₂ are very close to the values reported in table C4.

In conclusion, as the absorption column in the ABSORBER.xls model is foreseen to be working in a temperature range between -35 °C and -70 °C, we assumed an average value for (-ΔH abs)_{CO₂/MeOH} = 4500 kcal/kmol.

Note also that the partial pressure of CO₂ in the ABSORBER.xls absorption column ranges between 6 and 0.5 bar: the pressure effect on (-ΔH abs) can definitely be neglected at this level of approximation.

C.3.4 Thermodynamic model

For the gas/liquid equilibrium, we took into account the ideal Henry law, even though this is expected to be completely reliable only at pressures close to the atmospheric:

Equation 1 – Henry law

$$yP = H(P,T)x$$

The Henry constant H(P,T) was expressed at 1 bar as a function of the temperature using an Aspen Plus simulation quite similar to the one represented in fig. C17. The values obtained were interpolated obtaining the relationships in (2) & (3) and they were verified using experimental data published in Literature [Ref. 3].

Equation 2

$$H(1bar,T)_{H_2S / MeOH} = 0.039T^2 + 0.5679T + 22.188$$

T is expressed in °C.

Equation 3

$$H(1bar,T)_{CO_2 / MeOH} = 0.0116T^2 + 1.9985T + 87.941$$

T is expressed in °C.

C.3.5 Heat and material balance equations in the absorption column

The heat and material balance equations referred to each column theoretic stage (considered as an adiabatic system) are reported here below (refer to fig. C18).

The basic assumptions behind the equations (4-10) are the followings:

- on the liquid side, methanol does not vaporize
- on the gas side, only H₂S and CO₂ are possibly transferred into the liquid phase
- the contribution of H₂S absorption to the liquid and gas enthalpy changes can be neglected with respect to the CO₂ contribution

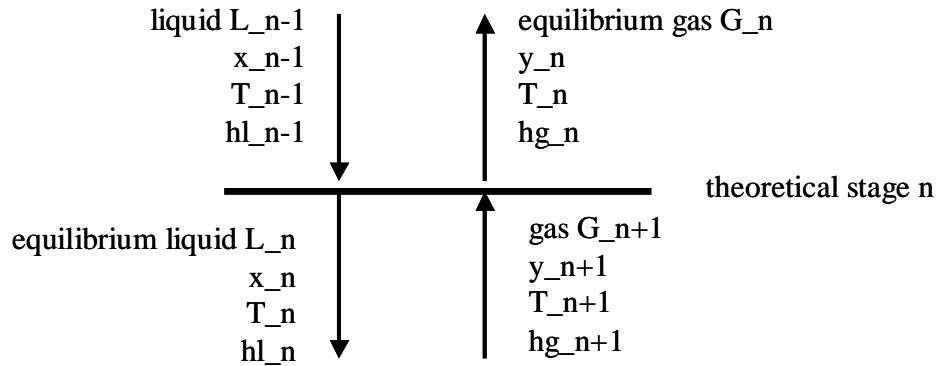


Figure C18: Theoretic stage in the absorption column

Considering a cross section in the absorber with an infinitive thickness, the enthalpy and mass balances can be written in differential terms as follows:

Equation 4 Mass balance

$$d(Gy) + d(Lx) = 0$$

Equation 5 Enthalpy balance

$$d(Gh_g) + d(Lh_l) = d\dot{Q}_{abs}$$

Equation 6

$$d\dot{Q}_{abs} = (-\Delta H_{abs})d(Lx)$$

Equation 7

$$Gc_{pg}dT_g + dGc_{pg}T_g + Lc_{pl}dT_l + dLc_{pl}T_l = (-\Delta H_{abs})d(Lx)$$

Considering the previous equations applied to each theoretic stage:

Equation 8

$$y_{n+1}G_{n+1} + x_{n-1}L_{n-1} = y_nG_n + L_nx_n$$

Equation 9

$$y_nP = H(P, T_n)x_n$$

Equation 10

$$T_{n-1} = \frac{c_{pg}((G_{n+1}(T_n - T_{n+1}) + T_{n+1}(G_n - G_{n+1})) + L_{n-1}c_{pl}T_n - (-\Delta H_{abs})(x_nL_n - x_{n-1}L_{n-1}))}{c_{pl}(G_n - G_{n+1} + L_{n-1})}$$

This implies that the temperature, concentration, gas and liquid flow profiles can be calculated throughout the absorber starting, for example, from the bottom theoretic stage and calculating the various “upwards” unknowns, stage by stage, using eqs. 8-10.

The calculation procedure can be verified in the ABSORBER.xls file described in the next paragraph.

C.3.6 ABSORBER.xls user interface

As the “bottom column calculation approach” was adopted, the process inputs required to ABSORBER.xls are the followings:

- absorber pressure (pressure drops throughout the column neglected)
- feed gas molar composition
- feed gas temperature
- feed gas molar flow
- product liquid temperature
- feed liquid molar composition
- duty specification for the H₂S and CO₂ composition in the product gas

At this point, the ABSORBER.xls calculates the minimum liquid product flow at the column bottom section, the actual liquid product (with a factor of 120%) and its composition and it proceeds “upwards” through the column providing the following outputs, for each theoretic stage:

- gas and liquid composition
- liquid and gas molar flow
- temperature
- number of theoretic stage required to achieve the separation of the duty specification

Please note that ABSORBER.xls is not “self-adjusting” and it requires of course a proper tuning of the input parameters and a proper verification of the system thermodynamics.

C.3.7 Results and discussion

A calculation example for the absorber column is reported in this paragraph: in this case the absorption column is designed for the complete abatement of H₂S only.

The feed gas properties and the column pressure were fixed in the *Core Study*: the main results are summarized here below:

- the theoretic stages required for the separation are usually < 10
- the temperature profile is always roughly constant in the first 3,4 bottom absorber theoretic stages, while it steeply decreases moving upwards in the absorber
- the CO₂ gas concentration decreases continuously moving upwards in the absorber, but the concentration drops much less rapidly than in the case of H₂S, which is entirely absorbed in the first 2,3 bottom absorber stages
- provided a pure methanol scrubbing liquid on top of the column, its required temperature, in order to achieve the specified separation, is considerably lower than the feed gas temperature: in the reported example the liquid is heated from –70°C (absorber top) to –20°C (absorber bottom).
- the liquid/gas molar ratio is always around 2
- the liquid temperature might generate a “hot spot” due to the CO₂ absorption because either its feed temperature is not low enough or the scrubbing liquid flowrate is not high enough.

The reported results, which do vary consistently when the inlet conditions are changed, lead to the following considerations:

- the CO₂ absorption in methanol is highly exothermic and if the system is not over designed using a much larger liquid flow than what is calculated by the material balance, the feed scrubbing methanol is considerably heated when it flows downwards through the absorber.
- This implies that the feed methanol stream must be cold enough to maintain the temperature in the absorber low enough to allow for the CO₂ absorption (which is much less soluble than H₂S) and to avoid any methanol vaporization.
- In effect, at the absorber bottom section, where the majority of CO₂ is absorbed, the temperature does not rapidly decrease because of the large absorption heat released: this has in turn an effect on the CO₂ absorption rate.
- If at a certain stage the temperature reaches a “hot spot” the CO₂ absorption is prevented.
- The results are consistent with the information available in Literature, mostly in the original Patent [Ref. 1].

	C1	C2	C3	C4	C5	T min, °C	T, ref	cp _g , kJ/kmol·K
CO	2,91E+04	8,77E+03	3,09E+03	8,46E+03	1,54E+03	-23	230	29,1
CO2	2,94E+04	3,45E+04	1,43E+03	2,64E+04	5,88E+02	-213	230	33,5
H2	2,76E+04	9,56E+03	2,47E+03	3,76E+03	5,68E+02	-213	230	28,3
N2								
CO2 latent heat of vaporization	kcal/kmol	3052						
cp_liquid CO2 @ -23°C	kcal/kmolK	21						
CO2 heat of solution in MeOH (-DELTA_h)	kcal/kmol	4500						
cp_liquid MeOH (cons const)	kcal/kmolK	17,6						
source: Perry								

Table C6: Physical constants of ABSORBER.xls file

CO2 heat of solution in MeOH (-DELTA_h)					
		kcal/kmol	4500		
absorber bottom					
pressure	bar	30			
ideal stages		5			
syngas in			syngas out		
	y_CO2	0.2		y_CO2 input	0.01
	y_H2S	0.017		y_CO2 calc'ed	0.016
	y_CO	0.4		y_H2S	1.43E-06
	y_H2	0.383		y_CO	0.50
	°C	-35.0		y_H2	0.46
	kmol/s	1.15		°C	-47
				kmol/s	0.92
liquid out					
	x_CO2	0.10	liquid in		
	x_H2S	0.01		x_CO2	0.00
	°C	-20		x_H2S	0.00
	L/G @ bottom	2.30		°C	-71
				kmol/s	2.07

Legend	user input
	output

Table C7: Input and output data of ABSORBER.xls file

<i>input data to absorption columns</i>			
column const pressure	bar		30
T @ bottom C1	°C		-20
T syngas @ C1 inlet	°C		-35
y_CO2 @ syngas to BCTBOL unit			0.2
y_H2S @ syngas to BCTBOL unit			0.017
y_CO @ syngas to BCTBOL unit			0.4
y_H2 @ syngas to BCTBOL unit			0.366
syngas flowrate to BCTBOL unit	kmol/s		1.15
x_CO2 to top stage			0.00
x_H2S to top stage			0.00
x_CO2 (equilibrium with CO2 @ syngas inlet)			0.114
x_H2S (equilibrium with H2S @ syngas inlet)			0.041
y_CO2 @ column exit (user design)			0.010
y_H2S @ column exit (user design)			0.000
(L/G)*based on CO2			1.67
(L/G)*based on H2S			0.41
(L/G)	1.2		2.00
x_CO2 @ liquid from absorber			0.10
x_H2S @ liquid from absorber			0.01
L @ C1 bottom	kmol/s		2.30
	initial CO flowrate	kmol/s	0.46
	initial H2 flowrate	kmol/s	0.42
	hert gas	kmol/s	0.90
CO2 heat of solution (-BLT Ah)	kcal/kmol		4500

Table C8: Input to ABSORBER.xls file

			<i>ideal stage number that best fits specified separation</i>		5						
heat capacity gas (approx const)	kcal/kmol-K	28,7	y_CO2, gas out		0,016						
CO	kcal/kmol-K	29,1	y_H2S, gas out		1,43E-06						
H2	kcal/kmol-K	28,3	y_CO2, gas in		0,200						
CO2	kcal/kmol-K	33,5	x_CO2, liquid in		0,002						
heat capacity MeOH (approx const)	kcal/kmol-K	17,6	x_CO2, liquid out		0,095						
heat capacity liquid CO2 (approx const)	kcal/kmol-K	21	x_H2S, liquid in		0,000						
			x_CO2, liquid out		0,076						
			G (kmol/s), gas out		0,92						
			L (kmol/s), liquid in		2,07						
			T (°C), gas out		-46,7						
			T(°C), liquid in		-70,6						
			gas out, composition								
			CO		0,50						
			H2		0,46						
bottom absorber column											
ideal stage		1		2		3		4		5	
		CO2	H2S	CO2	H2S	CO2	H2S	CO2	H2S	CO2	H2S
G_n+1 gas flowrate	kmol/s	1,152		1,09		1,06		1,02		0,97	
T_n+1, gas	°C	-35		-20		-16,79		-19,44		-28,61	
T @ stage n	°C	-20		-16,79		-19,44		-28,61		-46,74	
CO2 Henry in methanol at stage n		52,6	12,4	57,7	13,8	53,5	12,6	40,3	9,1	19,9	4,2
H/total P	1/bar	1,75	0,41	1,92	0,46	1,78	0,42	1,34	0,30	0,66	0,14
gas inlet-stage n composition (mol fraction)											
y_CO @ stage n		0,42		0,44		0,45		0,48		0,50	
y_H2 @ stage n		0,39		0,40		0,41		0,44		0,46	
y_n+1		0,200	1,70E-02	0,167	3,51E-03	0,146	7,82E-04	0,115	1,57E-04	0,065	2,25E-05
x_n		0,095	8,50E-03	0,076	1,71E-03	0,065	3,74E-04	0,049	7,40E-05	0,024	1,03E-05
y_n		1,67E-01	3,51E-03	1,46E-01	7,82E-04	1,15E-01	1,57E-04	6,54E-02	2,25E-05	1,61E-02	1,43E-06
x_n-1		0,076	1,71E-03	0,065	3,74E-04	0,049	7,40E-05	0,024	1,03E-05	0,002	6,32E-07
T @ stage n-1 (my method)	°C	-16,79		-19,44		-28,61		-46,74		-70,57	
T @ stage n-1 (standard method)	°C	-16,90		-19,47		-28,70		-46,71		-70,54	
Gas G_n	kmol/s	1,09		1,06		1,02		0,97		0,92	
liquid L_n	kmol/s	2,30		2,24		2,21		2,17		2,12	
Liquid L_n-1		2,24		2,21		2,17		2,12		2,07	
y_CO2 - target		0,157		0,136		0,105		0,055		0,006	
acid gas balance check		0,000E+00	0,000E+00	0,000E+00	0,000E+00	0,000E+00	0,000E+00	0,000E+00	0,000E+00	0,000E+00	0,000E+00
% acid gas absorbed		21,37%	80,51%	33,18%	99,64%	49,12%	99,93%	72,62%	99,99%	93,58%	100,00%
cpL, Ln		17,95		17,86		17,82		17,77		17,68	
cpL, Ln-1		17,86		17,82		17,77		17,68		17,61	
cpL, avg		17,91		17,84		17,79		17,72		17,64	

Table C9: Absorber model in the ABSORBER.xls file

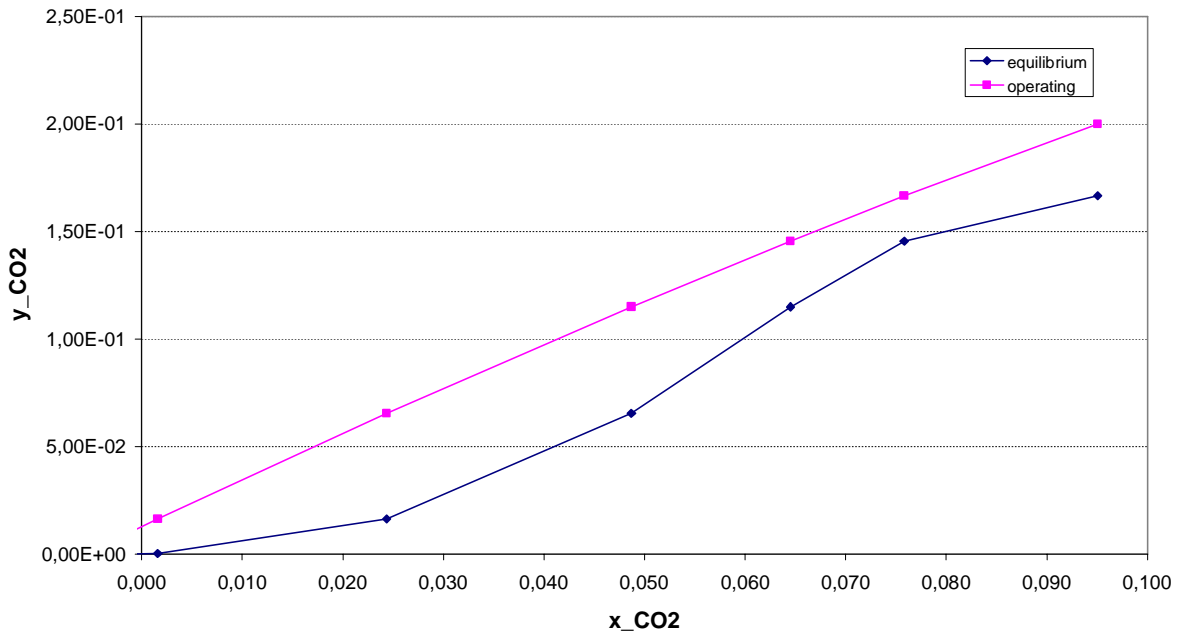


Fig. C19: Equilibrium & operation curves

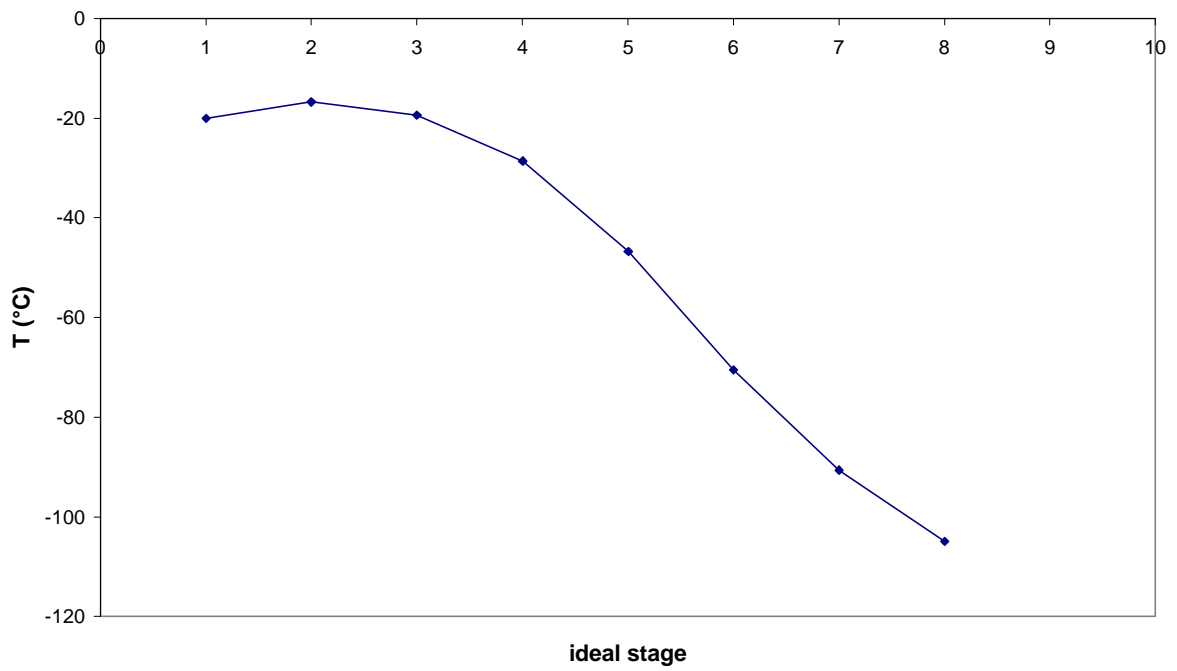


Fig. C20: Temperature profile in the absorption column

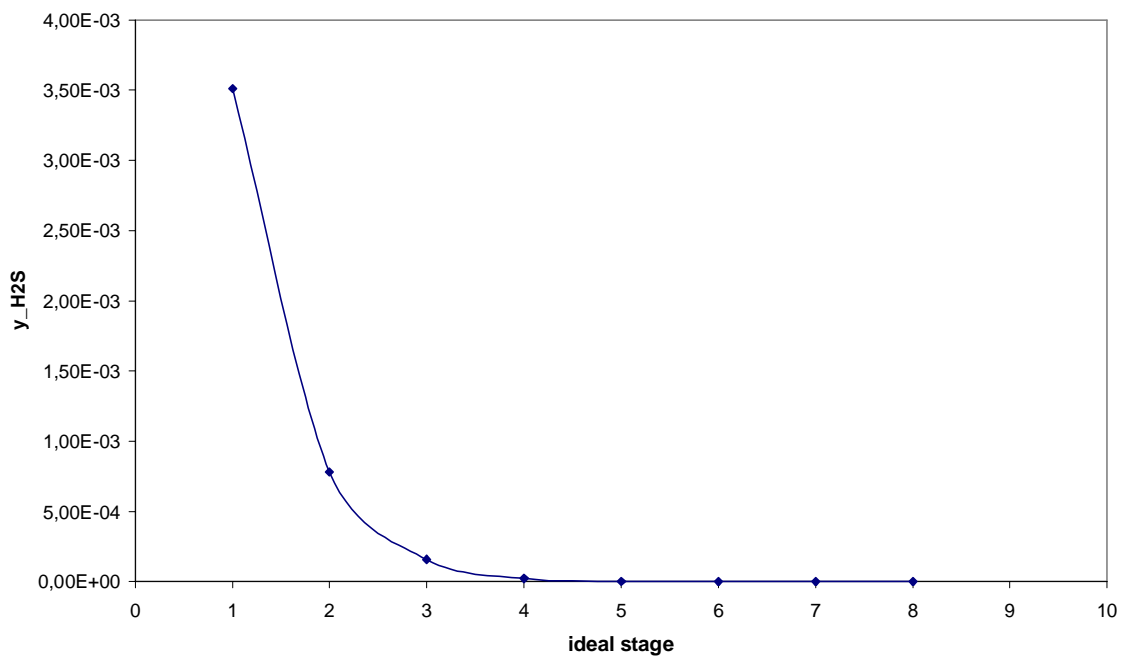


Fig. C21: H₂S gas concentration profile in the absorption column

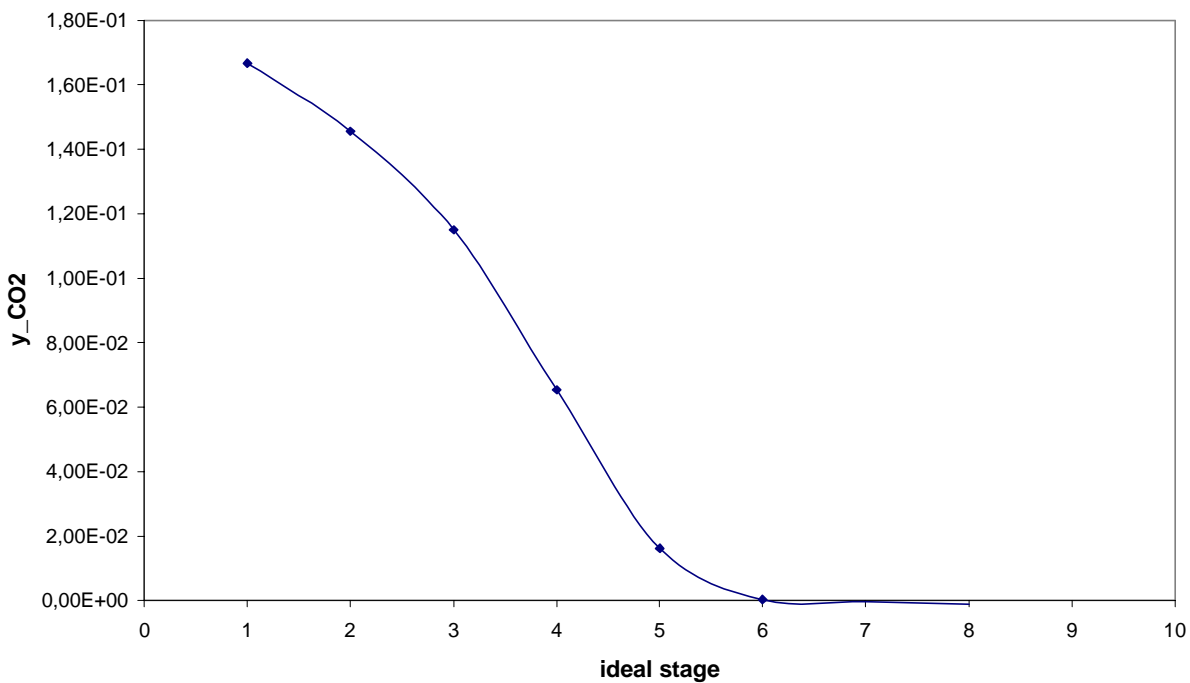


Fig. C22: CO₂ gas concentration profile in the absorption column

C.4 Aspen Plus thermodynamic model

The Aspen Plus Helpdesk provides a specific advice for the thermodynamic models that fit the acid gas absorption by a methanol solvent and a clear reference is made to the *Rectisol* process.

The list is reported here below:

- PRWS
- RKSWS
- PRMHV2
- PSRK
- SR-POLAR

The Aspen Support Service experts (email: AES.Support@aspentech.com) suggested that PSRK does not have adjustable parameters because it is based on the UNIFAC equation of state and it might not give the best results. The other listed models, though, require binary parameters (methanol/acid gas): Aspen Plus is not provided with data for the system methanol/COS and on the other hand these parameters were not available.

Actually, the only thermodynamic model which can process the COS without any external intervention is the SR-POLAR one.

It was decided therefore to use the PSRK model and to remove the COS from the raw gas feed stream (its composition is 0.02 % vol) and replacing the flow of this component by a molar-equivalent amount of H₂S. This was done in the hypothesis that the binary parameters of the systems MeOH/COS and MeOH/H₂S are quite similar.

This hypothesis could not be verified directly as we lacked of the parameters, but the following sensitivity analysis was performed:

- a sample raw gas streams quite similar to the Aspen Model one in term of composition and properties was fed to a single stage absorber: in one case though the raw gas stream contained 1% vol of H₂S, on the other case 1% vol of COS. An Aspen Plus simulation calculated the methanol flow (@ the raw gas T and P) required to absorb 99 % of the molar flow of the raw S-containing gas (H₂S or COS).
- All the thermodynamic model listed here above were used, but as we anticipated only the SR-POLAR one performed the calculations for the COS case.
- The results reported in Table C10 show that:
 1. for the H₂S case, the MeOH required flowrate and the absorption heat data are of the same order of magnitude for the different models, even though the PSRK and PRWS ones provide the largest estimation for the methanol flow and a relatively small heat of absorption;
 2. The SR-POLAR model, which allows comparing the MeOH/COS and MeOH/H₂S performances, shows the same value for the heat and two equal order of magnitude values for the required methanol flow.

Based on the previous considerations and on the fact that the COS concentration is roughly 1% mol/mol of the H₂S one, the error due to replacing the COS flow by a molar-correspondent flow of H₂S was considered negligible to the degree of approximation of the results provided in the present Study.

H2S CAPTURE				
	RAWGAS	MODEL USED	METHANOL FLOW REQUIRED TO CAPTURE 99% OF THE INCOMING H2S GAS FLOW	HEAT released
	VAPOR		kmol/s	MW
Mole Flow kmol/sec		RKSWS	3	4.9
METHANOL	0	PRMHV2	1.47	8.9
NITROGEN	0.07	PRWS	8.55	4.7
COS	0	PSRK	8.55	4.7
H2S	0.01	SRPOLAR	4.81	3.6
CO	0.35			
CO2	0.20			
CH4	0.02			
H2	0.35			
Total Flow kmol/sec	1.00			
Temperature K	238.15			
Pressure N/sqm	3.20E+06			
COS CAPTURE				
	RAWGAS	MODEL USED	METHANOL FLOW REQUIRED TO CAPTURE 99% OF THE INCOMING COS GAS FLOW	HEAT released
	VAPOR		kmol/s	MW
Mole Flow kmol/sec		SRPOLAR	8.68	3.6
METHANOL	0			
NITROGEN	0.07			
COS	0.01			
H2S	0			
CO	0.35			
CO2	0.20			
CH4	0.02			
H2	0.35			
Total Flow kmol/sec	1.00			
Total Flow kg/sec	21.93			
Total Flow cum/sec	0.58			
Temperature K	238.15			
Pressure N/sqm	3.20E+06			

Table C10

C.5 References

- [Ref. 1]: “Separation of Gaseous Components from a Gaseous Mixture by Physical Scrubbing”, Ranke, G.; Weiss, H., United States patent 4,324,567, 1982
- [Ref. 2]: Gas Processes 2004, Hydrocarbon Processing®
- [Ref. 3]: Gas Purification, II Edition, Riesenfeld, F.C.; Kohl, A., Gulf Publishing Company, 1974.
- [Ref. 4]: The Rectisol® Process for Gas Purification, Lurgi Engineering Oel-Gas-Chemie, brochure available @ <http://www.lurgi.com> (in attachment to the present Study).
- [Ref. 5]: Dr. Ulrich Koss, Ulrich_Koss@lurgi.de, Private Communication, 2005.